Universitat Autònoma de Barcelona

INVESTIGATION OF THE ROLE AND MODULATION OF AUTOPHAGY FOR NEUROPROTECTION AND NERVE REGENERATION USING MODELS OF PERIPHERAL NERVE INJURY

TATIANA LEIVA RODRIGUEZ

Universitat Autònoma de Barcelona

INVESTIGATION OF THE ROLE AND MODULATION OF AUTOPHAGY FOR NEUROPROTECTION AND NERVE REGENERATION USING MODELS OF PERIPHERAL NERVE INJURY

Presented by

TATIANA LEIVA RODRIGUEZ

ACADEMIC DISSERTATION

To obtain the degree of PhD in Neuroscience of the Universitat Autònoma de Barcelona, September 2018

Supervised by	PhD Student
Dra. Caty Casas Louzao	Tatiana Leiva Rodríguez

Group of Neuroplasticity and Regeneration (UAB)

The research described in this thesis is performed at the "Departament de Biologia Cel·lular, Fisiologia I Immunologia, Institut de Neurociències, of the Universitat Autònoma de Barcelona" in the Group of Neuroplasticity and Regeneration.

Financial funding:

The research funding was from La Marató, MINECO and CIBERNED.

NeuroPlasticity
& Regeneration

Table of contents

Summary

Summary

Severe peripheral nerve injury (PNI) cause axonal disruption and may produce retrograde neurodegeneration. Axotomized neurons undergo a series of phenotypic changes at the molecular and cellular levels, some of them called endogenous mechanisms of neuroprotection, that promote neuronal survival that includes the unfolded protein response (UPR), the heat-shock response, the autophagy pathway, the ubiquitin-proteasome system, chaperone, the endoplasmic reticulum (ER)-associated degradation machinery (ERAD) and the antioxidant defence. The intensity and time course of the neuronal response are mainly influenced by the severity of the injury, distance of the lesion to cell body, type of neuron and age. However, when the injury is proximal to the soma, such in the case of peripheral nerve root avulsion (RA), the endogenous mechanisms of neuroprotection might not be properly activated contributing to neurodegeneration. We reasoned that the correction or potentiation of these mechanisms might be effective for neuroprotection.

We first characterize the state of autophagy flux after PNI in vivo and found a blockage of these pathway, alterations in microtubule related proteins and vesicle trafficking proteins at 5-7 days post-injury Subsequently, we modelize some concomitant events associated with autophagy failure such as cytoskeleton abnormalities in *in vitro* model. Furthermore, we analyse the time course response of autophagy and cytoskeleton in vitro. These revealed that neurodegeneration might occur due to initial microtubule alteration followed autophagy blockage. These cytoskeleton alterations increase astrogliosis and MN death in vivo. Finally, we explored the role of autophagy potentiation. Time-course analysis of pharmacological autophagy induction using rapamycin revealed to be neuroprotective only as a pre-treatment before RA injury. In addition, autophagy activation mediated by ATG5 overexpression resulted in a MN preservation accompanied by improved internal trafficking and autophagy flux.

Previous data demonstrated neuroprotective capacities mediated by GRP78/BiP overexpression that it has been found downregulated in degenerated

MNs after the lesion. Considering its relationship with autophagy, we aimed to clarify the mechanisms of these neuroprotection by proteomic analysis. We discovered that GRP78/BiP overexpression induces the downregulation of mitochondrial proteins by the induction of mitophagy. In this activation of mitophagy by GRP78/BiP is implicated IP3R and PINK1

Finally, considering that an effective therapy after PNI should promote axonal regrowth and nerve regeneration, we explored if autophagy stimulation might be pro-regenerative as well. We did so by overexpressing ATG5 or by genetic and pharmacological activation of SIRT1. We discovered that autophagy mediated by SIRT-1/HIF1α promotes neurite outgrowth in vitro. In addition, autophagy potentiation by ATG5 or SIRT1 overexpression enhances functional recovery and axonal growth after the lesion.

Overall, these findings suggested that correction or potentiation of endogenous mechanisms such as autophagy may be an effective therapy to increase the survival of disconnected MNs and enhanced axonal regrowth after the peripheral nerve injuries.

Articles

Articles produced from the work of this thesis:

Peer reviewed publication:

- **Leiva-Rodríguez, T**., Romeo-Guitart, D., Marmolejo-Martínez-Artesero, S., Herrando-Grabulosa, M., Bosch, A., Forés, J., & Casas, C. (2018). ATG5 overexpression is neuroprotective and attenuates cytoskeletal and vesicle-trafficking alterations in axotomized motoneurons. Cell Death & Disease. https://doi.org/10.1038/s41419-018-0682-y

In preparation:

- **Leiva-Rodríguez, T**., Romeo-Guitart, D., Muñoz-Guardiola,P., Polo M., Bañuls C, Herrando-Grabulosa M, Petegnief V., Bosch A., Lizcano JM, Apostolova N, Forés J, Casas C. GRP78/BiP Overexpression Triggers PINK1/IP3R-Mediated Neurorotective Mitophagy

- Romeo-Guitart, D., **Leiva-Rodríguez T**., Forés Q., Casas C. Autophagy induced by SIRT1/Hif1α axis promotes nerve regeneration

Other publications during the thesis:

- Romeo-Guitart, D., Forés, J., Herrando-Grabulosa, M., Valls, R., **Leiva-Rodríguez, T**., Galea, E., Casas, C. (2018). Neuroprotective Drug for Nerve Trauma Revealed Using Artificial Intelligence. Scientific Reports, 8(1), 1879.

- Romeo-Guitart, D., **Leiva-Rodríguez, T**., Espinosa-Alcantud, M., Sima, N., Vaquero, A., Martín, H. D.-, Casas, C. (2018). SIRT1 activation with neuroheal is neuroprotective but SIRT2 inhibition with AK7 is detrimental for disconnected motoneurons. Cell Death & Disease. https://doi.org/10.1038/s41419-018-0553-6

- Mancuso, R., Martínez-Muriana, A., **Leiva, T**., Gregorio, D., Ariza, L., Morell, M., Navarro, X. (2016). Neuregulin-1 promotes functional improvement by enhancing collateral sprouting in SOD1G93A ALS mice and after partial muscle denervation. Neurobiology of Disease, 95, 168–178. https://doi.org/10.1016/j.nbd.2016.07.023

Introduction

Introduction

1. Motor system, motoneurons and peripheral motor compounds

The motor system encompasses several areas and circuits of the brain, spinal cord and peripheral nervous system to produce movement in animals. The primary motor cortex, or M1, located in the frontal lobe, is one of the principal brain areas

involved in motor function. The role of the primary motor cortex is to generate impulses that control the execution of movement. Other regions of the cortex involved in motor function are called the secondary motor cortices. These regions include the posterior parietal cortex, the premotor cortex, and the supplementary motor area (SMA). Neurons in M1, SMA and premotor cortex give rise to the fibers of the corticospinal tract, the only direct pathway from the cortex to the spine. The corticospinal tract is the main pathway for control of voluntary movement in humans. There are other motor pathways which originate from subcortical groups of motor neurons (nuclei). These pathways control posture and balance, coarse movements of the proximal muscles, and coordinate head, neck and eye movements in response to visual targets. Subcortical pathways can modify voluntary movement through interneuronal circuits in the spine and through projections to cortical motor regions. The cerebellum is involved in the timing and coordination of motor programs. The actual motor programs are generated in the basal ganglia. The basal ganglia are several subcortical regions that are involved in organizing motor programs for complex movements.

Like many other large fiber bundles, the corticospinal tract courses through the lateral white matter of the spinal cord (SC). Fibers in the corticospinal tract synapse onto motor neurons and interneurons in the ventral horn of the spine. Fibers coming from hand regions in the cortex end on MNs higher up in the spine (in the cervical levels) than fibers from the leg regions which terminate in the lumbar levels.

At the spinal cord MNs are surrounded by other non-neuronal cells such as microglia, astrocytes, oligodendrocytes and ependymal cells. support neurons by carrying out homeostatic functions and controls neurotransmission as part of the tripartite synapse whereas oligodendrocytes produce myelin, hereby sustaining saltatory nerve conduction. Adult microglia are highly ramified cells with phagocytic capacity and morphological plasticity, important in development and after injury. These types of cells have different functions and its characterized by their molecular heterogeneity profile, but their main role is to sustain, feed and ensure a correct health of neurons to allow the optimal performance of the CNS and protects the neurons after several insults. It has been demonstrated that gene profiling of astrocytes and microglia has been heterogenous among diseases. The cellular

restoration is very focused on the oligodendrocyte and the neuron in CNS diseases perhaps not sufficiently for astrocytes and microglia, despite signs of functional impairment in both cell types(Masgrau et al., 2017). Therefore, it is important to know the molecular mechanisms of each cell type that underlie CNS diseases, to design specific therapies. On the same way, CNS is protected by the blood brain barrier that selecting molecules between the bloodstream and the CNS. Therefore, it maintains a correct homeostatic environment and isolates neurons from damaging compounds and the blood immune system (Rasband, 2016).

Within the ventral horn, motoneurons (MNs) projecting to distal muscles are located more laterally than neurons controlling the proximal muscles. Neurons projecting to the trunk muscles are located the most medially. Furthermore, neurons of extensors (muscles that increase the joint angle such as the triceps muscle) are found near the edge of the gray matter, but the flexors (muscles which decrease the joint angle such as the biceps muscle) are more interior. It is important to note that a single motor neuron in the spine can receive thousands of inputs from the cortical motor regions, the subcortical motor regions and through interneurons in the spine. These interneurons receive input from the same regions and allow complex circuits to develop. Each motor neuron in the spine is part of a functional unit called the motor unit. The motor unit is composed of the MN, its axon and the muscle fibers it innervates. Smaller motor neurons typically innervate smaller muscle fibers. Motor neurons can innervate any number of muscles fibers, but each fiber is only innervated by one motor neuron. When the motor neuron fires, all its muscle fibers contract. The size of the motor units and the number of fibers that are innervated contribute to the force of the muscle contraction. There are three types: α, β and γ. The α-MNs innervate muscle fibers that contribute to force production. The γ-MNs innervate fibers within the muscle spindle. The muscle spindle is a structure inside the muscle that measures the length, or stretch, of the muscle. And β-MNs dually innervate skeletal muscle and spindles (Squire et al., 2008). Motor neurons of these classes have significantly different molecular, morphological, and functional properties (Kanning et al, 2010).

MNs can classify according it cell body location, neurotransmitter, targeting, and symptoms upon lesion. MNs are easily identified by histochemical staining of

choline acetyltransferase (ChAT), which synthesizes acetylcholine (ACh) and vesicular acetylcholine transporter protein (VAChT), which is responsible for the transportation of ACh from the cytoplasm into the synaptic vesicles.

MNs located at different of the CNS have differences in their excitability and therefore the action potentials. Nowadays these are not fully understood but these differences can be related with the ionic channel conformation of their membrane(Tadros et al., 2016).

The pool of MNs that innervates an individual muscle forms an elongated column that typically extends over two or three spinal cord segments. Small γ-MNs that innervate muscle spindles are intermingled among large α-MNs that innervate skeletal muscle fibres and β-MNs innervate both types. Motor axons also give off small branches within the spinal cord, called recurrent collaterals. These axons have two differential domains: the axonal initial segment (AIS) and nodes of Ranvier that share their protein composition but differs in their mechanism of assembly (Nelson & Jenkins, 2017).

Nerves are composed of these axons, together with fibroblasts, blood vessels supplying the tissue, and Schwann cells that are the responsible to myelinate axons increasing their conduction velocity. Peripheral nerves are surrounded by connective tissue component and is divided into endoneurium, perineurium and epineurium, according to their topography. The endoneurium are enriched of collagen fibrils which run longitudinally along the nerve fibres between the basal lamina of the Schwann cells and the perineurium. This thin layer contains the endoneurial fluid and serves to support capillary blood vessels. The perineurium envelope a nerve bundle or fascicle and it is denser than the endoneurium, the epineurium is the outermost layer that surround and connect the nerve bundles in a single beam.

The neuromuscular junction (NMJ), also called motor end plates is the site of connection between motor nerve axons and skeletal muscle fibres. NMJ are specialised chemical synapses of acetylcholine formed at the sites where the terminal branches of the axon of a MN contact to a target muscle cell (Pavelka, 2010). Innervation is achieved by interaction of acetylcholine released from the motor axon

endings with its receptor in the plasma membrane of the muscle cell that triggers the action potential. Mutations or changes in receptor expression have been related to neuromuscular pathologies (Cooper & Jan, 1999) and with apparition of neuropathic pain after nerve injuries (Seltzer et al., 1991).

When the whole nerve is stimulated at an intensity that activates all the contained axons, the recorded wave is a compound nerve action potential, that is the algebraic sum of the individual action potentials of all the axons stimulated and able to propagate it. The size and shape of this compound is determined by the number of functional axons, the amplitude of single action potentials, the range of conduction velocity and the distance impulses travel along the nerve. Stimulation of a mixed or a motor nerve elicits a twitch in the innervated muscles. The impulse conducted by α-MNs causes synaptic transmission at the NMJ and the production of an action potential in the membrane of the skeletal muscle fibers, that can be recorded with electrodes placed on the muscle. The compound muscle action potential (CMAP) represents the summation of the action potentials of all excited muscle fibers that respond to the nerve stimulation. Therefore, motor nerve conduction tests provide selective information on the function and regeneration of α-motor axons in vivo (Navarro, 2009a).

The amplitude of the CMAP response is determined by the number of muscle fibres innervated and the size of the axons. By measuring the latency and the distance between stimulating and recording electrodes the conduction velocity (CV) can be calculated for each wave. In regenerating nerves, the CV is altered by changes in axon diameter and myelination and remains below normal values for long time after successful regeneration. These are the most useful indicators for nerve regeneration studies (Navarro, 2016) and the state of MNs in neurodegenerative diseases (Morales et al., 1987).

NMJ is formed by the pre-synaptic nerve terminal, post-synaptic muscle and perisynaptic glial cells, which are separated by 50-80 nm-wide gap also known as synaptic cleft. The axon terminal represents the presynaptic part of NMJ and it contains multiple mitochondria and synaptic vesicles where acetylcholine is stored (Tintignac et al., 2015).

The muscle fibers are enclosed by a basal lamina containing extracellular matrix material originating from the muscle fibers. The basal lamina in the synaptic cleft differs in its molecular composition from that outside the synapse as it contains molecules secreted by both nerve and muscle (Banke,et al, 1983). The nerve terminal is capped by Schwann cells. These cells also produce a basal lamina, which fuses with that of the muscle fiber at the edge of the NMJ. In addition, a fibroblast-like cell, referred to as kranocyte form a loose cover over the NMJ (Court et al., 2008).

2. Peripheral nerve injury

Trauma to peripheral nerve trunks may result in various extents of nerve fibers injury. Peripheral nerve injuries (PNIs) usually lead to devastating loss of motor, sensory and autonomic functions, acute or progressive, of the areas innervated by the injured nerve fibers (Seddon, 1943). Due to the complex requirements for adequate axonal regeneration, functional recovery is often poorly achieved. The degree of deficits depends mainly on the severity and proximity of the lesion to the spinal cord. The functions might be recovered if it was possible that axotomized neurons survive, regrow the sectioned axons through the distal stump, and re-establish functional connections with appropriate peripheral target organs. Surgical repair to re-establish nerve continuity has a great impact on the prognosis of PNI. Although peripheral axons are able to regenerate when the circumstances and the environment allow it to happen, functional recovery is not guaranteed (Allodi , 2012).

2.1 Types

The insults that can damage a peripheral nerve are very diverse (mechanical, thermal, biochemical, ischemic, etc.). PNIs can be classified according to the morphology of the lesion, their therapeutic requirements and their prognosis. The two widely used classifications for nerve injury are the Seddon and Sunderland classifications. While Seddon classification is simpler to follow for electrophysiologists, Sunderland grading is more often used by surgeons.

Mackinnon and Dellon have identified another addition to Sunderland classification by describing a mixed type of injury (Chhabra, 2014) **(Fig 1).**

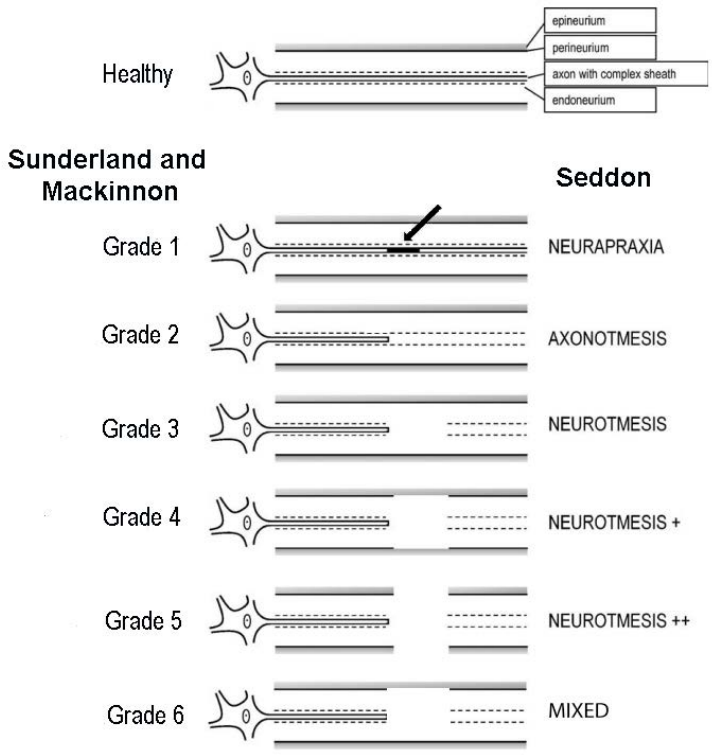

Figure 1. Schematic representation of 6 degrees of nerve injury according to Sunderland and Mackinnon. Grade 1: conduction block indicated by arrow, Grade 2: transection of axon with an intact endoneurium (axonotmesis). Grade 3: transection of the nerve fiber (axon and endoneurium) within an intact perineurium (neurotmesis), Grade 4: transection of funiculi, epineurial tissue maintains nerve trunk continuity (neurotmesis +), Grade 5: transection of the whole nerve trunk (neurotmesis), Grade 6: mixture between 2 and 4. The classification depending on the affected layer, which can be the axon, endoneurium, perineurium and epineurium. (Adapted from Deumens et al., 2010)

The first degree corresponds to neuropraxia, related with alterations on myelin without disruption of the axon continuity that cause a temporary loss of motor and sensory function due to blockage of nerve conduction. In the grade 2, the axon continuity is disrupted, but the endoneurium remains intact and completely recovery is expected over months. The Grades 2, 3 and 4 (Axonotmesis of Seddon) imply the anatomical affectation of the axon, axon-endoneurium or axon-endoneurium-perineurium, respectively. The Grade 5 (Neurotmesis of Seddon) is a complete transection of the nerve. The Grade 6 or Mixed is a mixture of grades 2 and 4, which involves a more common clinical scenario of PNI. In these injuries, since the connective tissue sheaths are disrupted, the regenerating axons are misdirected and

may not be able to innervate the sensory endings or muscle end plates, and the pattern of recovery indicated by muscle unit potentials is mixed, and, often, incomplete (Chhabra et al., 2014. For the grade 4 and 5 the surgical repair is mandatory to guarantee some degree of recovery.

The mechanical injuries (avulsions) that affect the nerve root, at the interface between CNS and PNS, lead to neurotmesis and represent one of the most severe types of PNI. This type of lesion can be produced to a single or some nerve roots from brachial, lumbar and facial zones and causes a disruption of the neuron-muscle connection. Nerve root avulsion (RA) may occur after traffic, sportive or work accidents or after iatrogenic injuries or during complicate obstetric interventions at birth (Pondaag et al., 2007)(Feinberg et al., 2008). The same lesion in adults exhibits poor functional recovery in compared to infants. This is due to the reduced regenerative capacity at older age and to the diverging anatomical dimensions between infants and adults patients because the distance of nerve ends and the distance that regenerating axons must transverse are substantially larger (Hulleberg et al, 2014).

Following peripheral nerve injury, while Schwann cells located in the NMJ guide regenerating axons to denervated endplates they start retracting their processes from the endplates after prolonged denervation (Reynolds & Woolf, 1992). Besides, these cells eventually atrophy and the basal lamina and bands of Büngner degenerate. Muscle endplates also lose postsynaptic receptors, the size of muscle fibers decrease, and the ability of satellite cells to proliferate declines (Kang et al., 2014). Therefore, the prolonged loss of NMJ function would cause both a contraction failure and a loss of the NMJ synaptic machinery. These impairment impedes the recovery of motor function after muscle denervation (Sakuma et al., 2016)

The peripheral nerves also can be damaged by metabolic, infectious, degenerative, or toxic mechanisms. The principle effect of neuromuscular disorders that affect mainly the peripheral nervous system and muscle include some of the most devastating diseases including amyotrophic lateral sclerosis (ALS), congenital muscular dystrophies and myopathies. This type of disorders causes significant incapacity, including at the most extreme, almost complete paralysis (Laing, 2012).

2.2 Neuroprotection and nerve regeneration

PNI is a major clinical and public health calling and occurring in 2.8-5% of polytrauma patients derived from multiple scenarios. In the United States of America (USA) about 20 million Americans suffer from PNI caused by trauma and medical disorders (Jones et al., 2016). Obstetrical brachial plexus injury is seen 1.24 per 1000 births and iatrogenic PNI is seen after surgery, anaesthesia injections, chemotherapy, and radiation for breast or head and neck tumours (Brull et al. , 2015). Severe injuries have devastating effects on patient's quality of life.

Peripheral nerve root avulsion (RA) leads to the most severe degree of nerve injury because nerves are completely separated from the spinal cord and sensory ganglia, thus causing loss of motor, sensory, and autonomic functions in the affected extremities. Detached nerves may be reimplanted but successful repair is time-dependent due to the existence of massive retrograde degeneration of MNs (Koliatsos et al ., 1994) (Penas et al., 2009). MNs can regenerate their axons if nerve root reimplantation is performed soon after the injury. In patients with brachial plexus avulsion, direct re-implantation of injured roots has allowed some functional recovery (Chew et al., 2011) There is the assumption that in chronic axotomy and chronic muscle denervation, insufficient retrogradely support of neurotrophic factors from Schwann cells and target organs arrived and its progressive diminution over time leads to poorer outcomes. Three months has been established as the critical time-point where the effects of medical intervention start to decrease (Jonsson et al., 2013). The effective recovery of motor function after spinal root injuries depends on neuroprotection and axonal regeneration toward the muscle targets.Several therapeutically approximations to sustain MN viability after RA have been found experimentally but translation to the human has never been performed (**Table 1**). Most of these agents have been tested after root avulsion lesions without reimplantation, so that only its neuroprotective action is known and not if they have a role in regeneration. In addition, neuroprotectants only increase survival up to 60%. It is important to emphasize that the time of administration of the drug could be decisive. This is because the activation of neuroprotective mechanisms or the inhibition of detrimental mechanisms could be good in certain stages after the

injury. For this reason, it is important to know the underlying mechanisms of degeneration to design specific and effective therapies in a time-dependent manner.

Table 1. Published therapies to sustain MN survival in different RA models (David Romeo-Guitart, 2017)

Drug	Model	Ref
GM-1 Ganglioside	Spinal Root Avulsion	(Oliveira & Langone, 2000)
Riluzole	Spinal Root Avulsion + Reimplantation	(Nógrádi et al., 2001)
MK801, DAP5, NBQX	Spinal Root Avulsion	(Nagano et al., 2003)
Cerebrolysin	Spinal Root Avulsion	(Haninec et al., 2003)
T-588	Facial nerve avulsion	(Ikeda et al., 2003)
Nitroarginine	Spinal root avulsion	(Wu & Li, 1993)
BDNF+GDNF	Facial nerve avulsion	(BLITS et al., 2004)
N-Acetyl-cysteine	Spinal Root Avulsion	(Zhang et al., 2005)
Vitamin E	Facial nerve avulsion	(Hoshida et al., 2009)
Glatiramer acetate	Spinal Root Avulsion	(Scorisa et al., 2009)
Pre084	Spinal Root Avulsion	(Clara Penas, Pascual-Font, et al., 2011)
Phorbol-12-myristate-13-acetate	Spinal Root Avulsion	(Zhao et al., 2012)
Valproic acid	Spinal Root Avulsion	(Wu et al., 2013)
Paclitaxel	Spinal Root Avulsion	(Sim et al., 2015)
ISP	Spinal Root Avulsion + Reimplantation	(H. Li et al., 2015)
Lithium	Spinal Root Avulsion + Reimplantation	(Fang et al., 2016)
Pregabalin	Facial nerve Avulsion	(Moriya et al., 2017)
Minocycline	Spinal Root Avulsion	(Chin et al., 2017)
Neuroheal	Spinal Root Avulsion + Reimplantation	(Romeo-Guitart et al., 2017)

After PNI, a few percentages of axons will regenerate until target organs after the nerve transection. The principal treatment after nerve transection when direct suture between stumps cannot be achieves, is the nerve grafting. This graft can be from the same patient (autograft) or from a donor (allograft)(Glaus et al., 2011). These grafts can be replaced by conductive tubes based on chitosan or cell therapy (Georgiou et al., 2015). Therefore, a co-adjuvant therapy is needed after PNI to increase nerve regeneration and block the muscle atrophy.

A multitude of agents have been investigated to improve outcomes in peripheral nerve repair. Betamethasone, vitamin E, thyroid hormone, pyrroloquinoline and erythropoietin have been shown to improve neuronal recovery (Mohammadi et al., 2013)(Mohammadi et al., 2013)(Elfar et al., 2008)(Azizi et al., 2014). FK506, a calcineurium inhibitor, enhances peripheral nerve regeneration and increases axonal sprouting (Gold et al.,1995). Related proteins have similar neurotrophic activity without the immunosuppressive qualities (Gold et al., 1997). These agents

have not been widely adopted due to limited demonstrable efficacy in humans and/or side effect profiles. Recently, it has been discovered a new combination of drugs, called Neuroheal using the systems biology approach. These combination neuroprotected motoneurons, exerted anti-inflammatory properties and promoted functional locomotor recovery in a preclinical model(Romeo-Guitart, Forés, et al., 2018a). Furthermore, chronic treatment exerted long-lasting neuroprotection, reduced gliosis and matrix proteoglycan content, accelerated nerve regeneration, promoted the formation of functional neuromuscular junctions, and reduced denervation-induced muscular atrophy (Romeo-Guitart et al., 2017). This combination would be a promising therapy for clinical translation.

Even so, novel therapies that sustain survival of cell bodies, NMJ, and distal axonal targets while accelerating the rate and quality of regeneration need to be discovered for clinical translation. A potential product could be a "neurobiologic cocktail" consisting of such additive or synergistic pro-neurotherapeutics to increase the MN survival and to augment or accelerate nerve functional outcomes after PNI (Janjic & Gorantla, 2017).

3. Murine models of peripheral nerve injury

To investigate the molecular mechanisms underlying after PNL and to develop neuroprotective drugs/therapies to increase MNs survival after the lesion, *in vitro* and *in vivo* models are needed.

3.1 *In vitro* models

Several specific elements of the peripheral nerve regeneration or the molecular mechanisms underlying after root avulsion can be effectively reproduced in vitro although the complexity of the nerve structure or the spinal cord complexity are impossible to entirely reproduce in vitro. Due to the responsibility to respect the 3Rs (Replacement, Reduction, Refinement) in using live animals, researchers have been required to design and optimize *in vitro* models before testing their hypothesis using *in vivo* animal models (Geuna et al., 2016).

In vitro models could help to elucidate the underlying mechanism of various pathological processes since they allow their manipulation by molecular techniques of transgenesis to express or overexpress a particular molecule or protein of interest. Furthermore, *in vitro* models offer certain advantages over *in vivo* studies since interpretation of results may be easier and more conditions can be assessed.

Several models of immortalized cell lines of peripheral glial cells (JS-1& RT4-D6P2T) and neuronal cells (PC-12 & NSC-34) serve to study basic elements of neurodegeneration and regeneration. These serve us to obtain preliminary data on several aspects including the signalling pathways activated by drugs or molecules, the biocompatible of new or modified materials and cell behaviour changes due to environmental alterations induced by physical agents. These cell lines provide the great advantage that completely replaced the animal manipulation and the cheapest cost and rapidly results. Even though the biological properties of these cells are far distant from those of corresponding mammalian cells in normal conditions due to neoplastic features.

The culture of the whole tissue explant, called organotypic model preserve both cytoarchitecture and cell interactions that form the tissue, providing a closer approximation to *in vivo* models in comparison with dissociated cell cultures. MNs in the spinal cord organotypic culture (SCOC) remain embedded in their natural environment in contact with glial cells and maintain interneuronal connections and the general response to each single neurotrophic factor is maintained (Gähwiler et al., 1997). Therefore, SCOC can give a closer indication to *in vivo* responses than dissociated cell cultures, where the disruption of their environment may affect the neuronal phenotype. These cultures provide information about the effect of some modulators and it impact on molecular pathways that can provoke or rescue MN cell death (Guzmán-Lenis et al., 2009a)(Guzmán-Lenis ., 2009b). Furthermore, the SCOC in combination with a matrix of a material that allows axonal regeneration (i.e collagen), will permit to extend the axons in neurons and provides information about the axonal growth of MNs(Allodi et al.,2011).

Despite the results obtained *in vitro* shed important information that could help to corroborate some aspects relevant to the unknown mechanisms of PNI, we are aware of the limitations in transferring conclusions from *in vitro* models to *in vivo*.

3.2 *In vivo* models

In the face of acute or chronic axonal damage, neurons and their axons undergo a high number of molecular, cellular, and morphological changes. These changes facilitate two types of responses, axonal degeneration and regeneration, both of which are remarkably conserved in both vertebrates and invertebrates. Invertebrate model organisms including *D. melanogaster* and *C. elegans* have offered a powerful platform with accessible genetic tools for manipulation and amenable nervous system for visualization after axonal injury (J. Li & Collins, 2017).

Various large animal models have been employed for nerve regeneration including rabbits, sheep, pigs and primates. Nevertheless, the majority of studies have been done using rodents, rats and mice taking advantage of size to perform microsurgeries and the anatomical resemblance.

Two main experimental lesion paradigms can be used for nerve regeneration studies. Axonotmesis, in particularly the grade 2 of Seddon or crush which interrupts nerve fibers without severing the connective tissue of the nerve trunk. This model is suitable for the study of biological mechanism of regeneration of new therapeutic agents. Neurotmesis, the other lesion, which is based in a complete nerve transection (with or without removal of a nerve segment). This requires surgical repair to re-establish epineural continuity and should be preferred for preclinical studies of new therapeutic agents (Tos et al., 2009). The advantages of axonotmesis over neurotmesis are: less technically challenging, low interanimal variability in the postoperative outcome. In neurotmesis, axonal regeneration is much slower, in terms of both morphological and functional predictors, thus making it easier to disclose differences between experimental groups. Besides, the differences on these models rely also on the distance from the soma and the age of the animals.

To study the degeneration of MNs after injury a model for peripheral nerve avulsion (Neurotmesis)in the brachial or lumbar have been employed. This model could be used to understand the mechanisms that underlie the degeneration of MNs and therefore could be translational to degenerative diseases that affect MN.

4. Molecular mechanisms of motoneuron response after PNI

After PNI, several factors contributing to poor functional recovery include the damage to the neuronal cell body due to axotomy and retrograde degeneration, inability for axonal growth due to the nerve lesion, poor specificity of reinnervation and changes in the central circuits in which the injured neurons participate due to plasticity of neuronal connections (Lundborg, 2000).

The recovery from traumatic injuries depends primarily on the severity of the axonal injury and its proximity to the CNS. Spinal cord MNs can regenerate and survive by initiating molecular programs shortly after injury known as a chromatolysis and neuronal reaction (Navarro, 2009b).

Chromatolysis is the fragmentation of stacks of rough endoplasmic reticulum (RER) accompanied by the disaggregation of polyribosomes. These cell body response involve the dispersion to the periphery of ribonucleoprotein and movement of the nucleus to the eccentric position that causes the disarray of key parts of the protein synthesis machinery (Moon, 2018). Regenerated neurons after crush has been shown an increase of newly synthesized total RNA due to an increase of anabolic processes in brief chromatolysis. This rapidly chromatolysis reassembles protein machinery, resulting in axonal regeneration. In contrast, various experiments have been demonstrated than transection or SCI (which prevent regeneration) cause persistent chromatolysis and reduced protein synthesis in MNs. Therefore, the functional consequences of chromatolysis is the disruption of protein synthesis which can be transient or permanent depending on a variety of factors including the type and the location of injury (Moon, 2018).

The neuronal reactivation after injury starts with the activation of pro-regenerative machinery, which requires profound changes in transcription and translation in the cell body. The initiated events are classified in early and late events (Rishal & Fainzilber, 2014). The breach of the axonal membrane upon injury is accompanied by rapid changes in intracellular ion concentrations, which leads to the propagation of a calcium wave and the firing of action potentials. Calcium-mediated regulation of immediate-early genes and (Ben-Yaakov et al., 2012) and

epigenetic modifications of the genome by histone acetyltransferases at CNS or by histone deacetyltransferases at the PNS (Shin & Cho, 2017).

The genes that are upregulated after PNI and are directly linked with axonal regrowth, are termed as Regeneration-Associated Genes (RAGs)(Ma & Willis, 2015). Axotomy of PNS neurons induces broad and coordinated gene transcription, a response that is lacking following CNS injury that could correlate with the incapability to regenerate after the injury. The expression of RAGs is a tightly regulated process that needs the neuronal specific activation of determined TFs, and the consequent coordinated modulation of gene expression by them (Ben-Yaakov et al., 2012). The late events are directed by signalling macromolecular networks trafficked on dynein motors that include the molecular axis of the JUN amino-terminal kinase 3 (JNK3), the signal transducer and activator of transcription 3 (STAT3) and the extracellular signal-regulated kinases (ERKs)(Rishal & Fainzilber, 2014).

After nerve injuries, axon distal to the lesion site are disconnected from the neuronal body and degenerate. The axotomized neurons undergo a series of phenotypic changes at the molecular and cellular levels and shift to a regenerative phenotype, activating molecular pathways that promote neuronal survival and axonal regeneration. The intensity and time course of the neuronal response are mainly influenced by the severity of the injury, distance of the lesion to cell body (pre-or postganglionic), type of neuron and age (Navarro, 2009). Spinal MNs from rat are susceptible to the avulsion transection of the roots form brachial or lumbosacral plexus (Penas et al., 2009), but when injury is at postganglionic level MNs do not degenerate (Vanden et al.,1993). However, the immature MNs present susceptibility to the postganglionic injury of the sciatic nerve (Lowrie et al.,1994). Degeneration of MNs and their peripheral axons it has been observed in other disorders: ALS, sarcopenia or following SCI (Bucchia et al., 2018).

In animal models of RA, it was observed that the lesion leads to a massive retrograde death of the 80% of MN and the molecular pathways that underlie these death are controversial (Koliatsos et al., 1994; Penas et al., 2009).

The molecular mechanisms leading to retrograde MN degeneration remains unclear. After RA, where the lesion occurs close to the MN soma, the effects are more sever than after distal axotomy (DA) (Penas et al., 2011; Penas et al., 2009). Recent advances suggest that the mechanisms between these two models differs from 7 days post-injury (dpi). These differing events are characterized by the unbalanced response of pro-survival mechanisms and pro-death mechanisms that determines MN destiny (Casas et al., 2015).The pro-death mechanisms related to the MN degeneration are: apoptosis, necrosis, anoikis, ER stress, nucleolar stress, cytoskeletal rearrangements, selective autophagy and mitochondrial dysfunction. In contrast, the endogenous mechanisms of neuroprotection engaged by MNs are: the unfolded protein response (UPR), the heat-shock response, the autophagy pathway, the ubiquitin-proteasome system (UPS), chaperone, the endoplasmic reticulum (ER)-associated degradation machinery (ERAD) and the antioxidant defence.

Often, neurodegeneration appears concomitantly with anomalies in these corrective mechanisms preventing complete recovery. Correction or potentiation of these endogenous mechanisms of neuroprotection might ensure success of neuroprotective therapy. Therefore, its important to study the molecular cascade related with these endogenous mechanisms to design better therapeutic strategies.

4.1 Apoptosis/Antiapoptosis

Type I programmed cell death (PCD) or apoptosis is critical for cellular self-destruction for a variety of processes that maintains the integrity of cell plasma membrane and of organelles, and it is mediated by the activation of caspases. must be tightly controlled since dysregulated cell death is involved in the development of a large number of different pathologies (Portt et al., 2011). To date, research indicates that there are two main apoptotic pathways: the extrinsic or death receptor pathway and the intrinsic or mitochondrial pathway However, there is now evidence that the two pathways are linked and that molecules in one pathway can influence the other (Elmore, 2007).

The extrinsic signalling pathways that initiate apoptosis, involve transmembrane receptor-mediated interactions with TNF receptors family. However, the intrinsic pathway involves a diverse array of non-receptor-mediated

stimuli that produce intracellular signals that act directly on targets. The stimuli that initiate the intrinsic pathway produce intracellular signals that may act in either a positive or negative fashion (Elmore, 2007). Upon initiation, the initiator caspases (Caspase 1, 2, 4, 6, 9, 10, 12 and 14) will become active and the activation leads to the cleavage of the effector caspases (3,6 and 7), which will run apoptosis (Ichim & Tait, 2016).

The aggressiveness of the process after RA is characterized by a drastic reduction of MN survival, which achieves around 80% of MN death after 3 weeks post-injury(Koliatsos et al., 1994; Penas et al.,, 2009; Wu & Li, 1993). In contrast, distal axotomy of spinal nerves does not cause any motoneuron death due to the presence of the remaining part of peripheral nerves.

This retrograde MN degeneration caused by RA was classified as apoptotic (Martin et al., 2005; Martin et al.,1999) although the use of caspase inhibitors failed to rescue them(Chan et al ., 2001). In contrast, other researchers speculated that the process might be rather necrotic (Li et al., 1998). Nevertheless, Penas and collaborators, had previously reports the lack of any end-step of caspase 3-dependent apoptosis that pointed to the existence of a more severe and non-apoptotic-end in that model. In that sense, some light previously shed by Park and collaborators using KO mice for Bax revealed that these mice presented a phenotype with a too wide range of MN loss after RA. These study revealed that MN may die by Bax-dependent and other by Bax-independent process (Park et al., 2007). Besides, Penas and collaborators had previously reported the lack of any end-step of caspase 3 dependent apoptosis (Penas et al., 2011). However, recent proteomic data revealed that RA induces apoptotic-pathways, but its final execution is prevented by the concurrence of anti-apoptotic factors (Casas et al., 2015).

The anti-apoptosis pathways are regulated by three protein families: FLICE-inhibitory proteins, Bcl-2 and Inhibitors of Apoptosis Proteins (IAPs)(Portt et al., 2011). After RA, has been observed an activation of XIAP in MNs which reaffirms the activation of the intrinsic mechanisms to scape of apoptosis (Casas et al., 2015). The activation of protein kinase B (AKT) has been correlated as a pro-survival protein by it apoptosis blockage. AKT inhibits p53 (a molecular player in apoptosis) and blocks its pro-apoptotic abilities (Gottlieb et al., 2002). In contrast, AKT was cleaved

by caspases during apoptosis and accelerates the cell death (Rokudai et al., 2000). The phosphorylation of FOXOs by AKT impedes the induction of pro-apoptotic genes such BIM or BNIP3 (Dijkers et al, 2000; Tran et al., 2002).

Furthermore, after RA MNs activates apoptotic pathways but also anti-apoptotic ones. These balance could determine the MN destiny after the injury to an alternative death (Casas et al., 2015).

4.2 Rearrangements of cytoskeleton

The cytoskeleton of neurons comprises three distinct, interacting structural complexes that have very different properties: neurofilaments (NFs) and actin filaments and microtubules (MTs). These structures have important functions in the establishment and maintenance of neuronal polarity, morphology and integrity of axons (Luo, 2002 ;Barnes & Polleux, 2009). The main function of neurofilaments which are particularly abundant in axons, is to control the axon diameter, and mechanical resistance (Yuan et al., 2012). MTs and actin filaments mainly affect axon specification and growth and axonal transport (Luo, 2002);(Kapitein & Hoogenraad, 2011). Both MTs and actin filaments are dynamic structures which facilitates the continuous remodelling of the cytoskeleton.

MTs are composed of α- and β-tubulin heterodimers to form linear protofilaments that associate laterally to create the MT. These structures are extremely dynamic, existing in an either growing state (polymerization) or shrinking state (depolymerization). The plus ends of MTs can rapidly switch between these two states, going from growth to shrinkage (catastrophe), or from shrinkage to growth (rescue), a process called "dynamic instability"(Mitchison & Kirschner, 1984). The assembly and dynamics are further regulated by other components, including microtubule-assembly-promoting factors, microtubule stabilizing factors (such as structural or classical microtubule-associated proteins (MAPs)), microtubule destabilizing factors, microtubule severing proteins, post-translational modifications such as acetylation and microtubule-based motors of the kinesin and dynein superfamilies (Conde & Cáceres, 2009). Alterations related with

the stability of MTs have been described in neurodegenerative diseases such ALS, Alzheimer and peripheral neuropathies (Almeida-Souza et al.,2011).

The process of axonal transport depends on the integrity of the MT within the neuron, as serve as the conduits upon which cellular constituents are shuttled in both the anterograde by kinesins (towards the axonal terminus) and retrograde by dyneins (towards the neuronal soma) (Brunden, et al., 2017). Therefore, motor complexes are essential for the proper trafficking and MN survival. MNs are enriched by the family of kinesin-1 (KIF5A and KIF5C) and its genetic ablation or mutation are linked with MN diseases (Hirokawa et al., 2008; De Vos & Hafezparast, 2017). Alterations in the complex dynein/dynactin has been reported to cause MN degeneration (De Vos & Hafezparast, 2017).

The cytoskeleton ensures the active transport of proteins, vesicles and organelles along the axonal shaft besides promoting the forward movement of the axon tip. After RA, MNs undergo cytoskeletal rearrangements (Penas et al., 2009; Casas et al., 2015). These alterations in cytoskeleton may affect the transport and promote MN degeneration (Casas et al., 2015). Furthermore, it is described a dramatic reduction of the tubulin acetylation in degenerate MNs, which is considered an important regulator of microtubule dynamics (Almeida-Souza et al., 2011)(Casas et al., 2015). Actin and MT disturbances are described in different neurodegenerative diseases (Voelzmann et al.,2016). The axonopathy present in AD and ALS is characterized by a "dying back" phenomena and by the MTs loss (Baas et al., 2016). Mutations in the interaction sites of tubulin are present in mouse models characterized by the degeneration of motor axons (Piermarini et al., 2016). The MT stabilization has been proven to block neuronal death. In contrast, modulation of MT stability has been successful to accelerate axonal growth in the CNS after the injury (Ruschel et al., 2015).

Thus, the reduction in axonal transport observed in many neurodegenerative diseases and after injury could results from alterations in MT structure and/or molecular motors required for axonal transport. Proper axonal transport is critical to the normal functioning of neurons, and impairments in this process contribute to the neuronal damage and death. Therefore, the modulation of MT after the injury could be a key role to face up the insult and for axonal regeneration.

4.3 Secretory pathway and protein trafficking

The secretory pathway is where synthesis and delivery of soluble proteins. Most of the cellular transmembrane proteins (except those of the mitochondria) use this pathway to reach their destination. The pathway comprises the rough endoplasmic reticulum (rough ER), ER exit sites (ERES), the ER-to-Golgi intermediate compartment (ERGIC), the Golgi complex and post-Golgi carriers in route to their final destination. The organelles have a precise regulation in order to provide a proper environment for protein folding and post-translational modifications(Mellman & Warren, 2000). The exit of newly synthesised proteins from the ER depends on these proteins being properly folded, but also on the ability of the export machinery to incorporate them into carriers that are coated into the membrane-coating coat protein II (COPII) and that leave the ER (Jackson & Hauri, 2009). Assembly of the COP-II coat is initiated at ERES by the guanosine triphophatase (GTPase) Sar1 that couples membrane curvature with the recruitment of the inner COPII coat (Sec23) to capture cargo into the vesicle. The coat adaptor recruits the outer shell Sec31, which leads to membrane deformation and vesicle budding (Lord et al., 2013). Deficiency and/or loss of protein activity due to mutations in genes encoding coat complex proteins are implicated in a number of autosomal recessive human diseases.

The Golgi comprises of three functional compartments: the cis-Golgi, which being the nearest compartment to ER, forms to the entry face to the Golgi, the medial-golgi which is responsible for the modification, sorting and packing of proteins for transportation, and finally the trans Golgi network, which forms the exit face of the Golgi. Specific types of intracellular vesicles are associated with the Golgi. Here an extensive machinery of glycosylation enzymes completes N-linked glycosylation and initiates and extends O-linked oligosaccharides. In addition to glycosylation, the Golgi apparatus is also a major site of protein sulfation and phosphorylation (Puertollano et al., 2003).

Both, late-endosomes and lysosomes are highly enriched in distinctive, highly glycosylated and conserved proteins, LMP, that reach their destination directly from the Trans-Golgi network or from the endocytic pathway. The majority of newly

synthesized lysosomal hydrolases to lysosomes is mediated by mannose 6-phosphate receptors (M6PRs). Early in the Golgi, select mannose residues on oligosaccharide chains of lysosomal enzymes are modified with phosphate groups to form mannose 6-phosphate. Upon arrival to the trans-Golgi network (TGN), lysosomal hydrolases encounter two distinct classes of M6PRs, cation-independent (CI-M6PRs) and cation-dependent (CD-M6PRs), both mediating the exit of lysosomal enzymes in clathrin–coated vesicles (Kornfeld and Mellman, 1989). The bound hydrolases are released from the receptors in the endosomes as a result of acidic luminal pH, allowing the receptors to cycle back to the TGN (Seaman, 2004). Unlike soluble hydrolases, newly synthesized lysosomal membrane proteins (LMPs) are delivered from the TGN without the requirement for M6PR binding. Sorting of these proteins is accomplished by adaptor and clathrin coat complexes that bind with high specificity to sorting signals present within the cytosolic domains of transmembrane cargo. Transport of LMPs can occur through direct intracellular pathway or indirect route involving passage via the plasma membrane and subsequent endocytosis. All these processes are dependent of cytoskeleton integrity and if this structure was impaired, the secretory pathway was affected.

4.4 Unfolded protein response

The endoplasmic reticulum (ER) is a major site of protein synthesis and transport, protein folding and calcium storage. ER is the site of folding most of proteins by a complex family of chaperones, cofactors and enzymes that mediate different post-translational modifications. All proteins that transit the secretory pathway first enter the ER where they fold and assemble into multi-subunit complexes prior to transit to the Golgi compartment. Misfolded proteins are either retained within the ER lumen in complex with molecular chaperones or are direct toward degradation through the 26s proteasome in a process called ER-associated degradation (ERAD) or through autophagy (Malhotra et al., 2007).

Accumulation of unfolded protein initiates activation of an adaptative signalling cascade known as the unfolded protein response (UPR). Three main type-I transmembrane proteins initiate the UPR: inositol-requiring protein 1α (IRE1α; a β isoform is selectively expressed in the lung and intestine), activating transcription factor-6 (ATF6, α and β), and protein kinase RNA-like ER kinase (PERK). In non-

stressed cells, the luminal domains of these three proteins are bound to the protein chaperone GRP78/BiP and they are maintained in an inactive state. Sufficiently high levels of expression of any protein that binds GRP78/BiP can activate UPR (Ng et al., 1992) **(Fig 2).**

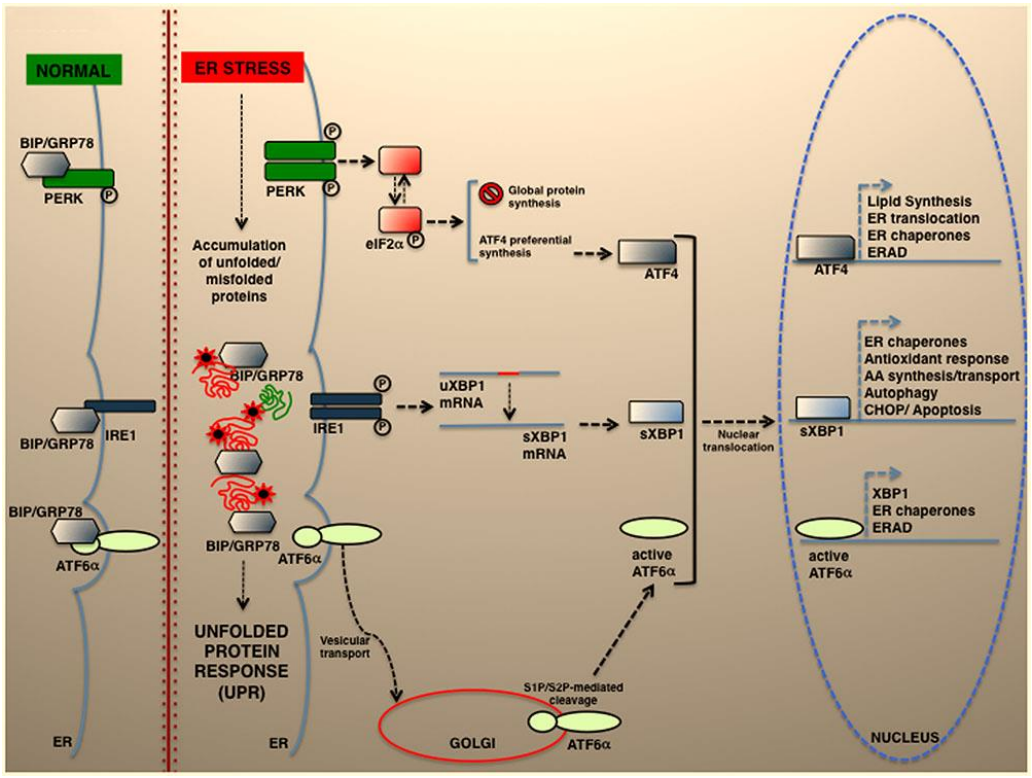

Fig 2. UPR signalling pathways. UPR is controlled by three transducers: IRE1, ATF6α, and PERK. Upon ER stress, BIP/GRP78 dissociates and enables UPR activation. ATF6 is transported from the ER to the Golgi, where it undergoes proteolytic cleavage by S1P/S2P proteases. These is translocated into the nucleus where it acts as a transcription factor of genes required for ERAD and modulates XBP1 transcription. ER stress also activates PERK, which phosphorylates eIF2α to attenuate protein translation. In parallel, preferential ATF4 translation drives the expression of ER chaperones and other genes controlling autophagy, redox control and nutrient metabolism. Under severe ER stress, the PERK–ATF4 pathway controls the proapoptotic genes, including CHOP, which leads to programmed cell death. Once activated, IRE1 operates the alternative splicing of XBP1. The active XBP1(s) up-regulates, among others, genes encoding for ER chaperones, ERAD components and proteins involved in the lipid biosynthesis pathways. (Remondelli & Renna, 2017)

The most immediate response to ER stress is the attenuation of mRNA translation to preventing influx of newly synthesized into the ER lumen mediated by PERK. Upon BiP unbounds, PERK it autophosphorylates, homodimerizes and transphosphorylates itself (p-PERK) to become active (Harding et al., 2000). PERK

activates and phosphorylates elF2α to inhibits general translational initiation. Several stress-response mRNA are translate by elF2α, the most important is the transcription factor 4 (ATF4)(Scheuner et al., 2001). Upon ER stress, PERK phosphorylates Nuclear respiratory factor 2 (NRF2) to promote the nuclear entry and the activation of the transcription of detoxifying enzymes by the binding to the antioxidant response element (ARE)(Cullinan et al., 2003).

The second branch is mediated by IRE1α. Upon UPR response, IRE1 is released from BiP and undergoes homodimerization and trans-autophosphorylation to activates its RNAse activity(Cox & Walter, 1996). IRE RNase activity initiates removal of an intron of a X-box binding protein (XBP1). This spliced XBP1 is a transcriptional activator that plays a fundamental role of a wide variety of UPR target genes involved in ERAD response, chaperones and lipid synthesis (Hiderou Yoshida et al., 2003).

ATF6 was identified as another regulator protein like XBP1, binds to the ERSE1 element in the promoters of UPR-responsive genes (Yoshida et al., 1998). In response to ER stress, BiP dissociation permits trafficking of ATF6 to the Golgi complex, where is cleaved by two proteases: S1P and S2P(Ye et al., 2000). The processed forms of ATF6 translocate to the nucleus and bind to CRE and ERSE-1 to activate target genes such as BiP, GRP74 and XBP1, enhancing the ability of the cell to correctly fold proteins (Yoshida et al., 2001).

Accumulating evidence indicates that endoplasmic reticulum (ER) proteostasis is altered after injury in both PNS and CNS, generating a protein folding stress reaction in neurons and glial cells(Penas et al., 2011; Li et al., 2013;Oñate et al., 2016). Several lines of evidence support the contribution of UPR branches to axonal injury induced events. For example. Activation of XBP1 enhances motor recovery after spinal cord injury and injury-induced by CHOP, a downstream of PERK, results in the induction of apoptosis and tissue damage after optic nerve injury(Li et al., 2013;Ohtake et al., 2018). After RA, XBP1 and ATF4 proteins are still present but misfolded proteins are not detected in the axonal ER after injury (Penas et al., 2011;Hu, 2016). Interestingly, UPR modulation has positive effects and increases the axonal regeneration when it is activated partially(Oñate et al., 2016; Valenzuela, Oñate, & Court, 2016).

Several physiological and pathological conditions that alter the function of the secretory pathway results in ER stress: this perturbation activates the UPR, which controls the stability of RNAs and the rate of protein synthesis, and activates the transcription of several genes involved in protein folding, ERAD, vesicular trafficking, autophagy, ER redox control and lipid synthesis (Hetz & Saxena, 2017).

The function of the ER and the secretory pathway are key elements of the proteostasis network that are altered in neurodegenerative diseases and nerve injury. Nowadays, it is not clear how activation of UPR response elements is globally coordinated leading to a delicate balance between adaptive and pro-apoptotic responses.

4.4.1 78-kDa glucose-regulated protein (GRP78/BiP)

GRP78/BiP is encoded by the gene Hsp5a. It is the most abundant protein within the hat shock protein-70 (Hsp70) family but it is not induced by heat shock because the promoter lacks the heat shock element.

GRP78/BiP it is traditionally regarded as a major ER chaperone but recently is described the multiple functions in maintaining cell viability. BiP appears to orchestrate several of the beneficial mechanisms that are activated under circumstances of damage or intrinsic pro-survival pathways (Casas, 2017).

Its expression is highly regulated at different time points by transcription factors that binds to the promoter and the post-transcriptional regulation of GRP78/BiP mediated by the activation of internal ribosome entry sequence (Macejak et al., 1991). Another post-transcriptional regulatory mechanism is mediated by PI3K/AKT that stabilizes the protein by unknown mechanisms(Dai et al., 2010).

GRP78/BiP acts as a molecular chaperon is mainly found in ER lumen but it is redistributed to the cytosol, nucleus, mitochondria, the plasma membrane or is secreted **(Fig 3)**. This localization determines it function that trigger different molecular signalling events (Suzuki et al., 1991).

At the ER, GRP78/BiP has diverse functions and relies on several interaction partners and co-chaperones, nucleotide exchange factors, and signal transducers. The diversity of functions includes the translocation of nascent polypeptides, in

protein folding and assembly, ERAD machinery and the maintenance of calcium homeostasis.

ERAD in combination with the ubiquitin-proteasome system (UPS) are responsible for the quality control in neurons. When the ERAD system is saturated under stress conditions, macroautophagy removes unfolded proteins and dysfunctional organelles. GRP78/BiP acts at several stages of macroautophagy. It is described that AMPK is stimulated by GRP78/BiP overexpression. In addition, GRP78/BiP also interacts at late stages of autophagy flux since GRP78/BiP interacts with p62 and misfolded proteins. This binding provoke the conformational change of p62 that facilitates the entrance of the cargo in the autophagosomes for its subsequent degradation (Molstad et al., 2015;Malek et al., 2015). Recently, Lee and collaborators demonstrated that cytosolic form of GRP78/BiP interacts with PARK7 and p62 to modulate autophagic removal of misfolded protein cargoes(Lee et al., 2018).

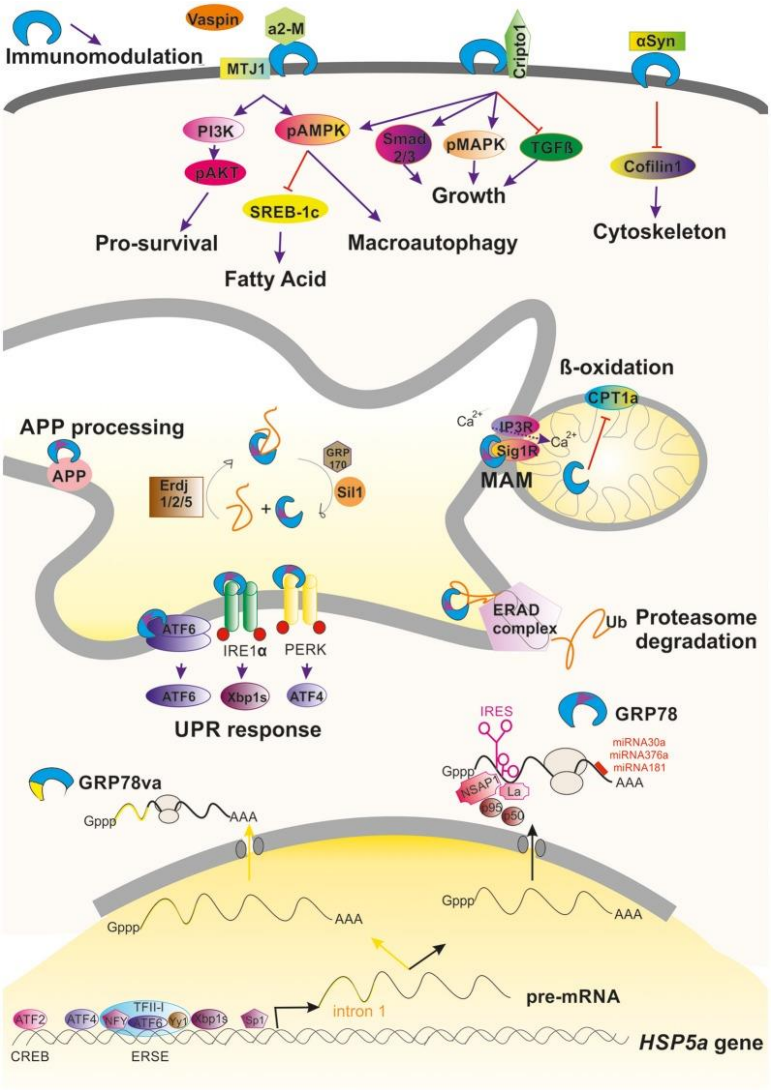

Fig 3. Graphical summary of the regulation and activities promoted by GRP78 within a cell.(Casas, 2017)

GRP78/BiP has also been observed in mitochondria in association with co-chaperones known to be involved in calcium-mediated signalling between ER and mitochondria that is important for bioenergetics and cell survival. Some studies showed that GRP78/BiP is mainly located in the intermembrane space, inner membrane and mitochondria matrix (Sun et al., 2006). GRP78/BiP plays an important role in the control of efflux of calcium ions from the ER. In addition, upon calcium deletion from the ER via IP3R, the calcium-sensitive co-chaperone sigma receptor 1 (SIG1R) dissociated from GRP78/BiP and associates with IP3R, thereby protecting the otherwise unstable IP3R from ERAD and prolonging calcium signalling to the mitochondria (Hayashi & Su, 2007). Finally, BiP has also found in cytosol and the plasma membrane where plays a protective role.

Age-related diseases are commonly related with the accumulation of misfolded proteins and mitochondrial dysfunction, particularly at the mitochondria-associated ER membrane (MAM). Neurodegenerative disorders, such as AD, PD and ALS have common events that also occurs in brain ischaemia or trauma. In AD has been shown that GRP78/BiP protect cells from Aβ toxicity but induced tau hyperphosphorylation via activating glycogen synthase kinase-3β (GSK-3β)(Yerbury et al., 2010)(Z.-C. Liu et al., 2016). In animal and culture models of PD, has been demonstrated that GRP78/BiP translocate from the ER to the nucleus and cytosol (Casas, 2017). Furthemore, GRP78/BiP was found to be neuroprotective, through a mechanism that involves decreases in the levels of UPR target genes, preventing the loss of dopaminergic neurons and dopamine in the SNc (Ni et al., 2011). Genetic inactivation of GRP78/BiP itself results in spontaneous degeneration and motor alterations during ageing in association with aggregation of wild-type SOD1 in mice (Jin et al., 2014).

After trauma, it has been demonstrated that GRP78/BiP plays an important role. After avulsion of the nerve root, GRP78/BiP is downregulated in neurodegenerative motoneurons but it has been found overexpressed in the regenerative conditions such as axotomy (Penas et al., 2009). Indeed, forced expression of BiP or pharmacological activation of its co-chaperone Sig-R1 in a root avulsion model leads to neuroprotection (Guzmán-Lenis et al., 2009; Penas et al., 2011a,b). These observations suggested that GRP78/BiP plays a relevant role activating endogenous neuroprotection.

4.5 Mitochondria related-events

Mitochondria play a critical role in the generation of metabolic energy in eukaryotic cells. They provide essential energy and metabolites, and maintain calcium balance, which is imperative for proper neuronal function. Mitochondria are divided in four main compartments: the outer mitochondrial membrane (OMM), the inner mitochondrial membrane (IMM), the intermembrane space (IMS), and the matrix, located in the interior.

Their main function is energy production through the tricarboxylic acid cycle (TCA) and oxidative phosphorylation (OXPHOS) via the mitochondrial electron

transport chain (ETC). The inevitable products of OXPHOS are the reactive oxygen species (ROS) where physiological levels are related with differentiation, autophagy and immune response(Sena & Chandel, 2012). Supra-physiological ROS levels are harmful to proteins that cause damage in cellular lipids, proteins and DNA. These alterations have been linked to multiple pathologies, including neurodegenerative diseases, spinal cord injury (SCI) and traumatic brain injury. Most mitochondrial proteins are encoded in the nucleus and imported into the mitochondria that requires the mitochondrial membrane potential (ΔΨm)(Zorova et al., 2018). For import, mitochondrial proteins first use translocases of the outer membrane (TOMs). Some proteins are inserted into the outer membrane and either transported to the matrix and processes there or inserted into the inner membrane using TIM translocases, ΔΨm, and ATP, and finally the export of the processes inner membrane protein from matrix to inner membrane(Zorova et al., 2018)

Mitochondria are not static organelles. They can change shape, size, number, or localization inside the cell and have the ability to fuse into each other or divide by fission to adapt to changes. Mitochondrial fusion utilizes three dynamin-related GTPases: the Mitofusins 1and 2 (Mfn1/Mfn2) that control outer membrane fusion and optic atrophy (OPA1) that controls inner membrane fusion (Song et al., 2007) . In contrast, mitochondrial fission is controlled by dynamin related protein 1 (Drp1) that form a ring around the mitochondria and causes their division, after being recruited by primary mitochondrial fission 1 (FIS1) and mitochondrial fission factor (MFF)(Toyama et al., 2016). The fission of mitochondria permits the isolation of damaged mitochondrial components for their removal (Suárez-Rivero et al., 2016) .

Mitochondria are transported around the cell by cytoskeleton, motor proteins and appropriate adaptors. In neurons are primarily trafficked on microtubules with the adaptors of Miro and Milton/TRAK proteins(Devine et al.,2016). Mitochondria often localize close to ER forming mitochondria-associated ER membranes or MAMs. These membrane microdomains are reversible tethers that co-regulate and influence a variety of cellular processes, i.e., synthesis/transport of lipids, Ca2+dynamics/signalling, autophagy, mitochondrial shape and size, apoptosis and energy metabolism (Annunziata et al., 2018).

It is important to point out the contribution of mitochondria as core regulators of neuronal survival through their involvement in pathways that facilitate cell death A variety of internal or external triggers are capable to trigger signalling cascades that converge at the mitochondria and then re-diverge into one or more cell death pathways (Galluzzi et al., 2018). The most known pathway is the intrinsic apoptosis pathway but mitochondria are also associated with some non-apoptotic forms of cell death: necroptosis and parthanatos (Princz et al., 2018).

Mitochondrial dysfunction arises from an inadequate number of mitochondria, an inability to provide necessary substrates to mitochondria, or a dysfunction in their electron transport and ATP-synthesis machinery. The high levels of ROS and the related reactive species (RNS) can be neutralize by dismutase enzymes and antioxidants(Nicolson, 2014). Alterations in these enzymes have been observed in some neurodegenerative diseases such as ALS, PD and HD but also after traumatic brain injury (Schon et al., 2003). Furthermore, impaired function of certain mitochondrial respiratory complexes has long been linked to the pathogenesis of chronic neurodegenerative disorders such as PD an HD. In HD, deficiency in complex II of electron transport chain and the repression of PGC-1α, involved in mitochondrial biogenesis are reported. In a model of PD, has been also observed a selectively and irreversibly impairs the function of mitochondrial complex I in dopaminergic neurons (Szalárdy et al., 2015).

Perturbations in mitochondrial number and function severely impair cellular homeostasis and trigger the onset of disease. Therefore, cells maintain a dynamic balance between the opposing processes of mitochondrial biogenesis and clearance. Therefore, the accumulation of dysfunctional mitochondria and/or the loss of mitochondrial biogenesis process could be producing the cell death of the cell.

4.6 Motor axon elongation

The reaction after PNI is characterized by an axonal reaction in injured neurons that changes the molecular pattern. The neuronal reactivation after injury starts with the activation of pro-regenerative machinery, which requires profound changes in transcription and translation in the cell body. Several factors determine the recovery of function after PNI: the time-response of pro-regenerative

machinery, neurite elongation, the distance to target and the rebuilding of synapse (Mahar & Cavalli, 2018) MNs of the spinal cord, .

The axis PI3K/AKT and ERK/MAPK are the most studied pathway and have shown to play a role in outgrowth after injury. When inhibitors of both pathways were applied to the axon, axon elongation was abolished. Neurotrophic factors are growth factors that can promote the survival and regeneration of the neurons, specifically nerve growth factor (NGF) plays a pivotal role in regeneration by the activation PI3K/AKT. This axis regulates local protein synthesis in the axon through the mTOR pathway, where adult CNS require this signalling for axon regeneration (Z. Huang et al., 2017). Deletion or inhibition of phosphatase and tensin homolog (PTEN), negative regulator of mTOR, enhances axon regeneration after nervous system injury. Although there are no studies performed in adult MNs, mTOR kinase activity has been linked with axonal growth in sensory neurons (Fischer & Leibinger, 2012).

The phosphorylation of Akt in Ser 473 is highly correlated with mTOR activation and therefore with axonal re-growth. At the same time mTOR can phosphorylate AKT in the same residue, forming a positive loop (Rahman & Haugh, 2017). The direct effector of mTOR. The effector of mTOR, p70s6K has been correlated with the increase of cell growth and protein synthesis, necessary for the regeneration of neurons after PNI (Yang et al., 2014). In contrast, acute inhibition of mTOR signalling by rapamycin results in the activation of autophagy and promotes nerve regeneration(Huang et al., 2016). Thus, indicate that the regulation of mTOR in a time-dependent manner after the lesion could be a promise therapeutic strategy to promote the axonal regeneration.

Another post translational modification that regulate Akt activity is reversible acetylation. SIRT1 can deacetylate and thus activate AKT and promotes axonogenesis (Li et al., 2013). After injury, several growth-associated proteins including GAP-43 and cytoskeletal components and pro-growth transcriptional factors, such as ATF3, HIF-1α, c-jun and STAT3 are up-regulated (Venkatesh & Blackmore, 2017). SIRT1 can stabilizes HIF-1α via deacetylation (Joo et al., 2015) and has been found that HIF-1-α enhances axon regeneration and accelerates

neuromuscular junction re-innervation(Cho et al., 2015). Therefore, the up-regulation of pro-regenerative machinery could be the best target to promote the functional recovery after the injury.

Identifying key signalling networks associated with axon regeneration allows us to experimentally manipulate these pathways, unveiling potential therapies for regeneration

5. Autophagy

The term autophagy ("self-eating" from Greek) describes lysosome-dependent degradative routes of eukaryotic cells, during which cytosolic material is delivered to the endo-lysosomal system for subsequent degradation. Its three major forms involve different mechanisms, which are responsible for the sequestration of different cargo. Chaperone-mediated autophagy (CMA) is a selective delivery pathway accomplished by lysosomal-associated membrane protein 2A (LAMP2A) (Cuervo & Dice, 1996) and chaperon complexes while cytoplasmic constituents are directly engulfed by the invaginations of lysosomes during microautophagy. (Mijaljica et al., 2011).The process of macroautophagy (popularly called autophagy) involves the formation of double-membrane autophagosomes to sequester cytosolic cargo either in a selective or in a non-selective way. Matured autophagosomes undergo fusion with late endosomes or lysosomes, and their degraded content is recycled(Glick et al., 2010).

5.1 Macroautophagy

In macroautophagy, the cytoplasmic content is enveloped into a double-membraned vesicle called autophagosome, trough non-specific encircling of the bulk cytoplasm. Precise regulation is required to facilitate selective engulfment and degradation when needed, in addition to preventing undesired removal of cytoplasmic contents. This process at its optimal level ensures cell homeostasis, while its deregulation compromises cell survival and it has been reported in many diseases such as neurodegenerative disorders. This dysregulation its produced at several levels in each disease (Wong et al., 2011). Macroautophagy involves a battery of proteins to initiate autophagosome formation, nucleation, elongation,

maturation, and degradation of autophagosomes. Macroautophagy regulators are also modified post-translationally that provides an additional level of control over macroautophagy.

The phagophore formation are control by two activating pathways and the source of membrane is controversial, since several studies have been suggested that it origins provides from Endoplasmic reticulum, mitochondria, Golgi Apparatus or plasma membrane (Mari et al., 2011). The most characterized trigger for induction of autophagy is deprivation of amino acids, which results in inhibition of the master cell growth regulator serine/threonine kinase mTOR. mTOR is found in two distinct protein complexes, mTORC1 and mTORC2, but only mTORC1 directly regulates autophagy(Dikic & Elazar, 2018). When mTOR is inhibited, ULK1 complex is activated and therefore starts the autophagy process. The adenosine monophosphate-activated protein kinase (AMPK) can be activated leading to mTOR inhibition and ULK1 complex activation. This pathway is known as a mTOR dependent. (Arbogast & Gros, 2018). Currently, it has been described several proteins that inhibits mTOR such as SIRT1(**See 5.1.2**) The other pathway involved in these phagophore formation are mediated by phosphatidylinositol-3-phosphate (PInst3p) by Beclin1-BECN1/Vsp34 complex, exerting a class III phosphatidylinositol 3 kinase (PIK3CIII) activity. ULK1 complex can activate Beclin1/Vsp34 complex after its recruitment to the initiation site (Arbogast & Gros, 2018). . This pathway is known as a mTOR dependent.

The elongation of membranes that evolve into autophagosomes is regulated by two ubiquitination-like reactions. First, the ubiquitin-like molecule Atg12 is conjugated to Atg5 by Atg7 and Atg10. The Atg5–Atg12 complex then interacts non-covalently with Atg16L1 This complex recognizes the site of elongation due to the interaction of WIPI and the complex Beclin1/Vsp34. ATG12-ATG5-ATG16L and ATG3 mediates the lipidation of Microtubule-associated protein 1 light chain 3 (MAP-LC3/Atg8/LC3) **(Fig 4)** Other members of LC3 family, such as GABARAP proteins can also associate with autophagosome membranes(Arbogast & Gros, 2018; Rubinsztein et al., 2012).

Subsequent to elongation step, autophagosomes are fused with lysosome for degradation of their contents, a process known as autophagosome maturation. Autophagosomes fuse with several types of vesicles from the endosomal/lysosomal pathways including endosomes and lysosomes. Autophagosome degradation require the action of late endosome marker protein Rab7 and lysosomal membrane protein. This fusion requires a microtubule-based transport machinery that involved dyneins, dynactin and kinesins to transport autophagosomes next to lysosomes (Reggiori & Ungermann, 2017).

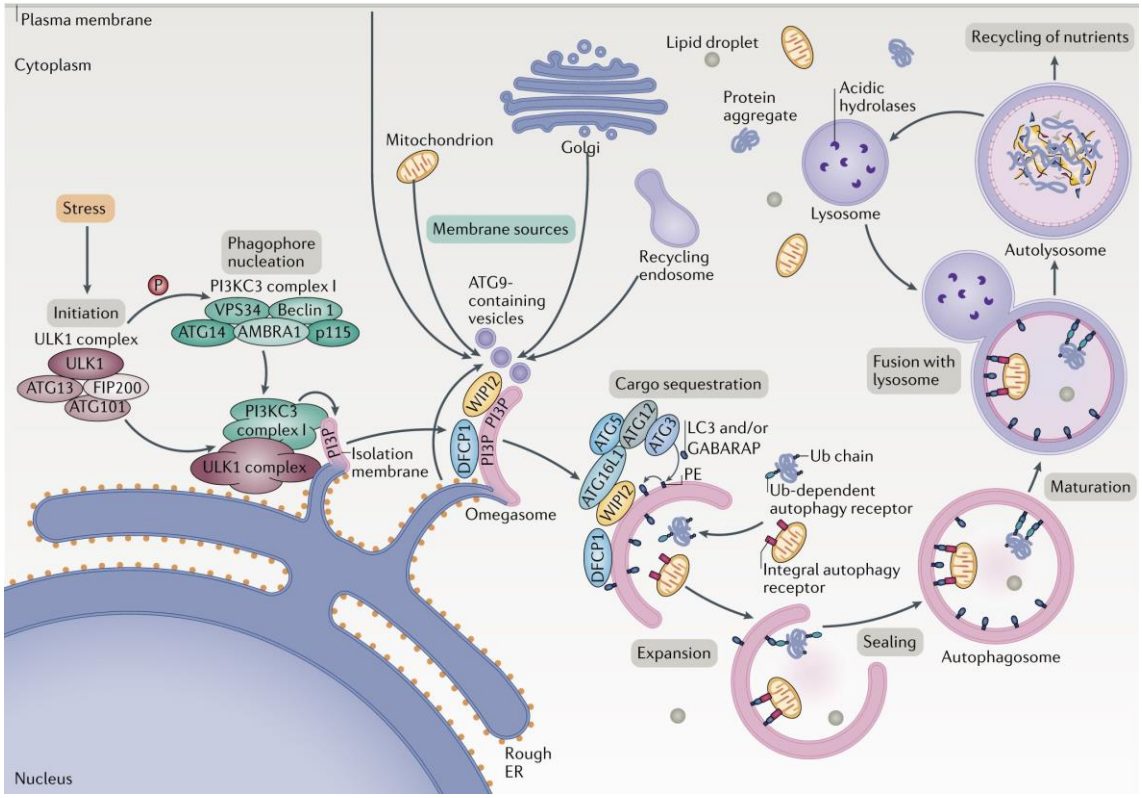

Fig 4. **Overview of the autophagy process.** ULK1 complex triggers nucleation of phagophore by the phosphorylation of components of the class III (PI3KC3) complex I which activates PI3P production at omegasome. PI3P recruits WIPI2 and binds to ATG16L1 directly, thus recruiting ATG12-ATG5-ATG16L complex that conjugates PE to LC3. Sealing of the autophagosomal membrane gives rise to a double-layered vesicle called the autophagosome, which matures and finally fuses with the lysosome (Dikic & Elazar, 2018)

Lysosomes break down macromolecules into their constituent parts, which are then recycled. These membrane-bound organelles contain two classes of proteins: soluble lysosomal hydrolases and integral membrane proteins (LMPs.) The lysosomal hydrolases can digest proteins, nucleic acids, lipids, and complex sugars.

The lumen of a lysosome is more acidic than the cytoplasm and therefore activates the hydrolases in a pH-dependent manner and confines their destructive work to the lysosome. LMPs reside mainly in the lysosomal limiting membrane and have diverse functions, including acidification of the lysosomal lumen, protein import from the cytosol, membrane fusion and transport of degradation products to the cytosol(Eskelinen et al., 2003). Newly synthesized lysosomal proteins can be direct, from the TGN to the endosomal system (**see 4.3**). Damage or genetic alterations in this organelle often results in lysosomal membrane permeabilization (LMP) and the release into the cytoplasm of the lysosomal content that has been observed in several diseases and cancer.

Neuronal survival requires the continuous recycling of cellular materials released by the machineries of autophagy and endocytosis to maintain homeostasis. Impaired or dysfunctional autophagy in neurons is associated with neurodegeneration, while its activation can have a therapeutic benefit. Lysosomes are abundant in the perinuclear region where fusion take place (Roberts & Gorenstein, 1987). In contrast, autophagosomes can be formed anywhere there are intracellular components to be eliminated. This process requires the retrograde transport of autophagosomes to the soma and this dependence upon axonal transport makes it dependent for its function.

Alterations of proteins related to the initial phases of autophagy and in p62 have been observed in ALS. Rapamycin, inductor of autophagy via mTORC1, exerts neuroprotection in cerebral ischemia, TBI and AD (Menzies et al., 2015)

After RA there are some changes in autophagy markers that could be related with alterations in autophagy flux and therefore the degeneration of MNs(Penas et al., 2011)(Casas et al., 2015). In TBI, autophagy is initiated but the autophagosomes are not cleared. This is caused by the lysosomal dysfunctions and therefore impedes autophagy resolution, what causes the neuronal death (Sarkar et al., 2014) Similar observations have been observed in human brains of AD (Boland et al., 2008). In a model of SCI, autophagy induction prevents the retraction of axons and enhances their regrowth, thus promoting the recovery of motor function. These effects were mediated by the degradation of a MT-destabilizing component, which turns on a better intraneuronal axonal transport (He et al., 2016).

These cell protective mechanism, also it has been reported as one type of cell death called autophagic cell death (Kroemer & Levine, 2008). In some diseases it has been described that he blockage of these pathway promotes an improvement of the pathology. The inhibition of autophagy after ischemia promoted neuron survival in adult and neonatal mice whereas autophagy flux blockage after spinal cord injury promotes functional recovery and avoids apoptotic cell death(Suzuki et al., 2008; Zhou et al., 2017)

It is important to emphasize that depending on the moment or stage of autophagy affected, the impact on pathological outcomes will differ. These may occur in the form of a lack of autophagic flux, accumulation of autophagolysosomes, accumulation of empty autophagosomes and lysosomal depletion, among others (Wong et al., 2011). Therefore, the elucidation of the origin of dysfunctional autophagic processes may help in the design of new therapeutic approaches based on autophagy modulation to ultimately attenuate or prevent neurodegeneration.

5.1.1 Autophagy related 5 (ATG5)

ATG5 and ATG7 are considered to be essential molecules for the induction of autophagy. Atg7 is required for the conjugation of Atg12 to Atg5 and the complex Atg5-Atg16L1-Atg12 facilitates autophagosome formation. Following the nucleation step, other Atg proteins are recruited to the membrane of the pre-autophagosomes to promote elongation and expansion. During the elongation and expansion steps, Atg7 and Atg10 promotes the interaction of Atg5-Atg12 which also interacts with Atg16L. This complex mediates the conjugation of PE to the microtubule associated protein 1 light chain (LC3-I) to form LC3-II leading to the translocation of LC3 from cytoplasm to the membrane of the autophagosomes. However, mouse cells lacking ATG5 or ATG7 can still form autophagosomes/autolysosomes and perform autophagy-mediated protein degradation when subjected to certain stressor in several embryonic tissues(Nishida et al., 2009).

Autophagy is critical for neuronal homeostasis and survival. Neural-specific depletion of genes required for autophagy such as ATG5 and ATG7 is sufficient to cause axon degeneration and neuron death in mice (Komatsu et al., 2007;

Nishiyama et al., 2007). Furthermore, ATG5 KO animals have a significant reduction in survival, as a delay in neuronal maturation (Xi et al., 2016).

In contrast, ATG5 overexpression increases lifespan and the resistance to the oxidative stress and (Pyo et al., 2013). Furthermore, neuroprotective effects has been observed in a model of PD after the up-regulation of ATG5 (Hu et al., 2017).

Moreover, ATG5 has been linked in apoptosis. It was shown that FADD can interact with ATG5, activating the caspases and promoting cell death (Pyo et al., 2005). This implication indicates that ATG5 can regulate components of the extrinsic apoptosis pathway. Another mechanism by which ATG5 can control apoptosis has been described. The cleavage of ATG5 by calpain create a truncated form of the protein that translocate to the mitochondria and promoting the release of cytochrome c and therefore, the activation of intrinsic apoptosis pathway (Yousefi et al., 2006). ATG5 represents another molecular link between autophagy and apoptosis.

5.1.2 Sirtuin 1 (SIRT1)

The Sirtuin family of class III histone deacetylases (SIRTs) has been extensively implicated in modulating multitudinous of cellular processes, including energy metabolism, stress response, cell/tissue survival and malignancy. There are seven SIRTs in mammals with varied subcellular localization and enzymatic activity influencing their in vivo substrates and cellular functions (Frye, 1999;Frye, 2000).

SIRT1/Sir2 was initially described as a nuclear protein that may also shuttle to the cytoplasm or mitochondria (Stünkel et al., 2007;Tang, 2016).Is a nicotinamide adenosine dinucleotide (NAD)-dependent deacetylase and removes acetyl groups from many histone and nonhistone proteins (Rahman et al., 2011). The list of SIRT1 substrates includes several transcription factors: p53, members of the FoxO family (forkhead box factors regulated by insulin/Akt),PPARγ (peroxisome proliferator-activated receptor gamma), p300, PGC-1α (PPARγ coactivator), and NF-κB (nuclear factor kappa B) and hypoxia-inducible factor-1α (HIF1α) among others(Joo et al., 2015;Rahman et al., 2011). Therefore, SIRT1 orchestrates several functions at neuron related with pro-survival mechanisms such as autophagy, mitochondrial activity and apoptosis.

Regulation of autophagy further involves post-translational modifications such as phosphorylation and acetylation. Acetylation of several ATG proteins including ATG5, ATG7, LC3 and ATG12 are inversely correlated with the cellular level of macroautophagy (Lee et al., 2008). Knockdown of acetyltransferase p300 reduces acetylation of Atg5, Atg7, LC3 and Atg12 and enhances macroautophagy, while overexpression of p300 inhibits macroautophagy(Lee et al, 2009). In tissues from SIRT1 KO, basal acetylation of autophagy component is increased. Furthermore, acetylation of ATG5. Furthermore, acetylation of Atg5 is markedly elevated in mice lacking deacetylase Sirtuin-1, which exhibit macroautophagy-deficit phenotypes. This phenotype is similar to ATG5 lacking mice (Lee et al., 2008).

SIRT1 can also induce autophagy by mediating the deacetylation of FoxO1. Specifically, SIRT1 can induce an increase in autophagic flux and upregulate the expression of Rab7, a small GTP-binding protein that mediates late autophagosome–lysosome fusion(Füllgrabe et al., 2013).

Other regulators of autophagy has been reported to associate with SIRT1 such as Histone 4, FoxO3, NK-KB, p53, HIF1 and TSC2, p70S6K(Qiu et al., 2015).

This autophagy activation mediated by SIRT1 exerts a positive neurite-growth effect via mTOR inactivation in primary cell cultures. Correspondingly, Rapamycin enhanced neurite outgrowth(Garza-Lombó et al., 2016). Furthermore, the cytosolic form of SIRT1 has also been described during neuronal differentiation and neurite outgrowth(Hisahara et al., 2008). SIRT1 has also been shown to promote axon development in embryonic hippocampal neurons via AKT and enhancing axonogenesis in cultures hippocampal neurons(Codocedo et al., 2012). Specifically, cytosolic presence of SIRT1 has been related to neurite elongation(Sugino et al., 2010). Therefore, activation of autophagy mediated by SIRT1 could be a promising target for nerve regeneration.

5.2 Selective autophagy

Over the past 20 years, the concept of mammalian autophagy as a nonselective degradation system has been repudiated, due in part to important discoveries in neurodegenerative diseases, which opened the field of selective autophagy.

Microautophagy, macroautophagy and CMA can operate in a specific manner, through a mechanism that involves the recognition of autophagy substrates by dedicated receptors(Farré & Subramani, 2016). It is defined instances of micro- and macroautophagy of a precise autophagy substrate, coupled to requirement of specific molecular factors which may be used to selectively monitor or experimentally manipulate the process(Galluzzi et al., 2017).

This selectivity in the cargo recognition results in a several new types of autophagy. Some of them include the selective degradation of mitochondria (mitophagy), peroxisomes (pexophagy), ER portions (ER-phagy), ribosomes (ribophagy), lipid droplets (lipophagy), intracellular pathogens (xenophagy) or ubiquitinated-aggregates (aggrephagy)(Martinez-Vicente, 2017).

Although all these types of selective macroautophagy degradations might be activated by different signals, they all require autophagy receptors to act as adaptor between the substrate and the autophagosome. Most of these adaptors contain the LIR (LC3 interacting region) and a ubiquitin-binding domain that recognizes the substrate with ubiquitinated chains(Wild et al., 2014)

Other specific forms of autophagy have been described, mostly based on cargo selectivity. These include: myelinophagy (targeting myelin in Schawnn cells)(Gomez-Sanchez et al., 2015), zymophagy (targeting zymogen granules in pancreatic acinar cells) (Grasso et al., 2011), ferritinophagy, targeting ferritin via the receptor nuclear coactivator 4 (Mancias et al., 2015).

5.2.1 Mitophagy

Among the different types of selective autophagy, mitophagy is the only known pathway via which whole mitochondria can be selectively eliminated. Mitophagy is responsible for the basal mitochondrial turnover that eliminates old mitochondria. However, mitophagy can also be induced under certain physiological conditions, examples of which are the maturation of erythrocytes, where mitochondria must remove from the cell, and the developmental of fertilized oocytes to remove paternal mitochondria (Sandoval et al., 2008)(Sato & Sato, 2011). In addition, mitophagy also can be induced as a stress response mechanism to eliminate selectively damaged mitochondria, but how the cell distinguishes between functional and non-functional

is not entirely elucidated (Martinez-Vicente, 2017). Loss of mitochondrial membrane potential and mitochondrial fragmentation precede mitophagy(Gomes, Di Benedetto, & Scorrano, 2011) (Twig et al., 2008). In cultured systems, mitophagy can be triggered by a number of stimuli, including hypoxia, energy stress and increased oxidative phosphorylation activity (Egan et al., 2011)(Wei, Liu, & Chen, 2015) (Melser et al., 2013).

All types of mitochondria keep the same pattern involving the receptor-mediated mechanism. The receptors connect the mitochondria with LC3-II via the LC3-interacting region (LIR) present in all receptors (Wild et al., 2014). The nature and origin of this receptors can vary depending on the type of mitophagy; some receptors are proteins or lipids located in mitochondrial membrane, while other receptors are non-mitochondrial proteins that recognize and simultaneously bind ubiquitinated chains on the surface of mitochondria and LC3-II on the autophagosome structure due to Ubiquitin binding domain that contain (Wild et al., 2014).

The most characterized mechanism regulating the recruitment of autophagosomes to mitochondria is that driven by phosphatase and tensin homolog (PTEN)-induced putative kinase 1 (PINK1) and Parkin (Youle & Narendra, 2011). This type of mitophagy its known as PINK1/Parkin mediated mitophagy and its activated in response to mitochondrial depolarization. PINK1 is imported from the cytosol to mitochondria in under basal conditions. In a mitochondrial transmembrane potential-dependent manner PINK1 is imported from the OMM to the IMM through translocase complex TOM and TIM. In the IMM its cleaved by mitochondrial matrix proteases such as mitochondrial processing peptidase (MPP) and prenisilin-associated rhomboid-like protease (PARL). This processing causes the externalization of the cleaved protein to the cytosol where it is degraded by the UPS. In a stress conditions of mitochondria where it loss it potential PINK1 is not imported and therefore PINK1 processing is not complete. Therefore, full-length is accumulate in mitochondria's surface (S. M. Jin et al., 2010) (Deas et al., 2011) (Greene et al., 2012)(Y. Yang et al., 2006).This accumulation can provoke the phosphorylation of ubiquitin (UB) at Ser65 tagged to OMM proteins that stimulates the recruitment and activation of Parkin to damaged mitochondria. PINK1

phosphorylates Parkin activating it and thereby promoting the ubiquitination of several proteins on the mitochondrial surface that will be phosphorylated by PINK1, generating a positive feedback loop. Therefore, the accumulation of ubiquitinated proteins in the mitochondrial surface generate a signal as an "eat-me" for mitophagy receptors. Currently, there are five receptors described (p62, NRB1, Optineurin (OPTN), NDP52 and TAX1BP1) involved in PINK/Parkin system but the primary receptors are OPTN and NDP52 (Lazarou et al., 2015). Autophagosomal membrane attachment is mediated through the LIR region, which targets damaged mitochondria to phagophores for clearance in the lysosome. Recently its described the direct interaction of LC3 with this ubiquitin tags at damaged mitochondria.

In any case, recent works was shown that parkin is important to amplify the signal but not essential for this process (Szargel et al., 2016). Alternative models to explain the role of Parkin in mitophagy have also been proposed in which Parkin acts more indirectly. This speculation about how Parkin promotes mitophagy in mitophagy emerges from evidence that targeted proteosomal degradation of Parkin substrates imbalances the ratio of mitochondrial to nuclear encode proteins at the mitochondria resulting in the mitochondria unfolded protein response (UPR ^{mt}) (Houtkooper et al., 2013).

Alternatively, Parkin may promote mitophagy indirectly by inhibiting fusion (as a result of Mnf-1/Mnf-2 degradation) (Dorn, Scorrano, & Dorn, 2010). Regulation of mitochondrial transport along MTs is another key consequence of Parkin recruitment to mitochondria. This is achieved through Parkin-mediated turnover of Miro, a protein that tethers MT-associated kinesin motor protein complexes to the OMM and through Parkin-dependent recruitment of HDAC6 that also promotes trafficking of mitochondria along MTs. Finally, Parkin has non- mitochondrial substrates that influence mitochondrial mass in cells, such as PARIS transcriptional regulator that repress PGC-1α expression to inhibit mitochondrial biogenesis (J.-H. Shin et al., 2011).

Other type of mitophagy is mediated by several proteins located in the OMM that contain LIR motif, which act as specific receptors (Bcl-2 nineteen-kilodalton interacting protein 3 (BNIP3), Nix, Bcl-2 like protein 13 (Bcl-L-13) and FUND1. BNIP3 and NIX are targets of Hypoxia-inducible factors(HIFs) (Bruick, 2000) (L. Liu

et al., 2012) but BNIP is also transcriptionally regulated by RB/E2Fs (Tracy et al., 2007), NF-KB (Shaw et al., 2008), FoxO3 (Mammucari et al., 2007), oncogenic Ras (S.-Y. Wu et al., 2011)(Kalas et al., 2011) and p53. The direct interaction with LC3B-II or GABARAP provoke the direct target of mitochondria to the autophagosome(Zhu et al., 2013). BNIP3 dependent mitophagy is preceded by mitochondrial fragmentation and perinuclear clustering of mitochondria. FUNDC1 is another protein located in the OMM that is also activated in response to hypoxia. Intriguingly, this renders the FUNDC1-LC3 interaction subject to negative regulation by SRC1.Conversely, phosphorylation of FUNDC1 by ULK-1 promotes the interaction with LC3.Cardiolipin is a mitochondrial phospholipid present in the IMM, when is externalized to the OMM, it can function as a mitophagy receptor to recruit LC3 and the autophagosome machinery (J. Zhang & Ney, 2009).

Although mitophagy is the only cellular process that eliminates whole mitochondria, other mechanisms exist to eliminate portions or components of mitochondria. One of these are UPR^{mt}**.** This is activated in a stress-response and activates genes related to mitochondrial proteostasis as an internal quality control. It is formed by several chaperones and proteases that promote proper protein folding and complex assembly (Haynes & Ron, 2010). Recently, it has been found a new mechanism involving in the partial elimination of mitochondria. It is called Mitochondrial-derived vesicles (MDVs) and can be formed by budding of the mitochondrial membrane, these vesicles are formed independently of the mitochondrial fission machinery and are targeted to lysosomes for degradation in an autophagosome-independent manner (Soubannier et al., 2012; Roberts et al., 2016).

Neurons represent a particularly interesting cell type for mitophagy because they combine high demand for mitochondria and high mitochondrial stress with a challenging cellular architecture. In addition, neurons are post-mitotic cells and therefore their mitochondria are particularly prone to accumulation of oxidative damage and high levels of calcium (Berthold, Fabricius, Rydmark, & Andersén, 1993). Nowadays, the process of mitophagy in neurons it is not well characterized but the mutations of PINK1 and Parkin were associated with neurodegeneration in hereditary PD (Batlevi & La Spada, 2011). Mitochondrial damage and dysregulation

of mitophagy have also observed in other neurodegenerative diseases such as Alzheimer, ALS and Huntington's disease (Khalil et al., 2015; Sun, Starovoytov, & Cai, 2015; Wong & Holzbaur, 2014).

Objectives

Objectives

Correction or potentiation of endogenous mechanisms of neuroprotection after injury such as autophagy might ensure success of neuroprotective and regenerative therapy. Therefore, our main objective is to investigate the features of autophagy induction after injury and provide related tools for neuroprotection and nerve regeneration after PNI.

With this aim the thesis has been divided in 3 different chapters that are composed by particular objectives.

Chapter 1: ATG5 Overexpression is Neuroprotective and Attenuates Cytoskeletal and Vesicle-Trafficking Alterations in Axotomized Motoneurons

1.1 To perform proteomic analysis and validate data to determine key molecular proteins involved in the degenerative processes after RA.

1.2 To characterize the Autophagy flux and related events in neurodegeneration of MNs after RA.

1.3 To modelling in vitro some key events of this neurodegenerative processes (e.g. cytoskeleton and autophagy abnormalities).

1.4 To analyse the impact of cytoskeleton alterations on MN survival in vivo

1.5 To evaluate if autophagy potentiation by ATG5 overexpression preserve injured MN population.

Chapter 2: Grp78/Bip Triggers PINK/IP3R-Mediated Protective Mitophagy

2.1. To perform proteomic analysis and validate data to determine key molecular events and nodes by which GRP78/BiP overexpression promote the survival of MNs after RA.

2.2 To asses if Grp78/ BiP overexpression triggers mitophagy *in vivo* and *in vitro*.

2.3 To determine the relevance of mitophagy in the neuroprotective effect of GRP78/BiP overexpression.

2.4 To discover possible partners for Grp78/BiP-induced mitophagy.

Chapter 3: Autophagy induced by SIRT1/Hif1α axis promotes nerve regeneration

3.1 To characterize SIRT1 localization and activity within MNs after PNI

3.2 To assess the role of SIRT1 in nerve regeneration after axotomy using several PNI models by pharmacologic and genetic approach.

3.3 To investigate the implication of Hif1a/autophagy pathway in SIRT1-mediated axon growth and neuritogenesis

3.4 To verify the importance of macroautophagy in nerve regeneration by inducing ATG5 overexpression

Chapter 1

Leiva-Rodríguez et al. *Cell Death and Disease* (2018)9:626
DOI 10.1038/s41419-018-0682-y

Cell Death & Disease

ARTICLE Open Access

ATG5 overexpression is neuroprotective and attenuates cytoskeletal and vesicle-trafficking alterations in axotomized motoneurons

Tatiana Leiva-Rodríguez[1], David Romeo-Guitart[1], Sara Marmolejo-Martínez-Artesero[1], Mireia Herrando-Grabulosa[1], Assumpció Bosch[2], Joaquim Forés[3] and Caty Casas[1]

Abstract

Injured neurons should engage endogenous mechanisms of self-protection to limit neurodegeneration. Enhancing efficacy of these mechanisms or correcting dysfunctional pathways may be a successful strategy for inducing neuroprotection. Spinal motoneurons retrogradely degenerate after proximal axotomy due to mechanical detachment (avulsion) of the nerve roots, and this limits recovery of nervous system function in patients after this type of trauma. In a previously reported proteomic analysis, we demonstrated that autophagy is a key endogenous mechanism that may allow motoneuron survival and regeneration after distal axotomy and suture of the nerve. Herein, we show that autophagy flux is dysfunctional or blocked in degenerated motoneurons after root avulsion. We also found that there were abnormalities in anterograde/retrograde motor proteins, key secretory pathway factors, and lysosome function. Further, LAMP1 protein was missorted and underglycosylated as well as the proton pump v-ATPase. In vitro modeling revealed how sequential disruptions in these systems likely lead to neurodegeneration. In vivo, we observed that cytoskeletal alterations, induced by a single injection of nocodazole, were sufficient to promote neurodegeneration of avulsed motoneurons. Besides, only pre-treatment with rapamycin, but not post-treatment, neuroprotected after nerve root avulsion. In agreement, overexpressing ATG5 in injured motoneurons led to neuroprotection and attenuation of cytoskeletal and trafficking-related abnormalities. These discoveries serve as proof of concept for autophagy-target therapy to halting the progression of neurodegenerative processes.

Introduction

Connectivity is needed for neuronal survival. Disruption of synaptic function and axonal connectivity precedes neuronal cell death in most neurodegenerative processes and diseases[1]. Accordingly, proximal axotomy leads to dysfunction, atrophy, and eventually neuronal death. Injured neurons may trigger endogenous mechanisms of neuroprotection that help them to rapidly recover from the insult. Macroautophagy (hereafter referred to as autophagy) and the unfolded protein response activated against the endoplasmic reticulum (ER) stress are examples of these mechanisms. Often neurodegeneration appears concomitantly with anomalies in these corrective mechanisms preventing complete recovery. Correction or potentiation of these endogenous mechanisms of neuroprotection might ensure success of neuroprotective therapy[2].

Correspondence: Caty Casas (Caty.Casas@uab.cat)
[1]Institut de Neurociències and Department of Cell Biology, Physiology and Immunology, Universitat Autònoma de Barcelona (UAB), Centro de Investigación Biomédica en Red sobre Enfermedades Neurodegenerativas (CIBERNED), 08193Bellaterra, Barcelona, Spain
[2]Department of Biochemistry and Molecular Biology, Center of Animal Biotechnology and Gene Therapy (CBATEG), UAB, CIBERNED, Barcelona, Spain
Full list of author information is available at the end of the article.
Edited by H.-U. Simon

Here, we used a non-transgenic model of spinal motor neurodegeneration based on surgical peripheral nerve root avulsion (RA) for axonal connectivity disruption. Spinal motoneurons (MNs) are located throughout the central nervous system (CNS) and send out their axons through peripheral nerves. This positioning facilitates experimental access to soma and axons. The model is commonly used to evaluate neuroprotective strategies for use in treatment of peripheral nerve trauma[2].

After axotomy, a neuronal retrograde response is initiated. The intensity and time course of this response are influenced by the distance from the axonal injury site, the age, and the animal species, among other factors. In contrast to neonatal MNs[3], in the adults, axonal transection does not lead to MN death unless the injury is in close proximity to the perikaryon as occurs after root mechanical traction or avulsion (RA)[4–6]. In contrast, after distal axotomy, MNs engage endogenous mechanisms that allow them to recover and even regenerate axons. Thus, we sought to characterize the molecular programs activated after distal axotomy that differ from the neurodegenerative process after RA using unbiased proteomics[7] with the goal of determining which programs should be activated to ensure neuroprotection. In this study, we demonstrate that selective autophagy[8] is an important endogenous neuroprotective mechanism engaged after distal axotomy. Since the autophagy process is necessary for MN survival and regeneration, we identified concomitant programs that may contribute to its failure with the goal of establishing a neuroprotective approach for RA.

Results

Impaired autophagy flux and aberrant lysosomal protein glycosylation early after RA

Autophagy sequesters cytoplasm and superfluous or dysfunctional organelles within an expanding phagophore, leading to the formation of the double-membrane autophagosome (Fig. 1a)[9]. We reported previously that autophagy was induced with the accumulation of lipidated form of microtubule-associated protein 1 light chain 3 (LC3II) at 3–5 days after RA[10]. Increasing levels of LC3II might indicate either enhanced conversion of LC3I to LC3II or impaired degradation through lysosomes. To distinguish between these possibilities, we analyzed autophagic flux using the reporter mCherry-GFP-LC3[11], which was cloned into the MN-specific adeno-associated viral vector serotype AAVrh10[12]. GFP signal quenches into acidic compartments, such as lysosome, whereas mCherry's persists (Fig. 1a)[13].

At 3 weeks after vector injection, the animals were subjected to surgical RA and sacrificed at 5 days post injury (dpi). In order to better detect LC3-associated puncta in sham-operated control animals, the mice were treated orally with rapamycin, an inducer of mTOR-dependent autophagy, for 3 days post operation. By confocal microscopy, we observed abundant LC3-positive autophagosomes and autolysosomes within the MN soma (Fig. 1b). We observed an increase in the number of yellow dots per MN in animals subjected to RA compared to control animals (Fig. 1c). Autophagic flux was significantly diminished to 48% of control levels after RA, suggesting a reduction of autolysosome formation or reduced function.

The existence of autophagy flux impairment after RA led us to focus on late events in autophagy related to fusion and autolysosome formation. We investigated the abundance of three lysosomal proteins critical for its function and fusion with the autophagosome: V-type proton ATPase subunit V0 isoform a1 (v-ATPase), indispensable for lysosome internal acidification; LAMP1, a major integral membrane glycoprotein localized to late endosomes and lysosomes and important for autolysosome fusion events[14]; and the polyubiquitin-binding protein p62/SQSTM1 (p62), an autophagic receptor. The H+ pump activity of v-ATPase depends on its glycosylated state[15]. We observed that the ratio of glycosylated to unglycosylated forms was 4-fold lower after RA than in controls at 7 dpi (Fig. 1d). From this time point, neurodegeneration of avulsed MNs is molecularly initiating as we previously reported[7,10]. LAMP1 was detected as a pattern of bands with different antibodies corresponding to different glycosylated isoforms as previously described[16] (Supplemental Fig. S1). The overall level of LAMP1 (≈100 kDa) was lower in RA samples than controls, and a particular decrease was observed in faster migrating bands (Fig. 1d). Finally, p62 accumulated in the RA model as expected, given that autophagy flux is impaired (Fig. 1d). These results suggest that RA provokes blockage of the autophagy flux and alterations in the glycosylation of some key intramembrane lysosomal proteins.

RA causes alterations in microtubule-related proteins and deficient protein sorting

In order to identify the causative events leading to autophagy flux blockage early after RA, we took advantage of our recently performed unbiased quantitative proteomic analysis[7]. From this analysis, we reported a list of protein signatures that determined the neurodegenerative condition. A Gene Ontology (GO) analysis of these data revealed significant enrichment for proteins related to microtubules and vesicle trafficking among those proteins modulated in RA relative to the control (Fig. 2a and Supplemental Table S1). Our proteomic data shed qualitative differences that can be interpreted as quantitative. Qualitative differences depend on both, the easy tripsinization processes for a particular protein and the easy

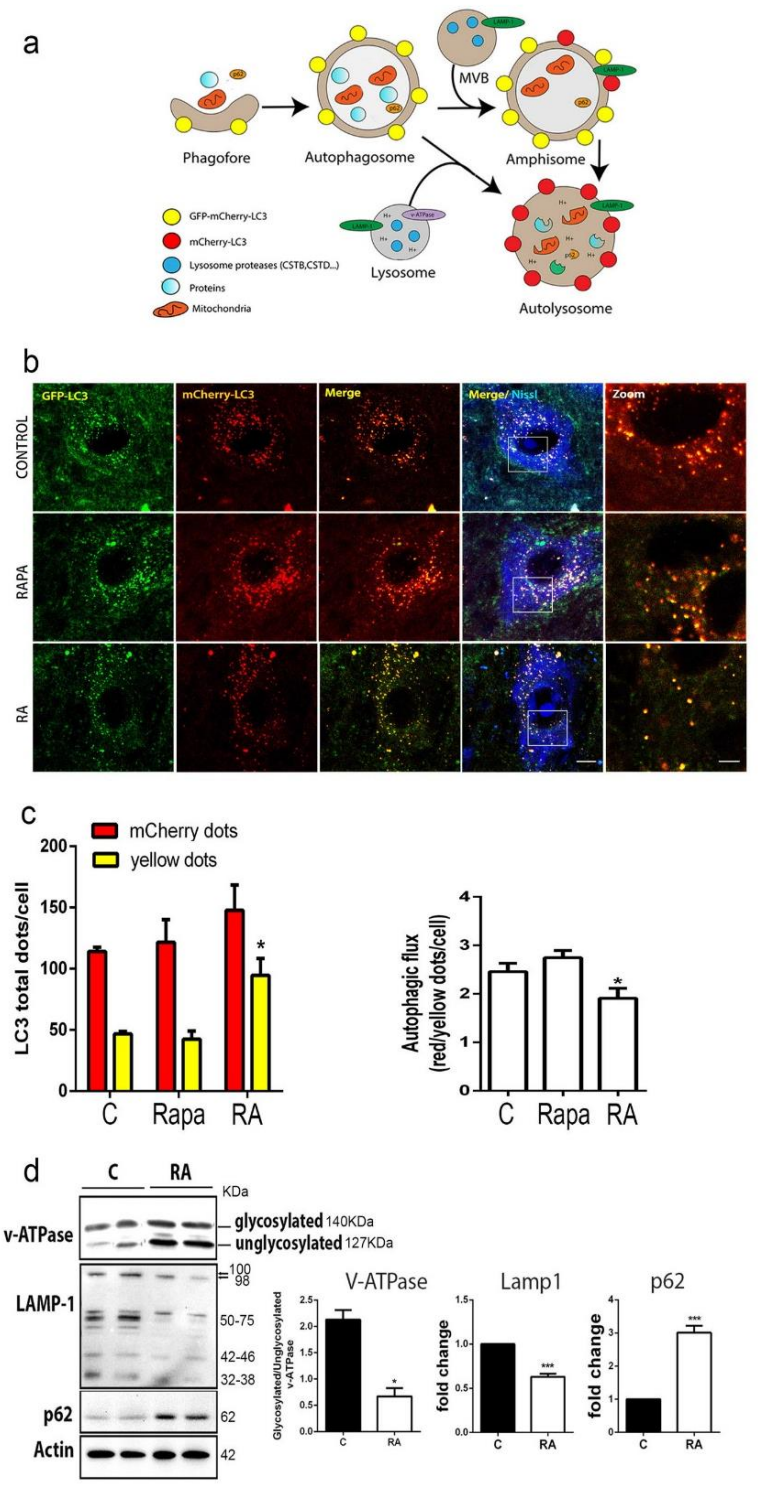

Fig. 1 (See legend on next page.)

(see figure on previous page)

Fig. 1 Impaired autophagy flux and aberrant lysosomal protein glycosylation after RA. a Schematic representation of the autophagy flux (modified from ref. [13]). Expression of the mCherry-GFP-LC3 reporter gene will generate yellow puncta upon activation of autophagy at the autophagosome/amphisome and red puncta in the autolysosome if the autophagy flux continues correctly and the lysosomes achieve their usual acidic pH which quenches the green GFP fluorescence. **b** Microphotographs of representative MNs from sham-operated control animals treated with rapamycin (Rapa) for 3 days before sacrifice, from RA injured and control sham rats at 5 dpi; all rats were infected with AAVrh10-mCherry-GFP-LC3. **c** Left, Bar graph of manual quantification of yellow and red puncta within MNs at L4 spinal cord segment in both conditions. Right, Bar graph of autophagic flux measured as the ratio of red to yellow puncta per MN. Non-parametric *t*-test was used to compare the statistical significance between the control and avulsed animal. **d** Left, Immunoblot for glycosylated and unglycosylated v-ATPase, LAMP1, and p62. Note the slight difference in electrophoretic mobility of higher LAMP1 band between control and RA samples and the different general band pattern. Right, Bar graph showing the average fold change protein level ± SEM in control (C) and root avulsed (RA) samples normalized to actin levels ($n = 4$). Scale bar = 10 µm; zoom = 5 µm; $^{*}p < 0.05$ vs. control, $^{***}p < 0.001$ vs. control (Student's *t*-test)

detection of its peptides by the mass spectrometer. Post-translational modifications present on proteins affect easy access for cleavage. Hence, less modified proteins might be easier cut into single peptides and therefore considered as more abundant. This seemed to be the apparent case for LAMP1, which was significantly better detected in RA than in the control group. However, we found less amount of the highly glycosylated 100 kDa band of LAMP1, in agreement with previous reports[10], and an altered glycosylation pattern in the RA group compared to control. Thus, proteomic data were consistent with an increase in deglycosylated forms.

We also validated other proteins related to either anterograde/retrograde transport, such as the kinesin family protein KIF5C and the dynactin subunit DCTN1, or the secretory pathway. Both KIF5C and DCTN1 diminished significantly after RA compared to control at 7 dpi (Fig. 2b, c). Similarly, there was a reduction in EEA1, at early endosomes, and Sec31A and p115 *cis*-Golgi markers (Fig. 2d)[17]. These data suggested that affectation in microtubule-related transport and vesicle trafficking are early events that occur concomitantly with impaired autophagy flux in this neurodegenerative process.

In vitro model of MN cell death reproduces transport and glycosylation alterations

An understanding of the relationship and causative sequence between microtubule-related and autophagy impairment after RA will help in the establishment of targets for future neuroprotective therapies. Hence, we aimed to model these features in vitro. We first evaluated the response over time of the MN-like NSC34 cells to treatment with 1 µM rapamycin. We evaluated the expression of Beclin1, involved in the initiation of autophagy, the conversion of LC3I to LC3II, and the level of LAMP1. We observed that the level of these proteins progressively increased from 2 to 4 h after rapamycin treatment (Supplemental Fig. S2).

In order to mimic cytoskeletal alterations, we treated the NSC34 cells with 10 µM nocodazole, which binds to β-III-tubulin and transitorily inhibits microtubule dynamics[18]. Nocodazole treatment caused NSC34 cells to become rounded in shape and drastically reduced the levels of acetylated α-tubulin, KIF5C, and DCTN1 during the first 2 h post treatment compared to control (Fig. 3).

Autophagy induction promoted by rapamycin use did not decrease NSC34 cell survival by MTT assay over 18 h unless used at high concentrations (Fig. 3e). In contrast, despite the transitory effect promoted by nocodazole[7], it drastically reduced the cell viability (by 41%) (Fig. 3e). To mimic simultaneous induction of autophagy and cytoskeletal alterations as they appear to occur in vivo after RA, the cells were treated with both rapamycin and nocodazole. Co-treatment enhanced cell viability with respect to single treatments at lower concentrations of rapamycin (Fig. 3e). Thus, it is unlikely that microtubule alterations and autophagy occurred at the same time in vivo as we observed MN degeneration.

Since LAMP1 levels are a neurodegenerative signature in our in vivo model, we assayed different sequential treatments with 10 µM nocodazole and 1 µM rapamycin and analyzed the impact on cell survival (Fig. 3f) and on LAMP1 levels (Fig. 3g). We observed that the most drastic effects on cell viability were obtained when nocodazole was added prior to rapamycin, suggesting that microtubule alterations might initiate neurodegeneration after RA. LAMP1 levels and the complexity of the bands observed were dramatically reduced when nocodazole was added prior to rapamycin (Fig. 3g). Considering that the first 2 h of nocodazole treatment should be enough to exert its effect, in subsequent experiments, the cells were first treated with nocodazole; 2 h later rapamycin was added, and analysis was performed 3 h after rapamycin addition (N2R3). Together these results suggest that microtubule alteration precedes autophagy induction after RA to promote neurodegeneration and aberrations in intramembrane lysosomal proteins that compromise lysosomal function.

Concurrent LAMP1 missorting, lysosomal dysfunction, and blocked autophagy flux in the in vitro model

We suspected that there are alterations in protein trafficking in the secretory pathway specific to the lysosome in

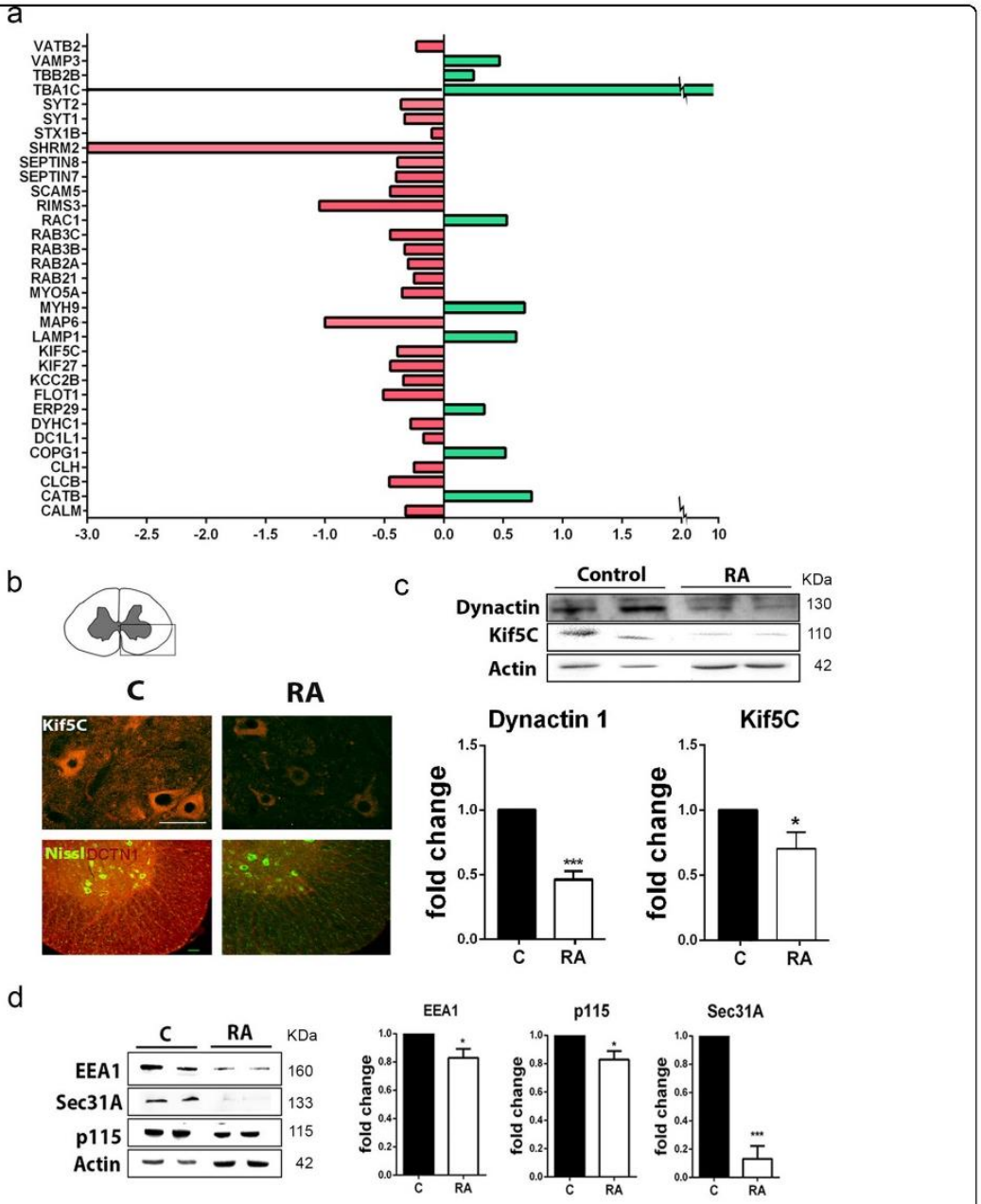

Fig. 2 Proteomic data validation. a Histogram of microtubule and vesicle-related protein fold changes in RA injured L4–L5 spinal cord segments with respect to sham-operated control obtained by analysis of proteomic data (upregulated in green; downregulated in red) obtained previously[7]. **b** Microphotographs of the ipsilateral spinal cord ventral horn from control (C) and RA-injured (RA) animals, showing immunostaining of KIF5C and DCTN1 with fluorescent Nissl counterstaining to reveal MNs at 7 dpi. Scale bar = 100 µm. **c** Western blot to quantify KIF5C and DCTN1 ($n = 4$; $^{*}p < 0.05$ vs. control, $^{***}p < 0.001$ vs. control Student's *t*-test). **d** Immunoblot and bar graph showing the analysis of EEA1, Sec31A, and p115 protein levels in L4 spinal cord segments ($n = 4$; $^{*}p < 0.05$ vs. control, $^{***}p < 0.001$ vs. control Student's *t*-test)

the in vitro model and in vivo after RA. By immunoblotting, we observed that the abundances of EEA1, Sec31A, and p115 were drastically reduced 5 h after nocodazole treatment alone or in N2R3 condition (Fig. 4a). Rapamycin alone affected only EEA1 levels. In order to verify that nocodazole treatment altered the lysosomal membrane protein sorting, we analyzed the localization of cathepsin B (CTSB), a lysosome marker, and LAMP1. The proteins did

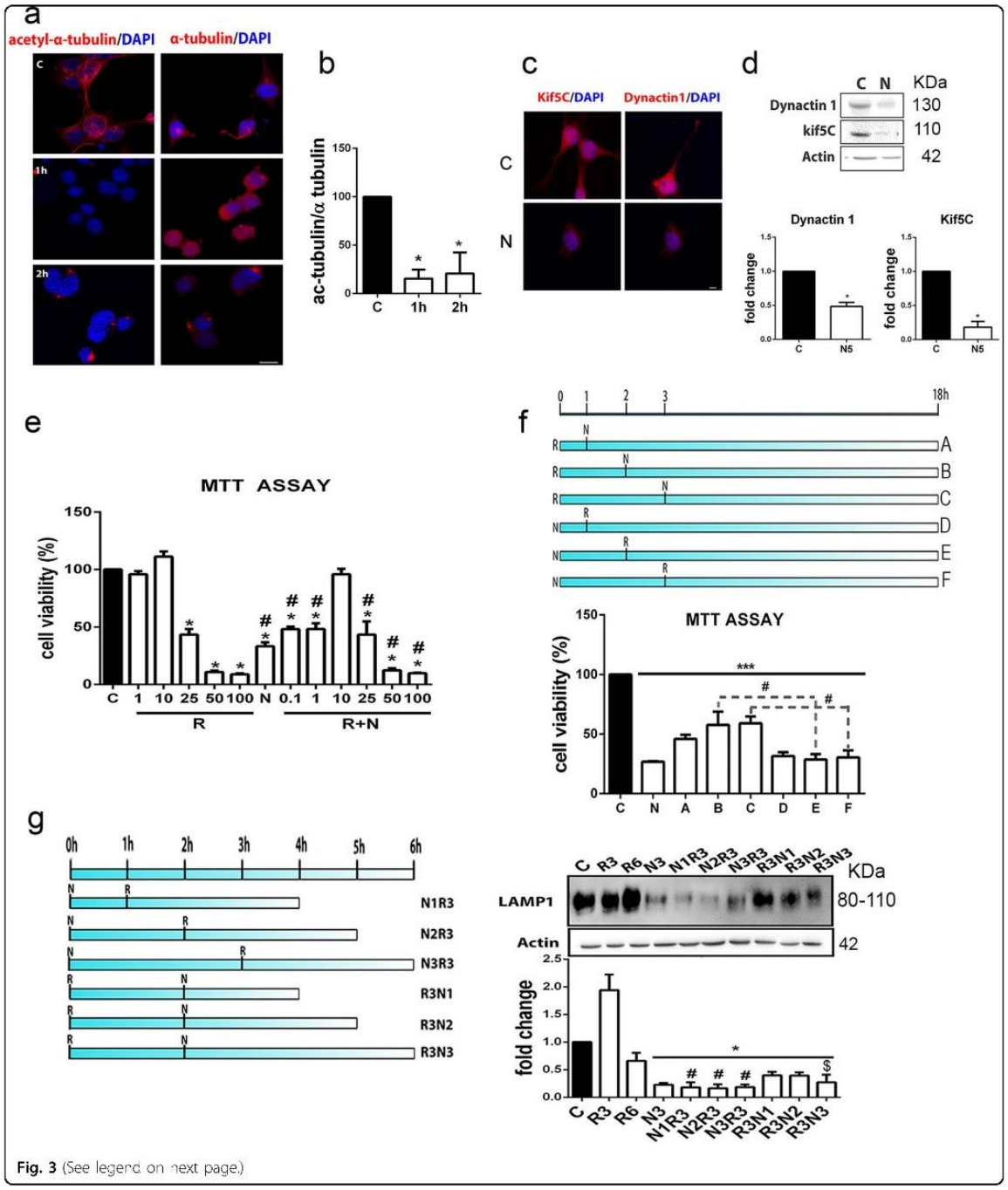

Fig. 3 (See legend on next page.)

not co-localize in cells treated with nocodazole alone or in combination with rapamycin (N2R3) suggesting impaired trafficking of membrane proteins toward the lysosome (Fig. 4b). In addition, the CTSB-positive lysosomes were located far from the perinuclear position observed in control or rapamycin-treated cells. LAMP1 rather co-localized with giantin (Fig. 4c), a Golgi-marker, distributed into Golgi mini-stacks upon nocodazole treatment[19,20]. This observation verified LAMP1 missorting in the in vitro model.

(see figure on previous page)

Fig. 3 In vitro model characterization. a Microphotographs showing merged images for α-acetyl-tubulin and α-tubulin fluorescent immunostaining (red) with DAPI nuclei counterstaining (blue) in control (C) NSC34 cells and cells treated with 10 μM nocodazole (N) for 1 h and 2 h. **b** Bar graph of ratios of mean immunofluorescence intensities (± SEM) of the acetylated vs. non-acetylated forms of α-tubulin (*$p < 0.001$ vs. control, one-way ANOVA). **c** Representative images of KIF5C and DCTN1 fluorescent immunostaining (red) with DAPI counterstaining (blue) in control cells and cells treated for 5 h with nocodazole. **d** Immunoblots and histograms of the levels of DCTN1 and KIF5C in control and nocodazole-treated cells ($n = 3$; *$p < 0.05$ vs. control). **e** Bar graph of the mean average percentage of NSC34 cell survival 18 h after vehicle (C), 1 μM rapamycin (R), 10 μM nocodazole (N), and concomitant R+N treatments analyzed by MTT assay ($n = 4$; *$p < 0.001$ vs. control, one-way ANOVA). **f** Schematic of different culture conditions assayed where either R was added at the beginning of the experiment and N was added after 1, 2, or 3 h (A, B, C conditions) or the reverse (D, E, F conditions). After 18 h of each condition, cell survival was assessed by MTT. **g** Left, Schematic of culture conditions. N was added at time zero and R was added after 1, 2, or 3 h (N1-N3R3) or the reverse (i.e., R was added at time zero and N was added after 1, 2, or 3 h; R3N1-N3). Cells were harvested at 6 h. Right, Immunoblot and histogram of LAMP1 protein levels in cells treated as described in **g** ($n = 3$–5; *$p < 0.05$ vs. control, $^{\$}p < 0.05$ vs. R6, $^{\#}p < 0.05$ vs. R3, one-way ANOVA)

We next assessed lysosomal acidification, which is necessary for proper function, using acridine orange (AO) as a sensor that emits red fluorescence in acidic compartments[21,22]. As a control for the evaluation of the ratio of signal at 498 nm (acid) to signal at 511 nm (basic) fluorescence, we treated the cells with 1 μM bafilomycin A1 (BafA1), an inhibitor of v-ATPases[23], for 3 h. The ratio of acidic to basic signal in BafA1-treated cells was reduced by 15.7±4.2% compared to untreated cells (Fig. 5a). Treatment with nocodazole also decreased the acidity of the cytoplasm (by 11.41% in N2R3 and 32.77% in N5 compared to control cells).

Consequently, we investigated the proteolytic cleavage of cathepsin D (CTSD), which depends on the presence of the acidic pH in the lysosomal compartment. Procathepsin D can escape the transfer to lysosomes and can be secreted into the extracellular space[24]. Hence, in our in vitro system, we could only detect the processed isoform which was drastically reduced after nocodazole, alone or with rapamycin, treatment as expected when acidification of the lysosome is reduced (Fig. 5b). This is in agreement with our previous work reporting altered CTSD processing after RA in vivo[7].

We next sought to determine whether these alterations were concurrent with autophagy flux impairment in vitro. Western blot analyses revealed that LC3II and p62 accumulated in all conditions that included nocodazole treatment (Fig. 5b). Cells transfected with the reporter LC3-GFP-mCherry had higher numbers of yellow LC3-GFP puncta at the N2R3 condition than when treated only with rapamycin (Fig. 5c). These results suggest that early cytoskeletal alterations severely compromise the function of lysosomes probably due to missorting of important glycoproteins into the lysosomal membrane. This in turn impairs autophagy or other lysosome-related events (Fig. 5d).

The early induction of autophagy appears to be necessary for neuroprotection against cytoskeleton-induced alterations, which are also presented after RA. We hypothesized that nocodazole administration would be sufficient to promote neurodegeneration by itself. And also, we wondered if the effect of autophagy induction would yield opposite results depending on pre- or post-treatment to the RA lesion. To explore this, we first intrathecally injected a dose of nocodazole in control rats, without any RA lesion, and let them up to 21 days post injection to analyze MN survival. We observed that nocodazole treatment caused early and transitory reduction of b-tubulin staining of the cytoskeleton as expected (Supplemental Fig. S3a). By the same time, astrogliosis around MNs was significantly increased (Supplemental Fig. S3b). These abnormalities were enough to trigger a slow neurodegenerative process that ends up with a significant decline in the number of MNs by 21 days post injection confirming our initial hypothesis (Fig. 6a). Secondly, we explored whether timing for autophagy induction was crucial for neuroprotection after RA lesions in vivo, as suggested by the in vitro results. On one side, we treated RA-injured animals with rapamycin for 3 days either previously or posteriorly to the lesion. By 21 dpi, similar results were obtained for vehicle administration in pre- and post-treatments. We observed that the number of survived MNs was notably higher in the animals treated with rapamycin previously to the lesion compared to vehicle group. In contrast, no benefit was observed when rapamycin treatment was initiated posterior to the RA lesion (Fig. 6b).

Since rapamycin may exert other effects in addition to autophagy induction, we performed a different approach based on autophagy induction by the overexpression of ATG5. In vitro, ATG5 overexpression increased the viability and notably recovered the normal levels of cleaved CTSD forms in nocodazole-treated cells compared to GFP-overexpressing group (Fig. 7a, b). To observe the effects in vivo, we generated the AAVrh10-ATG5 vector and, at 3 weeks after injection, we found (i) a significant overexpression of ATG5 by immunoblotting; (ii) an increased LC3 II isoform, and LAMP1 (≈100 kDa), and (iii) normal p62 levels with respect to animals given the control AAVrh10-GFP vector, as expected for autophagy

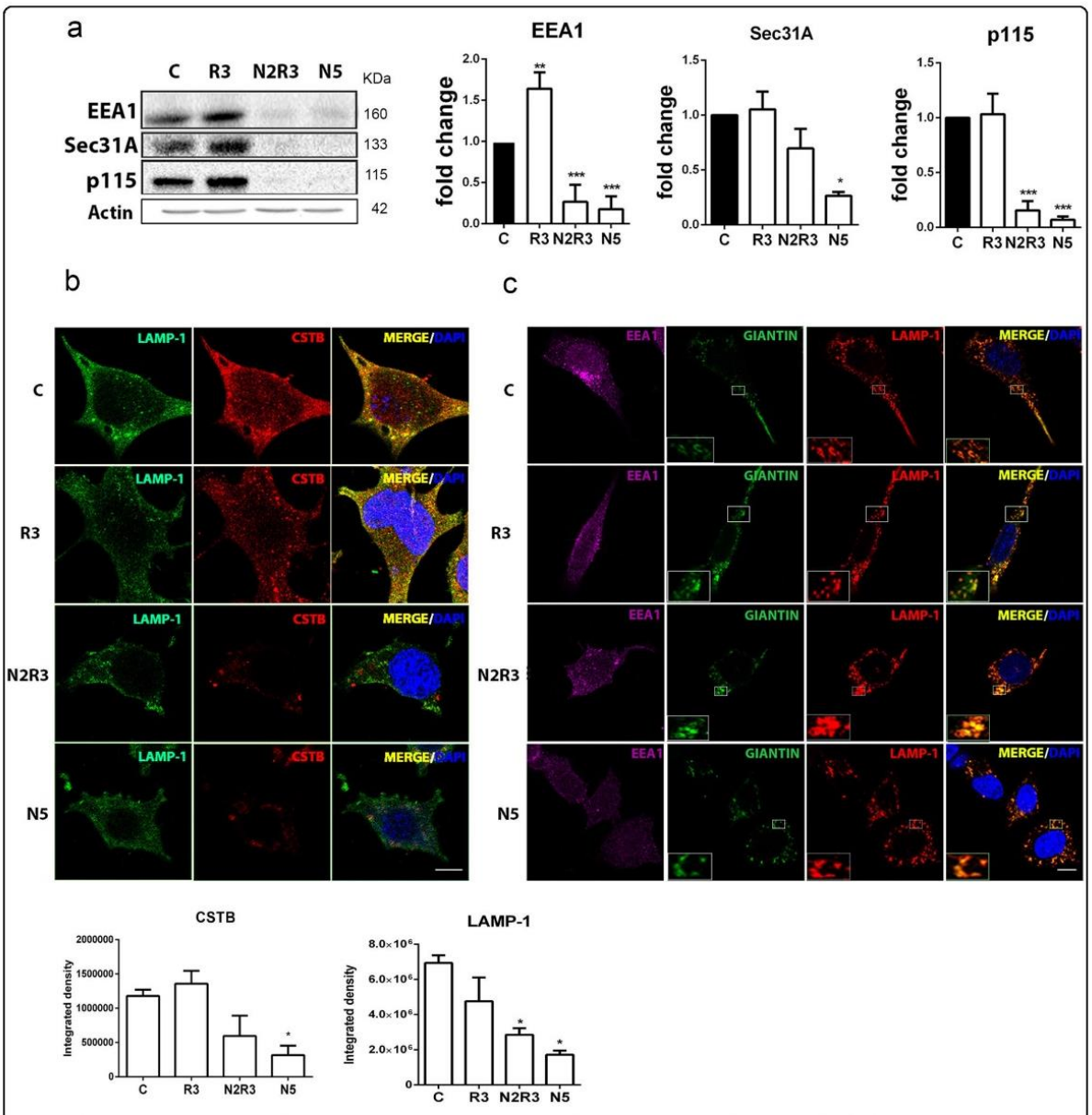

Fig. 4 Alterations in protein trafficking in the in vitro model. a Immunoblots and histogram showing the levels of EEA1, Sec31A, and p115 in control NSC34 cells and in cells treated with nocodazole (N), rapamycin (R), or the sequential combination (N2R3). **b** Microphotographs showing LAMP1 (green) and CTSB (red) immunostaining and co-localization (merged images) in indicated conditions. Below, graph bars of immunofluorescent quatification for each marker. Scale bar = 15 µm. **c** Representative confocal images of LAMP1 (red) co-immunolocalization (merged) with EEA1 (magenta) and giantin (green). Insets are two-fold magnifications of regions in boxes. Note that LAMP1 and giantin co-localized in cells treated with nocodazole. Scale bar = 30 µm

induction (Fig. 7c). Seven days post RA, ATG5 over-expressing group presented a marked reduction of p62 levels, increase of LAMP1 (≈100 kDa) and LC3-II isoform, and a tendency to rise in Beclin I compared to GFP-overexpressing animals, confirming autophagy induction and proper flux (Fig. 7d). Consistently, we observed increased levels of vesicle trafficking-related proteins such as Sec31 and KIF5C and a tendency to increase in EEA1 and DCTN1 in the AAVrh10-ATG5 compared to the AAVrh10-GFP groups suggesting recovery from a vesicle-

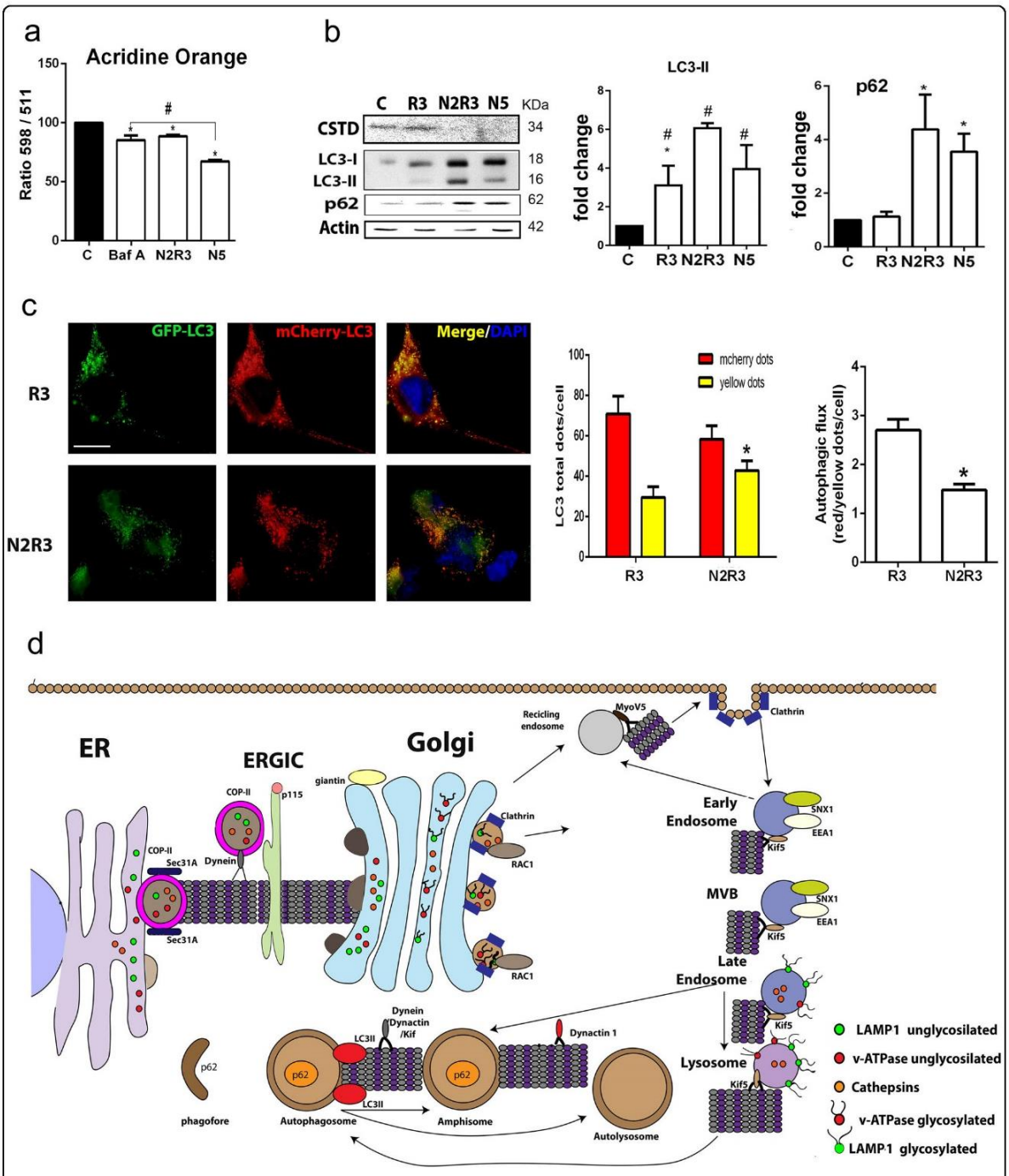

Fig. 5 Altered lysosomal function and autophagy flux blockage in the in vitro model. a Bar graph of the means (± SEM) of the ratios of the absorbance at 598 (red) to 511 (green) within the cytoplasm of cells stained with acridine orange. Shift toward the green indicates loss of acidity. BafA was used as a positive control ($^{*}p < 0.05$ vs. untreated control; $^{\#}p < 0.05$ vs. nocodazole, one-way ANOVA). **b** Western blot showing the levels of p62, cleaved CTSD, LC3I, and LC3II in control NSC34 cells and cells treated with nocodazole (N) or rapamycin (R) alone or sequentially with nocodazole and rapamycin (N2R3). Bar graphs show the average fold change of these proteins relative to control with normalization to actin. **c** Left, Microphotographs of NSC34 cells transfected with the mCherry-GFP-LC3 plasmid and treated as indicated. Scale bar = 30 μm. Right, Bar graphs with quantification of yellow and red puncta and the ratio ($^{*}p < 0.05$, non-parametric *t*-test). **d** Schematic of the secretory, endosomal, and autophagy pathways that are affected in MNs early in the neurodegenerative process after RA

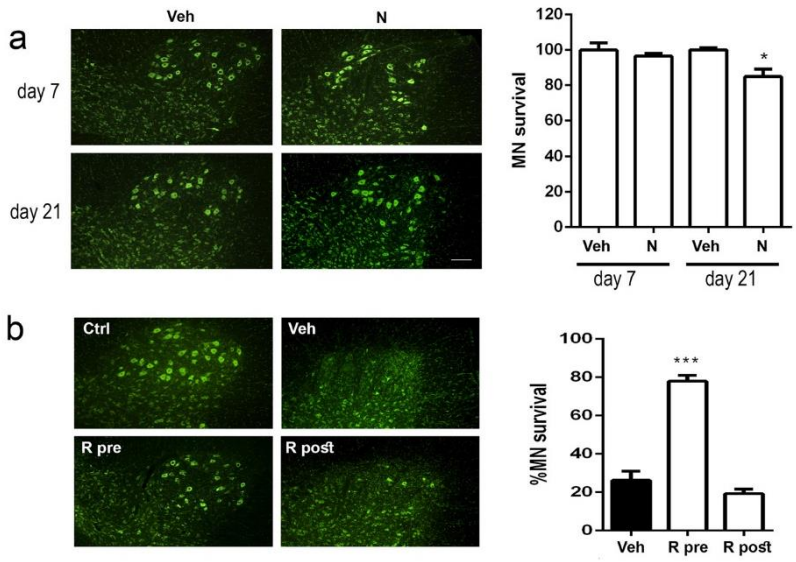

Fig. 6 Effects of nocodazole and rapamycin administration in vivo. a Left, Microphotographs of fluorescence Nissl stained MNs at the ventral horns of L4–L5 segments of the spinal cord of unlesioned rats treated with a single injection of nocodazole (N) or vehicle (Veh) taken at 7 and 21 days post injection. Right, Bar graphs of the average percentage of MNs at these spinal cord segments compared to control animals at different time-points. **b** Representative images of Nissl stained MNs and associated bar graphs of MN quantification at the ventral horns of L4–L5 segments of spinal cord from animals treated with vehicle (Veh) or rapamycin (R), previously (R pre) or posteriorly (R post) to RA lesion at 21 days post injury (dpi). Scale bar = 50 μm

trafficking defect after RA (Fig. 7d). By quantifying CTSD forms, we found a significant increase in the cleaved isoform in the ATG5 group suggesting better lysosomal functionality than in the GFP group. In agreement with these results, at 3 weeks post lesion, the number of surviving MNs was higher in the group treated with AAVrh10-ATG5 compared to AAVrh10-GFP-injected animals (Fig. 7e). In addition, the levels of acetyl α-tubulin, a marker of cytoskeletal dynamics[25,26], were higher in ATG5 with respect to GFP group (Fig. 7f) in agreement with previous results of increased levels in vesicle trafficking-related proteins.

Altogether, these results pointed that early ATG5 overexpression promoted better internal trafficking, autophagy flux, and functionality of the lysosome after RA leading to neuroprotection.

Overall, these results suggested that destabilization of the cytoskeleton is a primary cause sufficient to provoke neurodegeneration of MNs, even if they are still connected, not axotomized, and that primary induction of autophagy, but not late, is a key element for neuroprotection after proximal disconnection by RA.

Discussion

The nervous system has a remarkable ability for repair under stressful conditions. Under circumstances of damage, intrinsic pro-survival pathways, that are collectively termed endogenous neuroprotective mechanisms, are activated. Here, we addressed the question of why neurodegenerative processes occur even when beneficial mechanisms have been triggered. We confirm that disconnected MNs engage these mechanisms, such as autophagy, but the flux is blocked and anterograde/retrograde transport and secretory and endocytic trafficking are downregulated in vivo due to proximal axotomy. The relevant putative sequences of these events that lead to degeneration are initiated by cytoskeleton-related and vesicle-trafficking abnormalities that cause dysfunction in autophagy flux. We proof that the reverse sequence, i.e., early induction of autophagy, either by ATG5 overexpression or rapamycin pre-treatment, lead to neuroprotection in vitro and in vivo. In particular, precocious autophagy induction by ATG5 overexpression attenuates vesicle trafficking-related abnormalities, normalizes LAMP1 glycosylated pattern, and improves the lysosomal function and microtubule stability. We point to the importance of boosting autophagy at the very early stage in the neurodegenerative process to favor its own proper function and neuroprotection since late induction yields no benefits.

The evidences supporting these conclusions are based on analysis of proteomic data from a non-transgenic model of chronic disconnection by nerve RA (proximal axotomy). This analysis revealed that among the earliest events in the neurodegenerative process were the

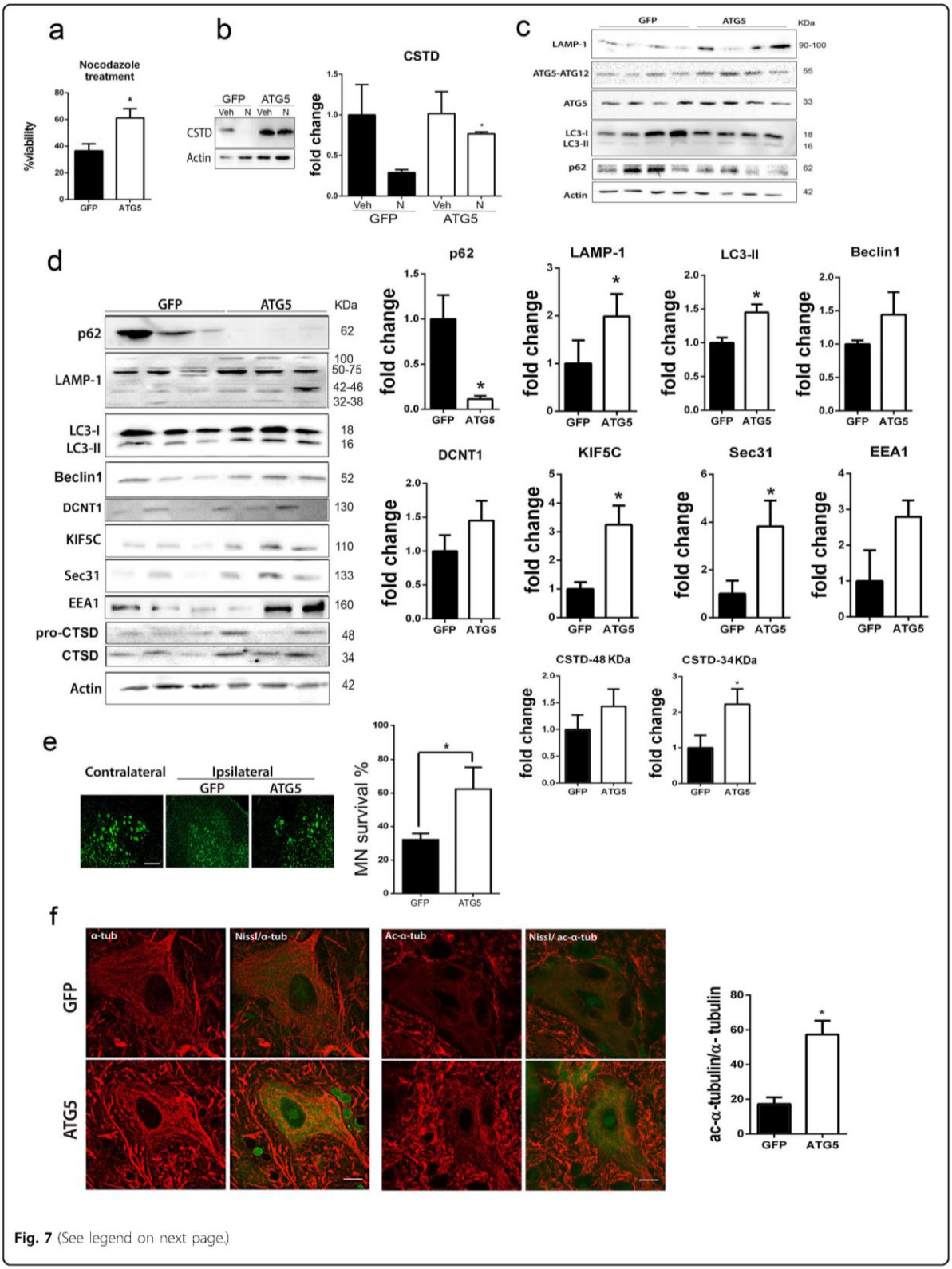

Fig. 7 (See legend on next page.)

(see figure on previous page)

Fig. 7 ATG5 overexpression neuroprotects and modulates motor and secretory pathway-related proteins and cytoskeleton. a Bar graphs of the mean average percentage of survival of NSC34 cells, transfected with CMV-GFP or CMV-ATG5 plasmids, at 18 h after nocodazole (N) treatment and analyzed by MTT assay ($n = 4$; $^*p < 0.001$ vs. control, one-way ANOVA). **b** Analysis of processed CTSD by western blot in transfected cells treated with vehicle (Veh) or nocodazole. **c** Western blot showing the levels of different autophagy hallmarks at the ipsilateral side of the spinal cord ventral horn from non-injured animals injected with AAVrh10-GFP or AAVrh10-ATG5 at 3 weeks post injection. Note LAMP1, ATG5-ATG12, ATG5, LC3II abundance, and normal p62 levels. **d** Western blot and corresponding bar graphs of the quantification of different proteins related to autophagy (p62, LAMP1, LC3, Beclin1), cytoskeleton (DCTN1, KIF5c), the secretory pathway (Sec31, EEA1), and lysosome function (CTSD) in the spinal cord from RA-injured animals injected with AAVrh10-GFP or AAVrh10-ATG5. **e** Left, Microphotographs showing green fluorescent Nissl stained MNs at the contralateral side and the ipsilateral side of the spinal cord ventral horn from RA-injured animals injected with AAVrh10-GFP or AAVrh10-ATG5. Right, Bar graphs showing the percentage of MN survival at the ipsilateral side with respect to the contralateral side of the same sample. **f** Representative microphotographs of MNs stained with α-tubulin (α-tub) or acetyl-α-tubulin (Ac-α-tub) from the different groups and associated bar graphs of the ratio of the percentage of immunoreactivity for Ac-α-tub with respect to α-tub. Scale bar = 10 µm

reduction of cytoskeletal and anterograde/retrograde motor forces (e.g., alterations in tubulins, α-actinin, myosins, kinesins, and dynactin). We previously reported abnormal progressive accumulation of phosphorylated neurofilaments within the soma of avulsed MNs[5], which is in agreement with defects in microtubules since neurofilaments rely entirely on them for the movement of phosphorylated forms toward the motor axon. KIF5C is a kinesin important for maintaining the MN population in adult mice[27], implicated in trafficking of mitochondria and vesicles[28] and in the passage of apical specific cargo molecules, to a post-Golgi endosomal compartment[29,30]. DCTN1 and dynein 1 are part of a multi-protein complex necessary for this trafficking[31]. Proteomic data suggested also a reduction in light and heavy chains of clathrin that may affect clathrin-dependent endocytic machinery or impaired maturation of vesicles emerging from the *trans*-Golgi network. Anterograde/retrograde transport dysfunction due to mutations in kinesins has been reported in patients with Charcot-Marie-tooth type 2A[32] and in the $p150^{Glued}$ subunit of dynactin in patients with late-onset progressive motor neuron degeneration[33,34]. Transport abnormalities are also observed in the mouse model of the fatal neurodegenerative disease amyotrophic lateral sclerosis (ALS)[1]. Thus, our model of RA reproduces some common key alterations in neurodegenerative conditions affecting MNs.

Correct microtubule dynamics is necessary for protein sorting, and we found alterations in genes encoding proteins involved in the secretory and exocytic pathway (Sec31[35], sintaxin1, Rac1, and myoVa) as well as the endocytic-lysosomal pathway (clathrin, LAMP1, v-ATPase). The observed reduction of around 90% in the amount of Sec31, which is necessary for the formation of COPII-coated vesicles created at the ER to drive vesicle release toward the *cis*-Golgi[35], certainly must diminish the transit at the secretory pathway. Mutations in these key components of the secretory pathway (Syntaxin 1b, CALM, CamKII, Rac1, and myoVa) are either lethal or cause severe disease[36–42].

Membrane proteins from different sources make up the lysosome membrane. Both late-endosomes and lysosomes are highly enriched in distinctive, highly glycosylated and conserved proteins such as LAMP1 that reach their destination directly from the *trans*-Golgi network or from the endocytic pathway. We observed LAMP1 missorting as a consequence of impaired microtubule dynamics in vitro and after RA in vivo[10]. One possible explanation might be saturation of transport at the *trans*-Golgi network since when overexpressed LAMP1 is found at the cell surface[43]. However, we did not observe LAMP1 in the cellular membrane of avulsed MNs in vivo or in nocodazole-treated cells suggesting that saturation is not the cause of missorting. We hypothesize that LAMP1 trafficking is severely reduced at all levels including the step from the ER to the Golgi post RA, resulting in the reduction of the hyperglycosylated forms that we observed both in our in vivo and in vitro models. The underglycosylated form of v-ATPase also accumulated. Absence or reduced function of this pump may prevent lysosomal acidification, explaining the reduction of mature forms of lysosomal enzymes that depend on an acidic environment for maturation, as is the case for CTSD after RA[7] and in our in vitro model. These observations are in agreement with the findings in other neurodegenerative disease studies: for example, Alzheimer's disease-linked mutations in presenilins cause reductions in the glycosylation of v-ATPase resulting in defective lysosome-mediated proteolysis during autophagy[44]. Hence, we speculate that this mechanism might be generalized to the neurodegenerative process regardless of specific mutations.

Treatment of cultured MN-like cells with nocodazole reproduced many of the events observed after RA in vivo. Nocodazole and related substances have been used to analyze the role of microtubules in autophagy (reviewed elsewhere[45]). LC3 associates with microtubules, and cells treated with nocodazole or vinblastine, which interfere with microtubule polymerization, are defective in fusion of autophagosomes with lysosomes, but autophagosome

biogenesis is not altered in the presence of these drugs[46,47]. It was proposed that nocodazole-induced blockage of autophagic flux is due to the inhibition of autophagosome trafficking toward lysosomes due to impaired microtubule dynamics. This is still a controversial question as in one study microtubule dynamics did not affect the co-localization and fusion of autophagosomes and lysosomes[48], which has been shown to occur in the absence of microtubules[49], although others argue that more efficient fusion is enabled by active transport along the microtubules[50]. Two previous studies demonstrated CTSD immaturity due to nocodazole treatment[51,52]. We propose that an altered membrane composition of lysosomes, devoid of proper glycosylated protein forms, in particular LAMP1, due to altered trafficking, contribute to preventing fusion and proper function. Relevant to neurodegeneration from our analysis is that microtubule alterations precede lysosome dysfunction and autophagy flux blockage after RA and hence may prevent induction of neuroprotective programs such as autophagy. Indeed, we provide evidence that a single intrathecal injection of nocodazole in vivo is sufficient to trigger MN degeneration and that autophagy induction before the appearance of any cytoskeletal alteration might prevent MN degeneration. This proof of concept is relevant in the field of neurodegenerative diseases. The targeted neuronal population used to have heterogeneous degrees of pathology, with some of them at late neuropathological stages, while others are still not affected, which gives an opportunity to autophagy induction as a way of halting progression. These results may resolve the questions raised due to controversial studies about the direction in autophagy modulation for therapy, whether being inhibited or activated, regarding some neurodegenerative diseases[53,54].

Finally, we collect evidence of a possible mechanism by which autophagy induction may prevent the apparition of a neurodegenerative process due to cytoskeletal alterations. By overexpressing ATG5, several issues are correcting: increase in vesicle trafficking-related proteins, improvement of lysosomal function and, importantly, attenuation of microtubule disorder after the lesion. How might this be possible? One explanation is that the lesion may lead to early aberrant accumulation of cytoskeletal proteins as hyperphosphorylated isoforms[5]. Ready autophagy machinery may help get rid off annoying accumulated material instantaneously before the situation worsens. Therefore, lack of cytoskeletal alterations allows the function of autophagy flux itself as a positive feedback loop.

Thus, enhancing and favoring proper function of the endogenous mechanisms of self-protection, such as autophagy, may be a way to design efficacious neuroprotective strategies to stop progression.

Materials and methods

Animal model and drug treatment

Sprague–Dawley female rats aged 12 weeks were kept under standard conditions of light and temperature and fed with food and water ad libitum. We performed surgical procedures under anesthesia with a cocktail of ketamine/xylazine (0.1 ml/100 g weight i.p.) essentially as reported previously[5]. To perform extravertebral nerve RA of the L4–L5 roots, we made a midline skin incision to identify sciatic nerves and applied a moderate traction on selected roots away from the intervertebral foramina, severing the mixed spinal nerves that contained the motor and sensory roots and dorsal root ganglia. The wound was sutured by planes, disinfected with povidone iodine, and the animals were allowed to recover in a warm environment. Sham-operated animals were used as controls. In the experiments for autophagy flux analysis, we administered rapamycin (Sigma-Aldrich) daily into the drinking water at concentrations of 0.2 μM for 3 days, a dose that in control animals favored the visualization of LC3 puncta. For this experiment, treatment of animals started 3 days before the sacrifice. Similarly, to analyze its neuroprotective effect, the animals received rapamycin or 0.1% ethanol as vehicle in the drinking water daily for 3 days either pre- or post-RA surgery. Fifteen microliters containing 50 μM nocodazole (Sigma-Aldrich) or DMSO as a vehicle was injected intrathecally at the dural cistern of L2 the same day of the surgery. All procedures involving animals were carried out in accordance with the guidelines of our institution, and the experimental protocols were approved by the Ethics Committee of our institution, and following the European Community Council Directive 86/609/EEC.

Autophagy flux analysis

The mCherry-EGFP-LC3B cDNA (kindly provided by Terje Johansen, University of Tromsøl, Oslo, Norway) was cloned into *Nhe*I and *Hind*III sites between the ITR domains of *AAV2* under the regulation of CMV promoter and the woodchuck hepatitis virus responsive element (WPRE)[55]. The AAV2/rh10 vector was generated as previously described[56] by triple transfection of HEK 293-AAV cells (Stratagene) with branched polyethylenimine (PEI; Sigma-Aldrich) with the plasmid containing the ITRs of AAV2, the AAV helper plasmid containing Rep2 and Cap for rh10 (kindly provided by JM Wilson, University of Pennsylvania, Philadelphia, USA), and the pXX6 plasmid containing helper adenoviral genes[57]. Recombinant vectors were clarified after benzonase treatment (50 U/ml, Novagen) and polyethylene glycol (PEG 8000, Sigma-Aldrich) precipitation. Vectors were purified by iodixanol gradient by the Vector Production Unit at CBATEG (UAB; http://sct.uab.cat/upv) following standard operating procedures. Viral

genomes per ml (vg/ml) were quantified using picogreen (Invitrogen)[57].

Intrathecal administration of viral vector was performed at the lumbar region of isoflurane-anesthetized animals using a 33-gauge needle and a Hamilton syringe. After lateral spine exposure, by paravertebral muscle dissection, 10 µl of viral vectors were slowly injected into the cerebrospinal fluid between vertebrae L3 and L4. Appropriate access to the intrathecal space was confirmed by the animal's tail movement. The needle was held in place at the injection site for 1 min after which the muscle and skin were sutured. For the analysis, we counterstained sections from rapamycin-treated control and RA-injured untreated rats injected with AAV-mCherry-GFP-LC3 with Fluorescent Nissl Stain (NeuroTrace, Molecular Probes) and analyzed the sections by confocal microscope. Images were acquired with the 63× oil immersion objective using GFP and TXRED filters and merged both channels for co-localization analysis (i.e., red and yellow puncta analysis). Quantitative analyses of LC3B-GFP-mCherry were performed using ImageJ software (National Institutes of Health; available at http://rsb.info.nih.gov/ij/). Image analyses were carried out by selecting the cells in the images and determining the co-localization between GFP and mCherry signals.

Sample preparation

Rats were deeply anesthetized with dolethal ($n = 4$–5) at 7 days post RA or sham operation to obtain L4–L5 spinal cord segments (5-mm length) for western blot analysis. Samples were snap frozen in liquid nitrogen for storage or were immediately processed by homogenization in lysis buffer (20 mM HEPES, pH 7.2, 250 mM sucrose, 1 mM EDTA, 1 mM EGTA, and a cocktail of protease (Sigma-Aldrich) and phosphatase inhibitors (Roche)) in a Potter homogenizer on ice. After centrifugation of lysates at 800×*g* for 20 min at 4 °C, we collected the supernatant as a cytosolic fraction and quantified the proteins by BCA assay (Pierce Chemical Co.). For western blotting, we loaded 30 µg of cytosolic fractions of L4–L5 segments from each animal onto 12% SDS-polyacrylamide gels to perform electrophoretic separation of the proteins, followed by transference to a PVDF membrane in a BioRad cuvette system in 25 mM Tris, pH 8.4, 192 mM glycine, 20% (v/v) methanol. Membranes were blocked with 5% BSA in phosphate-buffered saline (PBS) plus 0.1% Tween-20 for 1 h at room temperature and then incubated at 4 °C overnight with primary antibody. Antibodies used were the following: anti-β-Actin (A5316; 1:10000; Sigma-Aldrich), anti-ATP6V0A1 (ABIN487206; 1:500; Antibodies Online), anti-DCTN1 (ABIN1683528; 1:500; Antibodies Online), anti-EEA1 (ab50313; 1:1000; Abcam), anti-KIF5C (ab5630; 1:1000; Abcam), anti-LAMP1 (3629; 1:500; Prosci); anti-p62 (610833; 1:100; BD Transduction Laboratories), anti-p115 (612261; 1:1000; BD Transduction Laboratories), and anti-Sec31A (17913; 1:500; Proteintech). After several washes, the membranes were incubated for 2 h with an appropriate secondary antibody conjugated with horseradish peroxidase (1:5000, Vector). The membrane was visualized using a chemiluminescent mixture of one volume 0.5 M luminol, 79.2 mM p-coumaric acid, 1 M Tris-HCl, pH 8.5 and one volume 8.8 M hydrogen peroxide, 1 M Tris-HCl, pH 8.5. Images collected with the Gene Genome apparatus (Syngene) and analyzed with Gene Snap and Gene Tools softwares.

For glycosylation analysis, we used 30 µg protein and submitted to deglycosylation using the Protein Deglycosylation Mix II (New Legends Biolabs) and following the manufacturer's recommendations before loading the samples in 10% SDS-polyacrylamide.

For immunohistochemistry, at 7 dpi, we transcardially perfused the deeply anesthetized animals with a saline solution containing 10 U/ml heparin followed by 4% paraformaldehyde (PFA) in a 0.1-M phosphate buffer, pH 7.2, for tissue fixation ($n = 4$ at each time post lesion) and removed the L4 and L5 segments (5-mm total length) of the spinal cord, post-fixed in the same fixative for an extra 4 h and cryopreserved in 30% sucrose overnight. We cut the samples into serial transverse sections (20-µm thick) onto gelatinized slides using a cryotome (Leica) and preserved them at −20 °C until used. For immunohistochemistry, we treated the slides with blocking solution in Tris-buffered saline (TBS) with 0.03% Triton-X-100 and 10% bovine serum for 1 h and incubated thereafter with primary antibodies anti-DCTN1 (ABIN1683528; 1:500; Antibodies Online) or anti-KIF5C (ab5630; 1:1000; Abcam). After several washes with TBS, 0.05% Tween-20, the sections were incubated for 2 h with Cy-2- or Cy-3-conjugated donkey anti-rabbit antibodies (Jackson Immunoresearch). We counterstained the sections with DAPI (Sigma-Aldrich), or NeuroTrace Fluorescent Nissl Stain (Molecular Probes) and mounted the slices with Fluoromount-G mounting medium (Southern Biotech) or Mowiol. Sections of injured and control animals were processed in parallel for immunohistochemistry. Images of the ventral horn spinal cord samples were taken under the same exposure times, sensitivities, and resolutions for each marker analyzed with the aid of a digital camera (Olympus DP50) attached to the microscope (Olympus BX51). Confocal microscope examinations were performed with a Zeiss LSM 700 system.

In vitro model

NSC34 cells were grown in modified Eagle's medium high-glucose (DMEM) supplemented with 10% fetal bovine serum (Sigma-Aldrich), and 0.5× penicillin/streptomycin solution (Sigma-Aldrich). Cells were kept in a humidified incubator at 37 °C under 5% CO_2. For the

treatments, we coated plastic plates (Thermo) with 10% collagen dissolved in Milli-Q water at 37 °C for 2 h. After removing this solution, we seeded the cells at a density of 2.5×10^5 per cm^2. After 4 days of culture without changing the medium, NSC34 cells present with a differentiated-like phenotype characterized by the presence of long neurite extensions. At this time, we added different drugs to the cells. The drugs, prepared at a concentration 10-fold higher than the concentration to be tested, were dissolved in DMEM to the desired concentration and used to replace medium over cells. We used 1 μM rapamycin (Sigma-Aldrich) and 50 μM nocodazole (Sigma-Aldrich) unless otherwise stated. After 18 h, we assessed cell viability by incubating the cells with 0.4 mg/ml of MTT for 3 h. The formed blue formazan crystals were dissolved with DMSO, and the absorbance at 570 nm was measured with a microplate reader (Bio-tek, Elx800) ($n = 4–5$).

We transfected 1×10^5 cells with 2 μg GFP-LC3-mCherry plasmid (kindly provided by Terje Johansen, University of Tromsøl, Oslo, Norway) using the Amaxa Nucleofector II TM (Lonza) and the Nucleofactor V kit (Lonza) following the manufacturer's recommendations. LC3 puncta were analyzed as described above.

For western blot, the cells were harvested and homogenized in modified RIPA buffer (50 mM Tris-HCl, pH 7.5, 150 mM NaCl, 1 mM EGTA, 1% NP-40, 0.5% sodium deoxycholate, 0.1% SDS, protease and phosphatase cocktails). For immunocytochemistry, we coated 12-mm glass coverslips with 10% collagen placed in 24-well plates and seeded the cells onto them. After culture, we fixed the cells with 4% PFA, rinsed twice with PBS, and stored at −20 °C or added blocking buffer containing PBS plus 0.3% (v/v) Triton X-100 and 10% fetal bovine serum. We incubated with the following primary antibodies: anti-DCTN1 (ABIN1683528; 1:500; Antibodies Online), anti-giantin (324450; 1:100; Calbiochem), anti-KIF5C (AP52366; 1:100; Acris Antibodies), mouse-anti-α-tubulin (1:500; Sigma Aldrich), mouse-anti acetylated α-tubulin (AA4.3, 1:500; Hybridoma Bank, Iowa City, IA, USA), mouse anti-β-tubulin (1:500, Covance/biolegend, San Diego, CA, USA) or anti-LAMP1; (1D4B, 1:100, Hybridoma Bank) in 0.5× blocking buffer in PBS, at 4 °C overnight. The following day, after several washes with PBS plus 0.05% Tween-20, we incubated the coverslips with Cy3- or Cy2-conjugated secondary antibodies (Jackson Immunoresearch). Coverslips were counterstained with DAPI, and mounted with Mowiol. Images were taken under the same exposure times, sensitivities, and resolutions for each marker analyzed with the aid of a digital camera (Olympus DP50) attached to the microscope (Olympus BX51). Confocal microscope examinations were performed with a Zeiss LSM 700 system. Comparisons for tubulins or GFAP staining were performed taking microphotographs at 20× magnification from at least five spinal cord sections (separated by 200-μm between pairs), and transforming them to gray scale using ImageJ software. Immunoreactivity can be analyzed by measuring the integrated density of a region of interest (ROI) after defining a threshold for background correction 5. The ROIs were selected on the gray matter at the ventral horn and had an area of 0.11 mm^2. For tubulin immunoreactivity analysis, the ROI enclose the MN soma, determined by Nissl staining. Pictures were obtained for at least 15 MNs extracted from three different sections (separated by 100 μm between each section) per animal for each marker.

Motor neuron counting

Spinal cord sections were selected with a random start and then sampled systematically (every 12th section) to generate serial subsamples from each lumbar spinal cord of animals at 21 dpi. Eight series of 10 sections (separated by 100 μm) of each processed L4–L5 spinal cord were stained with fluorescent NeuroTrace (Life Technologies, Carlsbad, CA, USA) following the manufacturer's protocol. Sequential microphotographs were taken covering the lateral ventral horn at 10×. Large MNs were identified by their localization in the lateral ventral horn of lumbar spinal cord sections and only MNs with diameters of 30–70 μm with prominent nucleoli and polygonal shapes located at the layer IX of the ventral horn were counted[2,5,10]. The mean number of MNs per section was calculated. For comparisons, the estimated number of MNs present in the ventral horn of the avulsed side was expressed as a percentage of the contralateral side.

Analysis of acidic vesicular organelles

To evaluate the acidic vesicular organelles, we incubated cells with AO (Sigma-Aldrich) at a final concentration of 1 μg/ml for 10 min. We pre-treated NSC34 cells with 1 μM of BafA1 (Sigma-Aldrich) to specifically inhibit the vacuolar proton pump v-ATPase mainly at lysosomes. After two washes with pre-warmed PBS with calcium and magnesium, we immediately visualized and analyzed the slices using an Olympus 8160 fluorescence microscope. We collected and recorded the intensity for each excitation wavelength for independent images maintaining the same exposure conditions for all the experiments ($n = 30$ cells/condition). The ratio of 598–511 nm (red vs. green fluorescence) was calculated for each cell and condition.

Bioinformatics and statistics

We performed GO and pathway analyses of the signatures for degenerative process after RA[7] with STRING (http://string-db.org/)[58] and DAVID (http://david.niaid.nih.gov/david/version2/index.htm)[59] web tools. Data shown are means (±SEM) of a least three independent experiments. We used analyses of variance (ANOVA) to compare the values among different experimental groups for data

that met the normality assumption. Difference between groups was analyzed by using a one-way ANOVA, followed by Tukey's post hoc multiple-range test or Student's *t*-test. All statistical analyses were done using GraphPad Prism 5 software ($n = 3–5$; $p < 0.05$ for significance).

Acknowledgements
We thank Terje Johansen at the University of Tromsoe in Norway for the kind gift of the mCherry-GFP-LC3 plasmid and to Patrice Codogno and Nicolas Dupont at Institut Necker Enfants-Malades in Paris for the kind gift of CMV-ATG5 plasmid. We thank Marta Morell for animal care and Meritxell Puig for technical assistance. The 1D4B and AA4.3 antibodies were obtained from the Developmental Studies Hybridoma Bank developed under the auspices of the NICHD and maintained by the University of Iowa, Department of Biology. This work was supported by grants from Fundació La marató-TV3 (#110432) and to Ministerio de Economía y Competitividad of Spain (#SAF 2014-59701). We are also grateful for the support from CIBERNED.

Authors' contributions
T.L.R. carried out all the experiments in vitro and in vivo, analyzed the results, and wrote part of the paper. M.H.G. obtained the samples for the proteomic analysis. D.R.G., S.M.A., and J.F. helped with in vivo experiments and processing of the samples. A.B. helped with the construction of the viral vector. C.C. conceived, designed, and guided all the experiments, performed analysis of the results, and wrote the paper.

Author details
[1]Institut de Neurociències and Department of Cell Biology, Physiology and Immunology, Universitat Autònoma de Barcelona (UAB), Centro de Investigación Biomédica en Red sobre Enfermedades Neurodegenerativas (CIBERNED), 08193Bellaterra, Barcelona, Spain. [2]Department of Biochemistry and Molecular Biology, Center of Animal Biotechnology and Gene Therapy (CBATEG), UAB, CIBERNED, Barcelona, Spain. [3]Hand and Peripheral Nerve Unit, Hospital Clínic i Provincial, Universitat de Barcelona, Barcelona, Spain

Conflict of interest
The authors declare that they have no conflict of interest.

Supplementary Information accompanies this paper at (https://doi.org/10.1038/s41419-018-0682-y).

Received: 6 November 2017 Revised: 17 April 2018 Accepted: 2 May 2018
Published online: 24 May 2018

References

1. Casas, C., Manzano, R., Vaz, R., Osta, R. & Brites, D. Synaptic failure: focus in an integrative view of ALS. *Brain Plast.* **1**, 159–175 (2016).
2. Romeo-Guitart, D., Fores, J., Navarro, X. & Casas, C. Boosted regeneration and reduced denervated muscle atrophy by neuroheal in a pre-clinical model of lumbar root avulsion with delayed reimplantation. *Sci. Rep.* **7**, 1–12 (2017).
3. Snider, W. D., Elliott, J. L. & Yan, Q. Axotomy-induced neuronal death during development. *J. Neurobiol.* **23**, 1231–1246 (1992).
4. Koliatsos, V. E., Price, W. L., Pardo, C. A. & Price, D. L. Ventral root avulsion: an experimental model of death of adult motor neurons. *J. Comp. Neurol.* **342**, 35–44 (1994).
5. Penas, C., Casas, C., Robert, I., Forés, J. & Navarro, X. Cytoskeletal and activity-related changes in spinal motoneurons after root avulsion. *J. Neurotrauma* **26**, 763–779 (2009).
6. Valero-Cabré, A., Tsironis, K., Skouras, E., Navarro, X. & Neiss, W. F. Peripheral and spinal motor reorganization after nerve injury and repair. *J. Neurotrauma* **21**, 95–108 (2004).
7. Casas, C. et al. Network-based proteomic approaches reveal the neurodegenerative, neuroprotective and pain-related mechanisms involved after retrograde axonal damage. *Sci. Rep.* **5**, 9185 (2015).
8. Raiborg, C. & Stenmark, H. The ESCRT machinery in endosomal sorting of ubiquitylated membrane proteins. *Nature* **458**, 445–452 (2009).
9. Feng, Y., Yao, Z. & Klionsky, D. J. How to control self-digestion: transcriptional, post-transcriptional, and post-translational regulation of autophagy. *Trends Cell Biol.* **25**, 354–63 (2015).
10. Penas, C. et al. Autophagy, and BiP level decrease are early key events in retrograde degeneration of motoneurons. *Cell Death Differ.* **18**, 1617–1627 (2011).
11. Bjørkøy, G. et al. p62/SQSTM1 forms protein aggregates degraded by autophagy and has a protective effect on huntingtin-induced cell death. *J. Cell Biol.* **171**, 603–614 (2005).
12. Homs, J. et al. Intrathecal administration of IGF-I by AAVrh10 improves sensory and motor deficits in a mouse model of diabetic neuropathy. *Mol. Ther. Methods Clin. Dev.* **1**, 1–7 (2014).
13. Castillo, K. et al. Measurement of autophagy flux in the nervous system in vivo. *Cell Death Dis.* **4**, e917 (2013).
14. Saftig, P. & Klumperman, J. Lysosome biogenesis and lysosomal membrane proteins: trafficking meets function. *Nat. Rev. Mol. Cell Biol.* **10**, 623–635 (2009).
15. Nishi, T. & Forgac, M. The vacuolar (h+)-ATPases — nature's most versatile proton pumps. *Nat. Rev. Mol. Cell Biol.* **3**, 94–103 (2002).
16. Raval, K. K. et al. Pompe disease results in a Golgi-based glycosylation deficit in human induced pluripotent stem cell-derived cardiomyocytes. *J. Biol. Chem.* **290**, 3121–3136 (2015).
17. Dirac-Svejstrup, A. B., Shorter, J., Waters, M. G. & Warren, G. Phosphorylation of the vesicle-tethering protein P115 by a casein kinase II-like enzyme is required for golgi reassembly from isolated mitotic fragments. *J. Cell Biol.* **150**, 475–488 (2000).
18. Yoder, A. et al. Effects of microtubule modulators on HIV-1 infection of transformed and resting CD4 T cells. *J. Virol.* **85**, 3020–3024 (2011).
19. Beske, O., Reichelt, M., Taylor, M. P., Kirkegaard, K. & Andino, R. Poliovirus infection blocks ERGIC-to-Golgi trafficking and induces microtubule-dependent disruption of the Golgi complex. *J. Cell Sci.* **120**, 3207–3218 (2007).
20. Tie, H. C. et al. A novel imaging method for quantitative Golgi localization reveals differential intra-Golgi trafficking of secretory cargos. *Mol. Biol. Cell.* **27**, 848–861 (2016).
21. Klionsky, D. J. et al. Guidelines for the use and interpretation of assays for monitoring autophagy. *Autophagy* **8**, 445–544 (2012).
22. Traganos, Z. & Darzynkiewicz, F. Lysosomal proton pump activity: supravital cell staining with acridine orange differentiates leukocyte subpopulations. *Methods Cell Biol.* **41**, 185–194 (1994).
23. Ganley, I. G., Wong, P.-M., Gammoh, N. & Jiang, X. Distinct autophagosomal-lysosomal fusion mechanism revealed by thapsigargin-induced autophagy arrest. *Mol. Cell* **42**, 731–743 (2011).
24. Morikawa, W. et al. Angiostatin generation by cathepsin D secreted by human prostate carcinoma cells. *J. Biol. Chem.* **275**, 38912–38920 (2000).
25. Janke, C. & Chloë Bulinski, J. Post-translational regulation of the microtubule cytoskeleton: mechanisms and functions. *Nat. Rev. Mol. Cell Biol.* **12**, 773–786 (2011).
26. Dompierre, J. P. et al. Histone deacetylase 6 inhibition compensates for the transport deficit in Huntington's Disease by increasing tubulin acetylation. *J. Neurosci.* **27**, 3571–3583 (2007).
27. Kanai, Y. et al. KIF5C, a novel neuronal kinesin enriched in motor neurons. *J. Neurosci.* **20**, 6374–6384 (2000).
28. Smith, M. J., Pozo, K., Brickley, K. & Stephenson, F. A. Mapping the GRIF-1 binding domain of the kinesin, KIF5C, substantiates a role for GRIF-1 as an adaptor protein in the anterograde trafficking of cargoes. *J. Biol. Chem.* **281**, 27216–27228 (2006).
29. Astanina, K., & Jacob, R.. KIF5C, a kinesin motor involved in apical trafficking of MDCK cells. *Cell. Mol. Life Sci.* **67**, 1331–1342 (2010).
30. Willemsen, M. H. et al. Involvement of the kinesin family members KIF4A and KIF5C in intellectual disability and synaptic function. *J. Med. Genet.* **51**, 487–494 (2014).
31. Eschbach, J. & Dupuis, L. Cytoplasmic dynein in neurodegeneration. *Pharmacol. Ther.* **130**, 348–363 (2011).
32. Zhao, C. et al. Charcot-Marie-Tooth disease type 2A caused by mutation in a microtubule motor KIF1Bbeta. *Cell* **105**, 587–597 (2001).

33. Kuźma-Kozakiewicz, M. et al. Dynactin deficiency in the CNS of humans with sporadic ALS and mice with genetically determined motor neuron degeneration. *Neurochem. Res.* **38**, 2463 (2013).
34. Levy, J. R. & Holzbaur, E. L. F. Cytoplasmic dynein/dynactin function and dysfunction in motor neurons. *Int. J. Dev. Neurosci.* **24**, 103–111 (2006).
35. D'Arcangelo, J. G., Stahmer, K. R. & Miller, E. Vesicle-mediated export from the ER: COPII coat function and regulation. *Biochim. Biophys. Acta* **1833**, 2464–2472 (2013).
36. Mishima, T., Fujiwara, T., Sanada, M., Kofuji, T. & Kanai-azuma, M. Syntaxin 1B, but not syntaxin 1A, is necessary for the regulation of synaptic vesicle exocytosis and of the readily releasable pool at central synapses. *PLoS ONE* **9**, e90004 (2014).
37. Spang, A. The road not taken: less traveled roads from the TGN to the plasma membrane. *Membranes (Basel)* **5**, 84–98 (2015).
38. Okamoto, K.-I., Narayanan, R., Lee, S. H., Murata, K. & Hayashi, Y. The role of CaMKII as an F-actin-bundling protein crucial for maintenance of dendritic spine structure. *Proc. Natl Acad. Sci. USA* **104**, 6418–6423 (2007).
39. Bai, Y., Xiang, X., Liang, C. & Shi, L. Regulating Rac in the nervous system: molecular function and disease implication of Rac GEFs and GAPs. *Biomed. Res. Int.* **2015**, 632450 (2015).
40. D'Ambrosi, N., Rossi, S., Gerbino, V. & Cozzolino, M. Rac1 at the crossroad of actin dynamics and neuroinflammation in Amyotrophic Lateral Sclerosis. *Front. Cell. Neurosci.* **8**, 279 (2014).
41. Brown, M. E. & Bridgman, P. C. Myosin function in nervous and sensory systems. *J. Neurobiol.* **58**, 118–130 (2004).
42. Brandstaetter, H., Kishi-Itakura, C., Tumbarello, D. A., Manstein, D. J. & Buss, F. Loss of functional MYO1C/myosin 1c, a motor protein involved in lipid raft trafficking, disrupts autophagosome-lysosome fusion. *Autophagy* **10**, 2310–2323 (2014).
43. Mellman, I. Endocytosis and molecular sorting. *Annu. Rev. Cell Dev. Biol.* **12**, 575–625 (1996).
44. Lee, J. et al. Lysosomal proteolysis and autophagy require presenilin 1 and are disrupted by Alzheimer-related PS1 mutations. *Cell* **141**, 1146–1158 (2013).
45. Parker, A. L., Kavallaris, M. & McCarroll, J. A. Microtubules and their role in cellular stress in cancer. *Front. Oncol.* **4**, 153 (2014).
46. Aplin, A., Jasionowski, T., Tuttle, D. L., Lenk, S. E. & Dunn, W. A. Cytoskeletal elements are required for the formation and maturation of autophagic vacuoles. *J. Cell. Physiol.* **152**, 458–466 (1992).
47. Seglen, P. O. et al. in *Intracellular Protein Catabolism* (eds Suzuki, K. & Bond, J. S.) 103–111 (Springer US, Boston, MA, 1996).
48. Köchl, R. et al. Microtubules facilitate autophagosome formation and fusion of autophagosomes with endosomes. *Traffic* **7**, 129–145 (2006).
49. Fass, E., Shvets, E., Degani, I., Hirschberg, K. & Elazar, Z. Microtubules support production of starvation-induced autophagosomes but not their targeting and fusion with lysosomes. *J. Biol. Chem.* **281**, 36303–36316 (2006).
50. Kimura, S., Noda, T. & Yoshimori, T. Dynein-dependent movement of autophagosomes mediates efficient encounters with lysosomes. *Cell Struct. Funct.* **122**, 109–122 (2008).
51. Scheel, J., Matteoni, R., Ludwig, T., Hoflack, B. & Kreis, T. E. Microtubule depolymerization inhibits transport of cathepsin D from the Golgi apparatus to lysosomes. *J. Cell Sci.* **96**(Pt. 4), 711–720 (1990).
52. Renna, M. et al. Autophagic substrate clearance requires activity of the syntaxin-5 SNARE complex. *J. Cell Sci.* **124**, 469–482 (2011).
53. Nguyen, D. K. H., Thombre, R. & Wang, J. Autophagy as a common pathway in amyotrophic lateral sclerosis. *Neurosci. Lett.* https://doi.org/10.1016/j.neulet.2018.04.006 (2018).
54. Sheehan, P. & Yue, Z. Deregulation of autophagy and vesicle trafficking in Parkinson's disease. *Neurosci. Lett.* https://doi.org/10.1016/j.neulet.2018.04.013 (2018).
55. Loeb, J. E., Cordier, W. S., Harris, M. E., Weitzman, M. D. & Hope, T. J. Enhanced expression of transgenes from adeno-associated virus vectors with the woodchuck hepatitis virus posttranscriptional regulatory element: implications for gene therapy. *Hum. Gene Ther.* **10**, 2295–2305 (1999).
56. Zolotukhin, S. et al. Recombinant adeno-associated virus purification using novel methods improves infectious titer and yield. *Gene Ther.* **6**, 973–985 (1999).
57. Piedra, J. et al. Development of a rapid, robust, and universal picogreen-based method to titer adeno-associated vectors. *Hum. Gene Ther. Methods* **26**, 35–42 (2015).
58. Szklarczyk, D. et al. The STRING database in 2011: functional interaction networks of proteins, globally integrated and scored. *Nucleic Acids Res.* **39**, D561–D568 (2011).
59. Dennis, G. et al. DAVID: Database for Annotation, Visualization, and Integrated Discovery. *Genome Biol.* **4**, P3 (2003).

Chapter 2

GRP78/BiP Overexpression Triggers PINK1/IP_3R-Mediated Neuroprotective Mitophagy

Tatiana Leiva-Rodríguez[1], David Romeo-Guitart[1], Pau Muñoz-Guardiola[2], Miriam Polo[3], Celia Bañuls[3], Mireia Herrando-Grabulosa[1], Valerie Petegnief[4], Assumpció Bosch[2], Jose Miguel Lizcano[2], Nadezda Apostolova[5], Joaquim Forés[6], Caty Casas[1]

Affiliations

[1] *Institut de Neurociències* (INc) and Department of Cell Biology, Physiology and Immunology, *Universitat Autònoma de Barcelona* (UAB), & *Centro de Investigación Biomédica en Red sobre Enfermedades Neurodegenerativas* (CIBERNED), Bellaterra, Barcelona, Spain.

[2] INc and Department of Biochemistry and Molecular Biology, UAB.

[3]Service of Endocrinology. University Hospital Dr. Peset, Foundation for the Promotion of Health and Biomedical Research in the Valencian Region (FISABIO), Valencia.

[4]Department of Brain Ischemia and Neurodegeneration, Institute for Biomedical Research of Barcelona (IIBB), Spanish Research Council (CSIC), *Institut d'Investigacions Biomèdiques August Pi Sunyer* (IDIBAPS), Barcelona, Spain

[5]Departament de Farmacologia, Facultat de Medicina, Universitat de Valencia; CIBERehd.

[6]Hand and Peripheral Nerve Unit, Hospital Clínic i Provincial, *Universitat de Barcelona*, Barcelona, Spain Biotech, S.L, Barcelona, Spain

*Correspondence should be addressed to: Caty Casas Louzao, *Unitat de Fisiologia Mèdica*, *Facultat de Medicina*, *Universitat Autònoma de Barcelona*, E-08193 Bellaterra, Barcelona, Spain. Tel: +34-935811324, Fax: +34-935812986, E-mail: Caty.Casas@uab.cat

Running title: GRP78/BiP triggers mitophagy

ABSTRACT

Disconnection between the neuronal soma and their axon or dendrites can lead to neuronal dysfunction and death. This type of event is very common in the frame of neurodegenerative pathologies and understanding of the subjacent mechanisms is relevant to promote effective therapeutic strategies. In our model, based on traction of the L4-L5 root nerves (root avulsion (RA) model), a retrograde and complex network of processes is triggered to lead to spinal motoneurons (MN) death. One of the key signaling pathways engaged is the endoplasmic reticulum (ER) stress although with some defaults in its program. It is characterized by an important reduction of BiP, the luminal chaperone that orchestrate ER stress response. We previously demonstrated that BiP was relevant to promote neuroprotection after this type of injury and now we wanted to explore the mechanism by which BiP overexpression exerts this effect. Herein, bioinformatic analysis revealed that BiP overexpression clearly modulated mitochondrial function. We discovered that GRP78/BiP overexpression induces the downregulation of mitochondrial proteins by the induction of mitophagy *in vitro*. In this activation of mitophagy by GRP78/BiP is implicate IP3R and PINK1. In vivo, mitophagy activation seems to be involved in a PINK1 dependent. These discoveries serve as proof of concept for design effective therapies to halt neurodegenerative disorders.

INTRODUCTION

Functional connectivity disruption is a common early characteristic of the neurodegenerative processes (Conforti *et al.*, 2014). Axonal degeneration often leads to retrograde neuronal cell death or atrophy and the progressive and permanent loss of vital neuronal functions. Neurons react in front of damage engaging endogenous mechanisms of neuroprotection that encompass the unfolded protein response (UPR), the heat-shock response, the autophagy pathway, the ubiquitin-proteasome system, chaperone, the endoplasmic reticulum (ER)-associated degradation machinery (ERAD) and the antioxidant defence. Excess damage as well as aging can result in defective functioning of one or more of those programs what make neurons succumb. Boosting these endogenous mechanisms may be a smart strategy for neuroprotection (Romeo-Guitart *et al.*, 2017, 2018).

GRP78/BiP, also known as Heat Shock protein 5a (HSP5a), is a multifunctional protein with central activities of endogenous mechanisms of neuroprotection (Casas, 2017). It orchestrates the UPR, activated after endoplasmic reticulum (ER) stress, presents ATPase activity and is a major Ca^{2+} binding protein (Reddy *et al.*, 2003) (Wang and Kaufman, 2016). It also, acts to promote the proper folding of newly synthetized or misfolded proteins or to drive disassembled proteins for degradation by ERAD machinery (review in (Printsev et al., 2016)). Evidences also point to its participation also in triggering macroautophagy that removes both soluble and aggregated forms of unfolded proteins and dysfunctional organelles (Wen et al., 2012; Cook and Clarke, 2012(Li et al., 2015) (Cha-Molstad et al., 2016; Cha-Molstad et al., 2015; Abdel Malek et al., 2015; Jin et al., 2014; Kim et al., 2014). Overexpression of GRP78/BiP has been proven to be neuroprotective in several models (Kudo *et al.*, 2008)(Oida *et al.*, 2010)(Ni et al., 2011) (Ouyang *et al.*, 2011) (Guzmán-Lenis *et al.*, 2009; Penas, Font-Nieves, *et al.*, 2011; Penas, Pascual-Font, *et al.*, 2011) (Louessard 2017) and a reduction in GRP78/BiP levels has been observed during aging and throughout progression of degenerative disorders (Paz Gavilán et al., 2006). Some works reported that its neuroprotection was mediated by inhibition of apoptosis, however, apoptosis is rarely the main cause of neuronal cell death in many neurodegenerative processes.

By exploiting the anatomical and technical advantages of several models of axotomy, it has been revealed the concurrence of multiple signaling programs in neuronal soma during retrograde neurodegeneration, a process that does not end up with apoptosis (Penas, Font-Nieves, *et al.*, 2011; Casas, Isus, Herrando-Grabulosa, Francesco M Mancuso, *et al.*, 2015). Instead, the problem seem to be related to a difficulty to successfully override programs for self-repairing (Penas, Font-Nieves, *et al.*, 2011; Casas, Isus, Herrando-Grabulosa, Francesco M Mancuso, *et al.*, 2015; Leiva-Rodríguez *et al.*, 2018; Romeo-Guitart *et al.*, 2018). Comparing models of axotomy of spinal motoneurons either by mechanical traction of the sciatic nerve root (root avulsion, RA), that produces the progressive degeneration of more than 80% of MNs over a month post injury, or distal nerve transection and suture of the nerve that supports viability, we discovered that the chaperone GRP78/BiP was essential for MN survival (Penas et al., 2011). Thus, we aimed to clarify the mechanisms that mediate GRP78/BiP neuroprotection starting from unbiased proteomic analysis.

MATERIALS AND METHODS

Surgical procedures

Sprague–Dawley female rats aged 12 weeks were kept under standard conditions of light and temperature and fed with food and water ad libitum. We performed surgical procedures under anesthesia with a cocktail of ketamine/xylazine 0.1 mL/100 g weight i.p essentially as reported previously (Penas *et al.*, 2009)(Leiva-Rodríguez *et al.*, 2018)). To perform extravertebral nerve root avulsion of the L4–L5 roots we made a midline skin incision to identify each side sciatic nerve and applying a moderate traction on selected roots away from the intervertebral foramina, obtaining the mixed spinal nerves that contained the motor and sensory roots and dorsal root ganglia out. The wound was sutured by planes, disinfected with povidone iodine and the animals allowed recovering in a warm environment. Sham animals were used as controls. All the procedures that involved animals were approved by the of Universitat Autònoma de Barcelona and Generalitat de Catalunya and follow the European Community Council Directive 2010/63/EU.

Construction, purification, and infection with recombinant adenovirus vectors

cDNA encoding grp78 (ATCC, LGC Promochem) was cloned into the pAC.CMV shuttle vector. Recombinant adenoviruses were constructed by homologous recombination in HEK293 cells as described earlier,40. A control adenovirus-expressing bacterial b-galactosidase (Ad-β-gal) was a kind gift of C.B. Newgard (Duke University, Durham, NC, USA). Viruses were purified using the Vivapure AdenoPackTM 20 kit according to the instructions of the manufacturer (Sartorius, Goettingen, Germany). For viral infection, immediately after root avulsion the animals were injected with 14 ul of either Ad-GRP78/BiP or Ad-β-gal viruses (10^8 pfu/ml) by means of a 33-gauge needle and a Hamilton syringe into the thecal space at the lumbar site. Appropriate access to the intrathecal space was confirmed by animal tail flick. The needle was held in place at the injection site for one additional minute, after which muscle and skin were sutured. Untreated animals with root avulsion were also used as controls.

Construction, purification, and infection with recombinant adeno-associated vectors

The GRP78/BiP cDNA as cloned into NheI and HindIII sites between the ITR domains of AAV2 under the regulation of CMV promoter and the woodchuck hepatitis virus responsive element (WPRE). The AAV2/rh10 vector was generated as previously described56 by triple transfection of HEK 293-AAV cells (Stratagene) with branched polyethylenimine (PEI; Sigma-Aldrich) with the plasmid containing the ITRs of AAV2, the AAV helper plasmid containing Rep2 and Cap for rh10 (kindly provided by JM Wilson, University of Pennsylvania, Philadelphia, USA), and the pXX6 plasmid containing helper adenoviral genes57. Recombinant vectors were clarified after benzonase treatment (50 U/ml, Novagen) and polyethylene glycol (PEG 8000, Sigma-Aldrich) precipitation. Vectors were purified by iodixanol gradient by the Vector Production Unit at CBATEG (UAB; http://sct.uab.cat/upv) following standard operating procedures. Viral genomes per ml (vg/ml) were quantified using picogreen (Invitrogen).

Intrathecal administration of viral vector was performed at the lumbar region of isoflurane-anesthetized animals using a 33-gauge needle and a Hamilton syringe.

Sample preparation and proteomic analysis

We anesthetized the RA-injured groups of rats (n = 4–5), previously injected with either Ad-β-gal or Ad-GRP78/BiP viruses, at 7 dpi to obtain L4–L5 spinal cord segments (5-mm length) samples to be snap-frozen into liquid nitrogen. We homogenized the tissue in lysis buffer (Hepes 20 mM, Sucrose 250 mM, EDTA 1 mM, EGTA 1 mM and a cocktail of protease and phosphatase inhibitors) with potter homogenizer on ice. After centrifugation of lysates at 800 × *g* for 20 min at 4°C, we collected the supernatant as a cytosolic fraction and quantified by BCA assay (Pierce Chemical Co.; Rockford, IL, USA). For proteomic analysis, we solubilized 75 μg of each sample in 4% SDS, 8 M Urea, 0.1 M HEPES, 0.1 M DTT and subsequently reduced, alkylated in 0.05 M iodoacetamide and digested with trypsin (ratio enzyme:substrate 1:10) using the method FASP (Filter Aided Sample Preparation) as described. All samples were treated in parallel.

We analyzed samples using an LTQ-OrbitrapVelos mass spectrometer (Thermo Fisher Scientific) coupled to a ProxeonEasyLC (Thermo Fisher Scientific). We loaded the peptide mixtures directly onto the analytical column (2 μl·min−1) and separated them by reversed-phase chromatography using a 15-cm column with an inner diameter of 100 μm, packed with 5 μm C18 particles (NikkyoTechnos Co., Ltd.). Chromatographic gradients started at 97% buffer A (0.1% formic acid (FA) in water), and 3% buffer B (acetonitrile, 0.1% FA) with a flow rate of 500 nl·min−1, and gradually increased to 85% buffer A + 15% buffer B in 4 min, and to 55% buffer A + 45% buffer B in 120 min. We operated the instrument in TOP20 DDA (Data Dependent Acquisition) mode with one full MS scan in the Orbitrap at a resolution of 60,000, and a mass range of m/z 350–2,000 followed by MSMS spectra of the 20 most intense ions. We utilized the Ion Trap by CID (collision induced dissociation) to produce fragment ion spectra and used normalized collision energy at 35%. We acquired all data with Xcalibur software v2.1. We used Proteome Discoverer software suite (v1.3.0.339, Thermo Fisher Scientific) and the Mascot search engine (v2.3.01, Matrix Science50) for peptide identification and quantitation. We analysed the data against SwissProt Rat database (released July 2012) containing the most common contaminants (599 entries). We used a precursor ion mass tolerance of 7 ppm at the MS1 level and allowed up to three miscleavages for trypsin. The fragment

ion mass tolerance was set to 0.5 Da. Oxidation of methionine and N-terminal protein acetylation were set as variable modifications whilst cysteine carbamidomethylation was set as fixed modification. We filtered the peptides based on their false discovery rate (FDR > 5% not considered). For peptide quantification, we considered the chromatographic peak of the peptides calculated by Proteome Discoverer, and median normalized the areas by log2 transformation using R 3.0.2. We quantified the data using the R package MSstats (v. 2.0.1). For each ratio, we calculated the adjusted p-value ($p < 0.05$ for significance). Finally, we performed Gene Ontology and pathway analysis for regulated proteins with DAVID Annotation Web tools (http://david.niaid.nih.gov/david/version2/index.htm) and KEGG analysis (https://www.genome.jp/kegg/pathway.html) .

Immunohistochemistry and image analysis

After deep anaesthesia with pentobarbital, we transcardially perfused the animals with a saline solution containing 10 U/ml heparin, followed by 4% paraformaldehyde in a 0.1 M phosphate buffer, pH 7.2 for tissue fixation at 21 dpi (n=4 for each condition), and removed the L4 and L5 segments (5-mm total length) of the spinal cord, which were post-fixed in the same fixative for an extra 4 hours and cryopreserved in 30% sucrose overnight. Serial transverse sections (20-µm thick) were obtained on gelatinized slides using a cryotome (Leica, Heidelberg, Germany) and preserved them at -20 ˚C until use. For immunohistochemistry procedures see supplemental material. Sections to be compared were processed together on the same slide and on the same day. Images of the spinal cord samples from different treatments and controls were taken under the same exposure time, sensibility, and resolution for each marker analysed with the aid of a digital camera (Olympus DP50) attached to the microscope (Olympus BX51). We analysed signal intensity with the ImageJ software (National Institutes of Health; available at http://rsb.info.nih.gov/ij/). Confocal microphotographs of MNs were taken in identical conditions of exposure (Zeiss LSM 700; Zeiss, Jena, Germany).

Western Blot

We deeply anesthetized with dolethal a groups of rats (n=4) with control,root avulsion and root avulsion injected with Ad-ßgal or Ad-BiP virus at 7 dpi to obtain L4–L5 spinal cord segments (5-mm length) for western blot analysis. We snap-

frozen the samples into liquid nitrogen. Samples were stored or further processed by homogenization in lysis buffer (Hepes 20 mM, Sucrose 250 mM, EDTA 1 mM, EGTA 1 mM and a cocktail of protease (Sigma-Aldrich) and phosphatase inhibitors (Roche)) with potter homogenizer on ice. After centrifugation of lysates at 800 x *g* for 20 min at 4°C, we collected the supernatant as a cytosolic fraction and quantified proteins by BCA assay (Pierce Chemical Co.; Rockford, IL, USA). For western blotting, we loaded thirty micrograms of cytosolic fractions of L4–L5 segments from each animal model onto 12% SDS-polyacrylamide gels to perform electrophoretic separation of the proteins following by its transference to a PVDF membrane in a BioRad cuvette system in 25 mM Tris, 192 mM glycine, 20% (v/v) methanol, pH 8.4.We blocked the membranes with 5% BSA in phosphate-buffered saline (PBS) plus 0,1% Tween-20 for 1 h at room temperature and then incubated at 4°C overnight with primary antibody: mouse anti-β-Actin (1:10000; Sigma-Aldrich) , mouse anti-GRP78/BiP (1:500, Sigma-Aldrich), mouse anti-CVβ (1:1000, Invitrogen), rabbit anti-Hsp60 (1:500, Antibodies-online), mouse anti-NDUFA9 (1:1000, Invitrogen), mouse anti-OPA1 (1:1000, BD Biosciences), rabbit anti-PARKIN (1:500, Abcam), mouse anti-PINK1(1:500, Abcam), rabbit anti-NRF2 (1:500, Abcam), anti-MNF2 (1:500, Abcam), rabbit anti-GRP75 (1:500, Abcam). After several washes, membranes were incubated for 2 h with an appropriate secondary antibody conjugated with horseradish peroxidase (1:5000, Vector). The membrane was visualized using a chemoluminiscent mix 1:1 [0.5 M luminol, 79.2 mM p-coumaric acid, 1 M Tris-HCl; pH 8.5] and [8.8 M hydrogen peroxide, 1 M Tris-HCl; pH 8.5], and the images analyzed with Gene Snap and Gene Tools softwares, and Gene Genome apparatus (Syngene, Cambridge, UK).

In vitro model

NSC-34 cells were cultured in modified Eagle's medium high-glucose (DMEM, Biochrom, Berlin) supplemented with 10% Fetal Bovine Serum (FBS) (Sigma-Aldrich, Saint Louis, MO), 100 units/mL penicillin and 0.5 X penicillin/streptomycin solution (Sigma-Aldrich, Saint Louis, MO) and maintained with a humidified incubator at 37ºC under 5% CO2, essentially as described in (Leiva-Rodríguez *et al.*, 2018). After 4 days of cell culture without changing the medium, NSC-34 cells presented a differentiated-like phenotype characterized by the presence of long

neurites. By this time, we add different drugs to the cells which were prepared at a concentration of 10X and dissolved in DMEM. We used Tunicamycin0.1 ug/ul (Sigma-Aldrich) and Efavirenz 10uM (Sustiva ® 600mg, Bristol-Myers Squibb, Princeton, NJ, USA) unless otherwise statement. After 24h, we assessed cell viability by incubating the cells with 4 mg/mL 3-(4,5-dimethylthiazol-2-yl)-2,5-diphenyltetrazolium bromide (MTT) solution for 3h. The formed blue formazan crystals were dissolved with DMSO gently to measure the absorbance at 570 nm (optical density (DO) 570) with a microplate reader (Bio-tek, Elx800) (n=4-5).

Nucleofection

We transfected a million cells with 2 µg GFP, GRP78/BIP, HA-PARK, or mouse shRNA/eGFP, mouse shRNA/ PINK1 (ID 68943, Tebu-bio), mouse shRNA/Hspa5 (ID 14828, Tebu-bio) and mouse shRNA/ITPR3 (ID 16440, Tebu-bio) plasmid preparation using the Amaxa Nucleofector II TM (Lonza, Norwalk) and the Nucleofactor V kit (Lonza) following manufacturer's recommendations. For static cytometric analysis, we seeded the cells in 48-well plates coated with collagen 10%. After culture, we fixed the cells with 4% PFA, rinsed twice with PBS and stored or subsequently added blocking buffer containing PBS 0.3% (v/v) Triton X-100 and 10% of fetal bovine serum). After 3 days of cell culture, we add different drugs to the cells which were prepared at a concentration of 10X and dissolved in DMEM. We used Tunicamycin (Sigma-Aldrich), Carbonyl cyanide 3-chlorophenylhydrazone (CCCP, 10uM Sigma-Aldrich), Cyclosporin A (CsA, 5uM, Sigma-Aldrich) or BAPTA-AM (10uM, Sigma-Aldrich). After 5 hours we fixed the cells for immunocitochemistry or we homogenized the cells for western blot. After 24 h of treatment we assessed cell viability by MTT as a mentioned previously.

For western blot, the cells were harvested and homogenized in modified RIPA buffer (50 mM Tris-HCl, pH 7.5, 150 mM NaCl, 1 mM EGTA, 1% NP-40, 0.5% sodium deoxycholate, 0.1% SDS, protease and phosphatase cocktails). For immunocytochemistry, we plated the cells in 12-mm glass coverslips coated with 10% collagen placed in 24-well plates. After culture, we fixed the cells with 4% PFA, rinsed twice with PBS, and stored at −20 °C or added blocking buffer containing PBS plus 0.3% (v/v) Triton X-100 and 10% fetal bovine serum. We incubated with the following primary antibodies: rabbit anti-IP3R (1:200, Abcam), mouse anti-HA

(1:2000, Abcam) ,mouse anti-GRP78/BiP (1:200, Sigma-Aldrich) and rabbit anti-HSP60 (1:500, Antibodies-online).

Mitochondrial Superoxide Production and Mitochondrial Membrane Potential (ΔΨm)

We treated the Control, GFP or BIP/GRP78 transfected in vehicle (DMSO), Tun, vehicle (Methanol) or EFV and fluorochromes, 1μM Hoescht 33 342, and either 2.5 μM MitoSOX (superoxide analysis) or 2.5 μM TMRM (for ΔΨm analysis), both from Molecular Probes, Invitrogen, Eugene, OR were added for the last 30 minutes of treatment. EFV were used as positive controls for analysis of superoxide production and ΔΨm, respectively. Fluorescence was detected with an IX81 Olympus microscope (Hamburg Germany) and quantified by static cytometry software.

Electrochemical Measurement of Oxygen (O2) consumption

Cells ($1x10^6$ per 1mL of HBSS) were agitated in a gas-tight chamber at 37ºC. Measurements were taken with a Clark-type 02 electrode (Rank Brothers, Bottisham, UK) and recorded with the Dup.18 data acquisition device (WPI, Stevenage, United Kingdom) immediately after 5h treatment with vehicle or Tunicamycin.

Mitochondrial isolation

Cells were homogenized in lysis buffer (HEPES 10 mM pH 7.4, EGTA 1 mM, Sucrose 250 mM and a cocktail of protease (Sigma-Aldrich) and phosphatase inhibitors (Roche)) with potter homogenizer on ice. After centrifugation of lysates at 2,000 x *g* for 5 min, the supernatant was centrifuged at 10,000 x *g* for 12 min. Supernatant was considered the soluble fraction (S2) and contains cytosolic proteins and microsomes. The pellet (P2) was the enriched mitochondrial fraction which was resuspended in modified RIPA buffer (50 mM Tris-HCl, pH 7.5, 150 mM NaCl, 1 mM EGTA, 1% NP-40, 0.5% sodium deoxycholate, 0.1% SDS, protease and phosphatase cocktails) and protein concentration was determined by BCA assay. Samples were then processed for western blot.

Transmission electron microscopy

We submerged spinal cord L4-L5 segments (1mm/slice) in a fixative solution of 2% (w/v) PFA and 2.5% (v/v) glutaraldehyde (EM grade, Merck, Darmstadt, Germany) in PB 0.1M, pH7.4 and placed them on a rocking platform for 2h and then fixed in 1% (w/v) PFA and subsequently post-fixed with 1% (w/v) osmium tetroxide (TAAB Lab., UK) containing 0.08% (w/v) potassium hexocyanoferrate (Sigma-Aldrich, Steinheim, Germany) in PB for 2 additional hours. We performed four washes with deionized water and sequential dehydration in acetone. All procedures were performed at 4ºC (Rodríguez-Cariño et al., 2011). We embedded samples in EPON resin and polymerized at 60ºC for 48h. Samples were processed to obtain semithin sections (1µm) with a Leica ultracut UCT microtome (Leica Microsystems GmbH, Wetzlar, Germany), stained with 1% (w/v) aqueous toluidine blue solution and examined with a light microscope to identify the ventral horn areas enriched with motoneurons. To obtain ultrathin sections (70nm) we cut with diamond knife, placed on coated grids and contrasted with conventional uranyl acetate and Reynolds lead citrate solutions. Finally, we observed the sections with a transmission electron microscope (EM) (Jeol1400 Ltd, Tokyo, Japan) equipped with a GatanUltrascan ES1000CCD Camera. We selected 3 slices/condition, analyzed 3 MNs/section and measure the area of their nucleus compared to the total area of the MN using ImageJ tools.

Bioinformatics and Statistics

Data shown are means (±SEM) of a least three independent experiments. We used analyses of variance (ANOVA) to compare the values among different experimental groups for data that met the normality assumption. Difference between groups was analyzed by using a one-way ANOVA, followed by Tukey's post hoc multiple-range test or Student's t-test. All statistical analyses were done using GraphPad Prism 5 software ($n = 3–5$; $p < 0.05$ for significance).

RESULTS

Proteomic analysis of GRP78/BiP overexpression revealed mitochondria as main target

In order to identify the molecular mechanisms leading to neuroprotection mediated by GRP78/BiP overexpression, we performed a comparative label free proteomic analysis that allowed finding out both quantitative and qualitative differences between RA injured animals infected with an adenovirus that either overexpress GRP78/BiP (Ad- GRP78/BiP), previously found to be neuroprotective of MNs, or beta-galactosidase (Ad-ß-Gal) as a control (Penas, Font-Nieves, *et al.*, 2011). Seven days post injury (dpi) was the targeted time-point where specific neurodegenerative signalling mechanisms emerged in the RA model, as previously observed (Penas, Font-Nieves, *et al.*, 2011)(Casas, Isus, Herrando-Grabulosa, Francesco M. Mancuso, *et al.*, 2015). The LC-MS/MS label free analysis of the cytosolic fractions from L4-L5 spinal cord segments resulted in the identification of a total of 1,420 proteins with at least two peptides per protein. A total of 566 and 732 proteins or peptides were significantly altered due to Ad-GRP78/BiP or Ad-ß-Gal overexpression in RA injured animals respect to the control, respectively ($p<0.05$) **(Tables S1, S2)**. We compared both lists and found that 220 were unique signatures to be specifically altered due to Ad-GRP78/BiP overexpression **(Table S3)**. We attempted for functional annotation of these proteins using the DAVID annotation tool, which allowed identifying the most significant biological functions in the data set (FDR <0.05). The analysis of the comparative data revealed that enriched clusters pointed to mitochondrial processes, function and components (**Table S4, Fig 1A)**. Gene Ontology (GO) terms and KEGG pathways enrichment analysis of these data revealed significant decrease for many proteins related with mitochondria function due to GRP78/BiP overexpression; from the outer, and inner mitocondrial face, several proteins of the respiratory complex and matrix proteins. The most highly downregulated were the Mitochondrial 2-Oxoglutarate/Malate Carrier (OGC, SCL25A11), a tumor suppressor gene that participates to malate-asparate shuttle and regenerates NADH pool in mitochondrial matrix to allow complex I function, or MT-ND3, a NADH Dehydrogenase, Subunit 3 of Complex I, and in minor degree the responsible for catabolism of gamma-aminobutyric acid

(GABA), GABA Aminotransferase (ABAT GABAT), or the Ubiquinol-Cytochrome C Reductase, subunit of Complex III **(Fig 1B).** In contrast, very few proteins were upregulated. One of them was located outside mitochondria but close to it; the glucose-regulated protein 75 (GRP75) located at sites of ER-mitochondrial coupling, termed the mitochondria-associated membranes (MAM), together to the inositol 1,4,5 triphosphate receptor (IP_3R) and voltage dependent anion channel 1 (VDAC1). VDAC in the mitochondria membrane was also detected by the spectrophotometer but was found, in contrast, downregulated in GRP78/BiP overexpressing group. The other proteins up-regulated were the Excitatory Amino Acid Transporter 2 (EAAT2), located in plasma membrane and sometimes in mitochondria at excitatory synapses, and the Hydroxyacyl-CoA Dehydrogenase Trifunctional (HADHA) that catalyzes the last three steps of mitochondrial beta-oxidation of long chain fatty acids. We used western blot to further confirm some of the proteome data and validated mitochondria affectation due to GRP78/BiP overexpression in RA animals. We first analyzed whether mitochondria-related proteins were altered in RA respect to control uninjured animals and observed that Ubiquinone 1 Alpha (NDUFA9), the PTEN Induced Putative Kinase 1 (PINK1), involved in mitophagy, the Nuclear Factor Erythroid 2-Related Factor 2 (NRF2), the encoded transcription factor that regulates genes which contain antioxidant response elements (ARE), and the subunit β of complex V (CVβ) were already diminished in damaged tissue while no-changes were observed in other related proteins as the mitochondrial Dynamin Like GTPase (optic atrophy 1, OPA1) involved in fusion, and the E3 Ubiquitin-Protein Ligase PARKIN (**Fig. 1C).** Next, we analyzed the differences in the levels of some mitochondria-related proteins between GRP78/BiP overexpressing RA-injured animals versus the β-Gal-RA group. We confirmed a significant raise in GRP75 levels ($p<0.05$) and a tend to raise in the Lon peptide (LONP1), an ATP-dependent protease that mediates the selective degradation of misfolded polypeptides while a trend of downregulation of the mitochondrial matrix, OPA1 and CVβ levels ($p<0.1$). No differences in NRF2, mitofusin 2 (MNF2), that participates in mitochondrial fusion, or NDUFA9 were found **(Fig 1D).** Altogether these data confirmed overall alteration of mitochondria protein content due to RA injury but even more pronounced by GRP78/BiP overexpression.

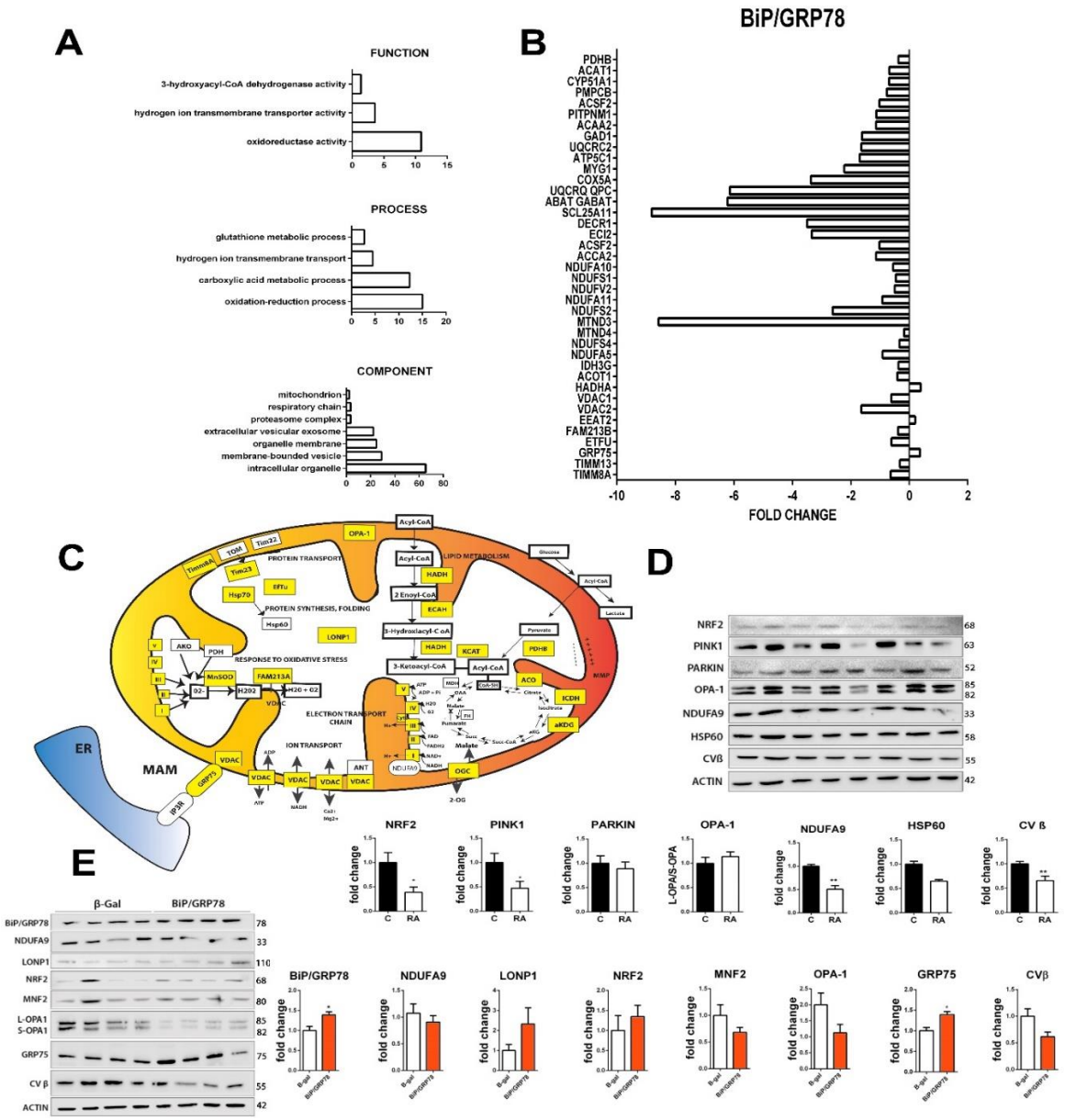

Figure 1. Bioinformatic Analysis of Proteomics. A) DAVID bioinformatic analysis of the comparative data revealed that enriched clusters pointed to mitochondrial processes, function and components. **(B)** Histogram of mitochondrial protein fold changes in GRP78/BiP overexpressed animals after RA respect to β-galactosidase (β-Gal) obtained by analysis of proteomic data. **(C)**Schematic draw of several reduced mitochondrial proteins represented in yellow promoted by GRP78/BiP overexpression in the RA model (7 dpi). **(D)** Immunoblot and bar graph showing the analysis of NRF2, PINK1, PARKIN, OPA-1, NDUFA9, HSP60 and CVβ protein levels in L4 spinal cord segments in control conditions and after RA (n = 4; *p < 0.05 vs. control, *p < 0.05 vs. control Student's t-test). (**E**)ImmunoblotGRP78/BiP, NDUFA9, LONP1, NRF2, MNF2, OPA-1, GRP75 and CVβ. Bar graph showing the average fold change protein level ± SEM in β-galactosidase (β-Gal) and GRP78/BiP treated root avulsed (RA) samples normalized to actin levels (n = 4) *p < 0.05 vs. β-Gal (Student's t-test).

GRP78/BiP overexpression restores damaged mitochondrial function

We then further investigated the particular action of GRP78/BiP overexpression onto mitochondria using an *in vitro* model of ER stress since response to this type of insult appears early after RA injury in vivo, as reported previously (Penas, Font-Nieves, *et al.*, 2011)(Leiva-Rodríguez *et al.*, 2018). We firstly verified that overexpression of GRP78/BiP by nucleofection of the NSC34 motoneuron-like cells produced neuroprotection 24h after tunicamycin (Tun) addition to the culture medium, an ER stress inductor by inhibition the formation of N-acetylglucosamine-lipid intermediates, thereby preventing the glycosylation of newly synthesized proteins **(Fig. 2A, B).** We also found neuroprotection in another *in vitro* model of RA that we previously reported to reproduce several characteristics of the RA injury process of neurodegeneration based on cytoskeletal damage using nocodazole as inductor that interferes with the polymerization of microtubules **(Fig. 2B).**

We assessed mitochondrial function by measuring the generation of reactive oxygen species (ROS) in mitochondria, using MitoSOX; the mitochondrial membrane potential (ΔψM), using Tetramethylrhodamine methyl ester (TMRM), and the O_2 consumption rate (OCR) in the ER stress *in vitro* model. As a positive control, we used Efavirenz (Efv), a mitotoxic agent that affects the three parameters (Funes *et al.*, 2014). NSC-34 cells were nucleofected with a vector that either overexpress GRP78/BiP or the green fluorescent protein (GFP) as control and submitted to the different tests. We observed that MitoSOX levels progressively increased after Tun addition to the culture until reaching statistical significance by 24 h, in contrast to Efv that increased ROS generation from the first hour post-treatment respect to the use of corresponding vehicles as controls **(Fig. S1A).** Cells overexpressing GRP78/BiP significantly reduced the levels of MitoSOX respect to GFP group at 24h after Tun but did not reach significance after Efv treatment despite a clear tendency **(Fig. 2C).** Regarding ΔψM, the reduction of TMRM fluorescence diminished after 5 h of Tun treatment and by 24 h using either Tun or Efv **(Fig. S1B).** We observed no-differences between control and cells overexpressing GRP78/BiP and submitted to Efv treatment although this caused redcution of ΔψM **(Fig.2D).** After tun treatment, recovery of ΔψM by GRP78/BiP was not so clear at 24 h **(Fig. 2D).** Finally, we

observed that the rate of O_2 consumption was inhibited during 80 min of analysis after Tun addition in the GFP group (slope -0.063, R^2=0.98) but it was sustained in GRP78/BiP overexpressing cells (slope -0.221, R^2=0.99) **(Fig. 2E)**. After 5h, respiration function was normal in GRP78/BiP overexpressing cells while severely compromised in the GFP group **(Fig. 2F)**. Altogether, these results suggested that GRP78/BiP attenuated overall mitochondria dysfunction both after ER stress or due to mitotoxicity, particularly regarding ROS generation and respiration.

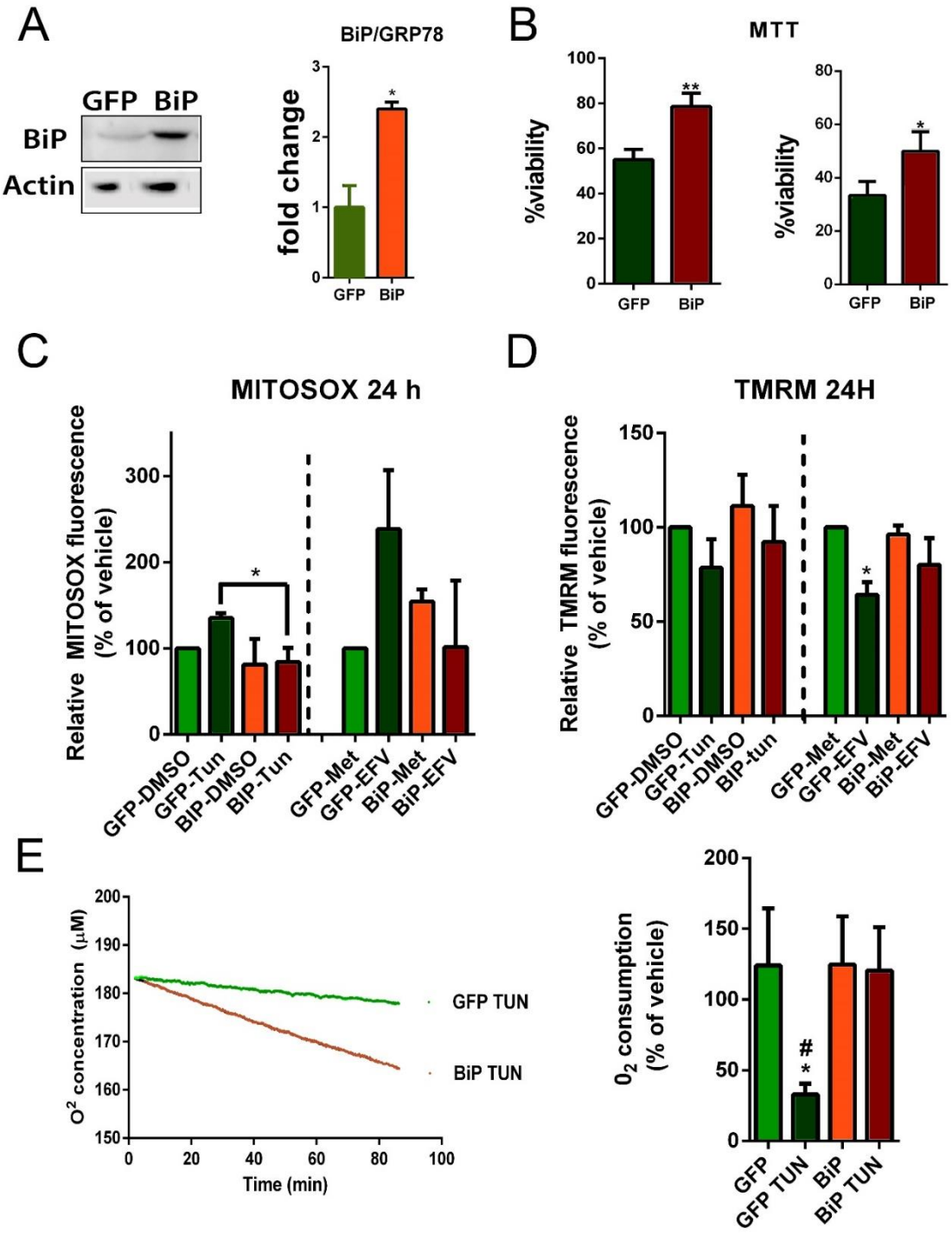

Figure 2. GRP78/BiP overexpression rescues mitochondrial dysfunction in stressed NSC-34 cells (A) Immunoblot and bar graph showing the levels of GRP78/BiP in transfected cells of GRP78/BiP or GFP. (B)Left, Bar graph of the mean average percentage of NSC34 cell survival 24 after Tun 1µg/mL in transfected cells with GFP or GRP78/BiP/GRP78 analysed by MTT assay (n = 4; **p < 0.001 vs. GFP (Student's t-test). Right, Bar graph of the mean average percentage of NSC34 cell survival 24 after Nocodazole 10µM in transfected cells with GFP or GRP78/BiP/GRP78 analysed by MTT assay (n = 4; *p < 0.05 vs. GFP (Student's t-test) (C) Quantitative analysis of mitochondrial superoxide production (MitoSOX fluorescence) after Tun or EFV at 24h in transfected cells with GFP

or GRP78/BiP/GRP78 by fluorescence microscopy. (D) Quantitative analysis of mitochondrial superoxide production (MitoSOX fluorescence) after Tun or EFV treatment at different time-points 24h in transfected cells with GFP or GRP78/BiP/GRP78 by fluorescence microscopy. (E, F) GRP78/BiP increases 0_2 consumption after Tunicamycin treatment. Representative traces and quantification of data showing the rate of 02 consumption (Clark-type O2 electrode) after 5h of Tunicamycin treatment in cells transfected with GFP or GRP78/BiP. n = 4; *p < 0.05 vs. control, one-way ANOVA.

Mitophagy is present in GRP78/BiP overexpressing cells

Considering these results, we hypothesized that GRP78/BiP may be handling selective autophagy of mitochondria or mitophagy to accelerate removal of defective organelles. First, and considering that GRP78/BiP has been proved to promote macroautophagy (Casas, 2017), we sought to determine whether autophagy was necessary for GRP78/BiP induced neuroprotection using several inhibitors of this process: 3-Methyladenine (3-MA), an inhibitor of class III phosphatidylinositol 3-kinases (PI3K), LY294002, an inhibitor of class I PI3K, and Bafilomycin A1 (BAF-A), that inhibits vacuolar H^+ ATPase (V-ATPase) and hence prevents late autophagy events. We observed that all three autophagy inhibitors affected the neuroprotective effect of GRP78/BiP overexpression in ER-stressed cells compared to GFP control group **(Fig 3A)** suggesting that the correct initiation of autophagy, through PI3K-Beclin1 pathway, and late flux are necessary**.**

Mitophagic degradation of mitochondria, e.g. following depolarization, is triggered by the increased stabilization of PINK1 on mitochondria and the subsequent recruitment of the in-between-ring ubiquitin ligase PARKIN and activation of MOM protein ubiquitylation (Lazarou *et al.*, 2015a). However, PARKIN is not always participating in mitophagy because it can be triggered through alternative mechanisms (Villa *et al.*, 2018). To ascertain whether PARKIN was involved in GRP78/BiP-mediated effect, we nucleofected NSC34 cells to express HA-tagged PARKIN and determined its subcellular localization after ER stress by immunocytochemistry. By confocal microscopy, we observed PARKIN widely distributed throughout the NSC-34 cell either after 5h of vehicle or Tun treatment **(Fig. 3B).** In contrast, in cells overexpressing GRP78/BiP there was an increase of

the co-localization of PARKIN and Hsp60, a mitochondria protein, suggesting taggeted organelle for mitophagy **(Fig 3B, C)**.

In addition, we isolated the mitochondrial and cytosolic fraction in cells treated with vehicle or Tun of GFP or GRP78/BiP groups. By immunoblotting, we verified the purity of the mitochondrial fraction analyzing the presence of OPA1 and CV ß in the corresponding fractions **(Fig. 3D)**. Interestingly, we observed an increase of the presence of GRP78/BiP mainly in the mitochondria fraction of cells overexpressing the protein, more prominent in tun-treated cells than after vehicle-treatment. We also observed increased levels of both PINK1, PARKIN in mitochondrial enriched fractions of GRP78/BiP overexpressing cells as it corresponds to PINK/PARKIN mitophagy (**Fig. 3D**). In agreement, we found that some differences in the protein ubiquitylation profile were apparent in the GRP78/BiP group respect to GFP group within the mitochondrial fraction (**Fig. 3D**). Mitochondrial protein ubiquitylation leads to recruitment of autophagosome machinery components starting with accumulation of lipidated isoform of LC3, LC3II. The accumulation of LC3II in the mitochondria fraction was higher in the cells overexpressing GRP78/BiP than control (**Fig. 3D**). Taken together, these data suggested that the overexpression of GRP78/BiP may promote its subcellular distribution increasing at mitochondria environment and promoting mitophagy.

To determine the relevance of mitophagy induction on the neuroprotective effect mediated by GRP78/BiP overexpression we assessed alterations due to the use of activators and inhibitors of mitophagy. We used carbonyl cyanide m-chlorophenyl hydrazine (CCCP) to activate mitophagy and two mitophagy inhibitors: the cell-permeant chelator of intracellular Ca^{2+} BAPTA-AM (BAPTA,) and the mitochondrial permeability transition pore (mPTP) inhibitor Cyclosporin A (CSA) that avoid Ca2+ efflux from mitochondria (Halestrap *et al.*, 1997). Curiously, we observed that CCCP treatment significantly increased survival of ER-stressed cells independently whether they overexpressed GRP78/BiP or GFP suggesting that mitophagy induction contributed determinately to cope with this type of stress **(Fig 3E)**. In agreement, using either CSA or BAPTA inhibitors, the neuroprotective effect promoted by GRP78/BiP overexpression was blocked **(Fig 3E)**.

These findings suggested that PINK1-PARKIN triggered protective mitophagy triggered by CCCP in ER-stressed cells and GRP78/BiP overexpression cells also presented this effect which was also Ca^{2+}-flux dependent.

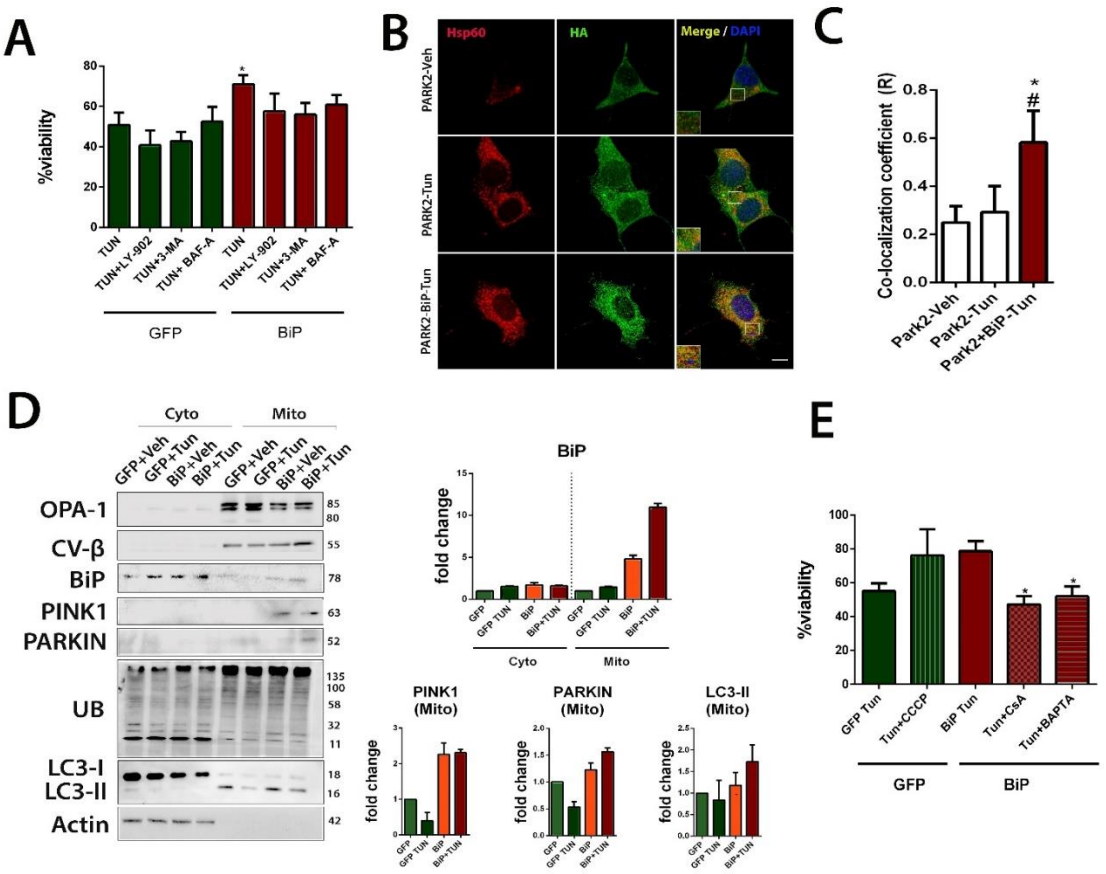

Figure 3. (A) Bar graph showing the percentage of cell survival ± SEM with Tun or combination with Tun+3MA, Tun+LY-902 Tun+Baf-A in transfected cells with GFP or GRP78/BiP by MTT assay after 24h adding treatments (n=4-8, *p<0.05 vs. GRP78/BiP) **(B)** Representative confocal images of transfected cells with PARK2 or PARK2 with GRP78/BiP treated with vehicle of Tunicamycin at 5h showing an increase of colocalization between PARK2-HA (green) and Hsp60(red). Scale bar = 10 µm. (**C**)Pearson's correlation coefficient of Parkin and Hsp60 (n = 4; *p < 0.05 vs. control), one-way ANOVA. . **(D)** Letf**,** Western blot and bar graphs of OPA-1, CVβ PINK1 and PARKIN, UB LC3 and GRP78/BiP in the mitochondrial (mito) and cytosolic (cyto) fraction in GFP or GRP78/BiP overexpressed cells treated with vehicle or tunicamycin by 5 hours. Bar graphs show the average fold change of these proteins relative to GFP with normalization to actin in the cytosolic fraction or the complex V in the mitochondrial fraction. **(E**) Bar graph showing the percentage of cell survival ± SEM with Tun or combination with Tun+CCCP, Tun+CSA, Tun+BAPTA in transfected cells with GFP or GRP78/BiP by MTT assay after 24h adding treatments (n=4-8, *p<0.05 vs. GRP78/BiP Tun).

Neuroprotection mediated by GRP78/BiP depends on IP3R and PINK1

We aimed to determine the molecules important for GRP78/BiP-related mitophagy and neuroprotection.

Using shRNA technology, we confirmed that it was the expression of GRP78/BiP itself and no other artifacts what was necessary for neuroprotection since the use of GRP78/BiP-shRNA abolished the neuroprotective effect promoted by its overexpression in ER-stressed cells **(Fig.4A)**. Even, neuroprotection promoted by CCCP in tun-treated GFP control cells was blocked when knockdown GRP78/BiP **(Fig. 4A)**. These results suggested that GRP78/BiP was relevant for PINK1/PARKIN-mediated protective mitophagy.

Then, we analysed the effect of PINK1 downregulation and we observed that the nucleofection with PINK1-shRNA caused a reduction in viability of tun-treated cells either overexpressing GRP78/BiP or under CCCP treatment what further confirmed its main role in the induced protective mitophagy in both mechanisms **(Fig. 4B)**.

One possibility to allow GRP78/BiP to directly drive any Ca^{2+}-mediated action related to mitophagy is across the ER-mitochondria communication sites at MAMs, particular through the action of the ER-resident IP_3R whose opening allow Ca^{2+} flow from ER to mitochondria. IP_3R downregulation using shRNA diminished cell viability promoted by GRP78/BiP overexpression or by CCCP treatment in ER-stressed cells **(Fig. 4C)**. PINK1 silencing alone did not increase tun toxicity but it completely blocked BiP overexpression-induced protection against Tun toxicity.

Altogether these results suggested that GRP78/BiP overexpression activates protective mitophagy in a PINK/ IP_3R dependent manner.

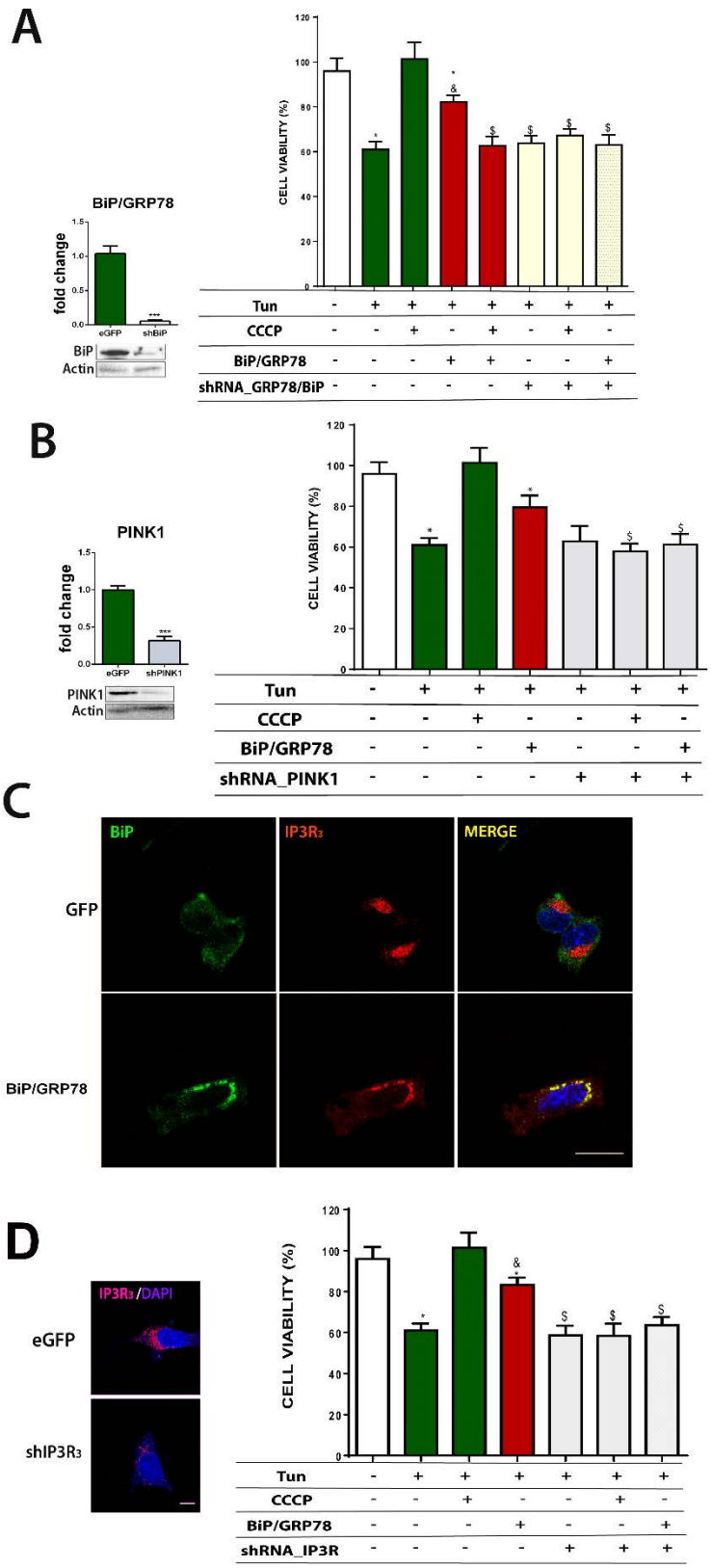

Figure 4. (A) Left, western blot and bar graph showing a reduction of GRP78/BiP levels in shRNAGRP78/BiP cells in compared to shRNAeGFP cells (n =3; *p < 0.05 vs. control), Student's t-test. **Right,** Bar graph showing the percentage of cell survival ± SEM with Tun or combination with CCCP

in transfected cells with GFP ,GRP78/BiP, shRNAGRP78/BiP or GRP78/BiP+shRNAGRP78/BiP by MTT assay after 24h adding treatments (n=4-8, *p<0.05 vs. GRP78/BiP-tun) **(B**) Left, western blot and bar graph showing a reduction of PINK1 levels in shRNAPINK1 cells in compared to shRNAeGFP cells (n =3; *p < 0.05 vs. control), Student's t-test. **Right,** bar graph showing the percentage of cell survival ± SEM with Tun or combination with CCCP in transfected cells with GFP, GRP78/BiP, shRNAPINK1 or GRP78/BiP+shRNAPINK by MTT assay after 24h adding treatments (n=4-8, *p<0.05 vs. GRP78/BiP-tun). (**C**) Representative confocal images of GRP78/BiP (red) co-immunolocalization (merged) with IP3R green in transfected cells with GFP or GRP78/BiP/GRP78. Scale bar=10 um **(D**) Left, representative microphotographs of transfected cells with shRNAIP3R or eGFP showing a decrease of IP3R(red) expression, Scale bar = 10 μm. Right, Bar graph showing the percentage of cell survival ± SEM with Tun or combination with CCCP in transfected cells with GFP ,GRP78/BiP, shRNAIP3R or GRP78/BiP+shRNAIP3R by MTT assay after 24h adding treatments (n=4-8, *p<0.05 vs. GRP78/BiP-tun) **(D)** Left**,** Representative microphotographs of transfected cells with shRNAIP3R or eGFP showing a decrease of IP3R(red) expression, Scale bar = 10 μm. Right, bar graph showing the percentage of cell survival ± SEM with Tun or combination with CCCP in transfected cells with GFP ,GRP78/BiP, shRNAIP3R or GRP78/BiP+shRNAIP3R by MTT assay after 24h adding treatments (n=4-8, *p<0.05 vs. GRP78/BiP-

Evidences of Mitophagy promoted by GRP78/BiP overexpression after RA

Searching for evidences of mitophagy induction by GRP78/BiP overexpression after RA *in vivo*, we assessed the levels of PINK1 and PARKIN by immunoblotting. We observed opposite effects in both proteins with a significantly diminution on PARKIN but an increase of PINK1 levels in the GRP78/BiP group respect to β-Gal group at the L4-L5 spinal cord segments after 7 dpi (**Fig. 5A**). PINK1 upsurge was consistent with the presence of mitophagy since it accumulates on the surface of the damaged mitochondria however, the reduction on PARKIN levels were unexpected.

Further evidence of the presence of mitophagy were obtained by immunohistochemistry when observed extensive co-localization of mitochondria, labeled using anti-COXIV, with punta of LC3 autophagosome marker using confocal microscopy (**Fig. 5B**). Finally, analyzing the injured ventral horns by transmission electronic microscopy, we observed a high number of vacuoles with engulfed mitochondria, or close to them, within MNs of the GRP78/BiP overexpressing group respect to control (**Fig. 5C**).

Hence, a proposal working model of actuation may considered that GRP78/BiP can interact with IP3R at ER-interconnected structures and favour controlled Ca2+ flow

to entry and ensure proper mitophagy activation. It might be possible that GRP78/BiP can also enter mitochondria and help buffering excessive calcium influx and favour efflux through mPTP that can trigger autophagy for proper autophagosome formation and engulfment of tagged mitochondria (**Fig.5D**).

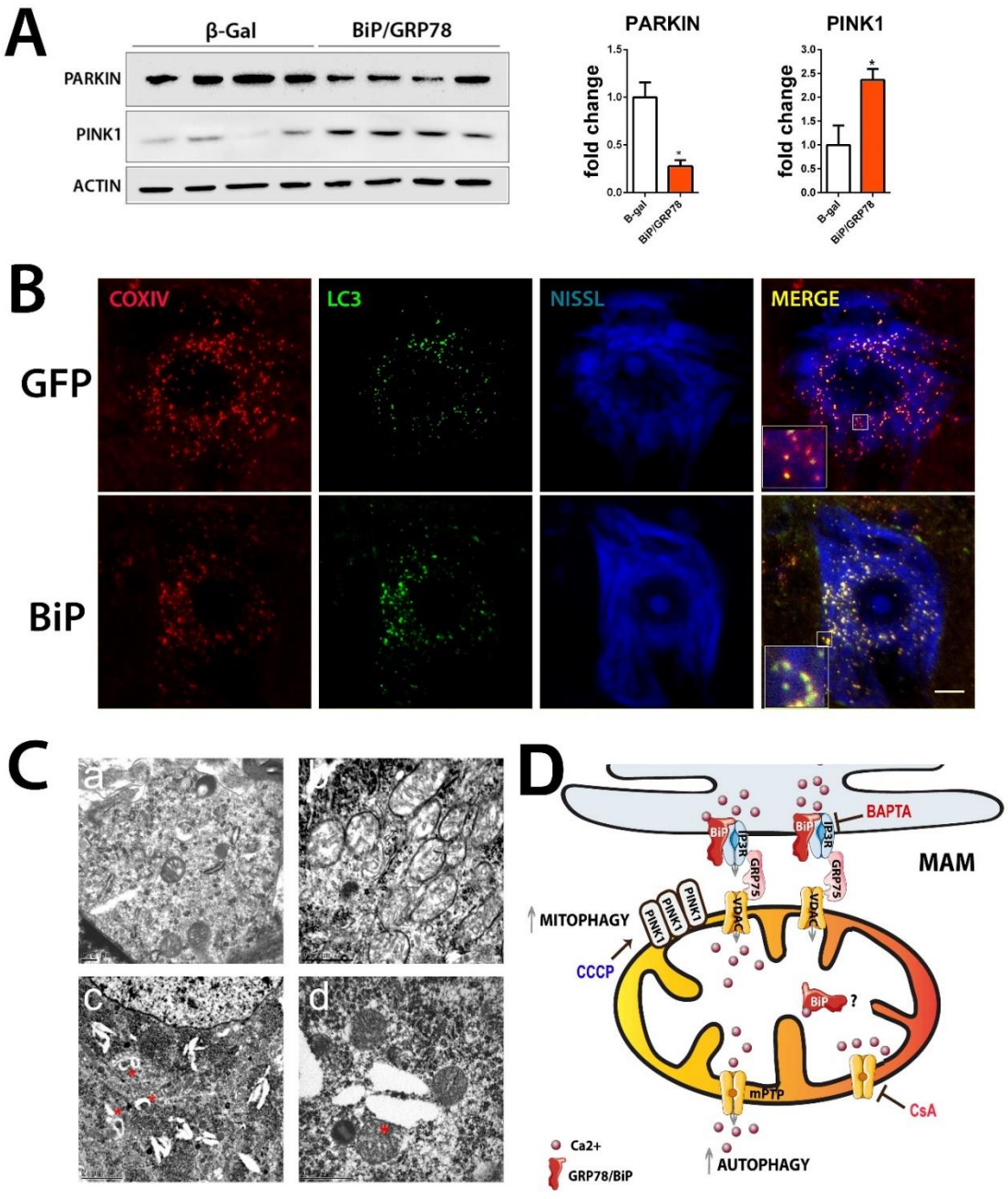

Figure 5. (A) Immunoblot of PINK1 and PARK. Bar graph showing the average fold change protein level ± SEM in β-galactosidase (β-Gal) and GRP78/BiP root avulsed (RA) samples normalized to actin levels (n = 4) *p < 0.05 vs. control (Student's t-test). **(B)** Microphotographs of representative MNs at the ipsilateral site from injured animals of AAVrh10-GFP or AAVrh10-GRP78/BiP overexpressed at 7 dpi. Co-immunolocalization (merged) with COX IV (red) and LC3 (green) staining with Nissl blue. Scale bar=10 um **(C)** Representative transmission electron microscopy (TEM) images of mitochondria within MNs of spinal cord. a, overview of MN cytoplasm showing mitochondria in control animal b: accumulation of mitochondria at the RA-injured MNs overexpressing β-gal; c: Engulfed mitochondria (some pointed with red asteriscs) in RA-injured MNs overexpressing GRP78/BiP; d, Higher magnification of picture in c. **(D)** Working model of the conclusions derived from the study.

DISCUSSION

Finding the way of enhancing the endogenous mechanisms of neuroprotection may yield efficient therapeutic tools for neuroprotection. ER-resident chaperone GRP78/BiP is at the crossroad of several of these mechanisms and its overexpression promote neuroprotection in several models including to MNs suffering retrograde neurodegeneration due to proximal axotomy (Penas, Font-Nieves, *et al.*, 2011). We aimed to deciphering the way GRP78/BiP mediated this protection using unbiass proteome analysis. Unexpectedly, we discovered that the main targeted organelle was mitochondria. In particular, we found that GRP78/BiP overexpression triggered protective mitophagy with implication by IP_3R and PINK1.

Proteomic analysis using our model of MN neurodegeneration by functional disconnection revealed that GRP78/BiP overexpression reduced the level of expression of a considerable number of mitochondria proteins at the ipsilateral injury site of the spinal cord. This was surprising considering that, although GRP78/BiP may be located in different subcellular places, it is mainly at the ER suggesting that it may be acting at the intercommunication site between these two organelles. The reduction of mitochondrial proteins may be consequence of a reduction in biogenesis or a higher turnover. Considering that the effect was beneficial to the cell and to recover mitochondria function after ER stress, the latest is more likely. Our investigation provides compelling evidences pointing that GRP78/BiP overexpression triggers mitophagy.

Firstly, using an *in vitro* model of ER stress, a prominent feature of the events that account after RA injury (Penas, Font-Nieves, *et al.*, 2011)(Leiva-Rodríguez *et al.*, 2018), we observed that macroautophagy induction was necessary for GRP78/BiP to exert neuroprotection. This is in agreement with several studies demonstrating that GRP78/BiP can promote autophagy acting at several points (Casas, 2017). Importantly, we previously reported that *in vivo* GRP78/BiP overexpression markedly reduced LC3II accumulation by 5 days post RA (Penas, Font-Nieves, *et al.*, 2011) what was caused probably by the existence of autophagy flux blockage (Leiva-Rodríguez *et al.*, 2018). Interestingly, GRP78/BiP can bind to SQSTM1/p62 that delivers ubiquitinated cargoes for autophagic degradation to unblock autophagy flux (Liu *et al.*, 2016)(Cha-Molstad *et al.*, 2015, 2016). Although this was not the focus of our investigation, that is an interesting hypothesis to be demonstrated. *In vivo*, we observed that GRP78/BiP increased PINK1 protein level, promoted LC3 target to mitochondria and the apparition of several figures with engulfed mitochondria what is consistent with the induction of mittophagy. Unexpectedly, PARKIN protein levels were downregulated by GRP78/BiP overexpression at 7 dpi. This might be due to the observation of a relative late event in the mitophagy process, where most mitochondria, including anchored PARKIN, was in the way of degradation, or it might indicate a rather PARKIN-independent mitophagic process that involve other receptors (Lazarou et al., 2015b). If this is the case or not it deserves further investigation.

In vitro model results suggested that IP_3R is involved in GRP78/BiP-mediated neuroprotection and that Ca^{2+} flow is important for protective mitophagy since it is blocked when using BAPTA and CsA. IP_3R are enriched in ER-mitochondria tethered by glucose-regulated protein 75 to the voltage-dependent anion channels (VDACs) in the mitochondria (Szabadkai et al., 2006). Consequently, ER-stored Ca^{2+} is rapidly and efficiently transferred into mitochondria through the MAM. PINK1, PARK2 and Beclin (BECN1) have been also observed all localized at MAM after CCCP treatment (Gelmetti et al., 2017). In addition to allow calcium transport from the ER to mitochondria, contributing to mitochondrial dynamics, and apoptosis control (Naon and Scorrano, 2014) MAM is the site for the formation of omegasomes, that represent autophagosome precursors (Gelmetti et al., 2017). Besides, basal IP3Rs activity and continuous, low-level Ca^{2+} flux from ER to mitochondria is essential to

promote mitochondrial respiration and cell bioenergetics (Cárdenas *et al.*, 2010). It has been observed that IP_3R functions in autophagy depending on the cellular condition. In normal cells, IP_3Rs suppress autophagic flux by fueling Ca^{2+} into the mitochondria to sustain ATP production, thereby preventing AMPK activity (Cárdenas and Foskett, 2012)(Cárdenas *et al.*, 2010). In contrast, in nutrient-deprived cells, IP_3Rs are required to promote Ca^{2+}-signaling events that are critical for up-regulating autophagic flux (J. P. Decuypere *et al.*, 2011) (J.-P. Decuypere *et al.*, 2011). However, extensive investigation on IP_3Rs implication on protective mitophagy is still pending regarding requirements about its subcellular localization and the resulting Ca^{2+} signals (cytosol or mitochondria) to determine the specific outcome or establishing which regulators may impinge on the cellular mitophagy. We herein highlight that one of its important partners may be GRP78/BiP to orchestrate the response. Oxidative stress evokes ER-mitochondria Ca2+ transfer at the MAM contributes to mitochondrial depolarization(Gerich et al., 2009) . We have observed ROS accumulation after ER stress that GRP78/BiP overexpression attenuated. Additionally, mitochondrial chaperone cyclophilin D (CypD), a composition of mPTP, also cooperates with the VDAC1/Grp75/IP3R1 complex as observed in some tissues modulating mitochondrial Ca^{2+} balance (Paillard et al., 2013).

In conclusion, this study shed light onto an effective way for neuroprotection when modulating autophagy or mitophagy and contribute to clarify doubts around their beneficial or detrimental role. The fact of the presence of mitophagy figures in the pathological specimens from postmortem tissue of Alzheimer or Parkinson patients might represent neuronal attempts to survive (Toulorge *et al.*, 2016). Numerous disease-modifying strategies targeting mitochondria are currently under investigation and we propose herein that overexpressing GRP78/BiP might be a promising strategy.

ACKNOWLEDGEMENTS

We thank Marta Monserrat, Ariadna Aransanz, Miguel Chillón, Julia Lorenzo, Sara Marmolejo and people of the Neuroplasticity and Regeneration Group for support and helping in different technical issues. Especially thanks to Carlos Guillem

(University Complutense de Madrid) for kindly provide the PARKIN-HA plasmid, and to Valerie Petegnief for adenovirus gift. Finally, also thanks to Elena Galea and Esther Dalfo for some antibody supply. **Funding:** This work was mainly supported by the Ministerio de Economía y Competitividad of Spain (#SAF 2014-59701). We are also grateful for support from CIBERNED and Generalitat de Catalunya fundings.

AUTHOR CONTRIBUTIONS

TLR designed, performed the experiments, analyzed the results, and wrote part of the manuscript. JF and DRG helped with in vivo experiments. PM and JML performed the mitochondrial purifications. MP, CB and NA helped with the mitochondria functional analysis. VP and AB prepared all the GRP78/BiP plasmids and viral vectors used. CC conceived, designed, supervised, and analyzed all the experiments and wrote the manuscript.

ADDITIONAL INFORMATION

Supplementary Information accompanies this paper.

Competing Financial Interest: There is no one.

SUPPLEMENTARY FIGURES

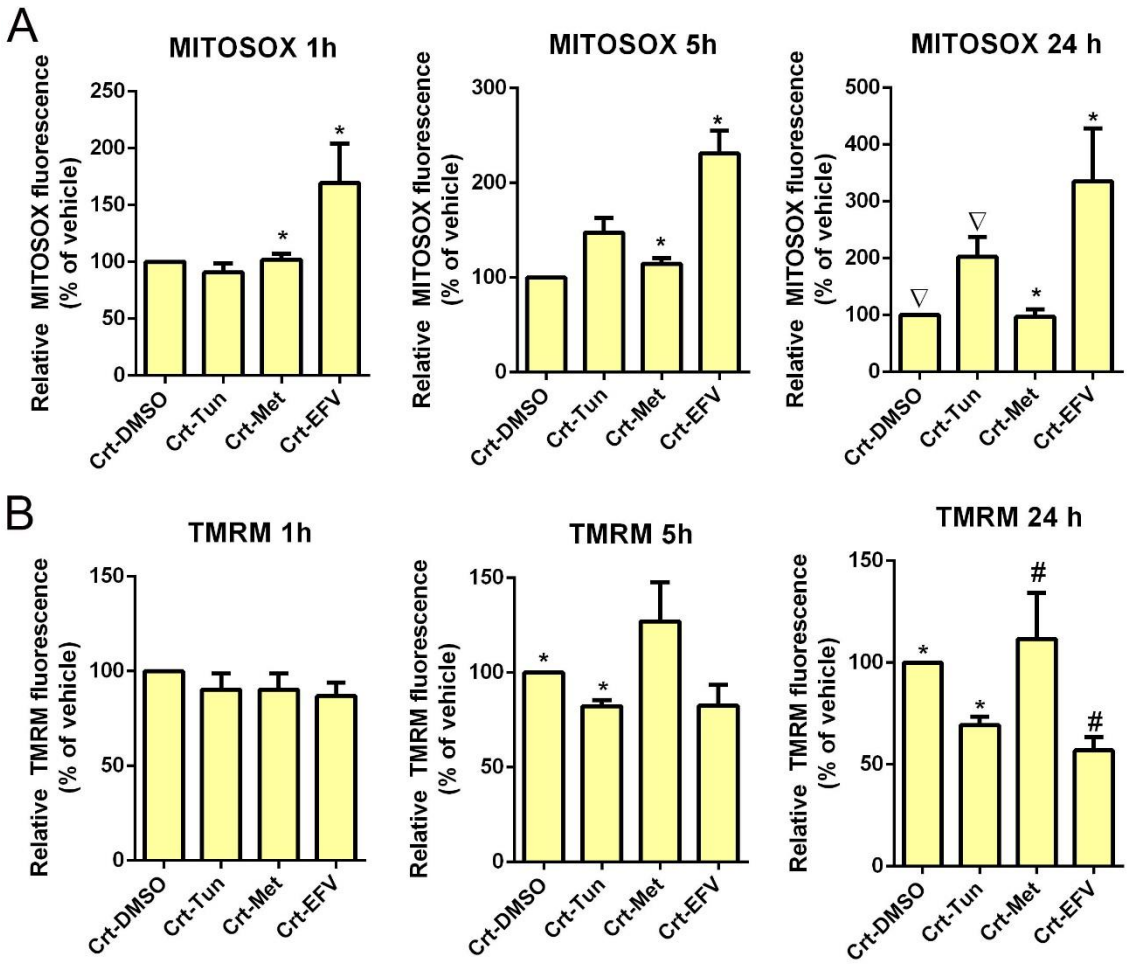

Figure S1 (A) Quantitative analysis of mitochondrial superoxide production (MitoSOX fluorescence) after Tun or EFV at different time-points (1,5 and 24h) in control cells by fluorescence microscopy. **(B)** Quantitative analysis of mitochondrial superoxide production (MitoSOX fluorescence) after Tun or EFV treatment at different time-points (1,5 and 24h) in in control cells by fluorescence microscopy.

REFERENCES

Abdel Malek MAY, Jagannathan S, Malek E, Sayed DM, Elgammal SA, Abd El-Azeem HG, et al. Molecular chaperone GRP78 enhances aggresome delivery to autophagosomes to promote drug resistance in multiple myeloma [Internet]. Oncotarget 2015; 6: 3098–3110.[cited 2016 Dec 12] Available from: http://www.ncbi.nlm.nih.gov/pubmed/25605012

Cárdenas C, Foskett JK. Mitochondrial Ca2+ signals in autophagy. Cell Calcium 2012

Cárdenas C, Miller RA, Smith I, Bui T, Molgó J, Müller M, et al. Essential Regulation of Cell Bioenergetics by Constitutive InsP3 Receptor Ca2+ Transfer to Mitochondria. Cell 2010

Casas C. Grp78 at the Centre of the Stage in Neurodegeneration and Cancer. Front. Neurosci. 2017; 11: 1–15.

Casas C, Isus L, Herrando-Grabulosa M, Mancuso FM, Borrás E, Sabidó E, et al. Network-based proteomic approaches reveal the neurodegenerative, neuroprotective and pain-related mechanisms involved after retrograde axonal damage [Internet]. Sci. Rep. 2015; 5: 1–13.Available from: http://www.nature.com/doifinder/10.1038/srep09185

Casas C, Isus L, Herrando-Grabulosa M, Mancuso FM, Borrás E, Sabidó E, et al. Network-based proteomic approaches reveal the neurodegenerative, neuroprotective and pain-related mechanisms involved after retrograde axonal damage. [Internet]. Sci. Rep. 2015; 5: 9185.[cited 2015 Mar 28] Available from: http://www.ncbi.nlm.nih.gov/pubmed/25784190

Cha-Molstad H, Sung KS, Hwang J, Kim KA, Yu JE, Yoo YD, et al. Amino-terminal arginylation targets endoplasmic reticulum chaperone BiP for autophagy through p62 binding [Internet]. Nat. Cell Biol. 2015; 17: 917–929.[cited 2016 Dec 12] Available from: http://www.ncbi.nlm.nih.gov/pubmed/26075355

Cha-Molstad H, Yu JE, Lee SH, Kim JG, Sung KS, Hwang J, et al. Modulation of SQSTM1/p62 activity by N-terminal arginylation of the endoplasmic reticulum chaperone HSPA5/GRP78/BiP. Autophagy 2016; 12: 426–428.

Conforti L, Gilley J, Coleman MP. Wallerian degeneration: an emerging axon death pathway linking injury and disease. Nat Rev Neurosci 2014; 15: 394–409.

Cook KL, Clarke R. Heat shock 70 kDa protein 5/glucose-regulated protein 78 'AMP'ing up autophagy [Internet]. Autophagy 2012; 8: 1827–1829.[cited 2017 Jan 5] Available from: http://www.ncbi.nlm.nih.gov/pubmed/22931685

Decuypere J-P, Welkenhuyzen K, Luyten T, Ponsaerts R, Dewaele M, Molgó J, et al. IP3 receptor-mediated Ca2+ signaling and autophagy induction are interrelated. Autophagy 2011

Decuypere JP, Bultynck G, Parys JB. A dual role for Ca 2+ in autophagy regulation. Cell Calcium 2011

Funes HA, Apostolova N, Alegre F, Blas-Garcia A, Alvarez A, Marti-Cabrera M, et al. Neuronal Bioenergetics and Acute Mitochondrial Dysfunction: A Clue to Understanding the Central Nervous System Side Effects of Efavirenz. J. Infect. Dis. 2014; 210: 1385–1395.

Gelmetti V, De Rosa P, Torosantucci L, Marini ES, Romagnoli A, Di Rienzo M, et al.

PINK1 and BECN1 relocalize at mitochondria-associated membranes during mitophagy and promote ER-mitochondria tethering and autophagosome formation [Internet]. Autophagy 2017; 13: 654–669.Available from: http://dx.doi.org/10.1080/15548627.2016.1277309

Gerich FJ, Funke F, Hildebrandt B, Faßhauer M, Müller M. H2O2-mediated modulation of cytosolic signaling and organelle function in rat hippocampus. Pflugers Arch. Eur. J. Physiol. 2009

Guzmán-Lenis M-S, Navarro X, Casas C. Selective sigma receptor agonist 2-(4-morpholinethyl)1-phenylcyclohexanecarboxylate (PRE084) promotes neuroprotection and neurite elongation through protein kinase C (PKC) signaling on motoneurons. [Internet]. Neuroscience 2009; 162: 31–8.[cited 2011 Jul 16] Available from: http://www.ncbi.nlm.nih.gov/pubmed/19345724

Halestrap AP, Connern CP, Griffiths EJ, Kerr PM. Cyclosporin A binding to mitochondrial cyclophilin inhibits the permeability transition pore and protects hearts from ischaemia/reperfusion injury. [Internet]. Mol. Cell. Biochem. 1997; 174: 167–72.[cited 2018 Sep 1] Available from: http://www.ncbi.nlm.nih.gov/pubmed/9309682

Jin H, Mimura N, Kashio M, Koseki H, Aoe T. Late-onset of spinal neurodegeneration in knock-in mice expressing a mutant BiP. [Internet]. PLoS One 2014; 9: e112837.[cited 2017 Jan 7] Available from: http://dx.plos.org/10.1371/journal.pone.0112837

Kim J-H, Hong S-K, Wu P-K, Richards AL, Jackson WT, Park J-I. Raf/MEK/ERK can regulate cellular levels of LC3B and SQSTM1/p62 at expression levels. Exp Cell Res.

2014; 327: 340–352.

Kudo T, Kanemoto S, Hara H, Morimoto N, Morihara T, Kimura R, et al. A molecular chaperone inducer protects neurons from ER stress [Internet]. Cell Death Differ 2008; 15: 364–375.Available from: http://www.ncbi.nlm.nih.gov/entrez/query.fcgi?cmd=Retrieve&db=PubMed&dopt=Citation&list_uids=18049481

Lazarou M, Sliter DA, Kane LA, Sarraf SA, Wang C, Burman JL, et al. The ubiquitin kinase PINK1 recruits autophagy receptors to induce mitophagy. Nature 2015a

Lazarou M, Sliter DA, Kane LA, Sarraf SA, Wang C, Burman JL, et al. The ubiquitin kinase PINK1 recruits autophagy receptors to induce mitophagy. Nature 2015b; 524: 309–314.

Leiva-Rodríguez T, Romeo-Guitart D, Marmolejo-Martínez-Artesero S, Herrando-Grabulosa M, Bosch A, Forés J, et al. ATG5 overexpression is neuroprotective and attenuates cytoskeletal and vesicle-Trafficking alterations in axotomized motoneurons article. Cell Death Dis. 2018; 9: 626.

Li Z, Wang Y, Newton IP, Zhang L, Ji P, Li Z. GRP78 is implicated in the modulation of tumor aerobic glycolysis by promoting autophagic degradation of IKKβ [Internet]. Cell. Signal. 2015; 27: 1237–1245.[cited 2016 Dec 12] Available from: http://www.ncbi.nlm.nih.gov/pubmed/25748049

Liu WJ, Ye L, Huang WF, Guo LJ, Xu ZG, Wu HL, et al. p62 links the autophagy pathway and the ubiqutin-proteasome system upon ubiquitinated protein degradation. Cell. Mol. Biol. Lett. 2016

Naon D, Scorrano L. At the right distance: ER-mitochondria juxtaposition in cell life and death. Biochim. Biophys. Acta - Mol. Cell Res. 2014

Ni M, Zhang Y, Lee AS. Beyond the endoplasmic reticulum: atypical GRP78 in cell viability, signaling and therapeutic targeting. 2011; 434: 181–188.

Oida Y, Hamanaka J, Hyakkoku K, Shimazawa M, Kudo T, Imaizumi K, et al. Post-treatment of a BiP inducer prevents cell death after middle cerebral artery occlusion in mice. [Internet]. Neurosci. Lett. 2010; 484: 43–6.[cited 2018 Aug 26] Available from: http://linkinghub.elsevier.com/retrieve/pii/S0304394010010499

Ouyang YB, Xu LJ, Emery JF, Lee AS, Giffard RG. Overexpressing GRP78 influences Ca2+ handling and function of mitochondria in astrocytes after ischemia-like stress. Mitochondrion 2011; 11: 279–286.

Paillard M, Tubbs E, Thiebaut PA, Gomez L, Fauconnier J, Da Silva CC, et al. Depressing mitochondria-reticulum interactions protects cardiomyocytes from lethal hypoxia-reoxygenation injury. Circulation 2013

Paz Gavilán M, Vela J, Castaño A, Ramos B, del Río JC, Vitorica J, et al. Cellular environment facilitates protein accumulation in aged rat hippocampus. Neurobiol. Aging 2006; 27: 973–982.

Penas C, Casas C, Robert I, Forés J, Navarro X. Cytoskeletal and activity-related changes in spinal motoneurons after root avulsion. [Internet]. J. Neurotrauma 2009; 26: 763–79.Available from: http://www.ncbi.nlm.nih.gov/pubmed/19331524

Penas C, Font-Nieves M, Forés J, Petegnief V, Planas A, Navarro X, et al. Autophagy,

and BiP level decrease are early key events in retrograde degeneration of motoneurons. [Internet]. Cell Death Differ. 2011; 18: 1617–1627.[cited 2011 Apr 1] Available from: http://www.ncbi.nlm.nih.gov/pubmed/21436843

Penas C, Pascual-Font A, Mancuso R, Forés J, Casas C, Navarro X. Sigma Receptor Agonist 2-(4-Morpholinethyl)1 Phenylcyclohexanecarboxylate (Pre084) Increases GDNF and BiP Expression and Promotes Neuroprotection after Root Avulsion Injury. [Internet]. J. Neurotrauma 2011; 28: 831–40.[cited 2011 May 13] Available from: http://www.ncbi.nlm.nih.gov/pubmed/21332255

Printsev I, Curiel D, Carraway KL. Membrane Protein Quantity Control at the Endoplasmic Reticulum [Internet]. J. Membr. Biol. 2016: 1–14.[cited 2016 Dec 12] Available from: http://www.ncbi.nlm.nih.gov/pubmed/27743014

Reddy RK, Mao C, Baumeister P, Austin RC, Kaufman RJ, Lee AS. Endoplasmic reticulum chaperone protein GRP78 protects cells from apoptosis induced by topkudoisomerase inhibitors. Role of ATP binding site in suppression of caspase-7 activation. J. Biol. Chem. 2003; 278: 20915–20924.

Romeo-Guitart D, Forés J, Herrando-Grabulosa M, Valls R, Leiva-Rodríguez T, Galea E, et al. Neuroprotective Drug for Nerve Trauma Revealed Using Artificial Intelligence [Internet]. Sci. Rep. 2018; 8: 1879.Available from: http://www.nature.com/articles/s41598-018-19767-3

Romeo-Guitart D, Fores J, Navarro X, Casas C. Boosted Regeneration and Reduced Denervated Muscle Atrophy by NeuroHeal in a Pre-clinical Model of Lumbar Root Avulsion with Delayed Reimplantation. Sci. Rep. 2017; 7: 1–12.

Szabadkai G, Bianchi K, Várnai P, De Stefani D, Wieckowski MR, Cavagna D, et al.

Chaperone-mediated coupling of endoplasmic reticulum and mitochondrial Ca2+ channels. J. Cell Biol. 2006

Toulorge D, Schapira AHV, Hajj R. Molecular changes in the postmortem parkinsonian brain. J. Neurochem. 2016

Villa E, Marchetti S, Ricci JE. No Parkin Zone: Mitophagy without Parkin [Internet]. Trends Cell Biol. 2018[cited 2018 Aug 26] Available from: https://linkinghub.elsevier.com/retrieve/pii/S0962892418301259

Wang M, Kaufman RJ. Protein misfolding in the endoplasmic reticulum as a conduit to human disease [Internet]. Nature 2016; 529: 326–335.Available from: http://www.ncbi.nlm.nih.gov/pubmed/26791723

Wen B, Lampe JN, Roberts AG, Atkins WM, Rodrigues AD, Nelson SD. Glucose-Regulated Protein 78 Controls Cross-talk between Apoptosis and Autophagy to Determine Antiestrogen Responsiveness. Cancer Res. 2012; 72: 3337–3349.

Chapter 3

Autophagy induced by SIRT1/Hif1α axis promotes nerve regeneration

David Romeo-Guitart[1], Tatiana Leiva-Rodriguez[1], Joaquim Forés[2], Caty Casas1*

Affiliations

[1] Institut de Neurociències (INc) and Department of Cell Biology, Physiology and Immunology, Universitat Autònoma de Barcelona (UAB), & Centro de Investigación Biomédica en Red sobre Enfermedades Neurodegenerativas (CIBERNED), Bellaterra, Barcelona, Spain

[2] Hand and Peripheral Nerve Unit, Hospital Clínic i Provincial, *Universitat de Barcelona*, Barcelona, Spain Biotech, S.L, Barcelona, Spain

*To whom correspondence should be addressed: Caty Casas Louzao, Unitat de Fisiologia Mèdica, Facultat de Medicina, Universitat Autònoma de Barcelona, E-08193 Bellaterra, Barcelona, Spain. Tel: +34-935811324, Fax: +34-935812986, E-mail: Caty.Casas@uab.cat

Running title: SIRT1/Hif1 axis on motoneuron regeneration

ABSTRACT

Neuron-target disconnection can occur after traumatic injuries, axonopathies or other affectations such as ischemia or cancer-induced compression. Nowadays, no effective therapies have been described to enhance nerve regrowth to recover the functional loss. SIRT1 has evolved as a well-known neuroprotectant, although its exact role in mammal axonal regeneration is not clarified because only *in vitro* approximations have been performed to depicter it. Recently, we described NeuroHeal (NH) as a feasible therapy for those nervous injuries in which motoneuron (MN) survival is compromised and long-distance regeneration is needed to obtain some functional recovery. Here, we describe that SIRT1 activation increases MN neurite elongation *in vitro* and motor axonal regeneration *in vivo*, and that those effects need the Hif1-dependent autophagy. Moreover, the overexpression of ATG5 increases axonal regeneration by autophagy induction. Thus, SIRT1 activity, and therefore that provided by NH treatment, are good therapeutic approaches to raise regeneration of MNs after peripheral nervous system injuries allowing to a better functional recovery.

INTRODUCTION

Peripheral nerve injury (PNI) directly affect about 13-23 people per 100,000 per year, carrying out important economics cost in healthcare of developed countries [1,2]. Mammal peripheral nervous system, and therefore the human one, has the intrinsic capability to regenerate and replace the unfunctional or injured axons to ensure a correct circuitry performance throughout a lifetime. Although this statement is true, the peripheral axons lose its ability to regrowth during aging [3], leading to a poor muscle reinnervation and therefore to an incipient functional recovery after traumatic injury to the peripheral nervous system. Indeed, although reparative surgeries can be performed after injury, an optimal recovery is not easily obtained [4]. Albeit several therapeutic approximations were described using pharmacotherapy [5], physical exercise [6] or electric stimulation [7], their effects on functional recovery are incipient and their molecular mechanisms are not fully understood. Therefore, no effective treatments exist nowadays in human healthcare to enhance nerve regeneration reducing the functional impairment that appears after a PNL.

Several molecular programs have been described as modulators of axonal regrowth within the peripheral and central nervous system [8]. Among them, the activation of (phosphatidylinositol-4,5-bisphosphate 3-kinase(PI3K)/AKT axis is highly related to the pro-neuritogenic effect of neurotrophic factors and it is activated after nerve injury by the motoneurons (MNs) to enhance its capability for re-extend their axons [9,10]. In the same way, AKT inhibition by the phosphatase and the tensin homolog (PTEN) completely blocks the spontaneous axon regrowth in the injured spinal cord, while its deletion [11] or its pharmacological inhibition [12] have raised axonal re-growth after nervous system injury. Unfortunately, these effects are accompanied by pro-oncogenic features because PTEN acts as a tumor suppressor [13], so the clinical translation of this therapeutic approach cannot be used

A widely described sensor of cellular stress is the NAD-dependent deacetylase sirtuin-1 (SIRT1) 18, which has positive roles in neurodegenerative disease and controls cellular homeostasis to deal with external insults [19,20]. Although SIRT1 was first described as a nuclear enzyme [21], it also has cytosolic functions as deacetylase

[22], although they exact roles are poorly understood. Regarding the cellular response after axonal injury, SIRT1 activity exerts a positive neurite-growth effect through the inhibition of mTOR pathway in cell culture [23]. We recently described that the crosstalk between SIRT1, AKT axis and FOXO3a leads to a fine-tuned autophagy that blocks MN apoptotic death during early stages of development.

Through a systems biology approach and using artificial intelligence, we discovered a drug combination named NeuroHeal (NH), which potentiates the endogenous protective mechanisms that cells intrinsically have to face proximal axotomies. NH maintains MN survival after nerve root avulsion (RA) by SIRT1 modulation, enhances functional recovery after PNL and activates the PI3K/AKT axis [14,24], although its exact mechanism to induce axonal regeneration is not yet described. Seeking to depict the role of SIRT1 on axonal regeneration, we found that its deacetylase activity at cytosol increases axonal regeneration and stabilizes Hif1a subunit. This stabilization leads to an increased autophagic flux, which accelerates axonal regeneration of MNs after PNL by giving them a more pro-regenerative phenotype.

MATERIALS & METHODS

Surgical procedures

All the experiments involving animals were approved by the Ethics Committee of our institution and followed the European Community Council Directive 2010/63/EU. Sprague-Dawley rats were kept under standard conditions of light, temperature and feeding and at 12 weeks of age, we performed surgical procedures. We deeply anesthetized rats with ketamine/xylazine cocktail 0.1mL/100 g i.p and prepared the animal for surgery. For crush injury, the sciatic nerve of right hindlimb was exposed ad mid-high and compressed with fine forceps (3 times of 30") at 90 mm from the third poe. For the cut and suture, we dissected the sciatic nerve as previously, transected it at 90mm from the third toe and immediately repaired it with fascicular suture (10-0, Ethicon). For the autograft, we transected the sciatic nerve at 80mm and 90mm from the third toe, flipped it and repaired it with fascicular suture (10-0, Ethicon). After all the surgeries, the wound was closed, disinfected and the animals were allowed to recover in a warm environment. For

the AAV injected rats, the surgery was performed three weeks after injection to ensure an optimal gene expression.

The ventral root avulsion (RA) and delayed root reimplantation (RE) was carried out as previously described (Ref). Briefly, we performed laminectomy at T11 vertebra to release the L3-L6 ventral roots from the meninges, and we separated detached them from the spinal cord with the help of a hook. Besides this, we introduced the four injured roots into a silicone tube, closed the wounds and allowed the animals to recover. Two weeks after RA, we anesthetized the animals and checked by electrophysiological tests a complete muscle denervation. We localized the silicone tube, dissected the injured ventral roots and inserted underneath the corresponding spinal cord segment. To ensure the reimplanted roots maintenance within the spinal cord, we opposed the paraventral muscles to the spinal cord and closed the wounds.

Construction, purification, and infection with recombinant adeno-associated vectors

SIRT1 cDNA was cloned into NheI and XhoI sites between the ITRs of AAV2, under the regulation of CMV promoter and the woodchuck hepatitis virus responsive element (WPRE)[66]. AAV2/rh10 vector was generated as previously described 36 by triple transfection of HEK 293-AAV cells (Stratagene) with branched polyethylenimine (PEI; Sigma) with the plasmid containing the ITRs of AAV2, the AAV helper plasmid containing Rep2 and Cap for rh10 (kindly provided by JM Wilson, University of Pennsylvania, Philadelphia, USA) and the pXX6 plasmid containing helper adenoviral genes 37. Recombinant vectors were clarified after benzonase treatment (50 U/mL, Novagen) and polyethylene glycol (PEG 8000, Sigma) precipitation. Vectors were purified by iodixanol gradient with the Vector Production Unit at UAB (http://sct.uab.cat/upv), following standard operating procedures. Viral genomes per ml (vg/ml) were quantified by picogreen (Invitrogen, Carlsbad, CA, USA)

We performed intrathecal or intramuscular injection of 4x10E10 viral genomes under ketamine/xylazine-anesthetized animals using a Hamilton syringe with a 33-gauge needle. For intrathecal injection, vertebral column was exposed after muscle

dissection at L3-L4 vertebrae, and 10 µL of viral vectors were slowly injected into the cerebrospinal fluid between vertebras. We introduced the needle and correct intrathecal placements was confirmed by the animal tail flick. The needle was fixed in the injection for 10 seconds to avoid fluid retraction and the wound was sutured.

Drug administration

NeuroHeal (NH) is composed of acamprosate calcium (Aca) and Ribavirin (Rib) compounds. Aca, Rib, Ex-527, and nicotinamide (NAM) (Sigma-Aldrich, Saint Louis, MO) and 3-MethyladeNine (3MA) (Tocris) for *in vitro* studies were diluted in sterile H_2O or DMSO. Aca, Rib, Ex-527, and NAM were added at final concentration of 1µM, 55µM, 10µm, 5mM and 10 µM mixed with the culture medium.

In vivo treatments consist of Aca (Merck, Darmstadt, Germany) and Rib (Normon, Madrid, Spain) pills grounded into fine powder and dissolved in drinking water at 2.2 mM and 1 mM respectively. NAM was dissolved also in the drinking water at 5mM and added jointly or not the NH treated animals. We changed the tap water every 3 days and freshly added the drug treatment.

Electrophysiological test and functional assessment

For electrophysiological evaluation, rats were anesthethized with ketamine/xylazine (100:10 mg/kg weight, i.p) at different times post-injury. The sciatic nerve was stimulated by transcutaneous electrodes placed at the sciatic notch by single pulses (20 µs), and the compound muscle action potential (CMAP) was recorded by placing electrodes on the tibialis anterior (TA), gastrocnemius and plantar interosseous muscles. Stimulus intensity was applied gradually until reach the supramaximal stimulus, which correspond to the maximum CMAP amplitude. The evoked action potentials were displayed on a storage oscilloscope (Synergy Medelec, Viasys HealthCare) at settings appropriate to measure the amplitude from baseline to peak and the latency to the onset after every stimulus. After testing, animals were allowed to recover in a warm environment.

Spinal organotypic culture (SOCs) on collagen 3D matrix

We prepared spinal organotypic cultures as previously described[34]**.** Summarizing, we prepared collagen solution at 3mg/mL mixing: rat tail collagen type I (Corning, Wiesbaden, Germany), PBS (Sigma-Aldrich), sodium bicarbonate at 0,3mg/mL( ) and 10x basal Eagle's medium (Gibco, Grand Island, USA). We deposited 30µL-single drops of collagen at 24-well Petri dishes pretreated with poly-D-Lysine (Sigma-Aldrich) and kept them in the incubator 1 hour at 37ºC and 5% CO2 to induce collagen gel formation. Therefore, we extracted lumbar spinal cord section from 7-day old Sprague-Dawley rats, placed in 30% glucose cold Gey's balanced salt solution (Sigma-Aldrich) and cleaned from meninges and nerve roots. Spinal cords were cut into 350µM–thickness slices and were placed onto collagen droplets. After 30 min in the incubator, were covered the sliced with 30µL of the same collagen solution mentioned above and after 30 at 37ªC for collagen polymerization, we added culture medium with Neurobasal (Life Technologies) supplemented with B27 (Life technologies), glutamine and penicillin/streptomycin (Sigma-Aldrich).

One day after culture, we removed the media and added the same combined with the different treatments: H_2O or DMSO as a vehicle, NH, NH + Ex-527, NH+NAM NH+3MA, DMOG, DMOG+3MA and 3-MA. We also changed the medium at 3 days post culture. After 4 days treatment, we removed the media, post-fixed the spinal cords with cold 4% PFA solution for 1 hour, washed them with TBS several times and incubated during 48h with primary antibodies at 4ºC. For neurite growth analyse the primary antibody was anti-mouse RT97 (1:200; Hybridoma Bank, USA). After washes with 0,1% Tween in TBS, we incubated the spinal cords with donkey conjugated Alexa 594 anti-mouse (1:200; Life Technologies) overnight at 4ºC, counterstained with DAPI, washed them and mounted with DPX (Sigma-Aldrich)

We took sequential microphotographs with a fluorescence microscope Olympus BX51 (Olympus, Germany) attached to a DP73 camera and merged them with Adobe Photoshop CS3 (Adobe System, USA) to obtain whole spinal cord slice body with their neurites. To analyse neurite growth and length, whole culture images were analysed with the help of the Neurite-J plug-in for ImageJ software[67]. The number of neurites for each intersection from the explant was calculated and compared between sets of cultures.

Cell culture

SH-SHY5 cells were grown in modified Eagle's medium high-glucose (DMEM) supplemented with 15% fetal bovine serum (Sigma-Aldrich), and 0.5× penicillin/streptomycin solution (Sigma-Aldrich). Cells were kept in a humidified incubator at 37 °C under 5% CO2. For the treatments, we coated plastic plates (Thermo) with 10% collagen dissolved in Milli-Q water at 37 °C for 2 h. After removing this solution, we seeded the cells at a density of 2.5×10^5 per cm2. For differentiated phenotype cells were grown in Neurobasal supplemented with B27 (Life technologies), 1uM of retinoic acid and 0.5x penicillin/streptomycin solution. After 3 days of culture without changing the medium, SH-SHY5 cells present with a differentiated-like phenotype characterized by the presence of long neurite extensions. At this time, we added different drugs to the cells. The drugs, prepared at a concentration 10-fold higher than the concentration to be tested, were dissolved in DMEM to the desired concentration and used to replace medium over cells. We used 1 mM DMOG (Tolcris) and 10 μM 3-MA(Merck-Millipore) unless otherwise stated. After 24h, we fixed the cells with 4% PFA, rinsed twice with PBS, and stored at −20 °C or added blocking buffer containing PBS plus 0.3% (v/v) Triton X-100 and 10% fetal bovine serum. We incubated with the following primary antibodies: mouse anti-β-tubulin (1:500, Covance/biolegend, San Diego, CA, USA), mouse anti-HIF1α (1:500, Novus Biological) and rabbit anti-SIRT1(1:200, Merck-Millipore) in 0.5× blocking buffer in PBS, at 4 °C overnight. The following day, after several washes with PBS plus 0.05% Tween-20, we incubated the coverslips with Cy3- or Cy2-conjugated secondary antibodies (Jackson Immunoresearch). Coverslips were counterstained with DAPI and mounted with Mowiol. Images were taken under the same exposure times, sensitivities, and resolutions for each marker analysed with the aid of a digital camera (Olympus DP50) attached to the microscope (Olympus BX51).

For transfection experiments, we transfected $1x10^6$ with 1 μg, shRNAGFP(CSHCTR001-CH1, Tebu-bio) shRNA HIF1α (HSH008832-32-CH1, Tebu-bio) and SIRT1 using the Amaxa Nucleofector II TM (Lonza) and the Nucleofactor V kit (Lonza) following the manufacturer's recommendations.

To analyse neurite growth, we took microphotographs at 20x magnification and culture images were analysed with the help of ImageJ software. The growth of neurites was measured manually and compared between sets of cultures.

Tissue processing for histology

At end stage, we euthanized the animals after dolethal injection (60 mg/kg i.p) and transcardially perfused them with a saline solution of heparin (10 U/mL) followed by 0.1M PBS buffer solution of 4% paraformaldehyde. Besides this, we harvested L4-L5 spinal cord segment and sciatic nerve from injury site to sciatic trifurcation, post-fixed them with PFA 1 hour and cryopreserved with the same sucrose solution. Serial spinal cord slices of 20-µm (20 slices of 10 slides each) were obtained with the aid of cryotome (Leica, Heidelberg, Germany) and kept at 20ºC until needed.

Immunohistochemistry and image analyse

Sections for each marker from different animals of each group to be analysed together were immunolabeled simultaneously on the same day and the analysis was performed concurrently. We washed the slices containing the spinal cords slides with Tris-buffered saline (TBS), blocked b them with TBS-Glycine 0,1mM during 101 and with blocking solution TBS with 0,3% Triton-X-100 and 10% donkey serum for 1h at RT. Next, we added the primary antibodies to be incubated overnight at 4ºC. The primary antibodies used were: rabbit-anti NAD-dependent deacetylase sirtuin-1 (SIRT1; 1:100, Millipore), rabbit anti-acetyl-Histone H3 (Lys9) (Acetyl H3-K9; 1:50, Millipore), rabbit anti-acetyl-p53 (Lys373) (Acetyl p53-K373; 1:500, Millipore), rabbit anti-phospho protein kinase B (Ser473) (pAKT; 1:500, Santa Cruz), rabbit anti-phospho FOXO3a (Ser-253) (pFOXO3a; 1:500, Abcam), anti-growth associated protein-43 (GAP43; 1:50, Millipore), mouse anti-hypoxia inducible factor 1α (Hif-1 α; 1:200 amplified with streptavidin-biotin, Novus Biologicals). We incubated with TBS with Tween-20 at 0,1% to wash the primary antibody excess and we added specific donkey-Cy3 or Alexa488 against primary antibody (1:200; Jackson Immunoresearch) during 1h and 30' at RT. Besides this, we washed with TBS-0,3Triton-X-100 the slices and we added fluorescent green NeuroTracer Nissl Stain (Molecular Probes, Leiden, Netherlands) and DAPI (Sigma,

St Louis, MO, USA) to counterstain them. After several washings with TBS and TB, the slices were mounted with Fluoromount-G mounting medium (SouthernBiotech).

We examined under confocal microscope with a Confocal Laser Scanning Microscope (Zeiss LSM 700; Zeiss, Jena, Germany) the immunolabeled spinal cords from different animals and experimental groups. Confocal images were systematically acquired using three separate photomultiplier channels with a 1.4 numerical aperture objective of 20x under the same conditions of exposure time, resolution and sensibility for each analysed marker. Images were separately projected and the signal intensity was analysed with the aid of the ImageJ software (National Institutes of Health; available at http://rsb.info.nih.gov/ij/). The Nissl labelling were used as ROI (Region of interest) to enclose the MN cytosolic area, and the integrated density within the ROI was obtained for at least 15 MNs extracted from three different sections (separated 100 µm between each one) per animal for each marker.

Western blotting

For immunoblotting studies, we collected the L4-L5 segment of the spinal cord from each animal (n=3/4 per experimental condition) at end-stage and added lysis buffer (50 Mm Tris, 2mM EDTA, 0.5% Triton-X-100, 10 mM Nicotinamide and a cocktail of protease (Sigma) and phosphatase inhibitors (Roche); pH=6.8). We homogenized it on ice with the aid of a Pellet pestle (Sigma-Aldrich, sonicated it with an Ultrasonic homogenizer (Model 3000, Biologics Inc) and we centrifuged at 13000g during 10 min at 4ºC. The supernatant is harvested and quantified by BCA assay (Pierce Chemical Co.; Rockford, IL, USA). An equal amount of protein of each animal (10µg/well) was resolved in SDS-Page and transferred to a nitrocellulose membrane in a BioRad cuvette system in 25 mM Tris, 192 mM glycine, 20% (v/v) methanol, pH 8.4. We blocked the membrane during 1 hour at RT with 5% milk solution in 0.1% Tween-TBS for 1 hour at RT and incubated it overnight with different primary antibodies: anti-growth associated protein-43 (GAP43; 1:1000, Millipore), rabbit anti-phospho FOXO3a (Ser-253) (pFOXO3a; 1:1000, Abcam), rabbit anti-FOXO3a (FOXO3a; Novus Biologicals, 1:500), rabbit anti-phospho Protein Kinase B/AKT (pAKT; 1:1000; Cell Signalling), rabbit anti-AKT (AKT, 1:1000; Cell Signalling) and anti-β-actin (Actin; 1:3000; Sigma Aldrich). After several

washes, we incubated the membrane for 1 h with an appropriate secondary antibody conjugated with horseradish peroxidase (1:5000, Vector). The proteins were visualized using a chemiluminiscent method (ECL Clarity kit, Bio-Rad Laboratories, Berkeley, CA, USA) and the images were captured and quantified with Image Lab Software (Bio-Rad Laboratories).

For Immunoprecipitation, we followed the manufacturer's protocol (Life Technologies). Briefly, we linked the anti-Acetylated lysine antibodies (Ac-Lys; 1:200; Sigma) to the magnetic particles on a rotatory wheel during 10 min at RT, washed them and incubated with 20µg of protein extract during 10 mins at RT on a rotatory wheel. After elution, proteins were denaturalized, resolved in SDS-Page gel of 10%, transferred to a nitrocellulose membrane, incubated with primary and secondary antibody as previously described.

Statistical analysis

Data are presented as a mean ± standard error of the mean (SEM). Results were statistically analysed using GraphPad Prism 5 software (San Diego, California, USA) by one or two-way analysis of variance (ANOVA) followed by Bonferroni's post hoc test between groups. Statistical significances were taken with a p-value of <0.05.

RESULTS

Cytosolic expression SIRT1 is increased within MNs during axonal regrowth

To further characterize the SIRT1 expression and aiming to seek how its activity is regulated after nerve injury, we used two different rat models of PNL in which MNs activate endogenous mechanisms to extend their injured axons: the sciatic nerve crush and the delayed reimplantation (RE) of avulsed-ventral roots into the spinal cord. In both injuries, the pro-regenerative machinery is needed within the MN to recover the lost function. We immunohistochemically analysed SIRT1 expression after crush injury and observed that the number of MNs expressing it was increased, and that it was overrepresented only at the cytosol of injured neurons (**Figure 1A**). Although SIRT1 is described as a nuclear deacetylase, we were unable to detect it at the nuclei of either contralateral or injured MNs after crush. Specifically, the axonal and cytosolic presence of SIRT1 has been related to

neurite elongation [25,26]. We confirmed that the nuclear activity of SIRT1 was not modified during nerve regeneration by the analysis of its nuclear substrates Ac-H3k9 and Ac-p53 (**Figure 1B**). In parallel, we also observed that those rats who received NH treatment had a significant increase in the cytosolic expression of SIRT1 (**Figure 1A, B, C**). In the other model of RA plus RE, SIRT1 was aberrantly accumulated within the nuclei of MNs after nerve injury as we described previously [14]. Otherwise, when these MNs had a proper root reconnection to re-extend their axons, SIRT1 was re-localized to the cytosol, which reinforces its putative cytosolic role during the axonal regrowth (Figure **1D)**. These results suggested us that SIRT1 cytoplasmic activity can be triggering some cytosolic pathways to refurnish machinery that MNs need to re-extend their axons after nerve injury, and that our drug therapy may act through SIRT1 activation.

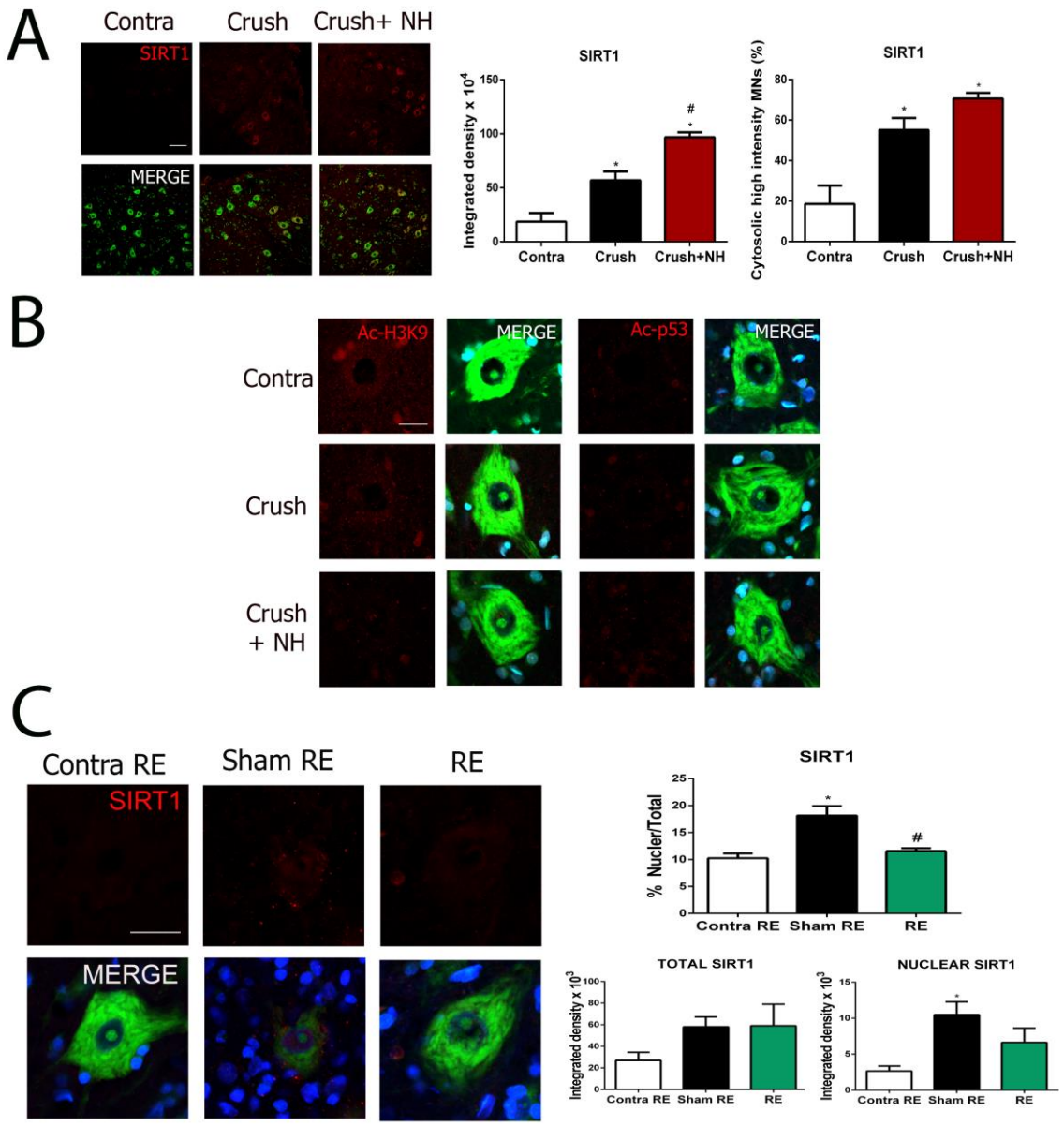

Figure 1. **(A)** Left, Confocal images of MNs immunolabeled for SIRT1 counterstained with Fluoro Nissl Green in injured spinal cord at 35 dpi days after peripheral nerve crush. Right, Histograms of the mean of the immunofluorescence intensity inside the cytoplasm of injured MNs (n = 3 animals,). Scale bar = 50 µM (n = 3 for each group, ANOVA, post hoc Bonferroni, *p < 0.05 vs. Contra and #p<0.05 vs Crush) **(B)** Confocal images of MNs immunolabelled to reveal Ac-H3K9 and Ac-p53 in red and counterstained with FluoroNissl (green) and DAPI (blue) from MNs of CTL, crush and NH-treated animals at 35 dpi. Scale bar = 20 µM. (C) ***Left,*** Confocal microphotographs and graphs showing levels of SIRT1 (red) co-labelled with FluoroNissl (green) from different experimental groups Scale bar=

25 μM. ***Right***, Graph of the means of the immunofluorescence intensity for each marker inside nuclei of MNs (n=3-4 per group, ANOVA, post hoc Bonferroni, *p<0.05 vs. Contra RE, #p<0.05 vs. Sham RE).

SIRT1 activation increase nerve regeneration in vivo

As we described previously, NH increases axonal growth after injury *in vivo* and promotes MN survival by SIRT1 activation[14]. To further examine if the SIRT1 can enhance nerve regeneration, we use the rat model of sciatic cut and suture, which recapitulates the main features of PNL in human and allows MNs to regenerate and reattach with the denervated muscle. To assess SIRT1 role, we orally treated rats with NH, the SIRT1 inhibitor Nicotinamide (NAM) and NH+NAM after injury and we tested them by electrophysiological techniques at tibialis anterior, gastrocnemius and plantar muscles at different days post-injury. Those animals that received the NH treatment had an increased compound muscle action potential (CMAP) at TA at early times and at GA and PL at end stages (Figure **2A**), which indicates that motor axons regeneration is increased. NH also accelerated the apparition of CMAP at the distal plantar muscle. Finally, the cotreatment of NH with NAM completely blocked these effects, giving similar results with those animals treated with NAM. These data suggested us that SIRT1 activation accelerates the reconnection between MNs and their target organ and that SIRT1 has low activity after nerve injury. To check that these effects are related to SIRT1, we overexpressed it at the spinal MNs using the infection with adeno-associated virus (AAV10). Three weeks after intrathecal injection of AAV-GFP or AAV-SIRT1, we cut and sutured the sciatic nerve and tested by electrophysiological techniques the CMAP recovery. In this case, those animals with AAV-SIRT1 had a significant increase of the CMAP at different muscles analysed above compared with AAV-GFP, obtaining similar muscle reinnervations than those treated with NH and presenting an early CMAP response at plantar muscle (Figure **2B**). These results confirmed us the pro-regenerative role of SIRT1 after nerve injury.

Then we wonder if the cytosolic levels of SIRT1 were modified after NH treatment or with AAV-SIRT1 overexpression in cut and suture paradigm. We observed that NH increased the cytoplasmic presence of this protein and that NAM was unable to block the NH effect at this point. To confirm that the nuclear activity of SIRT1 was not modified (**Figure 2C**), we analysed Ac-H3 within the MNs by

immunohistochemistry. The data revealed us the acetylation levels of H3k9 were unmodified between groups, reinforcing the putative cytoplasmic role of SIRT1 during axonal regrowth (**Figure 2C**). To confirm if MNs have a more pro-regenerative phenotype, we analysed the presence of growth associated protein 43 (GAP43), which is a regeneration-associated gene, by immunohistochemistry. Those animals treated with NH or with the overexpression of SIRT1 had an increase of this marker, being these effects blocked by the NAM, which indicates that these effects are SIRT1 activity dependents (**Figure 2C**).

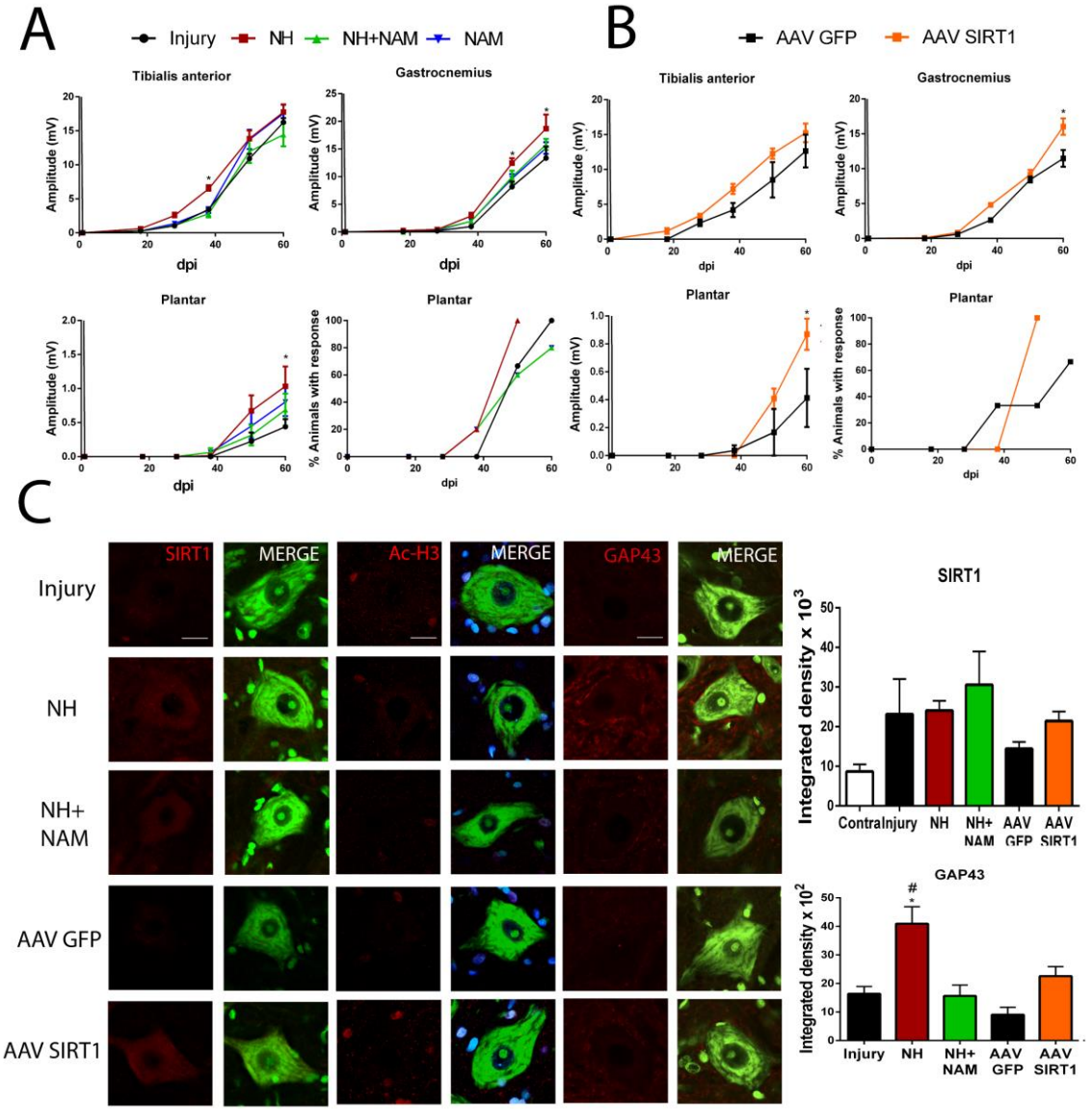

Figure 2 (A) Mean amplitudes (±SEM) values of CMAP recordings obtained during follow-up post-axotomy from TA, GA, Plantar muscles in animals treated with NH, NH+NAM or NAM (n=5-6, ANOVA, post hoc Bonferroni, *p < 0.05 vs. Injury) **(B)** Mean amplitudes (±SEM) values of CMAP recordings obtained during follow-up post-axotomy from TA, GA, Plantar muscles in animals overexpressing

GFP or SIRT1 (n=4-6, ANOVA, post hoc Bonferroni, *p < 0.05 vs AAV-GFP) **(C)** ***Left,*** Representative confocal images of SIRT1, Ac-H3k9 and GAP43 (red) counterstained with FluoroNissl (green) or DAPI in MNs from the different groups and the associated bar graphs of the mean (±SEM) intensity for each marker inside the cytoplasm of injured MNs at 60dpi (n=3-4, ANOVA, post hoc Bonferroni, *p < 0.05 vs Injury, #<0.05 vs NH+NAM).

Cytoplasmic activity of SIRT1 is increased during regeneration and induces SIRT1-dependent autophagy

To test if SIRT1 cytosolic activity is modulated during axonal regrowth, we analysed the cytosolic accumulation of the hypoxia-inducible factor 1α (HIF-1 α) as an indirect readout of its deacetylase activity [27]. Hif1α was overrepresented after crush injury within the cytosol of MNs and NH-treatment increases its presence (Fig **3A**). In parallel, we tested if NH has similar effects on HIF1α presence after cut and suture injury, and we observed that these effects are SIRT1-activity dependent, because the inhibition with NAM blocked them. Therefore, seems that SIRT1 stabilizes HIF1α when MNs shift their machinery to a pro-regenerative phenotype.

Next, we aimed to clarify if those animals had any changes in the autophagy flux, due to the previously described roles of SIRT1 and Hif1 on it. Some articles showed that nuclear SIRT1 activity induces autophagy by FOXO's and LC3 modulation [28,29], and that the cytosolic presence of this enzyme promotes it by ATG, mTOR or acetylproteome changes [30–32]. Moreover, Hif1 induces autophagy through an increased BNIP3 expression [33]. Therefore, we aimed to clarify if SIRT1 overexpression increases autophagic flux. Western blot analysis from L4-L6 spinal cord segment showed that AAV10-SIRT1 animals had a significant increase of ATG5-ATG12 and LC3II at 7dpi post cut and suture compared to AAV10-GFP, and that these effects were blocked when rats received oral NAM (Figure 3B). Furthermore, the inhibition of SIRT1 activity leads to an increase of p62 protein in AAV10-SIRT1 animals, indicating that autophagy was blocked. We also observed by immunohistochemically labelling that AAV10-SIRT1 animals had a significant increase of Hif1α and ATG5 within the MN cytosol, and that the phosphorylated form of p70s6k that depends of mTOR-activity was not modified by SIRT1 overexpression (Figure 3D). These data suggest us that autophagy induction was independent of mTOR and may be promoted by SIRT1/Hif1 axis.

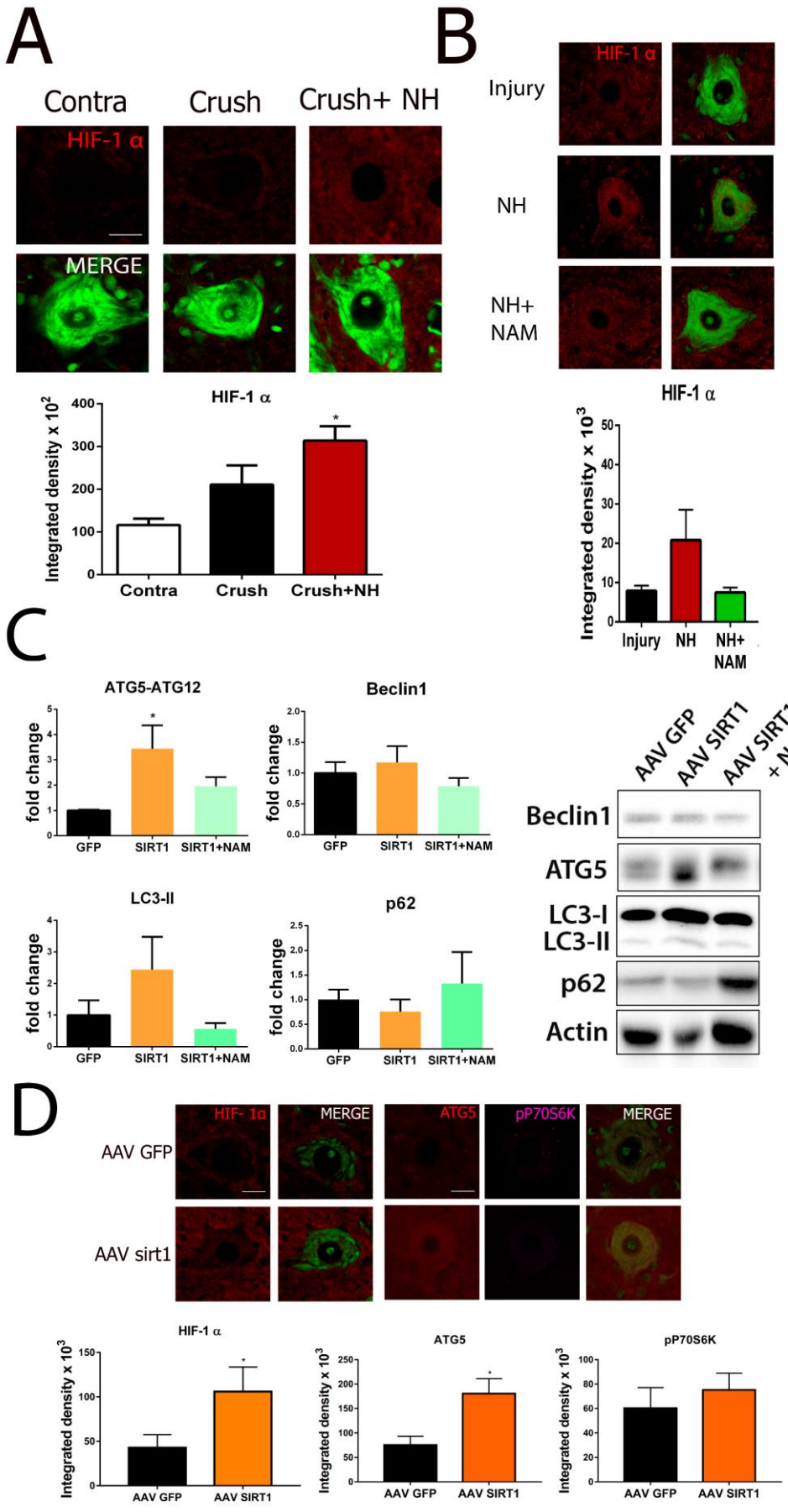
A
Contra
Crush
Crush+ NH
HIF-1 α
MERGE
HIF-1 α
Integrated density x 10²
400
300
200
100
0
Contra
Crush
Crush+NH
B
Injury
NH
NH+ NAM
HIF-1 α
HIF-1 α
Integrated density x 10³
50
40
30
20
10
0
Injury
NH
NH+ NAM
C
ATG5-ATG12
Beclin1
fold change
GFP
SIRT1
SIRT1+NAM
LC3-II
p62
AAV GFP
AAV SIRT1
AAV SIRT1 + NAM
Beclin1
ATG5
LC3-I
LC3-II
p62
Actin
D
HIF- 1α
MERGE
ATG5
pP70S6K
MERGE
AAV GFP
AAV sirt1
HIF-1 α
ATG5
pP70S6K
Integrated density x 10³
AAV GFP
AAV SIRT1

Figure 3 (A) ***Up***, confocal images of MNs immunolabeled for HIF1-α counterstained with Fluoro Nissl Green in injured spinal cord at 35 days after nerve crush in contralateral site, injured or NH treated animals Scale bar= 20 μM (n=3, ANOVA, post hoc Bonferroni, *p < 0.05 vs. Contra . ***Down***, bar graph of the mean of the immunofluorescence intensity of HIF in the MN for each group (STADISTICS) **(B)** ***Up,*** Representative confocal images of Hif-1α (red) counterstained with FluoroNissl (green) in MNs from the different groups at 60dpi. Scale bar = 20μM ***Bottom,*** bar graph of the mean (±SEM) intensity for Hif1-1α inside the cytoplasm of injured MNs at 60dpi (n=3-4, ANOVA, post hoc Bonferroni) **(C)** Western blot and corresponding bar graphs of the quantification of different proteins related to autophagy **(**Beclin1, ATG5, LC3-II and p62) in the spinal cord from axotomy injured animals injected with AAVrh10-GFP or AAVrh10-ATG5. *p < 0.05 vs. SIRT-1 (Student's t-test) **(D)** Representative confocal images of MNs stained with HIF1-α, ATG5 and p- p70S6K at T-389 with Fluoro Nissl green from the different groups and associated bar graphs of the mean (±SEM) intensity for each marker inside the cytoplasm of injured MNs. (n=4 animals per group, t-test, *p<0.05 vs. AAV-GFP) Scale bar= 20 μM.

NH increases neurite extension and elongation in vitro by SIRT-activity and autophagy induction

Thereby, we used an *in vitro* model to determine if the NH-induced SIRT1 activity after injury is necessary for the growth of motor axons. We assessed the neurite growth after NH treatment alone or in combination with two well-known inhibitors of SIRT1 activity, Ex-527, and NAM. We used SOCs with a 3D collagen matrix, which is a closer approximation to the *in vivo* situation [34]. NH treatment significantly increased the number of neurites that the SOCs projected within the 3D matrix, and also enhanced the length of these neurites (**Figure 4A**). The concomitant treatment of NH with the SIRT1 inhibitors completely blocked its pro-axonogenic effect and the maximum length of the extended neurites, pointing out that the effect of NH is mainly mediated by an increased activity of SIRT1. Furthermore, we analysed by immunohistochemistry the cytosolic presence of SIRT1 and of Hif1 α, as a readout of SIRT1 cytosolic activity. SIRT1 was overrepresented within the cytosol of those MNs treated with NH alone or in combination with the inhibitors, but Hif1α was only increased in those MNs treated with NH alone (**Figure 4B**), pointing out that the activity of SIRT1 is increased with the NH.

We further analysed if this effect was blocked by the PI3K inhibitor 3-Methyladenine (3MA) in SOCs, which is also a well-described inhibitor of autophagy-induction. This drug averted the increase in the number of neurites and the

maximum length promoted by NH (**Figure 4C).** Therefore, NH effect also needs the autophagy induction to promote it pro-regenerative effect. To confirm if these levels were correlated with the growth GAP43, we culture SOCs and we treated them with NH combined with Ex-527, NAM, and 3MA. NH-induces an increase of GAP43, and the blockage of either SIRT1 activity or autophagy by 3MA blocked this effect (Figure **4D**).

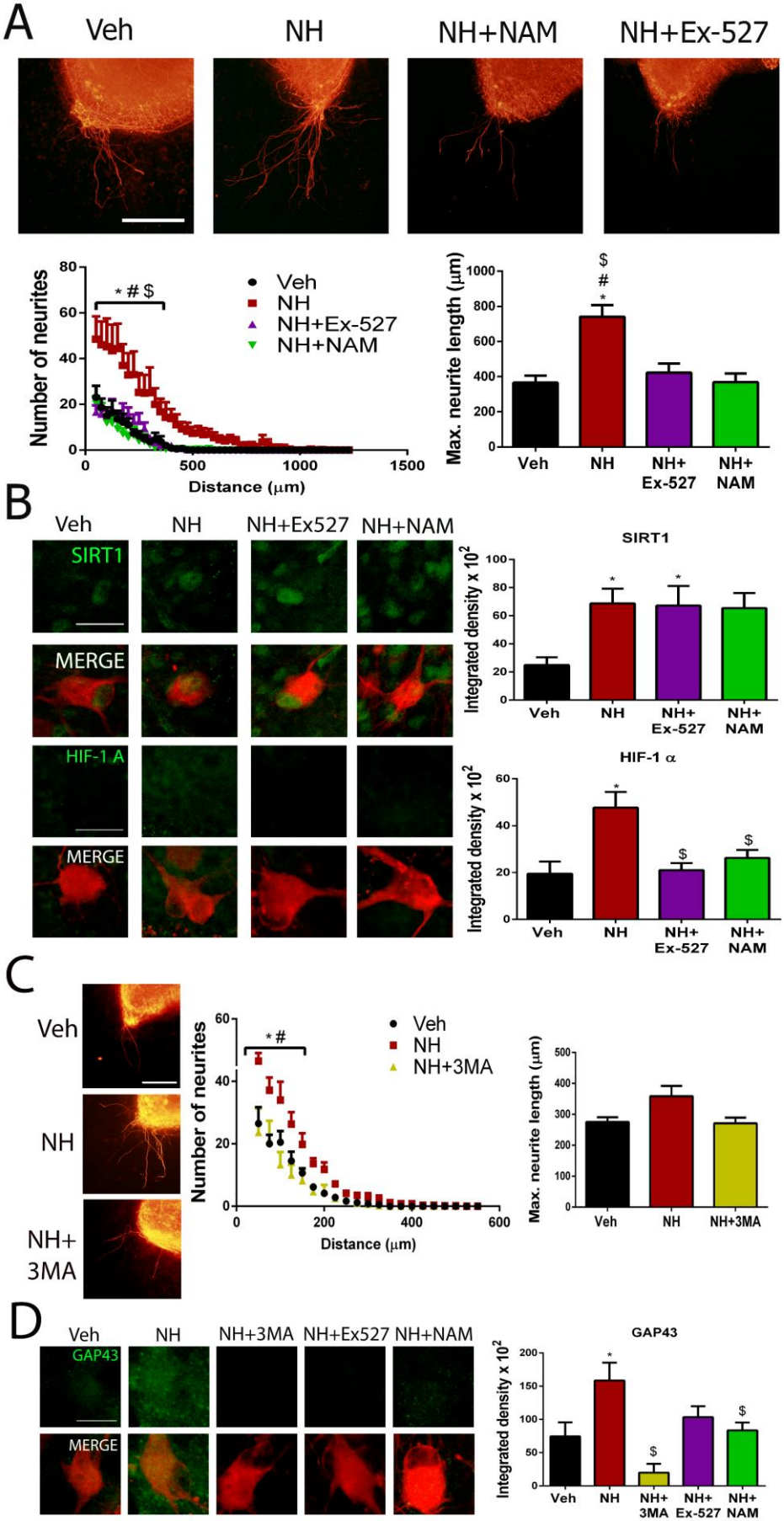
A
Veh
NH
NH+NAM
NH+Ex-527
Number of neurites
Distance (μm)
Veh
NH
NH+Ex-527
NH+NAM
Max. neurite length (μm)
Veh
NH
NH+ Ex-527
NH+ NAM
B
Veh
NH
NH+Ex527
NH+NAM
SIRT1
MERGE
HIF-1 A
MERGE
SIRT1
Integrated density x 10²
HIF-1 α
Integrated density x 10²
C
Veh
NH
NH+ 3MA
Number of neurites
Distance (μm)
Veh
NH
NH+3MA
Max. neurite length (μm)
D
Veh
NH
NH+3MA
NH+Ex527
NH+NAM
GAP43
MERGE
GAP43
Integrated density x 10²
Veh
NH
NH+ 3MA
NH+ Ex-527
NH+ NAM

Figure 4 (A) Representative microphotographs of Veh, NH, NH+Ex-527 and NH+NAM treated SOCs embeeded in collagen. Graphs show the number of neurites per intersection and the maximum neurite length in the SCOC **(n=8-10,** ANOVA, post hoc Bonferroni, *p < 0.05 vs. Veh, # p < 0.05 vs. NH+Ex-527, $ p < 0.05 vs. NH+NAM). Scale bar = 250 μM (**B**) ***Left,*** Representative confocal images of SIRT1 or Hif-1α (green) counterstained with RT-97 (red) of MNs from SOCs of different conditions. Scale bar= 20 μM ***Right,*** Bar graphs of the mean (±SEM) intensity for each marker inside the cytoplasm of MNs (n=10-18, ANOVA, post hoc Bonferroni, *p<0.05 vs. Veh, $<0.05 vs NH). (**C**). Representative microphotographs of Veh, NH and NH+3-MA treated SOCs embeeded in collagen. Graphs show the number of neurites per intersection and the maximum neurite length in the SCOC (n=6, ANOVA, post hoc Bonferroni, *p < 0.05 vs. Veh, # p < 0.05 vs. NH+3MA). Scale bar = 250 μM. (**D**) ***Left,*** Representative confocal images of GAP43 (green) counterstained with RT-97 (red) of MNs from SOCs of different conditions. Scale bar= 20 μM. ***Right,*** Bar graphs of the mean (±SEM) intensity for each marker inside the cytoplasm of MNs (n=14-29, ANOVA, post hoc Bonferroni, *p<0.05 vs. Veh, $<0.05 vs NH).

Autophagy induction by Hif1 stabilization induces neurite outgrowth

Seeking to understand if the Hif1-induced autophagy has pro-regenerative effects, we treated SOCs with DMOG, an inhibitor of the prolyl hydroxylases, the enzymes that drives Hif1 degradation by hydroxylation. DMOG treatment significantly increased the neurites emission and the longitude of them, indicating that Hif1 has neuritogenic effects (Figure **5A**). Aiming to depicter if those effected are mediated by Hif1-induced autophagy, we cotreated the SOC with DMOG and 3MA. In this case, we did not see significant differences compared with vehicle group, suggesting that autophagy modulates the effects observed in DMOG conditions. We also analysed by western blot the presence of the autophagy markers pUlk1 (Ser555), ATG5-ATG12, LCII and p62, observing that DMOG induces autophagy and that 3MA cotreatment blocks it (Figure **5B).**

To confirm if the SIRT1 pro-regenerative effect was mediated by Hif1α stabilization, we used another *in vitro* model based on SH-SY5Y cells culture, which is also widely used to analyse neurite outgrowth. Initially, we treated differentiated SH-SY5Y cells with DMOG, in combination or not with 3MA. DMOG treatment significantly increased the average of neurite length and the maximum neurite length ejected by these cells, while the treatment with the autophagy inhibitor 3MA averted both effects (Figure **6C**). On the other side, we genetically overexpressed SIRT1 or silenced Hif1α by shRNA (Figure **6D, S1)**. Interestingly, we also observed

in this model that SIRT1 is mainly cytosolic when neurons are ejecting their axons, as we observed *in vivo* (Figure **6D**). SIRT1 overexpression significantly increased neurite length in a similar fashion as DMOG did. shRNA_Hif1α alone significantly reduced the neurite length of the cells, and also blocked the pro-neuritogenic effects observed by SIRT1 overexpression, indicating that Hif1α is crucial to promote the SIRT1-dependent axonal regeneration that we observed *in vivo*.

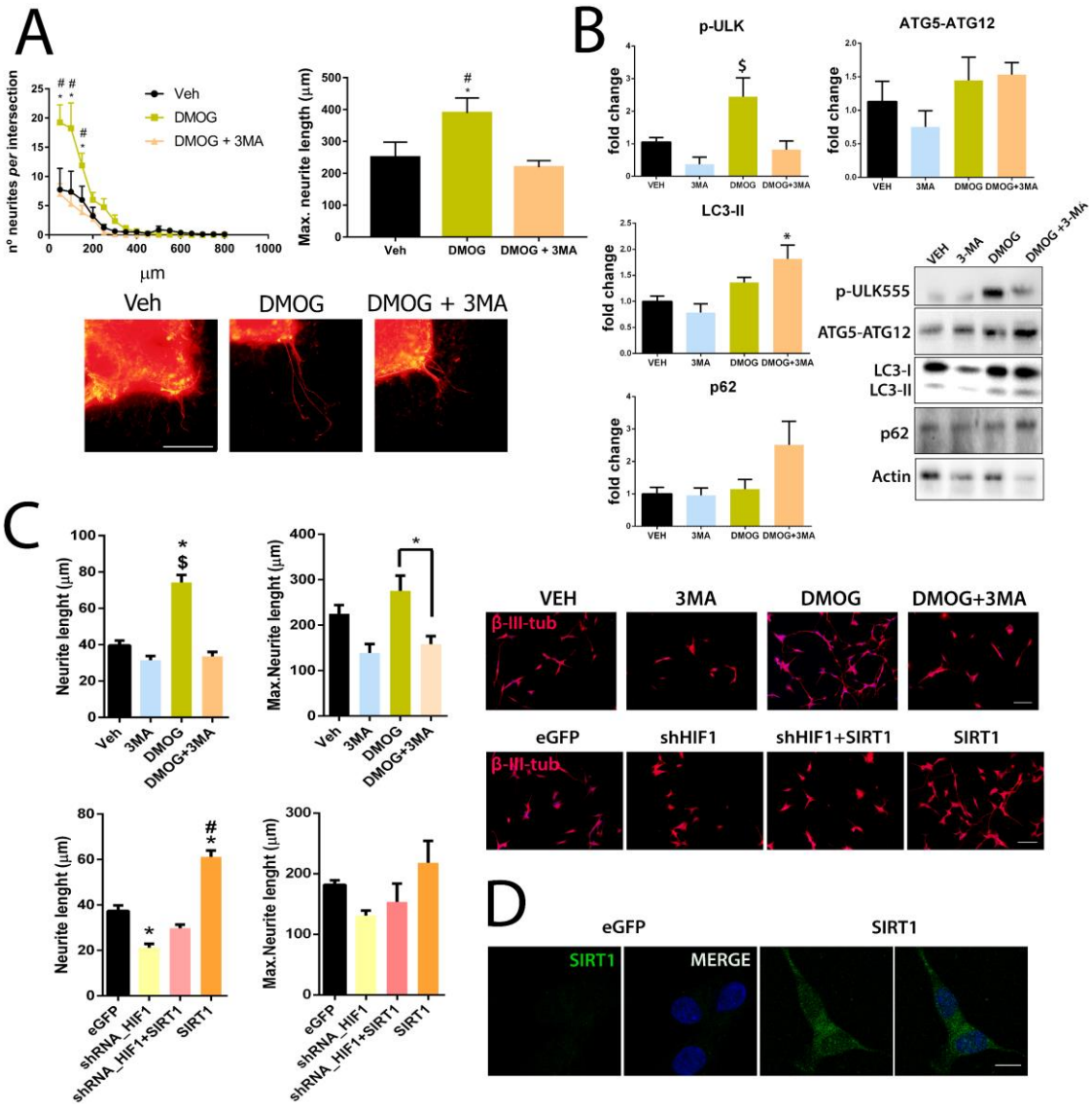

Figure 5 (A) Representative microphotographs of Veh, DMOG, DMOG+3-MA treated SOCs embeeded in collagen. Graphs show the number of neurites per intersection and the maximum neurite length in the SCOC (n=8-9, ANOVA, post hoc Bonferroni, *p < 0.05 vs. Veh, # p < 0.05 vs. DMOG+3MA). Scale bar = 250 µM **(B)** Western blots and histogram showing the analysis of analysis of pUlk1 (Ser555), ATG5-ATG12 LC3II and p62 protein level from SOCs after 2 days of treatment with Vehicle, DMOG, 3-MA or DMOG+3-MA (n=3-4, ANOVA, post hoc Bonferroni *p<0.05 vs DMOG, #p<0.05 vs Veh) **(C)** Representative microphotographs and bar graphs showing the mean (±SEM) values of neurite length

and maximum neurite length from SH-SHY5Y cells after 24h of treatment with Vehicle, DMOG, 3-MA or DMOG+3-MA or transfected cells with eGFP, shRNA/HIF1, SIRT-1 or the combination of shRNA/HIF+ SIRT-1. (n=3-4, ANOVA, post hoc Bonferroni *p<0.05 vs, #p<0.05 vs Veh). Scale bar=100 um**(D)**Representative microphotographs of SH-SHY5Y cells immunolabeled for SIRT1 counterstained with DAPI at 3 days post-culture in control and SIRT1 transfected cells. Scale bar=10 um.

ATG5-promoted autophagy accelerates nerve regeneration

We recently described that the AAV10-driven overexpression of ATG5 within the spinal MNs induces autophagy and increases MN survival after root avulsion [35]. Herein, to test if autophagy induction accelerates axonal regrowth, we intrathecally infected spinal MNs with AAV10-ATG5. Animals that overexpress ATG5 showed a significant increased CMAP amplitude at TA and gastrocnemius muscles as AAV-SIRT1 exhibited (Figure **6A**). Moreover, this was accompanied by a significant reduction of the sciatic functional index (SFI) analysed by walking track technique, which suggest a better motor performance of the hindlimb movements (Figure **6B**). We confirmed that ATG5-overexpressing MNs had a significant increase of ATG5 protein and GAP43 presence (Figure **6C**), reinforcing the hypothesis that autophagy induction promotes a higher regenerative capacity. To check that ATG5-induced autophagy is independent of AKT/mTOR axis, we analysed the phosphorylation state of p70s6k as we did above within injured MNs (Figure **6D**). The immunohistochemistry of this marker revealed no changes in the activation of this axis between AAV10-GFP and AVV10-ATG5 animals, supporting that mTOR-independent autophagy increases axonal regeneration and enhances functional recovery after PNL, as we described for SIRT1/Hif1α axis.

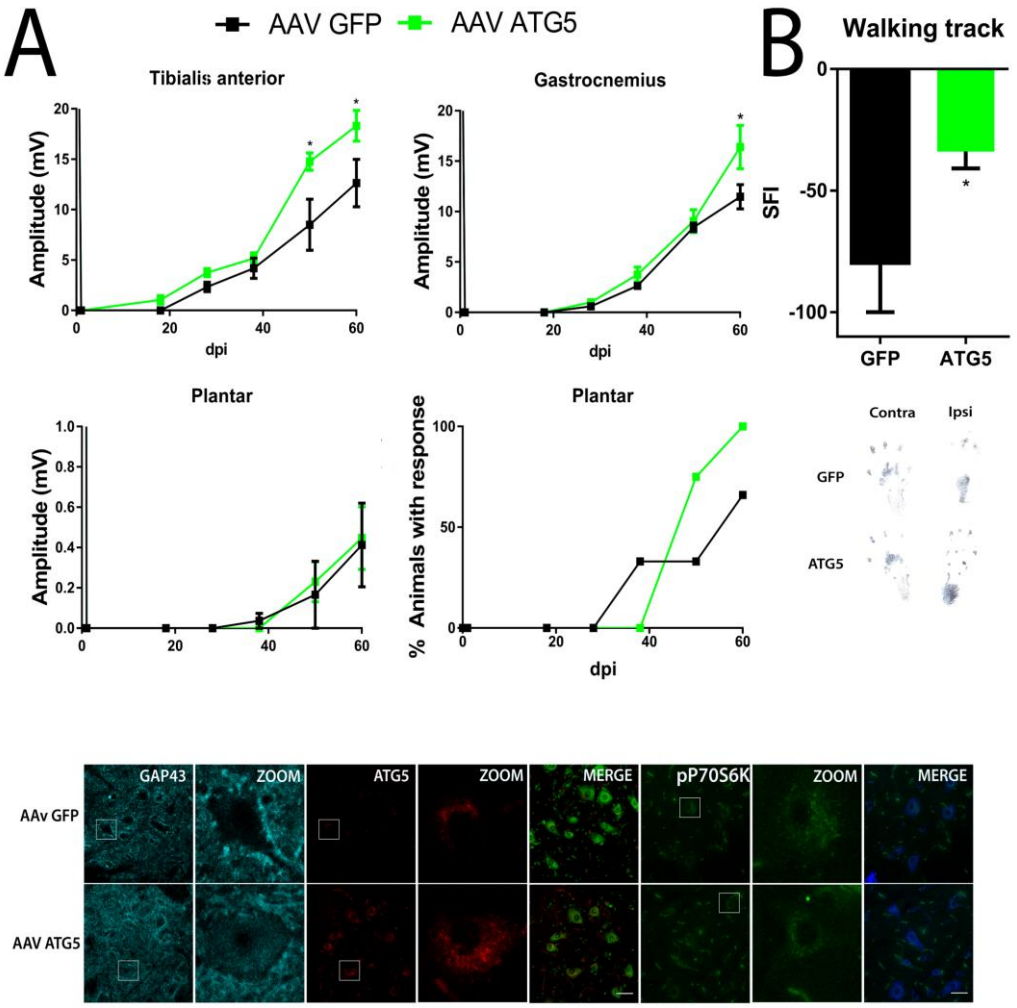

Figure 6. (A) Mean amplitudes (±SEM) values of CMAP recordings obtained during follow-up post-axotomy from TA, GA, Plantar muscles in animals overexpressing GFP or ATG5 (n=4-5, ANOVA, post hoc Bonferroni, *p < 0.05 AAV-GFP) **(B)** ***Up,*** representative footprints from ipsi- and contralateral paws at 60 days post injury (dpi). ***Down***, Graph of the sciatic functional index (SFI) obtained with walking track analysis of sciatic nerve in injured animals overexpressing ATG5 or GFP (t-test, *p<0.05 *vs.* AAV-GFP). **(C)** Representative confocal images of infected MNs with GFP or ATG5 immunolabeled for p-p70S6K at T-389, ATG5 and GAP-43 counterstained with Fluoro Nissl Blue or Fluoro Nissl Green at 60dpi after nerve axotomy.Scale bar=50 um.

NH treatment accelerates nerve regeneration in a more severe nerve injury.

Most of the surgical reparations of peripheral nerves need an autograft to reconnect the separated stumps. To test whether NH is an effective treatment for those injuries, we used a rat model of sciatic cut combined with autograft reparation. We treated the animals with NH and followed them by electrophysiological tests as explained above. Treated animals presented a significant increase on the CMAP of

TC, GA and PL muscle and an earlier apparition of CMAP at PL muscle as observed in the cut and suture model (**Figure 7A**). Finally, we analyzed the presence of Hif-1 α and GAP43 in the spinal cords from these animals by immunohistochemistry (**Figure 7B**), obtaining similar results to those obtained for the model of cut and suture. These data indicate that the NH acts in a similar fashion to enhance nerve regeneration in this model.

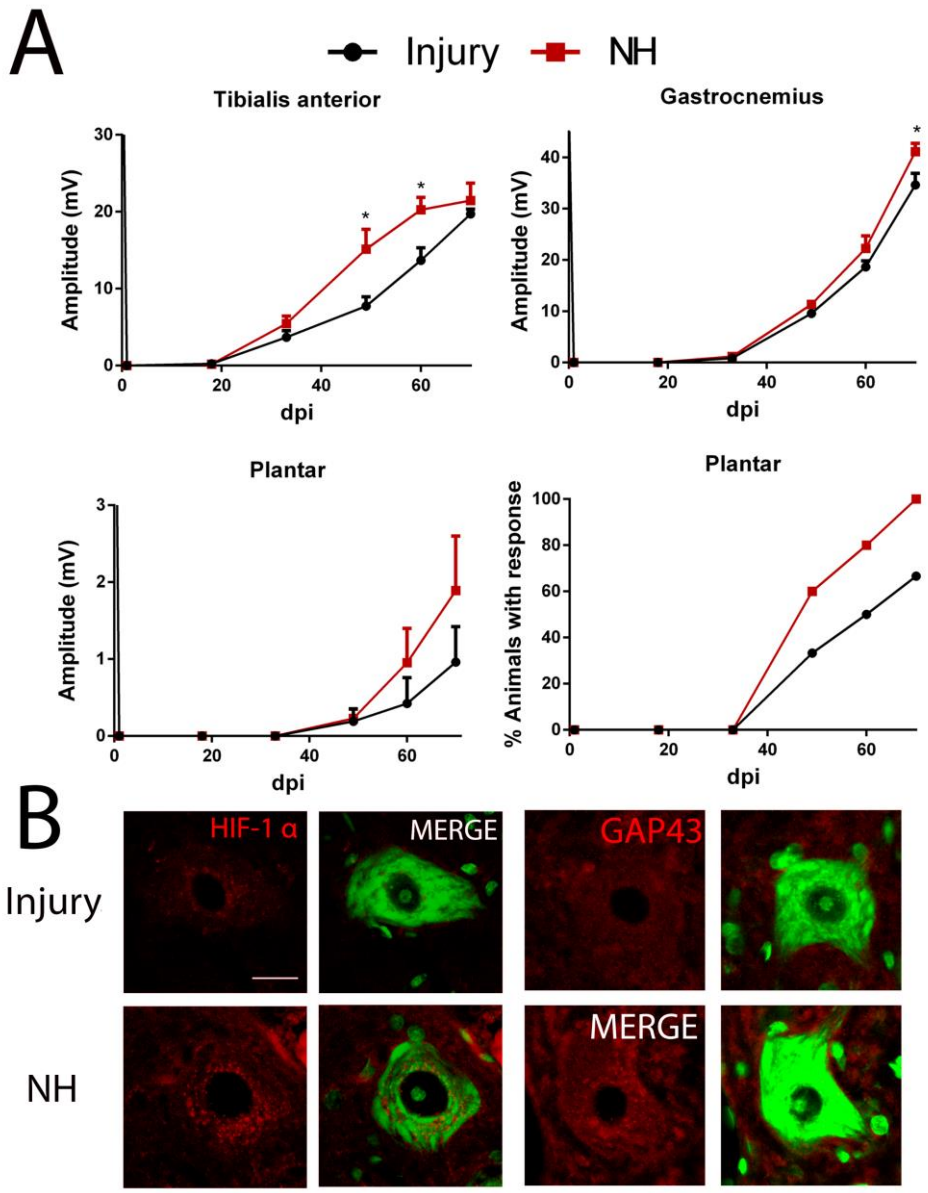

Figure 7 (A) Mean amplitudes (±SEM) values of CMAP recordings obtained during follow-up post-axotomy from TA, GA, Plantar muscles in animals treated with Vehicle or NH (n=5, ANOVA, post hoc Bonferroni, *p < 0.05 NH vs. Inj). **(B)** Representative confocal images of injured MNs immunolabeled for HIF1-α and GAP-43 counterstained with Fluoro Nissl Green at 75dpi Scale bar = 20µm.

DISCUSSION

In this work we aimed to depict the role of SIRT1 on the axonal regeneration of MNs after PNL and which are the underlying mechanisms. Although peripheral axons could regrowth after injury, a complete functional recovery is not always obtained due to a decline in their regenerative potency. Elucidate the programs that MNs engage during nerve regeneration can be helpful to discover new therapies to achieve a complete functional recovery after PNL. Here, we provide evidence that SIRT1 activity within the MN cytoplasm increases axonal regrowth and motor nerve regeneration after nerve injury, and that these effects involve the Hif1-dependent autophagy.

Initially, we described that MNs recruit SIRT1 to the cytosol when the pro-regenerative machinery is activated after PNL, while its deacetylase activity within the nuclei is significantly modified. We also described that an increased SIRT1 cytosolic activity is correlated with an overrepresentation of the Hif1α, GAP43 and with a higher pro-regenerative potency of the MNs *in vitro* and *in vivo*. These data fit with the pro-neuritogenic effect described *in vitro* for SIRT1, which is mediated by the modulation of AKT axis [25,26], although their exact mechanisms are poorly described and understood. Besides this, we described that Hif1α stabilization increases neuritogenesis and that these effects are autophagy-dependent. Finally, we check that an increased autophagic flux by the overexpression of ATG5 accelerates MN axonal regrowth.

Regarding SIRT1 localization, we were unable to find it at the MN nucleus. SIRT1 is located at the nucleus of other neuronal subtypes under normal conditions (i.e. neurons of dorsal root ganglia (DRG)). This location is related to neuronal differentiation [36–38] and the chronic inactivation of SIRT1 impairs neuronal maturation in oligodendrocytes [37]. SIRT1 is nuclear when it is overexpressed in retinal neurons, although it has not effect alleviating oxygen-induced retinopathy [39]. SIRT2, a SIRT1-family protein with controversial roles in neurodegeneration [40,41], is mainly cytosolic and essential for axonal remyelination after nerve injury [42]. Similarly, the NAD^+-synthesizing enzyme nicotinamide mononucleotide adenylyltransferase (NAMPT), which disruption provokes motor dysfunction [43],

only prevents axonal degeneration when it is located at cytosolic level [44]. Therefore, seems that those enzymes related to acetylproteome still have unrevealed functions in cytoplasmic compartment. Here, we provide evidences that SIRT1 has a novel function in the cytosol after PNL.

In the central nervous system, SIRT1 activity exerts neuroprotection in several models characterized by axonopathies and axonal degeneration as hallmarks. SIRT1 activation reduces axonal loss and spinal cord demyelination provoked after viral infection [45] and slows the progression of axonal degeneration present in WldS mice [46]. Regarding demyelinating diseases such as induced-multiple sclerosis in mice model, in which SIRT1 is downregulated, its active role is not clearly defined. SIRT1 activation reduces functional impairment, although another study suggests that its inactivation on nervous system delays the progression of the disease [37,47]. On another side, several studies report that SIRT1 activity can mediate axonal regeneration of injured cornea through the expression of miR-182 [48]. Its implication in the peripheral system seemed to be opposite since it stimulates axonal regenerationby repressing the miR-138 on neurons from DRG [38]. In fact, SIRT1 activation slows the degeneration of axons from DRG [49] and its inhibition reduces regeneration of sensory axons [38]. Nerve axotomy induces the expression of SIRT1 in DRGs as we have observed in MNs [38], and this can be related to changes on the expression of specific genes. We observed an increase of GAP43 presence, which is a marker well-correlated with axonal growth, within those MNs with higher SIRT1 activity. We have recently reported that the overexpression of SIRT1 mediated by AAV at spinal cord was not able to significantly increase the levels of GAP43 after root avulsion injury [14]. Albeit this, here we found that the same experimental approach increased GAP43 presence after cut and suture, which indicates that SIRT1 has different transcriptomic capabilities depending on the neuronal situation. Although it is not clear the underlying mechanism, SIRT1 activity and its Hif1-induced autophagy seems to have some role on GAP43 levels during axonal regeneration, but more studies are needed to elucidate which are the exact molecular mechanisms.

A recent study showed that Ulk1 and Ulk2 induces axonal guidance and its blockage stalls the axonal growth, indicating that autophagy can mediate axonal

regeneration [50]. After spinal cord injury, the autophagy induction avoids the retraction of the axons and enhances their regrowth leading to an increased recovery of motor function [51]. Besides, the blockage of the endolysosomal pathway causes defects on the remyelination and axonal regeneration after nerve injury and in Charcot-Marie-Tooth type 4J neuropathy [52]. Therefore, seems that the cell-protective mechanism of autophagy could modulate other cellular response to face the stress triggered after damage to the nervous systems.

Although unexplored, from this study raises other hypothesis related to SIRT1 regenerative potential by autophagy modulation. This is related to the Forkhead box protein (FOXO). SIRT1-mediated deacetylation of FOXO3a, FOXO1 and FOXO4 increases their transcriptomics activities in different biological paradigms. [53–55]. Besides, FOXO activity promotes axonal growth in the *C.elegans* model [56,57]. We recently described that SIRT1 modulates the transcriptomic program of FOXO3a by deacetylation, enhancing the presence of the phosphorylated form of FOXO3a within the MN nuclei, which is an event that does not happen under normal conditions due to the activation of AKT pathway. In fact, AKT phosphorylates FOXO3a blocking its induced gene expression [58] and avoiding neuronal death by apoptosis [59]. Experiments performed in *C. Elegans* described FOXO's as key players during axonal regeneration, and point out that the active role of SIRT1 is responsible for the transcriptomic program of FOXO that raises axonal regrowth [60]. Therefore, we hypothesized that this SIRT1-dependent deacetylation of pFOXO3a can shift the pro-apoptotic activities of FOXO3a towards the pro-regenerative ones, but this was out of the goal of the study and further studies are needed.

PNL provokes neuropathic pain apparition by central sensibilization processes and by the inflammatory response [61]. SIRT1 activity has anti-hyperalgesia effects, anti-allodynic and also attenuates neuropathic pain by epigenetic mechanisms [62–64]. In addition, it blocks the inflammatory reaction that sustains neuropathic pain [63,65]. Therefore, the finding that SIRT1 activity is beneficial for axonal regrowth can yield new therapeutic opportunities to treat the neuropathic pain, since there is a lack of effective therapies for this phenomena nowadays [61]. Finally, recent studies in our laboratory reported that NH treatment has anti-inflammatory effects in the model

of RA [14], pointing this therapy as a feasible treatment for PNL-induced neuropathic pain.

In summary, the present study demonstrates that the activation of autophagy at MN level enhances axonal regrowth after nerve injury and that this effect depends on SIRT1/Hif1 axis. Its activity did not modify AKT/mTOR axis activity, making this approach an attractive strategy because PTEN anti-oncogenic effects are not compromised. Therefore, pharmacological therapies aiming to increase the SIRT1 activity or autophagic flux may be a good strategy to treat those injuries that affect the peripheral nervous system. Albeit this, further studies are needed to discern if those mechanisms also induce axonal regrowth of DRG neurons and ameliorates the neuropathic pain, leading to the obtaining of a complete therapy for PNL.

ACKNOWLEDGEMENTS

This work was mainly supported by the Ministerio de Economía y Competitividad of Spain (#SAF 2014-59701). We are also grateful for support from CIBERNED and TERCEL. The RT97, antibodies were obtained from the Developmental Studies Hybridoma Bank developed under the auspices of the NICHD and maintained by the University of Iowa, Department of Biology.

COMPETING INTEREST

The authors declare no competing interests. NeuroHeal is currently under patent review.

SUPPLEMENTARY DATA

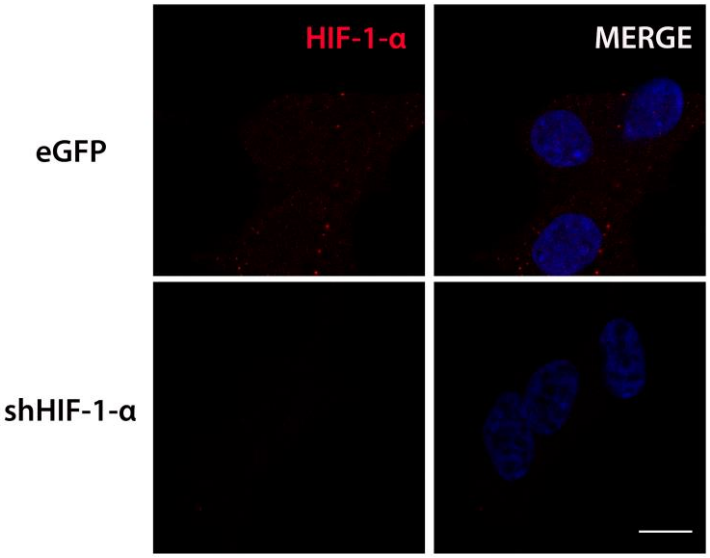

Figure S1 Immunocytochemistry against Hif-1α (red) in eGFP or shRNA/HIF1 transfected SH-SY5Y cells counterstained with DAPI. Scale bar= 25 um

REFERENCES

1. Grinsell D, Keating CP. Peripheral Nerve Reconstruction after Injury: A Review of Clinical and Experimental Therapies. *Biomed Res Int*. 2014;2014. doi:10.1155/2014/698256

2. Noble J, Munro CA, Prasad VS, Midha R. Analysis of upper and lower extremity peripheral nerve injuries in a population of patients with multiple injuries. *J Trauma*. 1998;45(1):116-122. doi:10.1097/00005373-199807000-00025

3. Pestronk A, Drachman DB, Griffin JW. Effects of aging on nerve sprouting and regeneration. *Exp Neurol*. 1980;70(1):65-82. doi:https://doi.org/10.1016/0014-4886(80)90006-0

4. Palispis WA, Gupta R. Surgical repair in humans after traumatic nerve injury provides limited functional neural regeneration in adults. *Exp Neurol*. 2017;290:106-114. doi:https://doi.org/10.1016/j.expneurol.2017.01.009

5. Chan KM, Gordon T, Zochodne DW, Power HA. Improving peripheral nerve regeneration: From molecular mechanisms to potential therapeutic targets. *Exp Neurol*. 2014;261:826-835. doi:https://doi.org/10.1016/j.expneurol.2014.09.006

6. Cannoy J, Crowley S, Jarratt A, et al. Upslope treadmill exercise enhances motor axon regeneration but not functional recovery following peripheral nerve injury. *J Neurophysiol*. 2016;116(3):jn.00129.2016. doi:10.1152/jn.00129.2016

7. Al-Majed AA, Neumann CM, Brushart TM, Gordon T. Brief electrical stimulation promotes the speed and accuracy of motor axonal regeneration. *J Neurosci*. 2000;20(7):2602-2608. http://www.ncbi.nlm.nih.gov/pubmed/10729340. Accessed January 23, 2017.

8. Tedeschi A. Tuning the orchestra: transcriptional pathways controlling axon

regeneration. *Front Mol Neurosci*. 2012;4(60):1-12. doi:10.3389/fnmol.2011.00060

9. Namikawa K, Honma M, Abe K, et al. Akt/Protein Kinase B Prevents Injury-Induced Motoneuron Death and Accelerates Axonal Regeneration. *J Neurosci*. 2000;20(8). http://www.jneurosci.org/content/20/8/2875.long. Accessed June 24, 2017.

10. Murashov AK, Haq IU, Hill C, et al. Crosstalk between p38, Hsp25 and Akt in spinal motor neurons after sciatic nerve injury. *Brain Res Mol Brain Res*. 2001;93(2):199-208. http://www.ncbi.nlm.nih.gov/pubmed/11589997. Accessed June 24, 2017.

11. Park KK, Liu K, Hu Y, et al. Promoting axon regeneration in the adult CNS by modulation of the PTEN/mTOR pathway. *Science*. 2008;322(5903):963-966. doi:10.1126/science.1161566

12. Ohtake Y, Park D, Abdul-Muneer PM, et al. The effect of systemic PTEN antagonist peptides on axon growth and functional recovery after spinal cord injury. *Biomaterials*. 2014;35(16):4610-4626. doi:10.1016/j.biomaterials.2014.02.037

13. Tolkacheva T, Chan a M. Inhibition of H-Ras transformation by the PTEN/MMAC1/TEP1 tumor suppressor gene. *Oncogene*. 2000;19(5):680-689. doi:10.1038/sj.onc.1203331

14. Romeo-Guitart D, Forés J, Herrando-Grabulosa M, et al. Neuroprotective Drug for Nerve Trauma Revealed Using Artificial Intelligence. *Sci Rep*. 2018;In press.

15. Oñate M, Catenaccio A, Martínez G, et al. Activation of the unfolded protein response promotes axonal regeneration after peripheral nerve injury. *Sci Rep*. 2016;6(February):21709. doi:10.1038/srep21709

16. Valenzuela V, Oñate M, Hetz C, Court FA. Injury to the nervous system: A look into the ER. *Brain Res*. 2016;1648:617-625. doi:10.1016/j.brainres.2016.04.053

17. Hervera A, De Virgiliis F, Palmisano I, et al. Reactive oxygen species regulate

axonal regeneration through the release of exosomal NADPH oxidase 2 complexes into injured axons. *Nat Cell Biol*. 2018;20(3):307-319. doi:10.1038/s41556-018-0039-x

18. Houtkooper RH, Pirinen E, Auwerx J. Sirtuins as regulators of metabolism and healthspan. *Nat Rev Mol Cell Biol*. 2012;13. doi:10.1038/nrn3209

19. Donmez G, Outeiro TF. SIRT1 and SIRT2: Emerging targets in neurodegeneration. *EMBO Mol Med*. 2013;5(3):344-352. doi:10.1002/emmm.201302451

20. Kupis W, Pałyga J, Tomal E, Niewiadomska E. The role of sirtuins in cellular homeostasis. *J Physiol Biochem*. 2016;72(3):371-380. doi:10.1007/s13105-016-0492-6

21. Michishita E, Park JY, Burneskis JM, Barrett JC, Horikawa I. Evolutionarily conserved and nonconserved cellular localizations and functions of human SIRT proteins. *Mol Biol Cell*. 2005;16(10):4623-4635. doi:10.1091/mbc.E05-01-0033

22. Stünkel W, Peh BK, Tan YC, et al. Function of the SIRTI protein deacetylase in cancer. *Biotechnol J*. 2007;2(11):1360-1368. doi:10.1002/biot.200700087

23. Guo W, Qian L, Zhang J, et al. Sirt1 overexpression in neurons promotes neurite outgrowth and cell survival through inhibition of the mTOR signaling. *J Neurosci Res*. 2011;89(11):1723-1736. doi:10.1002/jnr.22725

24. Romeo-Guitart D, Forés J, Navarro X, Casas C. Boosted Regeneration and Reduced Denervated Muscle Atrophy by NeuroHeal in a Pre-clinical Model of Lumbar Root Avulsion with Delayed Reimplantation. *Sci Rep*. 2017;7(1):12028. doi:10.1038/s41598-017-11086-3

25. Sugino T, Maruyama M, Tanno M, Kuno A, Houkin K, Horio Y. Protein deacetylase SIRT1 in the cytoplasm promotes nerve growth factor-induced neurite outgrowth in PC12 cells. *FEBS Lett*. 2010;584(13):2821-2826. doi:10.1016/j.febslet.2010.04.063

26. Li X, Chen C, Tu Y, Sun H. Sirt1 Promotes Axonogenesis by Deacetylation of Akt and Inactivation of GSK3. 2013;3:490-499. doi:10.1007/s12035-013-

8437-3

27. Laemmle A, Lechleiter A, Roh V, et al. Inhibition of SIRT1 impairs the accumulation and transcriptional activity of HIF-1α protein under hypoxic conditions. *PLoS One*. 2012;7(3):1-12. doi:10.1371/journal.pone.0033433

28. Ng F, Tang BL. Sirtuins' modulation of autophagy. *J Cell Physiol*. 2013;228(12):2262-2270. doi:10.1002/jcp.24399

29. Huang R, Xu Y, Wan W, et al. Deacetylation of nuclear LC3 drives autophagy initiation under starvation. *Mol Cell*. 2015;57(3):456-467. doi:10.1016/j.molcel.2014.12.013

30. Morselli E, Marino G, Bennetzen M V, et al. Spermidine and resveratrol induce autophagy by distinct pathways converging on the acetylproteome. *J Cell Biol*. 2011;192(4):615-629. doi:10.1083/jcb.201008167

31. Lee IH, Cao L, Mostoslavsky R, et al. A role for the NAD-dependent deacetylase Sirt1 in the regulation of autophagy. *Proc Natl Acad Sci U S A*. 2008;105(9):3374-3379. doi:10.1073/pnas.0712145105

32. Ghosh HS, McBurney M, Robbins PD. SIRT1 Negatively Regulates the Mammalian Target of Rapamycin. *PLoS One*. 2010;5(2):e9199. https://doi.org/10.1371/journal.pone.0009199.

33. Bellot G, Garcia-Medina R, Gounon P, et al. Hypoxia-induced autophagy is mediated through hypoxia-inducible factor induction of BNIP3 and BNIP3L via their BH3 domains. *Mol Cell Biol*. 2009;29(10):2570-2581. doi:10.1128/MCB.00166-09

34. Allodi I, Guzmán-Lenis MS, Hernàndez J, Navarro X, Udina E. In vitro comparison of motor and sensory neuron outgrowth in a 3D collagen matrix. *J Neurosci Methods*. 2011;198(1):53-61. doi:10.1016/j.jneumeth.2011.03.006

35. Leiva-Rodríguez T, Romeo-Guitart D, Marmolejo-Martínez-Artesero S, et al. ATG5 overexpression is neuroprotective and attenuates cytoskeletal and vesicle-trafficking alterations in axotomized motoneurons. *Cell Death Dis*. 2018;9(6):626. doi:10.1038/s41419-018-0682-y

36. Hisahara S, Chiba S, Matsumoto H, et al. Histone deacetylase SIRT1 modulates neuronal differentiation by its nuclear translocation. *Proc Natl Acad Sci U S A*. 2008;105(40):15599-15604. doi:10.1073/pnas.0800612105

37. Rafalski VA, Ho PP, Brett JO, et al. Expansion of oligodendrocyte progenitor cells following SIRT1 inactivation in the adult brain. *Nat Cell Biol*. 2013;15(6):614-624. doi:10.1038/ncb2735

38. Liu CM, Wang RY, Saijilafu, Jiao ZX, Zhang BY, Zhou FQ. MicroRNA-138 and SIRT1 form a mutual negative feedback loop to regulate mammalian axon regeneration. *Genes Dev*. 2013;27(13):1473-1483. doi:10.1101/gad.209619.112

39. Michan S, Juan AM, Hurst CG, et al. Sirtuin1 Over-Expression Does Not Impact Retinal Vascular and Neuronal Degeneration in a Mouse Model of Oxygen-Induced Retinopathy. *PLoS One*. 2014;9(1):e85031. https://doi.org/10.1371/journal.pone.0085031.

40. Chopra V, Quinti L, Kim J, et al. The Sirtuin 2 Inhibitor AK-7 Is Neuroprotective in Huntington's Disease Mouse Models. *Cell Rep*. 2012;2(6):1492-1497. doi:10.1016/j.celrep.2012.11.001

41. Romeo-Guitart D, Leiva-Rodríguez T, Sima N, et al. Neuroprotection of Disconnected Motoneurons requires Sirtuin 1 activation but Sirtuin 2 depletion or inhibition with AK-7 is detrimental. *Prep*. 2017.

42. Beirowski B, Gustin J, Armour SM, Yamamoto H, Viader A, North BJ. myelination through polarity protein Par-3 / atypical protein kinase C (aPKC) signaling. *October*. 2011;2. doi:10.1073/pnas.1104969108/-/DCSupplemental.www.pnas.org/cgi/doi/10.1073/pnas.1104969108

43. Wang X, Zhang Q, Bao R, et al. Deletion of Nampt in Projection Neurons of Adult Mice Leads to Motor Dysfunction, Neurodegeneration, and Death. *Cell Rep*. 2017;20(9):2184-2200. doi:10.1016/j.celrep.2017.08.022

44. Babetto E, Beirowski B, Janeckova L, et al. Targeting NMNAT1 to Axons and Synapses Transforms Its Neuroprotective Potency In Vivo. *J Neurosci*. 2010;30(40):13291-13304. doi:10.1523/JNEUROSCI.1189-10.2010

45. Khan RS, Dine K, Das Sarma J, Shindler KS. SIRT1 Activating compounds reduce oxidative stress mediated neuronal loss in viral induced CNS demyelinating disease. *Acta Neuropathol Commun*. 2014;2(1):3. doi:10.1186/2051-5960-2-3

46. Araki T, Sasaki Y, Milbrandt J. Increased nuclear NAD biosynthesis and SIRT1 activation prevent axonal degeneration. *Science*. 2004;305(5686):1010-1013. doi:10.1126/science.1098014

47. Shindler K, Ventura E, Dutt M. Oral Resveratrol Reduces Neuronal Damage in a Model of Multiple Sclerosis. *J Neuro- ….* 2010;30(4):328-339. doi:10.1097/WNO.0b013e3181f7f833.Oral

48. Wang Y, Zhao X, Wu X, Dai Y, Chen P, Xie L. MicroRNA-182 mediates sirt1-induced diabetic corneal nerve regeneration. *Diabetes*. 2016;65(7):2020-2031. doi:10.2337/db15-1283

49. Calliari A, Bobba N, Escande C, Chini EN. Resveratrol delays Wallerian degeneration in a NAD(+) and DBC1 dependent manner. *Exp Neurol*. 2014;251:91-100. doi:10.1016/j.expneurol.2013.11.013

50. Wang B, Iyengar R, Li-Harms X, et al. The autophagy-inducing kinases, ULK1 and ULK2, regulate axon guidance in the developing mouse forebrain via a noncanonical pathway. *Autophagy*. 2018;14(5):796-811. doi:10.1080/15548627.2017.1386820

51. He M, Ding Y, Chu C, Tang J, Xiao Q, Luo Z-G. Autophagy induction stabilizes microtubules and promotes axon regeneration after spinal cord injury. *Proc Natl Acad Sci*. 2016;113(40):11324-11329. doi:10.1073/pnas.1611282113

52. Vaccari I, Carbone A, Previtali SC, et al. Loss of Fig4 in both Schwann cells and motor neurons contributes to CMT4J neuropathy. *Hum Mol Genet*. 2015;24(2):383-396. doi:10.1093/hmg/ddu451

53. Brunet A, Sweeney LB, Sturgill JF, et al. Stress-dependent regulation of FOXO transcription factors by the SIRT1 deacetylase. *Science*. 2004;303(5666):2011-2015. doi:10.1126/science.1094637

54. Hughes KJ, Meares GP, Hansen PA, Corbett JA. FoxO1 and SIRT1 regulate β-

cell responses to nitric oxide. *J Biol Chem*. 2011;286(10):8338-8348. doi:10.1074/jbc.M110.204768

55. Kobayashi Y, Furukawa-Hibi Y, Chen C, et al. SIRT1 is critical regulator of FOXO-mediated transcription in response to oxidative stress. *Int J Mol Med*. 2005;16(2):237-243. doi:10.3892/ijmm.16.2.237

56. Byrne AB, Walradt T, Gardner KE, Hubbert A, Reinke V, Hammarlund M. Insulin/IGF1 Signaling Inhibits Age-Dependent Axon Regeneration. *Neuron*. 2014;81(3):561-573. doi:10.1016/j.neuron.2013.11.019

57. Calixto A, Jara JS, Court FA. Diapause Formation and Downregulation of Insulin-Like Signaling via DAF-16/FOXO Delays Axonal Degeneration and Neuronal Loss. *PLoS Genet*. 2012;8(12). doi:10.1371/journal.pgen.1003141

58. Motta MC, Divecha N, Lemieux M, et al. Mammalian SIRT1 Represses Forkhead Transcription Factors. *Cell*. 2004;116(4):551-563. doi:10.1016/S0092-8674(04)00126-6

59. Greer EL, Brunet A. FOXO transcription factors at the interface between longevity and tumor suppression. *Oncogene*. 24(50):7410-7425. http://dx.doi.org/10.1038/sj.onc.1209086.

60. Parker JA, Vazquez-Manrique RP, Tourette C, et al. Integration of -Catenin, Sirtuin, and FOXO Signaling Protects from Mutant Huntingtin Toxicity. *J Neurosci*. 2012;32(36):12630-12640. doi:10.1523/JNEUROSCI.0277-12.2012

61. Colloca L, Ludman T, Bouhassira D, et al. Neuropathic pain. *Nat Rev Dis Prim*. 2017;3:17002. doi:10.1038/nrdp.2017.2

62. Shao H, Xue Q, Zhang F, et al. Spinal SIRT1 activation attenuates neuropathic pain in mice. *PLoS One*. 2014;9(6). doi:10.1371/journal.pone.0100938

63. Lv C, Hu H-Y, Zhao L, Zheng H, Luo X-Z, Zhang J. Intrathecal SRT1720, a SIRT1 agonist, exerts anti-hyperalgesic and anti-inflammatory effects on chronic constriction injury-induced neuropathic pain in rats. *Int J Clin Exp Med*. 2015;8(5):7152-7159.

64. Zhou C-H, Zhang M-X, Zhou S-S, et al. SIRT1 attenuates neuropathic pain by epigenetic regulation of mGluR1/5 expressions in type 2 diabetic rats. *Pain*. 2017;158(1):130-139. doi:10.1097/j.pain.0000000000000739

65. To AM, Avulsion S, Pain I, et al. Segmental Spinal Root Avulsion in the Adult Rat : 2013;172:160-172. doi:10.1089/neu.2012.2481

66. Loeb JE, Cordier WS, Harris ME, Weitzman MD, Hope TJ. Enhanced expression of transgenes from adeno-associated virus vectors with the woodchuck hepatitis virus posttranscriptional regulatory element: implications for gene therapy. *Hum Gene Ther*. 1999;10(14):2295-2305. doi:10.1089/10430349950016942

67. Torres-Espín A, Santos D, González-Pérez F, del Valle J, Navarro X. Neurite-J: An Image-J plug-in for axonal growth analysis in organotypic cultures. *J Neurosci Methods*. 2014;236:26-39. doi:10.1016/j.jneumeth.2014.08.005

Discussion

General Discussion

After damage, the nervous system, as other tissues and cells in the body, has some ability for self-protection under mild stressful conditions activating pro-survival pathways, that are termed endogenous mechanisms of neuroprotection. These mechanisms are triggered at the same time as pro-death forces and the balance between them determine the vital destiny of the cells. When damage is severe, as it happens after proximal axotomy or nerve root avulsion, although these

mechanisms might activate, they used to be insufficient or presented as an incomplete program, that MNs degenerate (Casas et al., 2015). One of these mechanisms of neuroprotection is autophagy. In the present thesis we demonstrated that very early autophagy induction, through the overexpression of either GRP78/BiP, ATG5 or SIRT1, exerted neuroprotective effects. In addition, the overexpression of ATG5 or SIRT1 accelerated nerve regeneration and improved functional recovery in a model of PNI.

In the early stages after PNI, damaged or dysfunctional proteins, lipids, and organelles accumulate at the lesion site (Pereira et al .,2012). Autophagy, a cytoprotective process, maintain cellular homeostasis in which damaged or dysfunctional proteins, lipids and organelles are removed (Levine & Klionsky, 2004). Previous data reported autophagy induction in two different models of PNI, distal axotomy and root avulsion (Clara Penas, Font-Nieves, et al., 2011). This autophagy was induced by the same time, form 3 to 5 dpi as observed by increased abundance of Beclin1 and LC3-II but substantial differences were observed in LAMP-1 since it was totally absent in the RA model (Penas, Font-Nieves, et al., 2011). Autophagy was early activated in both cases, substantial differences make MNs to render vulnerable to cell death or not. Furthermore, proteomic analysis between these two models suggests that autophagy is a key determinant running program for the survival and regeneration in the axotomy model (Casas et al., 2015). This divergence could be due to a malfunction of this process after the avulsion. We demonstrated that autophagy flux is dysfunctional or blocked in degenerated motoneurons after root avulsion Alterations of proteins related to the initial phases of autophagy and in p62 have been observed in ALS. Autophagy potentiation by rapamycin, inductor of autophagy via mTORC1, exerts neuroprotection in cerebral ischemia, TBI and AD (Menzies et al.,2015). Importantly, proteomic analysis revealed an important aberration in cytoskeleton alterations in degenerated MNs. Dramatic reduction of acetylation of tubulin is described in degenerate MNs, which is considered an important regulator of microtubule dynamics (Almeida-Souza et al., 2011; Casas et al., 2015). Besides, an in vitro model that reproduced many of the events observed after RA in vivo demonstrated alterations in secretory pathway and lysosome function. We pointed that these alterations in cytoskeleton affects to

autophagy outcome and we demonstrate that these alterations promote neurodegeneration by itself. These results are in agreement with that MT stabilization has been proven to block neuronal death (Ruschel et al., 2015). Besides, Neuroheal a new neuroprotective agent, increase cytoskeletal dynamics after RA (Romeo-Guitart, Forés, et al., 2018a). These features are described in other neurodegeneratives diseases (Voelzmann et al.,2016). Besides, the axonopathy present in AD and ALS is characterized by a "dying back" phenomena and by the MTs loss (Baas et al., 2016). Accordingly, the study of these alterations of cytoskeleton and their contributions to the correct function of autophagy and to cell death may be applied to other types of pathologies.

Neuronal survival requires the continuous recycling of cellular materials released by the machineries of autophagy and endocytosis to maintain homeostasis. Impaired or dysfunctional autophagy in neurons is associated with neurodegeneration, while its activation can have a therapeutic benefit. Various studies have demonstrated the protective role of autophagy in the central nervous system with respect to cerebral trauma (Clark et al., 2008), hypoxia-ischemia brain injury (Balduini, 2012; Buonocore, & Balduini, 2008) and acute spinal cord injury(Hou et al., 2014). Besides, autophagy prevent neurodegeneration in PNS in animals of neuropathy (Kosacka et al., 2013). In the present work the demonstrated that autophagy potentiation at early stage sustains the survival after PNI. Rapamycin inhibits mTORC1 but long-term treatment modulates also the mTORC2 complex (Ballou & Lin, 2008). mTORC1 promotes anabolism, including mRNA translation, synthesis of lipids, purines, and pyrimidines, while inhibiting autophagy (Saxton & Sabatini, 2017). In the present study, we found neuroprotective capacities mediated by Rapamycin, only when is administrated previous than the lesion. Since mTOR inhibition affects the protein synthesis, essential for regenerative abilities after the lesion (Gumy, Tan, & Fawcett, 2010), other autophagy activators independent of mTOR are required for neuroprotection. Interestingly. Lithium treatment, that is an activator of autophagy independent of mTOR, after root avulsion increases MN survival (Fu et al., 2014). Thus, ATG5 overexpression, which activates autophagy in a mTOR independent, promotes MN preservation after the injury.

We also demonstrated that BiP overexpression mediates it neuroprotective capacities by the induction of selective autophagy, the mitophagy. This selective autophagy occurs to removal damaged or depolarized mitochondria and the most known pathway is via PINK1-Parkin dependent. These selective degradation of mitochondria is compromised in several neurodegenerative disorders i.e PD, ALS or AD (Martinez-Vicente, 2017). For example, different ALS-linked mutations in genes such as OPTN or p62 interfere with the process of mitophagy or reduces the efficiency of selective autophagy (Moore & Holzbaur, 2016)(Majcher, Goode, James, & Layfield, 2015). In the present work we found an increase of these mitophagy mediated by PINK1, but not of Parkin after the injury. Several studies suggests that Parkin might not be essential in neuronal mitophagy (Martinez-Vicente, 2017). These mitophagy activation is correlate with the previous data where GRP78/BiP overexpression markedly reduced LC3-II accumulation by 5 days post RA (Clara Penas, Font-Nieves, et al., 2011). In contrast, in vitro results suggest that BiP overexpression activates mitophagy with the recruitment of Parkin to the mitochondria and promotes neuroprotection in ER-stressed cells. Furthermore, ATG5 and BiP overexpression increases cell survival after the cytoskeleton alterations. This data could indicate that GRP78/BiP also activates the macroautophagy. With all of these data, we hypothesize that the activation of the autophagy machinery previous than the lesion, could help to remove accumulated material ie. cytoskeleton before the injury and protects the neuron in front of insult.

After PNI, several factors contributing to poor functional recovery include the damage to the neuronal cell body due to axotomy and retrograde degeneration, inability for axonal growth due to the nerve lesion, poor specificity of reinnervation and changes in the central circuits in which the injured neurons participate due to plasticity of neuronal connections (Lundborg, 2000). The effective recovery of motor function depends on axonal regeneration toward the muscles. After the injury, neurons activate their neuroprotective endogenous mechanisms. As mentioned previously, after PNI autophagy is activated. In the present work, we demonstrated that autophagy potentiation mediated by the axis SIRT1/HIF1 enhances axonal regeneration in vitro and in vivo and promotes better functional recovery. SIRT1/Sir2 was initially described as a nuclear protein that may also shuttle to the cytoplasm or mitochondria (Stünkel et al., 2007;Tang, 2016). SIRT1

have an impact on autophagy by the deacetylation of several ATG and the inhibition of mTOR, which promote autophagy(Ghosh, McBurney, & Robbins, 2010; I. H. Lee et al., 2008).This autophagy activation mediated by SIRT1 exerts a positive neurite-growth effect via mTOR inactivation in primary cell cultures. Correspondingly, Rapamycin enhanced neurite outgrowth (Garza-Lombó et al., 2016). Furthermore, the cytosolic form of SIRT1 has also been described during neuronal differentiation and neurite outgrowth (Hisahara et al., 2008). SIRT1 has also been shown to promote axon development in embryonic hippocampal neurons via AKT and enhancing axonogenesis in cultures hippocampal neurons (Codocedo et al., 2012). Specifically, cytosolic presence of SIRT1 has been related to neurite elongation (Sugino et al., 2010). This cytosolic activity of SIRT1 can stabilizes HIF-1α via deacetylation (Joo et al., 2015) and we demonstrated that the overexpression of SIRT-1 promotes the stabilization of HIF-1α in the cytosol in vivo. HIF-1-α enhances axon regeneration and accelerates neuromuscular junction re-innervation (Cho et al., 2015).This stabilization enhances neurite outgrowth in vitro and SIRT-1 regrowth capacities are dependent of HIF-1 α. BNIP3 is a known HIF-1 target gene (Greijer et al., 2005;Bruick, 2000) that has been implicated in autophagy (Hamacher-Brady et al., 2007). In fact, BNIP3 induce autophagy by disrupting interactions between Beclin-1 and Bcl2 (Maiuri et al., 2007). We found that HIF1 α promotes neurite outgrowth that is blocked by autophagy inhibition, which could indicate an effect mediated by autophagy. Finally, we demonstrated that specific activation of autophagy by ATG5 overexpression enhances the axonal regeneration and functional recovery after peripheral nerve axotomy. These ATG5 overexpression increases autophagy in a mTOR independent manner and promotes the expression of GAP-43, a pro-regenerative marker.

Research efforts to develop effective therapies for disorders affecting the function of the central nervous system have been aimed at elucidating the mechanisms of neuronal death to determine targets (genes, proteins or signalling pathways) that can be blocked pharmacologically. The process now aims to design alternative therapeutic strategies based on the enhancement of endogenous mechanisms of neuroprotection. After a complex neurodegenerative process that accounts after RA, it is necessary to modulate a whole network that characterizes the degeneration of MNs because it involves the crosstalk of several mechanisms

(Casas et al., 2015). In our laboratory generated several evidences with which proof that when MNs properly engage these mechanisms they can prevent dysfunction (Romeo-Guitart, et al., 2018b; Romeo-Guitart, et al., 2018; Romeo-Guitart et al., 2017). Furthermore, in the present work we demonstrate that the potentiation of these endogenous mechanisms such as autophagy using viral gene therapy promotes neuroprotection and regeneration after PNI. Nevertheless, the clinical studies based on viral gene therapy are generating undesired effects, due to the immune system reaction and the possibility of causing a tumour, among others (Brunetti-Pierri, 2017.) Perhaps, the future treatment of diseases are novel biotechnological techniques like nanotechnology, which allows the introduction of proteins and drugs to target several cells and therefore modulate pathways in a specific manner (Yu et al., 2016). Nanoparticles, such as liposomes, micelles, polymer nanoparticles and inorganic nanomaterials have considerable advantages as drug carriers. The best method to provides a direct access to the CNS is the intranasal delivery, without having to negotiate the BBB (Lochhead & Thorne, 2012). This tool yields promising effects in the cancer field (Platt et al., 2014) and in neurodegenerative diseases like PD, AD o ALS (Meredith et al., 2015) .

For this reason, the expected impact of the results includes a better understanding of the molecular mechanisms in neurodegeneration and neuroprotection of MNs to design better therapeutic strategies. This proof of concept is relevant in the field of neurodegenerative diseases and these results may resolve the questions raised due to controversial studies about the direction in autophagy modulation for therapy, whether being inhibited or activated, regarding some neurodegenerative diseases.

This proof of concept is relevant in the field of neurodegenerative diseases. The targeted neuronal population used to have heterogeneous degrees of pathology, with some of them at late neuropathological stages, while others are still not affected, which gives an opportunity to autophagy induction as a way of halting progression. These results may resolve the questions raised due to controversial studies about the direction in autophagy modulation for therapy, whether being inhibited or activated, regarding some neurodegenerative diseases.

Thus, enhancing and favour proper function of endogenous mechanisms of self-protection as autophagy may be a way to design efficacious neuroprotective strategies to stop progression.

Conclusions

Conclusions

Chapter 1: ATG5 Overexpression is Neuroprotective and Attenuates Cytoskeletal and Vesicle-Trafficking Alterations in Axotomized Motoneurons

- Peripheral nerve root avulsion provokes a blockage of the autophagy flux, alterations in microtubule-related transport and vesicle trafficking proteins at 5-7 days post-injury and altered LAMP1 and VATPase glycosylation.
- Nocodazole treatment of NSC34 neuronal cell line model cytoskeletal alterations and autophagy flux blockage observed in vivo.
- Sequential study analysis revealed that neurodegeneration might occur due to initial microtubule alteration followed by LAMP1 glycosilation alteration and autophagy blockage as observed in the in vitro model.
- Nocodazole treatment *in vivo* increases astrogliosis and MN death.
- Time-course analysis of pharmacological induction of autophagy using rapamycin revealed to be neuroprotective only as a pre-treatment before RA injury.
- Genetically-induced autophagy at the time of injury by overexpressing ATG5 with an adenoassociated vector resulted in improved internal trafficking, autophagy flux, and functionality of the lysosome.

Chapter 2: GRP78/BiP Triggers PINK1/IP_3R-Mediated Protective Mitophagy

- The overexpression of GRP78/BiP downregulated mitochondria-related proteins after peripheral nerve injury
- GR78/BiP overexpression in vitro attenuated mitochondrial dysfunction in ER stressed cells.

- GRP78/BiP overexpression activates mitophagy in a PINK1-Parkin dependent manner and it depends of the calcium transfer by IP3R in NSC34 cells after Tunicamycin treatment.
- Mitophagy activation could be involved in a PINK1 dependent GRP78/BiP after the peripheral nerve root avulsion

Chapter 3: Autophagy induced by SIRT1/Hif1α axis promotes nerve regeneration

- Cytosolic SIRT1 increased in two different models of PNL after Neuroheal treatment that enhances axonal regeneration after peripheral nerve axotomy.
- SIRT1 overexpression promoted HIF1 α stabilization in the cytosol and promoted autophagy induction mTOR independent after the injury.
- SIRT-1increased neurite outgrowth in vitro by autophagy activation mediates by SIRT-1/HIF1α axis
- ATG5-promoted autophagy accelerates nerve regeneration after peripheral nerve axotomy

References

References

Allodi, I., Guzmán-Lenis, M. S., Hernàndez, J., Navarro, X., & Udina, E. (2011). In vitro comparison of motor and sensory neuron outgrowth in a 3D collagen matrix. *Journal of Neuroscience Methods*, *198*(1), 53–61. https://doi.org/10.1016/j.jneumeth.2011.03.006

Allodi, I., Udina, E., & Navarro, X. (2012). Specificity of peripheral nerve regeneration: Interactions at the axon level. *Progress in Neurobiology*, *98*(1), 16–37. https://doi.org/10.1016/J.PNEUROBIO.2012.05.005

Almeida-Souza, L., Timmerman, V., & Janssens, S. (2011). Microtubule dynamics in the peripheral nervous system: A matter of balance. *BioArchitecture*, *1*(6), 267–270. https://doi.org/10.4161/bioa.1.6.19198

Annunziata, I., Sano, R., & d'Azzo, A. (2018). Mitochondria-associated ER membranes (MAMs) and lysosomal storage diseases. *Cell Death & Disease*, *9*(3), 328. https://doi.org/10.1038/s41419-017-0025-4

Arbogast, F., & Gros, F. (2018). Lymphocyte Autophagy in Homeostasis, Activation, and Inflammatory Diseases. *Frontiers in Immunology*, *9*, 1801. https://doi.org/10.3389/fimmu.2018.01801

Azizi, A., Azizi, S., Heshmatian, B., & Amini, K. (2014). Improvement of functional recovery of transected peripheral nerve by means of chitosan grafts filled with vitamin E, pyrroloquinoline quinone and their combination. *International Journal of Surgery*, *12*(1), 76–82. https://doi.org/10.1016/J.IJSU.2013.10.002

Baas, P. W., Rao, A. N., Matamoros, A. J., & Leo, L. (2016). Stability properties of neuronal microtubules. *Cytoskeleton (Hoboken, N.J.)*, *73*(9), 442–60. https://doi.org/10.1002/cm.21286

Balduini, W., Carloni, S., & Buonocore, G. (2012). Autophagy in hypoxia-ischemia induced brain injury. *The Journal of Maternal-Fetal & Neonatal Medicine*, *25*(sup1), 30–34. https://doi.org/10.3109/14767058.2012.663176

Ballou, L. M., & Lin, R. Z. (2008). Rapamycin and mTOR kinase inhibitors. *Journal of Chemical Biology*, *1*(1–4), 27–36. https://doi.org/10.1007/s12154-008-0003-5

Banker, B. Q., Kelly, S. S., & Robbins, N. (1983). Neuromuscular transmission and correlative morphology in young and old mice. *The Journal of Physiology*, *339*, 355–77. Retrieved from http://www.ncbi.nlm.nih.gov/pubmed/6310088

Barnes, A. P., & Polleux, F. (2009). Establishment of axon-dendrite polarity in developing neurons. *Annual Review of Neuroscience*, *32*, 347–81. https://doi.org/10.1146/annurev.neuro.31.060407.125536

Batlevi, Y., & La Spada, A. R. (2011). Mitochondrial autophagy in neural function, neurodegenerative disease, neuron cell death, and aging. *Neurobiology of Disease*. https://doi.org/10.1016/j.nbd.2010.09.009

Ben-Yaakov, K., Dagan, S. Y., Segal-Ruder, Y., Shalem, O., Vuppalanchi, D., Willis, D. E., … Fainzilber, M. (2012). Axonal transcription factors signal retrogradely in lesioned peripheral nerve. *The EMBO Journal*, *31*(6), 1350–63. https://doi.org/10.1038/emboj.2011.494

Berthold, C. H., Fabricius, C., Rydmark, M., & Andersén, B. (1993). Axoplasmic organelles at nodes of Ranvier. I. Occurrence and distribution in large myelinated spinal root axons of the adult cat. *Journal of Neurocytology*, *22*(11), 925–40. Retrieved from http://www.ncbi.nlm.nih.gov/pubmed/7507975

BLITS, B., CARLSTEDT, T., RUITENBERG, M., DEWINTER, F., HERMENS, W., DIJKHUIZEN, P., … Verhaagen, J. (2004). Rescue and sprouting of motoneurons following ventral root avulsion and reimplantation combined with intraspinal adeno-associated viral vector-mediated expression of glial cell line-derived neurotrophic factor or brain-derived neurotrophic factor. *Experimental Neurology*, *189*(2), 303–316. https://doi.org/10.1016/j.expneurol.2004.05.014

Boland, B., Kumar, A., Lee, S., Platt, F. M., Wegiel, J., Yu, W. H., & Nixon, R. A. (2008). Autophagy Induction and Autophagosome Clearance in Neurons: Relationship to Autophagic Pathology in Alzheimer's Disease. *Journal of Neuroscience*,

28(27), 6926–6937. https://doi.org/10.1523/JNEUROSCI.0800-08.2008

Bruick, R. K. (2000). Expression of the gene encoding the proapoptotic Nip3 protein is induced by hypoxia. *Proceedings of the National Academy of Sciences of the United States of America*, *97*(16), 9082–7. Retrieved from http://www.ncbi.nlm.nih.gov/pubmed/10922063

Brull, R., Hadzic, A., Reina, M. A., & Barrington, M. J. (2015). Pathophysiology and Etiology of Nerve Injury Following Peripheral Nerve Blockade. *Regional Anesthesia and Pain Medicine*, *40*(5), 479–90. https://doi.org/10.1097/AAP.0000000000000125

Brunden, K. R., Lee, V. M.-Y., Smith, A. B., Trojanowski, J. Q., & Ballatore, C. (2017). Altered microtubule dynamics in neurodegenerative disease: Therapeutic potential of microtubule-stabilizing drugs. *Neurobiology of Disease*, *105*, 328–335. https://doi.org/10.1016/J.NBD.2016.12.021

Brunetti-Pierri, N. (n.d.). *Safety and efficacy of gene-based therapeutics for inherited disorders*. Retrieved from https://books.google.es/books?id=y_okDwAAQBAJ&pg=PA7&lpg=PA7&dq=Yla-Herttuala,+2003;+Naldini,+2015&source=bl&ots=7-yT3dAt5g&sig=uJOwcsQl3nXUz-wjubCraizFVgw&hl=ca&sa=X&ved=2ahUKEwiPmM2Wk6HdAhVOxIUKHYLYC80Q6AEwB3oECBMQAQ#v=onepage&q=Yla-Herttuala%2C 2003%3B Naldini%2C 2015&f=false

Bucchia, M., Merwin, S. J., Re, D. B., & Kariya, S. (2018). Limitations and Challenges in Modeling Diseases Involving Spinal Motor Neuron Degeneration in Vitro. *Frontiers in Cellular Neuroscience*, *12*, 61. https://doi.org/10.3389/fncel.2018.00061

Carloni, S., Buonocore, G., & Balduini, W. (2008). Protective role of autophagy in neonatal hypoxia–ischemia induced brain injury. *Neurobiology of Disease*, *32*(3), 329–339. https://doi.org/10.1016/J.NBD.2008.07.022

Casas, C. (2017). GRP78 at the centre of the stage in cancer and neuroprotection. *Frontiers in Neuroscience*. Frontiers Media SA.

https://doi.org/10.3389/fnins.2017.00177

Casas, C., Isus, L., Herrando-Grabulosa, M., Mancuso, F. M., Borrás, E., Sabidó, E., … Aloy, P. (2015). Network-based proteomic approaches reveal the neurodegenerative, neuroprotective and pain-related mechanisms involved after retrograde axonal damage. *Scientific Reports*, *5*, 9185. https://doi.org/10.1038/srep09185

Cha-Molstad, H., Sung, K. S., Hwang, J., Kim, K. A., Yu, J. E., Yoo, Y. D., … Kwon, Y. T. (2015). Amino-terminal arginylation targets endoplasmic reticulum chaperone BiP for autophagy through p62 binding. *Nature Cell Biology*, *17*(7), 917–929. https://doi.org/10.1038/ncb3177

Chan, Y.-M., Wu, W., Yip, H. K., So, K.-F., & Oppenheim, R. W. (2001). Caspase inhibitors promote the survival of avulsed spinal motoneurons in neonatal rats. *Neuroreport*, *12*(3), 541–545. https://doi.org/10.1097/00001756-200103050-00022

Chew, D. J., Carlstedt, T., & Shortland, P. J. (2011). A comparative histological analysis of two models of nerve root avulsion injury in the adult rat. *Neuropathology and Applied Neurobiology*, *37*(6), 613–32. https://doi.org/10.1111/j.1365-2990.2011.01176.x

Chhabra, A., Ahlawat, S., Belzberg, A., & Andreseik, G. (2014). Peripheral nerve injury grading simplified on MR neurography: As referenced to Seddon and Sunderland classifications. *The Indian Journal of Radiology & Imaging*, *24*(3), 217–24. https://doi.org/10.4103/0971-3026.137025

Chin, T. Y., Kiat, S. S., Faizul, H. G., Wu, W., & Abdullah, J. M. (2017). The Effects of Minocycline on Spinal Root Avulsion Injury in Rat Model. *The Malaysian Journal of Medical Sciences : MJMS*, *24*(1), 31–39. https://doi.org/10.21315/mjms2017.24.1.4

Cho, Y., Shin, J. E., Ewan, E. E., Oh, Y. M., Pita-Thomas, W., & Cavalli, V. (2015). Activating Injury-Responsive Genes with Hypoxia Enhances Axon Regeneration through Neuronal HIF-1α. *Neuron*, *88*(4), 720–34. https://doi.org/10.1016/j.neuron.2015.09.050

Clark, R. S. B., Bayir, H., Chu, C. T., Alber, S. M., Kochanek, P. M., & Watkins, S. C. (2008). Autophagy is increased in mice after traumatic brain injury and is detectable in human brain after trauma and critical illness. *Autophagy*, *4*(1), 88–90. Retrieved from http://www.ncbi.nlm.nih.gov/pubmed/17957135

Codocedo, J. F., Allard, C., Godoy, J. A., Varela-Nallar, L., & Inestrosa, N. C. (2012). SIRT1 Regulates Dendritic Development in Hippocampal Neurons. *PLoS ONE*, *7*(10), e47073. https://doi.org/10.1371/journal.pone.0047073

Conde, C., & Cáceres, A. (2009). Microtubule assembly, organization and dynamics in axons and dendrites. *Nature Reviews Neuroscience*, *10*(5), 319–332. https://doi.org/10.1038/nrn2631

Cooper, E. C., & Jan, L. Y. (1999). Ion channel genes and human neurological disease: recent progress, prospects, and challenges. *Proceedings of the National Academy of Sciences of the United States of America*, *96*(9), 4759–66. https://doi.org/10.1073/PNAS.96.9.4759

Court, F. A., Gillingwater, T. H., Melrose, S., Sherman, D. L., Greenshields, K. N., Morton, A. J., … Ribchester, R. R. (2008). Identity, developmental restriction and reactivity of extralaminar cells capping mammalian neuromuscular junctions. *Journal of Cell Science*, *121*(23), 3901–3911. https://doi.org/10.1242/jcs.031047

Cox, J. S., & Walter, P. (1996). A novel mechanism for regulating activity of a transcription factor that controls the unfolded protein response. *Cell*, *87*(3), 391–404. Retrieved from http://www.ncbi.nlm.nih.gov/pubmed/8898193

Cuervo, A. M., & Dice, J. F. (1996). A receptor for the selective uptake and degradation of proteins by lysosomes. *Science (New York, N.Y.)*, *273*(5274), 501–3. https://doi.org/10.1126/SCIENCE.273.5274.501

Cullinan, S. B., Zhang, D., Hannink, M., Arvisais, E., Kaufman, R. J., & Diehl, J. A. (2003). Nrf2 is a direct PERK substrate and effector of PERK-dependent cell survival. *Molecular and Cellular Biology*, *23*(20), 7198–209. Retrieved from http://www.ncbi.nlm.nih.gov/pubmed/14517290

Dai, R. Y., Chen, S. K., Yan, D. M., Chen, R., Lui, Y. P., Duan, C. Y., … Li, H. (2010). PI3K/Akt promotes GRP78 accumulation and inhibits endoplasmic reticulum stress-induced apoptosis in HEK293 cells. *Folia Biologica*, *56*(2), 37–46. Retrieved from http://www.ncbi.nlm.nih.gov/pubmed/20492754

De Vos, K. J., & Hafezparast, M. (2017). Neurobiology of axonal transport defects in motor neuron diseases: Opportunities for translational research? *Neurobiology of Disease*, *105*, 283–299. https://doi.org/10.1016/j.nbd.2017.02.004

Deas, E., Plun-Favreau, H., Gandhi, S., Desmond, H., Kjaer, S., Loh, S. H. Y., … Wood, N. W. (2011). PINK1 cleavage at position A103 by the mitochondrial protease PARL. *Human Molecular Genetics*, *20*(5), 867–879. https://doi.org/10.1093/hmg/ddq526

Deumens, R., Bozkurt, A., Meek, M. F., Marcus, M. A. E., Joosten, E. A. J., Weis, J., & Brook, G. A. (2010). Repairing injured peripheral nerves: Bridging the gap. *Progress in Neurobiology*, *92*(3), 245–276. https://doi.org/10.1016/J.PNEUROBIO.2010.10.002

Devine, M. J., Birsa, N., & Kittler, J. T. (2016). Miro sculpts mitochondrial dynamics in neuronal health and disease. *Neurobiology of Disease*, *90*, 27–34. https://doi.org/10.1016/j.nbd.2015.12.008

Dijkers, P. F., Medema, R. H., Lammers, J. W., Koenderman, L., & Coffer, P. J. (2000). Expression of the pro-apoptotic Bcl-2 family member Bim is regulated by the forkhead transcription factor FKHR-L1. *Current Biology : CB*, *10*(19), 1201–4. Retrieved from http://www.ncbi.nlm.nih.gov/pubmed/11050388

Dikic, I., & Elazar, Z. (2018). Mechanism and medical implications of mammalian autophagy. *Nature Reviews Molecular Cell Biology*, *19*(6), 349–364. https://doi.org/10.1038/s41580-018-0003-4

Dorn, G. W., Scorrano, L., & Dorn, G. W. (2010). Two close, too close: sarcoplasmic reticulum-mitochondrial crosstalk and cardiomyocyte fate. *Circulation Research*, *107*(6), 689–99. https://doi.org/10.1161/CIRCRESAHA.110.225714

Egan, D. F., Shackelford, D. B., Mihaylova, M. M., Gelino, S., Kohnz, R. A., Mair, W., … Shaw, R. J. (2011). Phosphorylation of ULK1 (hATG1) by AMP-activated protein kinase connects energy sensing to mitophagy. *Science (New York, N.Y.)*, *331*(6016), 456–61. https://doi.org/10.1126/science.1196371

Elfar, J. C., Jacobson, J. A., Puzas, J. E., Rosier, R. N., & Zuscik, M. J. (2008). Erythropoietin Accelerates Functional Recovery After Peripheral Nerve Injury. *The Journal of Bone and Joint Surgery-American Volume*, *90*(8), 1644–1653. https://doi.org/10.2106/JBJS.G.00557

Elmore, S. (2007). Apoptosis: a review of programmed cell death. *Toxicologic Pathology*, *35*(4), 495–516. https://doi.org/10.1080/01926230701320337

Eskelinen, E.-L., Tanaka, Y., & Saftig, P. (2003). At the acidic edge: emerging functions for lysosomal membrane proteins. *Trends in Cell Biology*, *13*(3), 137–45. Retrieved from http://www.ncbi.nlm.nih.gov/pubmed/12628346

Fang, X.-Y., Zhang, W.-M., Zhang, C.-F., Wong, W.-M., Li, W., Wu, W., & Lin, J.-H. (2016). Lithium accelerates functional motor recovery by improving remyelination of regenerating axons following ventral root avulsion and reimplantation. *Neuroscience*, *329*, 213–225. https://doi.org/10.1016/j.neuroscience.2016.05.010

Farré, J.-C., & Subramani, S. (2016). Mechanistic insights into selective autophagy pathways: lessons from yeast. *Nature Reviews. Molecular Cell Biology*, *17*(9), 537–52. https://doi.org/10.1038/nrm.2016.74

Feinberg, J. H., Radecki, J., Wolfe, S. W., Strauss, H. L., & Mintz, D. N. (2008). Brachial plexopathy/nerve root avulsion in a football player: the role of electrodiagnostics. *HSS Journal : The Musculoskeletal Journal of Hospital for Special Surgery*, *4*(1), 87–95. https://doi.org/10.1007/s11420-007-9064-1

Fischer, D., & Leibinger, M. (2012). Promoting optic nerve regeneration. *Progress in Retinal and Eye Research*, *31*(6), 688–701. https://doi.org/10.1016/J.PRETEYERES.2012.06.005

Frye, R. A. (1999). Characterization of Five Human cDNAs with Homology to the

Yeast SIR2 Gene: Sir2-like Proteins (Sirtuins) Metabolize NAD and May Have Protein ADP-Ribosyltransferase Activity. *Biochemical and Biophysical Research Communications*, *260*(1), 273–279. https://doi.org/10.1006/bbrc.1999.0897

Frye, R. A. (2000). Phylogenetic Classification of Prokaryotic and Eukaryotic Sir2-like Proteins. *Biochemical and Biophysical Research Communications*, *273*(2), 793–798. https://doi.org/10.1006/bbrc.2000.3000

Fu, R., Tang, Y., Ling, Z.-M., Li, Y.-Q., Cheng, X., Song, F.-H., … Wu, W. (2014). Lithium enhances survival and regrowth of spinal motoneurons after ventral root avulsion. *BMC Neuroscience*, *15*(1), 84. https://doi.org/10.1186/1471-2202-15-84

Füllgrabe, J., Klionsky, D. J., & Joseph, B. (2013). Histone post-translational modifications regulate autophagy flux and outcome. *Autophagy*, *9*(10), 1621–3. https://doi.org/10.4161/auto.25803

Gähwiler, B. H., Capogna, M., Debanne, D., McKinney, R. A., & Thompson, S. M. (1997). Organotypic slice cultures: a technique has come of age. *Trends in Neurosciences*, *20*(10), 471–7. Retrieved from http://www.ncbi.nlm.nih.gov/pubmed/9347615

Galluzzi, L., Baehrecke, E. H., Ballabio, A., Boya, P., Bravo-San Pedro, J. M., Cecconi, F., … Kroemer, G. (2017). Molecular definitions of autophagy and related processes. *The EMBO Journal*, *36*(13), 1811–1836. https://doi.org/10.15252/embj.201796697

Galluzzi, L., Vitale, I., Aaronson, S. A., Abrams, J. M., Adam, D., Agostinis, P., … Kroemer, G. (2018). Molecular mechanisms of cell death: recommendations of the Nomenclature Committee on Cell Death 2018. *Cell Death & Differentiation*, *25*(3), 486–541. https://doi.org/10.1038/s41418-017-0012-4

Garza-Lombó, C., & Gonsebatt, M. E. (2016). Mammalian Target of Rapamycin: Its Role in Early Neural Development and in Adult and Aged Brain Function. *Frontiers in Cellular Neuroscience*, *10*, 157. https://doi.org/10.3389/fncel.2016.00157

Georgiou, M., Golding, J. P., Loughlin, A. J., Kingham, P. J., & Phillips, J. B. (2015). Engineered neural tissue with aligned, differentiated adipose-derived stem cells promotes peripheral nerve regeneration across a critical sized defect in rat sciatic nerve. *Biomaterials*, *37*, 242–251. https://doi.org/10.1016/J.BIOMATERIALS.2014.10.009

Geuna, S., Raimondo, S., Fregnan, F., Haastert-Talini, K., & Grothe, C. (2016, February). In vitro models for peripheral nerve regeneration. (D. Kirik, Ed.), *European Journal of Neuroscience*. https://doi.org/10.1111/ejn.13054

Ghosh, H. S., McBurney, M., & Robbins, P. D. (2010). SIRT1 Negatively Regulates the Mammalian Target of Rapamycin. *PLoS ONE*, *5*(2), e9199. https://doi.org/10.1371/journal.pone.0009199

Glaus, S. W., Johnson, P. J., & Mackinnon, S. E. (2011). Clinical strategies to enhance nerve regeneration in composite tissue allotransplantation. *Hand Clinics*, *27*(4), 495–509, ix. https://doi.org/10.1016/j.hcl.2011.07.002

Glick, D., Barth, S., & Macleod, K. F. (2010). Autophagy: cellular and molecular mechanisms. *The Journal of Pathology*, *221*(1), 3–12. https://doi.org/10.1002/path.2697

Gold, B. G., Katoh, K., & Storm-Dickerson, T. (1995). The immunosuppressant FK506 increases the rate of axonal regeneration in rat sciatic nerve. *The Journal of Neuroscience : The Official Journal of the Society for Neuroscience*, *15*(11), 7509–16. https://doi.org/10.1523/JNEUROSCI.15-11-07509.1995

Gold, B. G., Zeleny-Pooley, M., Wang, M.-S., Chaturvedi, P., & Armistead, D. M. (1997). A Nonimmunosuppressant FKBP-12 Ligand Increases Nerve Regeneration. *Experimental Neurology*, *147*(2), 269–278. https://doi.org/10.1006/EXNR.1997.6630

Gomes, L. C., Di Benedetto, G., & Scorrano, L. (2011). During autophagy mitochondria elongate, are spared from degradation and sustain cell viability. *Nature Cell Biology*, *13*(5), 589–98. https://doi.org/10.1038/ncb2220

Gomez-Sanchez, J. A., Carty, L., Iruarrizaga-Lejarreta, M., Palomo-Irigoyen, M.,

Varela-Rey, M., Griffith, M., … Jessen, K. R. (2015). Schwann cell autophagy, myelinophagy, initiates myelin clearance from injured nerves. *The Journal of Cell Biology*, *210*(1), 153–168. https://doi.org/10.1083/jcb.201503019

Gottlieb, T. M., Leal, J. F. M., Seger, R., Taya, Y., & Oren, M. (2002). Cross-talk between Akt, p53 and Mdm2: possible implications for the regulation of apoptosis. *Oncogene*, *21*(8), 1299–1303. https://doi.org/10.1038/sj.onc.1205181

Grasso, D., Ropolo, A., Lo Ré, A., Boggio, V., Molejón, M. I., Iovanna, J. L., … Vaccaro, M. I. (2011). Zymophagy, a Novel Selective Autophagy Pathway Mediated by VMP1-USP9x-p62, Prevents Pancreatic Cell Death. *Journal of Biological Chemistry*, *286*(10), 8308–8324. https://doi.org/10.1074/jbc.M110.197301

Greene, A. W., Grenier, K., Aguileta, M. A., Muise, S., Farazifard, R., Haque, M. E., … Fon, E. A. (2012). Mitochondrial processing peptidase regulates PINK1 processing, import and Parkin recruitment. *EMBO Reports*, *13*(4), 378–385. https://doi.org/10.1038/embor.2012.14

Greijer, A. E., van der Groep, P., Kemming, D., Shvarts, A., Semenza, G. L., Meijer, G. A., … van der Wall, E. (2005). Up-regualtion of gene expression by hypoxia is mediated predominantly by hypoxia-inducible factor I (HIF-I). *Journal of Pathology*, *206*(3), 291–304. https://doi.org/10.1002/path.1778

Gumy, L. F., Tan, C. L., & Fawcett, J. W. (2010). The role of local protein synthesis and degradation in axon regeneration. *Experimental Neurology*, *223*(1), 28–37. https://doi.org/10.1016/J.EXPNEUROL.2009.06.004

Guzmán-Lenis, M.-S., Navarro, X., & Casas, C. (2009). Drug screening of neuroprotective agents on an organotypic-based model of spinal cord excitotoxic damage. *Restorative Neurology and Neuroscience*, *27*(4), 335–49. https://doi.org/10.3233/RNN-2009-0482

Guzmán-Lenis, M.-S., Navarro, X., & Casas, C. (2009). Selective sigma receptor agonist 2-(4-morpholinethyl)1-phenylcyclohexanecarboxylate (PRE084) promotes neuroprotection and neurite elongation through protein kinase C (PKC) signaling on motoneurons. *Neuroscience*, *162*(1), 31–38.

https://doi.org/10.1016/j.neuroscience.2009.03.067

Hamacher-Brady, A., Brady, N. R., Logue, S. E., Sayen, M. R., Jinno, M., Kirshenbaum, L. A., … Gustafsson, Å. B. (2007). Response to myocardial ischemia/reperfusion injury involves Bnip3 and autophagy. *Cell Death and Differentiation*, *14*(1), 146–157. https://doi.org/10.1038/sj.cdd.4401936

Haninec, P., Houšťava, L., Stejskal, L., & Dubový, P. (2003). Rescue of rat spinal motoneurons from avulsion-induced cell death by intrathecal administration of IGF-I and Cerebrolysin. *Annals of Anatomy - Anatomischer Anzeiger*, *185*(3), 233–238. https://doi.org/10.1016/S0940-9602(03)80030-4

Harding, H. P., Zhang, Y., Bertolotti, A., Zeng, H., & Ron, D. (2000). Perk is essential for translational regulation and cell survival during the unfolded protein response. *Molecular Cell*, *5*(5), 897–904. Retrieved from http://www.ncbi.nlm.nih.gov/pubmed/10882126

Hayashi, T., & Su, T.-P. (2007). Sigma-1 Receptor Chaperones at the ER-Mitochondrion Interface Regulate Ca2+ Signaling and Cell Survival. *Cell*, *131*(3), 596–610. https://doi.org/10.1016/j.cell.2007.08.036

Haynes, C. M., & Ron, D. (2010). The mitochondrial UPR - protecting organelle protein homeostasis. *Journal of Cell Science*, *123*(Pt 22), 3849–55. https://doi.org/10.1242/jcs.075119

He, M., Ding, Y., Chu, C., Tang, J., Xiao, Q., & Luo, Z.-G. (2016). Autophagy induction stabilizes microtubules and promotes axon regeneration after spinal cord injury. *Proceedings of the National Academy of Sciences of the United States of America*, *113*(40), 11324–11329. https://doi.org/10.1073/pnas.1611282113

Hetz, C., & Saxena, S. (2017). ER stress and the unfolded protein response in neurodegeneration. *Nature Reviews Neurology*, *13*(8), 477–491. https://doi.org/10.1038/nrneurol.2017.99

Hirokawa, N., & Noda, Y. (2008). Intracellular Transport and Kinesin Superfamily Proteins, KIFs: Structure, Function, and Dynamics. *Physiological Reviews*, *88*(3), 1089–1118. https://doi.org/10.1152/physrev.00023.2007

Hisahara, S., Chiba, S., Matsumoto, H., Tanno, M., Yagi, H., Shimohama, S., … Horio, Y. (2008). Histone deacetylase SIRT1 modulates neuronal differentiation by its nuclear translocation. *Proceedings of the National Academy of Sciences*, *105*(40), 15599–15604. https://doi.org/10.1073/pnas.0800612105

Hoshida, S., Hatano, M., Furukawa, M., & Ito, M. (2009). Neuroprotective effects of vitamin E on adult rat motor neurones following facial nerve avulsion. *Acta Oto-Laryngologica*, *129*(3), 330–336. https://doi.org/10.1080/00016480802210431

Hou, H., Zhang, L., Zhang, L., & Tang, P. (2014). Acute spinal cord injury in rats should target activated autophagy. *Journal of Neurosurgery: Spine*, *20*(5), 568–577. https://doi.org/10.3171/2014.1.SPINE13237

Houtkooper, R. H., Mouchiroud, L., Ryu, D., Moullan, N., Katsyuba, E., Knott, G., … Auwerx, J. (2013). Mitonuclear protein imbalance as a conserved longevity mechanism. *Nature*, *497*(7450), 451–457. https://doi.org/10.1038/nature12188

Hu, Y. (2016). Axon injury induced endoplasmic reticulum stress and neurodegeneration. *Neural Regeneration Research*, *11*(10), 1557–1559. https://doi.org/10.4103/1673-5374.193225

Hu, Z.-Y., Chen, B., Zhang, J.-P., & Ma, Y.-Y. (2017). Up-regulation of autophagy-related gene 5 (ATG5) protects dopaminergic neurons in a zebrafish model of Parkinson's disease. *The Journal of Biological Chemistry*, *292*(44), 18062–18074. https://doi.org/10.1074/jbc.M116.764795

Huang, H.-C., Chen, L., Zhang, H.-X., Li, S.-F., Liu, P., Zhao, T.-Y., & Li, C.-X. (2016). Autophagy Promotes Peripheral Nerve Regeneration and Motor Recovery Following Sciatic Nerve Crush Injury in Rats. *Journal of Molecular Neuroscience : MN*, *58*(4), 416–23. https://doi.org/10.1007/s12031-015-0672-9

Huang, Z., Wang, W., Ma, J., Li, B., Chen, J., Yang, H., & Saijilafu. (2017). OUP accepted manuscript. *Acta Biochimica et Biophysica Sinica*, *49*(8), 689–695. https://doi.org/10.1093/abbs/gmx068

Hulleberg, G., Elvrum, A.-K. G., Brandal, M., & Vik, T. (2014). Outcome in adolescence of brachial plexus birth palsy. 69 individuals re-examined after 10–20 years. *Acta Orthopaedica*, *85*(6), 633–40. https://doi.org/10.3109/17453674.2014.964614

Ichim, G., & Tait, S. W. G. (2016). A fate worse than death: apoptosis as an oncogenic process. *Nature Reviews Cancer*, *16*(8), 539–548. https://doi.org/10.1038/nrc.2016.58

Ikeda, K., Sakamoto, T., Marubuchi, S., Kawazoe, Y., Terashima, N., Iwasaki, Y., … Watabe, K. (2003). Oral administration of a neuroprotective compound T-588 prevents motoneuron degeneration after facial nerve avulsion in adult rats. *Amyotrophic Lateral Sclerosis and Other Motor Neuron Disorders : Official Publication of the World Federation of Neurology, Research Group on Motor Neuron Diseases*, *4*(2), 74–80. Retrieved from http://www.ncbi.nlm.nih.gov/pubmed/14506937

Jackson, C. L., & Hauri, H. P. (2009). Mechanisms of transport through the Golgi complex. *Journal of Cell Science*, *122*(4), 443–452. https://doi.org/10.1242/jcs.032581

Janjic, J. M., & Gorantla, V. S. (2017). Peripheral Nerve Nanoimaging: Monitoring Treatment and Regeneration. *The AAPS Journal*, *19*(5), 1304–1316. https://doi.org/10.1208/s12248-017-0129-x

Jin, H., Mimura, N., Kashio, M., Koseki, H., & Aoe, T. (2014). Late-Onset of Spinal Neurodegeneration in Knock-In Mice Expressing a Mutant BiP. *PLoS ONE*, *9*(11), e112837. https://doi.org/10.1371/journal.pone.0112837

Jin, S. M., Lazarou, M., Wang, C., Kane, L. A., Narendra, D. P., & Youle, R. J. (2010). Mitochondrial membrane potential regulates PINK1 import and proteolytic destabilization by PARL. *The Journal of Cell Biology*, *191*(5), 933–42. https://doi.org/10.1083/jcb.201008084

Jones, S., Eisenberg, H. M., & Jia, X. (2016). Advances and Future Applications of Augmented Peripheral Nerve Regeneration. *International Journal of Molecular Sciences*, *17*(9). https://doi.org/10.3390/ijms17091494

Jonsson, S., Wiberg, R., Mcgrath, A. M., Novikov, L. N., Wiberg, M., Novikova, L. N., … Gillingwater, T. H. (2013). Effect of Delayed Peripheral Nerve Repair on Nerve Regeneration, Schwann Cell Function and Target Muscle Recovery. *Schwann Cell Function and Target Muscle Recovery. PLoS ONE*, *8*(2). https://doi.org/10.1371/journal.pone.0056484

Joo, H.-Y., Yun, M., Jeong, J., Park, E.-R., Shin, H.-J., Woo, S. R., … Lee, K.-H. (2015). SIRT1 deacetylates and stabilizes hypoxia-inducible factor-1α (HIF-1α) via direct interactions during hypoxia. *Biochemical and Biophysical Research Communications*, *462*(4), 294–300. https://doi.org/10.1016/j.bbrc.2015.04.119

Kalas, W., Swiderek, E., Rapak, A., Kopij, M., Rak, J., & Strzadala, L. (2011). H-ras up-regulates expression of BNIP3. *Anticancer Research*, *31*(9), 2869–75. Retrieved from http://www.ncbi.nlm.nih.gov/pubmed/21868531

Kang, H., Tian, L., Mikesh, M., Lichtman, J. W., & Thompson, W. J. (2014). Terminal Schwann cells participate in neuromuscular synapse remodeling during reinnervation following nerve injury. *The Journal of Neuroscience : The Official Journal of the Society for Neuroscience*, *34*(18), 6323–33. https://doi.org/10.1523/JNEUROSCI.4673-13.2014

Kanning, K. C., Kaplan, A., & Henderson, C. E. (2010). Motor Neuron Diversity in Development and Disease. *Annual Review of Neuroscience*, *33*(1), 409–440. https://doi.org/10.1146/annurev.neuro.051508.135722

Kapitein, L. C., & Hoogenraad, C. C. (2011). Which way to go? Cytoskeletal organization and polarized transport in neurons. *Molecular and Cellular Neuroscience*, *46*(1), 9–20. https://doi.org/10.1016/j.mcn.2010.08.015

Khalil, B., El Fissi, N., Aouane, A., Cabirol-Pol, M.-J., Rival, T., & Liévens, J.-C. (2015). PINK1-induced mitophagy promotes neuroprotection in Huntington's disease. *Cell Death & Disease*, *6*(1), e1617. https://doi.org/10.1038/cddis.2014.581

Koliatsos, V. E., Price, W. L., Pardo, C. A., & Price, D. L. (1994). Ventral root avulsion: An experimental model of death of adult motor neurons. *Journal of Comparative Neurology*, *342*(1), 35–44.

https://doi.org/10.1002/cne.903420105

Komatsu, M., Wang, Q. J., Holstein, G. R., Friedrich, V. L., Iwata, J. -i., Kominami, E., … Yue, Z. (2007). Essential role for autophagy protein Atg7 in the maintenance of axonal homeostasis and the prevention of axonal degeneration. *Proceedings of the National Academy of Sciences*, *104*(36), 14489–14494. https://doi.org/10.1073/pnas.0701311104

Kontos, H. A., & Povlishock, J. T. (1986). Oxygen radicals in brain injury. *Central Nervous System Trauma : Journal of the American Paralysis Association*, *3*(4), 257–63. Retrieved from http://www.ncbi.nlm.nih.gov/pubmed/3107844

Kosacka, J., Nowicki, M., Blüher, M., Baum, P., Stockinger, M., Toyka, K. V., … Klöting, N. (2013). Increased autophagy in peripheral nerves may protect Wistar Ottawa Karlsburg W rats against neuropathy. *Experimental Neurology*, *250*, 125–135. https://doi.org/10.1016/j.expneurol.2013.09.017

Kroemer, G., & Levine, B. (2008). Autophagic cell death: the story of a misnomer. *Nature Reviews. Molecular Cell Biology*, *9*(12), 1004–10. https://doi.org/10.1038/nrm2529

Laing, N. G. (2012). Genetics of neuromuscular disorders. *Critical Reviews in Clinical Laboratory Sciences*, *49*(2), 33–48. https://doi.org/10.3109/10408363.2012.658906

Lazarou, M., Sliter, D. A., Kane, L. A., Sarraf, S. A., Wang, C., Burman, J. L., … Youle, R. J. (2015). The ubiquitin kinase PINK1 recruits autophagy receptors to induce mitophagy. *Nature*, *524*(7565), 309–314. https://doi.org/10.1038/nature14893

Lee, D.-H., Kim, D., Kim, S. T., Jeong, S., Kim, J. L., Shim, S. M., … Lee, Y. J. (2018). PARK7 modulates autophagic proteolysis through binding to the N-terminally arginylated form of the molecular chaperone HSPA5. *Autophagy*, 1–16. https://doi.org/10.1080/15548627.2018.1491212

Lee, I. H., Cao, L., Mostoslavsky, R., Lombard, D. B., Liu, J., Bruns, N. E., … Finkel, T. (2008). A role for the NAD-dependent deacetylase Sirt1 in the regulation of

autophagy. *Proceedings of the National Academy of Sciences*, *105*(9), 3374–3379. https://doi.org/10.1073/pnas.0712145105

Lee, I. H., & Finkel, T. (2009). Regulation of autophagy by the p300 acetyltransferase. *The Journal of Biological Chemistry*, *284*(10), 6322–8. https://doi.org/10.1074/jbc.M807135200

Levine, B., & Klionsky, D. J. (2004). Development by self-digestion: molecular mechanisms and biological functions of autophagy. *Developmental Cell*, *6*(4), 463–77. https://doi.org/10.1016/S1534-5807(04)00099-1

Li, H., Wong, C., Li, W., Ruven, C., He, L., Wu, X., … Wu, W. (2015). Enhanced regeneration and functional recovery after spinal root avulsion by manipulation of the proteoglycan receptor PTPσ. *Scientific Reports*, *5*, 14923. https://doi.org/10.1038/srep14923

Li, J., & Collins, C. A. (2017). *Mechanisms of Axonal Degeneration and Regeneration*. (J. H. Byrne, Ed.) (Vol. 1). Oxford University Press. https://doi.org/10.1093/oxfordhb/9780190456757.013.33

Li, L., Houenou, L. J., Wu, W., Lei, M., Prevette, D. M., & Oppenheim, R. W. (1998). Characterization of spinal motoneuron degeneration following different types of peripheral nerve injury in neonatal and adult mice. *Journal of Comparative Neurology*, *396*(2), 158–168. https://doi.org/10.1002/(SICI)1096-9861(19980629)396:2<158::AID-CNE2>3.0.CO;2-#

Li, S., Yang, L., Selzer, M. E., & Hu, Y. (2013). Neuronal endoplasmic reticulum stress in axon injury and neurodegeneration. *Annals of Neurology*, *74*(6), 768–777. https://doi.org/10.1002/ana.24005

Li, X., Chen, C., Tu, Y., Sun, H., Zhao, M., Cheng, S., … Zhang, S. (2013). Sirt1 Promotes Axonogenesis by Deacetylation of Akt and Inactivation of GSK3. *Molecular Neurobiology*, *48*(3), 490–499. https://doi.org/10.1007/s12035-013-8437-3

Liu, D., Sybert, T. E., Qian, H., & Liu, J. (1998). Superoxide production after spinal injury detected by microperfusion of cytochrome c. *Free Radical Biology & Medicine*, *25*(3), 298–304. https://doi.org/10.1016/S0891-5849(98)00055-0

Liu, L., Feng, D., Chen, G., Chen, M., Zheng, Q., Song, P., … Chen, Q. (2012). Mitochondrial outer-membrane protein FUNDC1 mediates hypoxia-induced mitophagy in mammalian cells. *Nature Cell Biology*, *14*(2), 177–185. https://doi.org/10.1038/ncb2422

Liu, Z.-C., Chu, J., Lin, L., Song, J., Ning, L.-N., Luo, H.-B., … Tian, Q. (2016). SIL1 Rescued Bip Elevation-Related Tau Hyperphosphorylation in ER Stress. *Molecular Neurobiology*, *53*(2), 983–994. https://doi.org/10.1007/s12035-014-9039-4

Lochhead, J. J., & Thorne, R. G. (2012). Intranasal delivery of biologics to the central nervous system. *Advanced Drug Delivery Reviews*, *64*(7), 614–628. https://doi.org/10.1016/J.ADDR.2011.11.002

Lord, C., Ferro-Novick, S., & Miller, E. A. (2013). The Highly Conserved COPII Coat Complex Sorts Cargo from the Endoplasmic Reticulum and Targets It to the Golgi. *Cold Spring Harbor Perspectives in Biology*, *5*(2), a013367–a013367. https://doi.org/10.1101/cshperspect.a013367

Lowrie, M. B., Lavalette, D., & Davies, C. E. (1994). Time Course of Motoneurone Death after Neonatal Sciatic Nerve Crush in the Rat. *Developmental Neuroscience*, *16*(5–6), 279–284. https://doi.org/10.1159/000112120

Lundborg, G. (2000). A 25-year perspective of peripheral nerve surgery: Evolving neuroscientific concepts and clinical significance. *The Journal of Hand Surgery*, *25*(3), 391–414. https://doi.org/10.1053/jhsu.2000.4165

Luo, L. (2002). Actin Cytoskeleton Regulation in Neuronal Morphogenesis and Structural Plasticity. *Annual Review of Cell and Developmental Biology*, *18*(1), 601–635. https://doi.org/10.1146/annurev.cellbio.18.031802.150501

Ma, T. C., & Willis, D. E. (2015). What makes a RAG regeneration associated? *Frontiers in Molecular Neuroscience*, *8*, 43. https://doi.org/10.3389/fnmol.2015.00043

Macejak, D. G., & Sarnow, P. (1991). Internal initiation of translation mediated by the 5′ leader of a cellular mRNA. *Nature*, *353*(6339), 90–94.

https://doi.org/10.1038/353090a0

Mahar, M., & Cavalli, V. (2018). Intrinsic mechanisms of neuronal axon regeneration. *Nature Reviews. Neuroscience*, *19*(6), 323–337. https://doi.org/10.1038/s41583-018-0001-8

Maiuri, M. C., Le Toumelin, G., Criollo, A., Rain, J.-C., Gautier, F., Juin, P., … Kroemer, G. (2007). Functional and physical interaction between Bcl-XL and a BH3-like domain in Beclin-1. *The EMBO Journal*, *26*(10), 2527–2539. https://doi.org/10.1038/sj.emboj.7601689

Majcher, V., Goode, A., James, V., & Layfield, R. (2015). Autophagy receptor defects and ALS-FTLD. *Molecular and Cellular Neuroscience*, *66*(Pt A), 43–52. https://doi.org/10.1016/j.mcn.2015.01.002

Malek, M. A. Y. A., Jagannathan, S., Malek, E., Sayed, D. M., Elgammal, S. A., El-Azeem, H. G. A., … Driscoll, J. J. (2015). Molecular chaperone GRP78 enhances aggresome delivery to autophagosomes to promote drug resistance in multiple myeloma. *Oncotarget*, *6*(5), 3098–3110. https://doi.org/10.18632/oncotarget.3075

Malhotra, J. D., & Kaufman, R. J. (2007). The endoplasmic reticulum and the unfolded protein response. *Seminars in Cell & Developmental Biology*, *18*(6), 716–731. https://doi.org/10.1016/J.SEMCDB.2007.09.003

Mammucari, C., Milan, G., Romanello, V., Masiero, E., Rudolf, R., Del Piccolo, P., … Sandri, M. (2007). FoxO3 Controls Autophagy in Skeletal Muscle In Vivo. *Cell Metabolism*, *6*(6), 458–471. https://doi.org/10.1016/j.cmet.2007.11.001

Mancias, J. D., Pontano Vaites, L., Nissim, S., Biancur, D. E., Kim, A. J., Wang, X., … Harper, J. W. (2015). Ferritinophagy via NCOA4 is required for erythropoiesis and is regulated by iron dependent HERC2-mediated proteolysis. *ELife*, *4*. https://doi.org/10.7554/eLife.10308

Martin, L. J., Chen, K., & Liu, Z. (2005). Adult Motor Neuron Apoptosis Is Mediated by Nitric Oxide and Fas Death Receptor Linked by DNA Damage and p53 Activation. *Journal of Neuroscience*, *25*(27), 6449–6459.

https://doi.org/10.1523/JNEUROSCI.0911-05.2005

Martin, L. J., Kaiser, A., & Price, A. C. (1999). Motor neuron degeneration after sciatic nerve avulsion in adult rat evolves with oxidative stress and is apoptosis. *Journal of Neurobiology*, *40*(2), 185–201. https://doi.org/10.1002/(SICI)1097-4695(199908)40:2<185::AID-NEU5>3.0.CO;2-#

Martinez-Vicente, M. (2017). Neuronal Mitophagy in Neurodegenerative Diseases. *Frontiers in Molecular Neuroscience*, *10*, 64. https://doi.org/10.3389/fnmol.2017.00064

Masgrau, R., Guaza, C., Ransohoff, R. M., & Galea, E. (2017). Should We Stop Saying "Glia" and "Neuroinflammation"? *Trends in Molecular Medicine*, *23*(6), 486–500. https://doi.org/10.1016/j.molmed.2017.04.005

Mellman, I., & Warren, G. (2000). The road taken: past and future foundations of membrane traffic. *Cell*, *100*(1), 99–112. Retrieved from http://www.ncbi.nlm.nih.gov/pubmed/10647935

Melser, S., Chatelain, E. H., Lavie, J., Mahfouf, W., Jose, C., Obre, E., … Bénard, G. (2013). Rheb Regulates Mitophagy Induced by Mitochondrial Energetic Status. *Cell Metabolism*, *17*(5), 719–730. https://doi.org/10.1016/J.CMET.2013.03.014

Menzies, F. M., Fleming, A., & Rubinsztein, D. C. (2015). Compromised autophagy and neurodegenerative diseases. *Nature Reviews Neuroscience*, *16*(6), 345–357. https://doi.org/10.1038/nrn3961

Meredith, M. E., Salameh, T. S., & Banks, W. A. (2015). Intranasal Delivery of Proteins and Peptides in the Treatment of Neurodegenerative Diseases. *The AAPS Journal*, *17*(4), 780–7. https://doi.org/10.1208/s12248-015-9719-7

Mijaljica, D., Prescott, M., & Devenish, R. J. (2011). Microautophagy in mammalian cells Revisiting a 40-year-old conundrum. *Www.Landesbioscience.Com Autophagy Autophagy*, *6737*(7), 673–682. https://doi.org/10.4161/auto.7.7.14733

Mitchison, T., & Kirschner, M. (1984). Dynamic instability of microtubule growth. *Nature*, *312*(5991), 237–242. https://doi.org/10.1038/312237a0

Mohammadi, R., Amini, K., & Eskafian, H. (2013). Betamethasone-Enhanced Vein Graft Conduit Accelerates Functional Recovery in the Rat Sciatic Nerve Gap. *Journal of Oral and Maxillofacial Surgery*, *71*(4), 786–792. https://doi.org/10.1016/J.JOMS.2012.08.009

Mohammadi, R., Amini, K., Yousefi, A., Abdollahi-Pirbazari, M., Belbasi, A., & Abedi, F. (2013). Functional Effects of Local Administration of Thyroid Hormone Combined With Chitosan Conduit After Sciatic Nerve Transection in Rats. *Journal of Oral and Maxillofacial Surgery*, *71*(10), 1763–1776. https://doi.org/10.1016/j.joms.2013.03.010

Moon, L. D. F. (2018). Chromatolysis: Do injured axons regenerate poorly when ribonucleases attack rough endoplasmic reticulum, ribosomes and RNA? *Developmental Neurobiology*. https://doi.org/10.1002/dneu.22625

Moore, A. S., & Holzbaur, E. L. F. (2016). Dynamic recruitment and activation of ALS-associated TBK1 with its target optineurin are required for efficient mitophagy. *Proceedings of the National Academy of Sciences of the United States of America*, *113*(24), E3349-58. https://doi.org/10.1073/pnas.1523810113

Morales, F. R., Boxer, P. A., Fung, S. J., & Chase, M. H. (1987). Basic electrophysiological properties of spinal cord motoneurons during old age in the cat. *Journal of Neurophysiology*, *58*(1), 180–194. https://doi.org/10.1152/jn.1987.58.1.180

Moriya, S., Hasegawa, M., Inamasu, J., Kogame, H., Hirose, Y., Higashi, R., … Imai, F. (2017). Neuroprotective effects of pregabalin in a rat model of intracisternal facial nerve avulsion. *Journal of Neurosurgical Sciences*, *61*(5), 495–503. https://doi.org/10.23736/S0390-5616.16.03263-X

Nagano, I., Murakami, T., Shiote, M., Abe, K., & Itoyama, Y. (2003). Ventral root avulsion leads to downregulation of GluR2 subunit in spinal motoneurons in adult rats. *Neuroscience*, *117*(1), 139–46. Retrieved from

http://www.ncbi.nlm.nih.gov/pubmed/12605900

Navarro, X. (2009a). Chapter 27 Neural Plasticity After Nerve Injury and Regeneration (pp. 483–505). https://doi.org/10.1016/S0074-7742(09)87027-X

Navarro, X. (2009b). *Neural Plasticity After Nerve Injury and Regeneration*. *International Review of Neurobiology* (1st ed., Vol. 87). Elsevier Inc. https://doi.org/10.1016/S0074-7742(09)87027-X

Navarro, X. (2016, February). Functional evaluation of peripheral nerve regeneration and target reinnervation in animal models: A critical overview. (J. Foxe, Ed.), *European Journal of Neuroscience*. https://doi.org/10.1111/ejn.13033

Nelson, A. D., & Jenkins, P. M. (2017). Axonal Membranes and Their Domains: Assembly and Function of the Axon Initial Segment and Node of Ranvier. *Frontiers in Cellular Neuroscience*, *11*, 136. https://doi.org/10.3389/fncel.2017.00136

Ng, D. T., Watowich, S. S., & Lamb, R. A. (1992). Analysis in vivo of GRP78-BiP/substrate interactions and their role in induction of the GRP78-BiP gene. *Molecular Biology of the Cell*, *3*(2), 143–55. https://doi.org/10.1091/mbc.3.2.143

Ni, M., Zhang, Y., & Lee, A. S. (2011). Beyond the endoplasmic reticulum: atypical GRP78 in cell viability, signalling and therapeutic targeting. *The Biochemical Journal*, *434*(2), 181–8. https://doi.org/10.1042/BJ20101569

Nicolson, G. L. (2014). Mitochondrial Dysfunction and Chronic Disease: Treatment With Natural Supplements. *Integrative Medicine (Encinitas, Calif.)*, *13*(4), 35–43. Retrieved from http://www.ncbi.nlm.nih.gov/pubmed/26770107

Nishida, Y., Arakawa, S., Fujitani, K., Yamaguchi, H., Mizuta, T., Kanaseki, T., … Shimizu, S. (2009). Discovery of Atg5/Atg7-independent alternative macroautophagy. *Nature*, *461*(7264), 654–658. https://doi.org/10.1038/nature08455

Nishiyama, J., Miura, E., Mizushima, N., Watanabe, M., & Yuzaki, M. (2007). Aberrant Membranes and Double-Membrane Structures Accumulate in the Axons of *Atg5* -Null Purkinje Cells before Neuronal Death. *Autophagy*, *3*(6), 591–596. https://doi.org/10.4161/auto.4964

Nógrádi, A., & Vrbová, G. (2001). The effect of riluzole treatment in rats on the survival of injured adult and grafted embryonic motoneurons. *The European Journal of Neuroscience*, *13*(1), 113–8. Retrieved from http://www.ncbi.nlm.nih.gov/pubmed/11135009

Ohtake, Y., Matsuhisa, K., Kaneko, M., Kanemoto, S., Asada, R., Imaizumi, K., & Saito, A. (2018). Axonal Activation of the Unfolded Protein Response Promotes Axonal Regeneration Following Peripheral Nerve Injury. *Neuroscience*, *375*, 34–48. https://doi.org/10.1016/J.NEUROSCIENCE.2018.02.003

Oliveira, A. L., & Langone, F. (2000). GM-1 ganglioside treatment reduces motoneuron death after ventral root avulsion in adult rats. *Neuroscience Letters*, *293*(2), 131–4. https://doi.org/10.1016/S0304-3940(00)01506-8

Oñate, M., Catenaccio, A., Martínez, G., Armentano, D., Parsons, G., Kerr, B., … Court, F. A. (2016). Activation of the unfolded protein response promotes axonal regeneration after peripheral nerve injury. *Scientific Reports*, *6*(1), 21709. https://doi.org/10.1038/srep21709

Park, O., Lee, K. J., Rhyu, I. J., Geum, D., Kim, H., Buss, R., … Sun, W. (2007). Bax-dependent and -independent death of motoneurons after facial nerve injury in adult mice. *European Journal of Neuroscience*, *26*(6), 1421–1432. https://doi.org/10.1111/j.1460-9568.2007.05787.x

Pavelka, M., & Roth, J. (2010). Neuromuscular Junction. In *Functional Ultrastructure* (pp. 304–305). Vienna: Springer Vienna. https://doi.org/10.1007/978-3-211-99390-3_156

Penas, C., Casas, C., Robert, I., Fores, J., & Navarro, X. (2009). Cytoskeletal and activity-related changes in spinal motoneurons after root avulsion. *J Neurotrauma*, *26*(5), 763–779.

Penas, C., Casas, C., Robert, I., Forés, J., & Navarro, X. (2009). Cytoskeletal and activity-related changes in spinal motoneurons after root avulsion. *Journal of Neurotrauma*, *26*(5), 763–79. https://doi.org/10.1089/neu.2008-0661

Penas, C., Font-Nieves, M., Forés, J., Petegnief, V., Planas, A., Navarro, X., & Casas, C. (2011). Autophagy, and BiP level decrease are early key events in retrograde degeneration of motoneurons. *Cell Death and Differentiation*, *18*(10), 1617–27. https://doi.org/10.1038/cdd.2011.24

Penas, C., Font-Nieves, M., Forés, J., Petegnief, V., Planas, A., Navarro, X., & Casas, C. (2011). Autophagy, and BiP level decrease are early key events in retrograde degeneration of motoneurons. *Cell Death and Differentiation*, *18*(10), 1617–1627. https://doi.org/10.1038/cdd.2011.24

Penas, C., Pascual-Font, A., Mancuso, R., Forés, J., Casas, C., & Navarro, X. (2011). Sigma Receptor Agonist 2-(4-Morpholinethyl)1 Phenylcyclohexanecarboxylate (Pre084) Increases GDNF and BiP Expression and Promotes Neuroprotection after Root Avulsion Injury. *Journal of Neurotrauma*, *28*(5), 831–840. https://doi.org/10.1089/neu.2010.1674

Pereira, J. A., Lebrun-Julien, F., & Suter, U. (2012). Molecular mechanisms regulating myelination in the peripheral nervous system. *Trends in Neurosciences*, *35*(2), 123–34. https://doi.org/10.1016/j.tins.2011.11.006

Piermarini, E., Cartelli, D., Pastore, A., Tozzi, G., Compagnucci, C., Giorda, E., … Piemonte, F. (2016). Frataxin silencing alters microtubule stability in motor neurons: implications for Friedreich's ataxia. *Human Molecular Genetics*, *25*(19), 4288–4301. https://doi.org/10.1093/hmg/ddw260

Pondaag, W., Malessy, M. J. A., Van Dijk, J. G., & Thomeer, R. T. W. (2007). Natural history of obstetric brachial plexus palsy: a systematic review. *Developmental Medicine & Child Neurology*, *46*(2), 138–144. https://doi.org/10.1111/j.1469-8749.2004.tb00463.x

Portt, L., Norman, G., Clapp, C., Greenwood, M., & Greenwood, M. T. (2011). Anti-apoptosis and cell survival: A review. *Biochimica et Biophysica Acta (BBA) - Molecular Cell Research*, *1813*(1), 238–259.

https://doi.org/10.1016/J.BBAMCR.2010.10.010

Princz, A., Kounakis, K., & Tavernarakis, N. (2018). Mitochondrial contributions to neuronal development and function. *Biological Chemistry*, *399*(7), 723–739. https://doi.org/10.1515/hsz-2017-0333

Puertollano, R., van der Wel, N. N., Greene, L. E., Eisenberg, E., Peters, P. J., & Bonifacino, J. S. (2003). Morphology and dynamics of clathrin/GGA1-coated carriers budding from the trans-Golgi network. *Molecular Biology of the Cell*, *14*(4), 1545–57. https://doi.org/10.1091/mbc.02-07-0109

Pyo, J.-O., Jang, M.-H., Kwon, Y.-K., Lee, H.-J., Jun, J.-I., Woo, H.-N., … Jung, Y.-K. (2005). Essential Roles of Atg5 and FADD in Autophagic Cell Death. *Journal of Biological Chemistry*, *280*(21), 20722–20729. https://doi.org/10.1074/jbc.M413934200

Pyo, J.-O., Yoo, S.-M., Ahn, H.-H., Nah, J., Hong, S.-H., Kam, T.-I., … Jung, Y.-K. (2013). Overexpression of Atg5 in mice activates autophagy and extends lifespan. *Nature Communications*, *4*(1), 2300. https://doi.org/10.1038/ncomms3300

Qiu, G., Li, X., Che, X., Wei, C., He, S., Lu, J., … Fan, L. (2015). SIRT1 is a regulator of autophagy: Implications in gastric cancer progression and treatment. *FEBS Letters*, *589*(16), 2034–2042. https://doi.org/10.1016/J.FEBSLET.2015.05.042

Rahman, A., & Haugh, J. M. (2017). Kinetic Modeling and Analysis of the Akt/Mechanistic Target of Rapamycin Complex 1 (mTORC1) Signaling Axis Reveals Cooperative, Feedforward Regulation. *The Journal of Biological Chemistry*, *292*(7), 2866–2872. https://doi.org/10.1074/jbc.M116.761205

Rahman, S., & Islam, R. (2011). Mammalian Sirt1: insights on its biological functions. *Cell Communication and Signaling*, *9*(1), 11. https://doi.org/10.1186/1478-811X-9-11

Rasband, M. N. (2016). Glial Contributions to Neural Function and Disease. *Molecular & Cellular Proteomics : MCP*, *15*(2), 355. https://doi.org/10.1074/MCP.R115.053744

Reggiori, F., & Ungermann, C. (2017). Autophagosome Maturation and Fusion. *Journal of Molecular Biology*, *429*(4), 486–496. https://doi.org/10.1016/J.JMB.2017.01.002

Remondelli, P., & Renna, M. (2017). The Endoplasmic Reticulum Unfolded Protein Response in Neurodegenerative Disorders and Its Potential Therapeutic Significance. *Frontiers in Molecular Neuroscience*, *10*, 187. https://doi.org/10.3389/fnmol.2017.00187

Reynolds, M. L., & Woolf, C. J. (1992). Terminal Schwann cells elaborate extensive processes following denervation of the motor endplate. *Journal of Neurocytology*, *21*(1), 50–66. Retrieved from http://www.ncbi.nlm.nih.gov/pubmed/1346630

Rishal, I., & Fainzilber, M. (2014). Axon-soma communication in neuronal injury. *Nature Reviews. Neuroscience*, *15*(1), 32–42. https://doi.org/10.1038/nrn3609

Roberts, R. F., Tang, M. Y., Fon, E. A., & Durcan, T. M. (2016). Defending the mitochondria: The pathways of mitophagy and mitochondrial-derived vesicles. *The International Journal of Biochemistry & Cell Biology*, *79*, 427–436. https://doi.org/10.1016/J.BIOCEL.2016.07.020

Roberts, V. J., & Gorenstein, C. (1987). Examination of the Transient Distribution of Lysosomes in Neurons of Developing Rat Brains. *Developmental Neuroscience*, *9*(4), 255–264. https://doi.org/10.1159/000111628

Rokudai, S., Fujita, N., Hashimoto, Y., & Tsuruo, T. (2000). Cleavage and inactivation of antiapoptotic Akt/PKB by caspases during apoptosis. *Journal of Cellular Physiology*, *182*(2), 290–296. https://doi.org/10.1002/(SICI)1097-4652(200002)182:2<290::AID-JCP18>3.0.CO;2-8

Romeo-Guitart, D., Forés, J., Herrando-Grabulosa, M., Valls, R., Leiva-Rodríguez, T., Galea, E., … Casas, C. (2018a). Neuroprotective Drug for Nerve Trauma Revealed Using Artificial Intelligence. *Scientific Reports*. https://doi.org/10.1038/s41598-018-19767-3

Romeo-Guitart, D., Forés, J., Herrando-Grabulosa, M., Valls, R., Leiva-Rodríguez, T., Galea, E., … Casas, C. (2018b). Neuroprotective Drug for Nerve Trauma Revealed Using Artificial Intelligence. *Scientific Reports*, *8*(1), 1879. https://doi.org/10.1038/s41598-018-19767-3

Romeo-Guitart, D., Forés, J., Navarro, X., & Casas, C. (2017). Boosted Regeneration and Reduced Denervated Muscle Atrophy by NeuroHeal in a Pre-clinical Model of Lumbar Root Avulsion with Delayed Reimplantation. *Scientific Reports*, *7*(1), 12028. https://doi.org/10.1038/s41598-017-11086-3

Romeo-Guitart, D., Leiva-Rodríguez, T., Espinosa-Alcantud, M., Sima, N., Vaquero, A., Martín, H. D.-, … Casas, C. (2018). SIRT1 activation with neuroheal is neuroprotective but SIRT2 inhibition with AK7 is detrimental for disconnected motoneurons. *Cell Death & Disease*. https://doi.org/10.1038/s41419-018-0553-6

Rubinsztein, D. C., Shpilka, T., & Elazar, Z. (2012, January 10). Mechanisms of autophagosome biogenesis. *Current Biology*. Cell Press. https://doi.org/10.1016/j.cub.2011.11.034

Ruschel, J., Hellal, F., Flynn, K. C., Dupraz, S., Elliott, D. A., Tedeschi, A., … Bradke, F. (2015). Axonal regeneration. Systemic administration of epothilone B promotes axon regeneration after spinal cord injury. *Science (New York, N.Y.)*, *348*(6232), 347–52. https://doi.org/10.1126/science.aaa2958

Sakuma, M., Gorski, G., Sheu, S.-H., Lee, S., Barrett, L. B., Singh, B., … Woolf, C. J. (2016). Lack of motor recovery after prolonged denervation of the neuromuscular junction is not due to regenerative failure. *The European Journal of Neuroscience*, *43*(3), 451–62. https://doi.org/10.1111/ejn.13059

Sandoval, H., Thiagarajan, P., Dasgupta, S. K., Schumacher, A., Prchal, J. T., Chen, M., & Wang, J. (2008). Essential role for Nix in autophagic maturation of erythroid cells. *Nature*, *454*(7201), 232–235. https://doi.org/10.1038/nature07006

Sarkar, C., Zhao, Z., Aungst, S., Sabirzhanov, B., Faden, A. I., & Lipinski, M. M. (2014). Impaired autophagy flux is associated with neuronal cell death after traumatic brain injury. *Autophagy*, *10*(12), 2208–2222.

https://doi.org/10.4161/15548627.2014.981787

Sato, M., & Sato, K. (2011). Degradation of paternal mitochondria by fertilization-triggered autophagy in C. elegans embryos. *Science (New York, N.Y.)*, *334*(6059), 1141–4. https://doi.org/10.1126/science.1210333

Saxton, R. A., & Sabatini, D. M. (2017). mTOR Signaling in Growth, Metabolism, and Disease. *Cell*, *168*(6), 960–976. https://doi.org/10.1016/J.CELL.2017.02.004

Scheuner, D., Song, B., McEwen, E., Liu, C., Laybutt, R., Gillespie, P., … Kaufman, R. J. (2001). Translational Control Is Required for the Unfolded Protein Response and In Vivo Glucose Homeostasis. *Molecular Cell*, *7*(6), 1165–1176. https://doi.org/10.1016/S1097-2765(01)00265-9

Schon, E. A., & Manfredi, G. (2003). Neuronal degeneration and mitochondrial dysfunction. *The Journal of Clinical Investigation*, *111*(3), 303–12. https://doi.org/10.1172/JCI17741

Seddon, H. J., Medawar, P. B., & Smith, H. (1943). Rate of regeneration of peripheral nerves in man. *The Journal of Physiology*, *102*(2), 191–215. https://doi.org/10.1113/jphysiol.1943.sp004027

Seltzer, Z., Cohn, S., Ginzburg, R., & Beilin, B. (1991). Modulation of neuropathic pain behavior in rats by spinal disinhibition and NMDA receptor blockade of injury discharge. *Pain*, *45*(1), 69–75. Retrieved from http://www.ncbi.nlm.nih.gov/pubmed/1677750

Sena, L. A., & Chandel, N. S. (2012). Physiological Roles of Mitochondrial Reactive Oxygen Species. *Molecular Cell*, *48*(2), 158–167. https://doi.org/10.1016/j.molcel.2012.09.025

Shaw, J., Yurkova, N., Zhang, T., Gang, H., Aguilar, F., Weidman, D., … Kirshenbaum, L. A. (2008). Antagonism of E2F-1 regulated Bnip3 transcription by NF-kappaB is essential for basal cell survival. *Proceedings of the National Academy of Sciences of the United States of America*, *105*(52), 20734–9. https://doi.org/10.1073/pnas.0807735105

Shin, J.-H., Ko, H. S., Kang, H., Lee, Y., Lee, Y.-I., Pletinkova, O., … Dawson, T. M.

(2011). PARIS (ZNF746) repression of PGC-1α contributes to neurodegeneration in Parkinson's disease. *Cell*, *144*(5), 689–702. https://doi.org/10.1016/j.cell.2011.02.010

Shin, J. E., & Cho, Y. (2017). Epigenetic Regulation of Axon Regeneration after Neural Injury. *Molecules and Cells*, *40*(1), 10–16. https://doi.org/10.14348/molcells.2017.2311

Sim, S. K., Tan, Y. C., Tee, J. H., Yusoff, A. A., & Abdullah, J. M. (2015). Paclitaxel inhibits expression of neuronal nitric oxide synthase and prevents mitochondrial dysfunction in spinal ventral horn in rats after c7 spinal root avulsion. *Turkish Neurosurgery*, *25*(4), 617–24. https://doi.org/10.5137/1019-5149.JTN.14035-15.1

Song, Z., Chen, H., Fiket, M., Alexander, C., & Chan, D. C. (2007). OPA1 processing controls mitochondrial fusion and is regulated by mRNA splicing, membrane potential, and Yme1L. *The Journal of Cell Biology*, *178*(5), 749–55. https://doi.org/10.1083/jcb.200704110

Soubannier, V., Rippstein, P., Kaufman, B. A., Shoubridge, E. A., & McBride, H. M. (2012). Reconstitution of Mitochondria Derived Vesicle Formation Demonstrates Selective Enrichment of Oxidized Cargo. *PLoS ONE*, *7*(12), e52830. https://doi.org/10.1371/journal.pone.0052830

Squire, L. R., Bloom, F. E., Spitzer, N. C., Lac, S. du, Ghosh, A., & Berg, D. (2008). *Fundamental Neuroscience*. *Fundamental Neuroscience*. https://doi.org/10.1016/B978-0-12-385870-2.00032-9

Stünkel, W., Peh, B. K., Tan, Y. C., Nayagam, V. M., Wang, X., Salto-Tellez, M., … Wood, J. (2007). Function of the SIRT1 protein deacetylase in cancer. *Biotechnology Journal*, *2*(11), 1360–1368. https://doi.org/10.1002/biot.200700087

Suárez-Rivero, J., Villanueva-Paz, M., de la Cruz-Ojeda, P., de la Mata, M., Cotán, D., Oropesa-Ávila, M., … Sánchez-Alcázar, J. (2016). Mitochondrial Dynamics in Mitochondrial Diseases. *Diseases*, *5*(1), 1. https://doi.org/10.3390/diseases5010001

Sugino, T., Maruyama, M., Tanno, M., Kuno, A., Houkin, K., & Horio, Y. (2010). Protein deacetylase SIRT1 in the cytoplasm promotes nerve growth factor-induced neurite outgrowth in PC12 cells. https://doi.org/10.1016/j.febslet.2010.04.063

Sun, F.-C., Wei, S., Li, C.-W., Chang, Y.-S., Chao, C.-C., & Lai, Y.-K. (2006). Localization of GRP78 to mitochondria under the unfolded protein response. *Biochemical Journal*, *396*(1), 31–39. https://doi.org/10.1042/BJ20051916

Suzuki, C., Isaka, Y., Takabatake, Y., Tanaka, H., Koike, M., Shibata, M., … Imai, E. (2008). Participation of autophagy in renal ischemia/reperfusion injury. *Biochemical and Biophysical Research Communications*, *368*(1), 100–106. https://doi.org/10.1016/j.bbrc.2008.01.059

Suzuki, C. K., Bonifacino, J. S., Lin, A. Y., Davis, M. M., & Klausner, R. D. (1991). Regulating the retention of T-cell receptor alpha chain variants within the endoplasmic reticulum: Ca(2+)-dependent association with BiP. *The Journal of Cell Biology*, *114*(2), 189–205. Retrieved from http://www.ncbi.nlm.nih.gov/pubmed/1649196

Szalárdy, L., Zádori, D., Klivényi, P., Toldi, J., & Vécsei, L. (2015). Electron Transport Disturbances and Neurodegeneration: From Albert Szent-Györgyi's Concept (Szeged) till Novel Approaches to Boost Mitochondrial Bioenergetics. *Oxidative Medicine and Cellular Longevity*, *2015*, 498401. https://doi.org/10.1155/2015/498401

Szargel, R., Shani, V., Abd Elghani, F., Mekies, L. N., Liani, E., Rott, R., & Engelender, S. (2016). The PINK1, synphilin-1 and SIAH-1 complex constitutes a novel mitophagy pathway. *Human Molecular Genetics*, *25*(16), 3476–3490. https://doi.org/10.1093/hmg/ddw189

Tadros, M. A., Fuglevand, A. J., Brichta, A. M., & Callister, R. J. (2016). Intrinsic excitability differs between murine hypoglossal and spinal motoneurons. *Journal of Neurophysiology*, *115*(5), 2672–80. https://doi.org/10.1152/jn.01114.2015

Tang, B. L. (2016). Sirt1 and the Mitochondria. *Molecules and Cells*, *39*(2), 87–95.

https://doi.org/10.14348/molcells.2016.2318

Tintignac, L. A., Brenner, H.-R., & Rüegg, M. A. (2015). Mechanisms Regulating Neuromuscular Junction Development and Function and Causes of Muscle Wasting. *Physiological Reviews*, *95*(3), 809–852. https://doi.org/10.1152/physrev.00033.2014

Tos, P., Ronchi, G., Papalia, I., Sallen, V., Legagneux, J., Geuna, S., & Giacobini-Robecchi, M. (2009). Chapter 4 Methods and Protocols in Peripheral Nerve Regeneration Experimental Research: Part I—Experimental Models (pp. 47–79). https://doi.org/10.1016/S0074-7742(09)87004-9

Toyama, E. Q., Herzig, S., Courchet, J., Lewis, T. L., Losón, O. C., Hellberg, K., … Shaw, R. J. (2016). Metabolism. AMP-activated protein kinase mediates mitochondrial fission in response to energy stress. *Science (New York, N.Y.)*, *351*(6270), 275–281. https://doi.org/10.1126/science.aab4138

Tracy, K., Dibling, B. C., Spike, B. T., Knabb, J. R., Schumacker, P., & Macleod, K. F. (2007). BNIP3 is an RB/E2F target gene required for hypoxia-induced autophagy. *Molecular and Cellular Biology*, *27*(17), 6229–42. https://doi.org/10.1128/MCB.02246-06

Tran, H., Brunet, A., Grenier, J. M., Datta, S. R., Fornace, A. J., DiStefano, P. S., … Greenberg, M. E. (2002). DNA Repair Pathway Stimulated by the Forkhead Transcription Factor FOXO3a Through the Gadd45 Protein. *Science*, *296*(5567), 530–534. https://doi.org/10.1126/science.1068712

Twig, G., Elorza, A., Molina, A. J. A., Mohamed, H., Wikstrom, J. D., Walzer, G., … Shirihai, O. S. (2008). Fission and selective fusion govern mitochondrial segregation and elimination by autophagy. *The EMBO Journal*, *27*(2), 433–446. https://doi.org/10.1038/sj.emboj.7601963

Valenzuela, V., Oñate, M., & Court, F. A. (2016). Injury to the nervous system: A look into the ER. *Brain Research*, *1648*, 617–625. https://doi.org/10.1016/J.BRAINRES.2016.04.053

Vanden Noven, S., Wallace, N., Muccio, D., Turtz, A., & Pinter, M. J. (1993). Adult

spinal motoneurons remain viable despite prolonged absence of functional synaptic contact with muscle. *Experimental Neurology*, *123*(1), 147–56. Retrieved from http://www.ncbi.nlm.nih.gov/pubmed/8405274

Venkatesh, I., & Blackmore, M. G. (2017). Selecting optimal combinations of transcription factors to promote axon regeneration: Why mechanisms matter. *Neuroscience Letters*, *652*, 64–73. https://doi.org/10.1016/j.neulet.2016.12.032

Voelzmann, A., Hahn, I., Pearce, S. P., Sánchez-Soriano, N., & Prokop, A. (2016). A conceptual view at microtubule plus end dynamics in neuronal axons. *Brain Research Bulletin*, *126*(Pt 3), 226–237. https://doi.org/10.1016/j.brainresbull.2016.08.006

Wei, H., Liu, L., & Chen, Q. (2015). Selective removal of mitochondria via mitophagy: distinct pathways for different mitochondrial stresses. *Biochimica et Biophysica Acta*, *1853*(10 Pt B), 2784–90. https://doi.org/10.1016/j.bbamcr.2015.03.013

Wild, P., McEwan, D. G., & Dikic, I. (2014). The LC3 interactome at a glance. *Journal of Cell Science*, *127*(Pt 1), 3–9. https://doi.org/10.1242/jcs.140426

Wong, A. S. L., Cheung, Z. H., & Ip, N. Y. (2011). Molecular machinery of macroautophagy and its deregulation in diseases. *Biochimica et Biophysica Acta (BBA) - Molecular Basis of Disease*, *1812*(11), 1490–1497. https://doi.org/10.1016/J.BBADIS.2011.07.005

Wong, Y. C., & Holzbaur, E. L. F. (2014). Optineurin is an autophagy receptor for damaged mitochondria in parkin-mediated mitophagy that is disrupted by an ALS-linked mutation. *Proceedings of the National Academy of Sciences*, *111*(42), E4439–E4448. https://doi.org/10.1073/pnas.1405752111

Wu, D., Li, Q., Zhu, X., Wu, G., & Cui, S. (2013). Valproic acid protection against the brachial plexus root avulsion-induced death of motoneurons in rats. *Microsurgery*, *33*(7), 551–559. https://doi.org/10.1002/micr.22130

Wu, S.-Y., Lan, S.-H., Cheng, D.-E., Chen, W.-K., Shen, C.-H., Lee, Y.-R., … Liu, H.-S.

(2011). Ras-Related Tumorigenesis Is Suppressed by BNIP3-Mediated Autophagy through Inhibition of Cell Proliferation. *Neoplasia*, *13*(12), 1171-IN28. https://doi.org/10.1593/neo.11888

Wu, W., & Li, L. (1993). Inhibition of nitric oxide synthase reduces motoneuron death due to spinal root avulsion. *Neuroscience Letters*, *153*(2), 121–124. https://doi.org/10.1016/0304-3940(93)90303-3

Xi, Y., Dhaliwal, J. S., Ceizar, M., Vaculik, M., Kumar, K. L., & Lagace, D. C. (2016). Knockout of Atg5 delays the maturation and reduces the survival of adult-generated neurons in the hippocampus. *Cell Death & Disease*, *7*(3), e2127–e2127. https://doi.org/10.1038/cddis.2015.406

Yang, L., Miao, L., Liang, F., Huang, H., Teng, X., Li, S., … Hu, Y. (2014). The mTORC1 effectors S6K1 and 4E-BP play different roles in CNS axon regeneration. *Nature Communications*, *5*(1), 5416. https://doi.org/10.1038/ncomms6416

Yang, Y., Gehrke, S., Imai, Y., Huang, Z., Ouyang, Y., Wang, J.-W., … Lu, B. (2006). Mitochondrial pathology and muscle and dopaminergic neuron degeneration caused by inactivation of Drosophila Pink1 is rescued by Parkin. *Proceedings of the National Academy of Sciences of the United States of America*, *103*(28), 10793–8. https://doi.org/10.1073/pnas.0602493103

Ye, J., Rawson, R. B., Komuro, R., Chen, X., Davé, U. P., Prywes, R., … Goldstein, J. L. (2000). ER stress induces cleavage of membrane-bound ATF6 by the same proteases that process SREBPs. *Molecular Cell*, *6*(6), 1355–64. Retrieved from http://www.ncbi.nlm.nih.gov/pubmed/11163209

Ye, X., Sun, X., Starovoytov, V., & Cai, Q. (2015). Parkin-mediated mitophagy in mutant hAPP neurons and Alzheimer's disease patient brains. *Human Molecular Genetics*, *24*(10), 2938–2951. https://doi.org/10.1093/hmg/ddv056

Yerbury, J. J., & Wilson, M. R. (2010). Extracellular chaperones modulate the effects of Alzheimer's patient cerebrospinal fluid on Aβ1-42 toxicity and uptake. *Cell Stress and Chaperones*, *15*(1), 115–121. https://doi.org/10.1007/s12192-009-0122-0

Yoshida, H., Haze, K., Yanagi, H., Yura, T., & Mori, K. (1998). Identification of the cis-acting endoplasmic reticulum stress response element responsible for transcriptional induction of mammalian glucose-regulated proteins. Involvement of basic leucine zipper transcription factors. *The Journal of Biological Chemistry*, *273*(50), 33741–9. https://doi.org/10.1074/JBC.273.50.33741

Yoshida, H., Matsui, T., Hosokawa, N., Kaufman, R. J., Nagata, K., & Mori, K. (2003). A Time-Dependent Phase Shift in the Mammalian Unfolded Protein Response. *Developmental Cell*, *4*(2), 265–271. https://doi.org/10.1016/S1534-5807(03)00022-4

Yoshida, H., Okada, T., Haze, K., Yanagi, H., Yura, T., Negishi, M., & Mori, K. (2001). Endoplasmic Reticulum Stress-Induced Formation of Transcription Factor Complex ERSF Including NF-Y (CBF) and Activating Transcription Factors 6 and 6 That Activates the Mammalian Unfolded Protein Response. *Molecular and Cellular Biology*, *21*(4), 1239–1248. https://doi.org/10.1128/MCB.21.4.1239-1248.2001

Youle, R. J., & Narendra, D. P. (2011). Mechanisms of mitophagy. *Nature Reviews Molecular Cell Biology*, *12*(1), 9–14. https://doi.org/10.1038/nrm3028

Yousefi, S., Perozzo, R., Schmid, I., Ziemiecki, A., Schaffner, T., Scapozza, L., … Simon, H.-U. (2006). Calpain-mediated cleavage of Atg5 switches autophagy to apoptosis. *Nature Cell Biology*, *8*(10), 1124–1132. https://doi.org/10.1038/ncb1482

Yu, M., Wu, J., Shi, J., & Farokhzad, O. C. (2016). Nanotechnology for protein delivery: Overview and perspectives. *Journal of Controlled Release*, *240*, 24–37. https://doi.org/10.1016/J.JCONREL.2015.10.012

Yuan, A., Rao, M. V., Veeranna, & Nixon, R. A. (2012). Neurofilaments at a glance. *Journal of Cell Science*, *125*(14), 3257–3263. https://doi.org/10.1242/jcs.104729

Zhang, C.-G., Welin, D., Novikov, L., Kellerth, J.-O., Wiberg, M., & Hart, A. M. (2005). Motorneuron protection by N -acetyl-cysteine after ventral root avulsion and

ventral rhizotomy. *British Journal of Plastic Surgery*, *58*(6), 765–773. https://doi.org/10.1016/j.bjps.2005.04.012

Zhang, J., & Ney, P. A. (2009). Role of BNIP3 and NIX in cell death, autophagy, and mitophagy. *Cell Death and Differentiation*, *16*(7), 939–46. https://doi.org/10.1038/cdd.2009.16

Zhao, X.-C., Wang, L.-L., Wang, Y.-Q., Song, F.-H., Li, Y.-Q., Fu, R., … Zhou, L.-H. (2012). Activation of phospholipase-Cγ and protein kinase C signal pathways helps the survival of spinal motoneurons injured by root avulsion. *Journal of Neurochemistry*, *121*(3), 362–372. https://doi.org/10.1111/j.1471-4159.2012.07696.x

Zhou, K., Sansur, C., Xu, H., & Jia, X. (2017). The Temporal Pattern, Flux, and Function of Autophagy in Spinal Cord Injury. *International Journal of Molecular Sciences*, *18*(2), 466. https://doi.org/10.3390/ijms18020466

Zhu, Y., Massen, S., Terenzio, M., Lang, V., Chen-Lindner, S., Eils, R., … Brady, N. R. (2013). Modulation of serines 17 and 24 in the LC3-interacting region of Bnip3 determines pro-survival mitophagy versus apoptosis. *The Journal of Biological Chemistry*, *288*(2), 1099–113. https://doi.org/10.1074/jbc.M112.399345

Zorova, L. D., Popkov, V. A., Plotnikov, E. Y., Silachev, D. N., Pevzner, I. B., Jankauskas, S. S., … Zorov, D. B. (2018). Mitochondrial membrane potential. *Analytical Biochemistry*, *552*, 50–59. https://doi.org/10.1016/J.AB.2017.07.009

Acknowlegdments

Acknowledgements